VOLUME: 17 NO: 3 YEAR: 2020

Indexed in PMC and Web of Science
ULAKBİM, Tr Dizin, Scopus

ISSN: 1304-530X

TURKISH JOURNAL OF PHARMACEUTICAL SCIENCES

An Official Journal of the Turkish Pharmacists' Association, Academy of Pharmacy

TURKISH
JOURNAL OF PHARMACEUTICAL SCIENCES

TURKISH
JOURNAL OF PHARMACEUTICAL SCIENCES

TURKISH JOURNAL OF PHARMACEUTICAL SCIENCES

AIMS AND SCOPE

The Turkish Journal of Pharmaceutical Sciences is the only scientific periodical publication of the Turkish Pharmacists' Association and has been published since April 2004.
Turkish Journal of Pharmaceutical Sciences journal is regularly published 6 times in a year (February, April, June, August, October, December). The issuing body of the journal is Galenos Yayinevi/Publishing House level.
The aim of Turkish Journal of Pharmaceutical Sciences is to publish original research papers of the highest scientific and clinical value at an international level. The target audience includes specialists and professionals in all fields of pharmaceutical sciences.
The editorial policies are based on the "Recommendations for the Conduct, Reporting, Editing, and Publication of Scholarly Work in Medical Journals (ICMJE Recommendations)" by the International Committee of Medical Journal Editors (2013, archived at http://www.icmje.org/) rules.

Editorial Independence

Turkish Journal of Pharmaceutical Sciences is an independent journal with independent editors and principles and has no commerical relationship with the commercial product, drug or pharmaceutical company regarding decisions and review processes upon articles.

ABSTRACTED/INDEXED IN

PubMed Central
Web of Science-Emerging Sources Citation Index (ESCI)
SCOPUS SJR
TÜBİTAK/ULAKBİM TR Dizin
Directory of Open Access Journals (DOAJ)
ProQuest
Chemical Abstracts Service (CAS)
EBSCO
EMBASE
GALE
Index Copernicus
Analytical Abstracts
International Pharmaceutical Abstracts (IPA)
Medicinal & Aromatic Plants Abstracts (MAPA)
British Library
CSIR INDIA
GOALI
Hinari
OARE
ARDI
AGORA
Türkiye Atıf Dizini
Türk Medline
UDL-EDGE
J- Gate
Idealonline
ROOTINDEXING

OPEN ACCESS POLICY

This journal provides immediate open access to its content on the principle that making research freely available to the public supports a greater global exchange of knowledge.
Open Access Policy is based on the rules of the Budapest Open Access Initiative (BOAI) http://www.budapestopenaccessinitiative.org/. By "open access" to peer-reviewed research literature, we mean its free availability on the public internet, permitting any users to read, download, copy, distribute, print, search, or link to the full texts of these articles, crawl them for indexing, pass them as data to software, or use them for any other lawful purpose, without financial, legal, or technical barriers other than those inseparable from gaining access to the internet itself. The only constraint on reproduction and distribution, and the only role for copyright in this domain, should be to give authors control over the integrity of their work and the right to be properly acknowledged and cited.

CORRESPONDENCE ADDRESS

All correspondence should be directed to the Turkish Journal of Pharmaceutical Sciences editorial board;

Post Address: Turkish Pharmacists' Association, Mustafa Kemal Mah 2147.Sok No:3 06510 Çankaya/Ankara, TURKEY
Phone: +90 (312) 409 81 00
Fax: +90 (312) 409 81 09
Web Page: http://turkjps.org
E-mail: teb@teb.org.tr

PERMISSIONS

Requests for permission to reproduce published material should be sent to the publisher.
Publisher: Erkan Mor
Adress: Molla Gürani Mah. Kaçamak Sok. 21/1 Fındıkzade, Fatih, Istanbul, Turkey
Telephone: +90 212 621 99 25
Fax: +90 212 621 99 27
Web page: http://www.galenos.com.tr/en
E-mail: info@galenos.com.tr

ISSUING BODY CORRESPONDING ADDRESS

Issuing Body : Galenos Yayınevi
Address: Molla Gürani Mah. Kaçamak Sk. No: 21/1, 34093 İstanbul, Turkey
Phone: +90 212 621 99 25 Fax: +90 212 621 99 27
E-mail: info@galenos.com.tr

MATERIAL DISCLAIMER

The author(s) is (are) responsible for the articles published in the JOURNAL.
The editor, editorial board and publisher do not accept any responsibility for the articles.

galenos yayınevi

Galenos Publishing House
Owner and Publisher
Derya Mor
Erkan Mor

Publication Coordinator
Burak Sever

Web Coordinators
Fuat Hocalar
Turgay Akpınar

Graphics Department
Ayda Alaca
Çiğdem Birinci
Gülşah Özgül

Project Coordinators
Hatice Sever
Gamze Aksoy
Saliha Tuğçe Evin
Melike Eren
Duygu Yıldırm
Pınar Akpınar

Project Assistants
Gülay Akın
Özlem Çelik
Rabia Palazoğlu

Research&Development
Mert Can Köse
Mevlüde Özlem Akgüney

Finance Coordinator
Sevinç Çakmak

Publisher Contact
Address: Molla Gürani Mah. Kaçamak Sk. No: 21/1
34093 İstanbul, Turkey
Phone: +90 (212) 621 99 25 **Fax:** +90 (212) 621 99 27
E-mail: info@galenos.com.tr/yayin@galenos.com.tr
Web: www.galenos.com.tr | Publisher Certificate Number: 14521

Printing at: Üniform Basım San. ve Turizm Ltd. Şti.
Matbaacılar Sanayi Sitesi 1. Cad. No: 114 34204 Bağcılar, İstanbul, Turkey
Phone: +90 (212) 429 10 00 | Certificate Number: 42419
Printing Date: June 2020
ISSN: 1304-530X
International scientific journal published quarterly.

TURKISH
JOURNAL OF PHARMACEUTICAL SCIENCES

INSTRUCTIONS TO AUTHORS

Turkish Journal of Pharmaceutical Sciences journal is published 6 times (February, April, June, August, October, December) per year and publishes the following articles:

• Research articles

• Reviews (only upon the request or consent of the Editorial Board)

• Preliminary results/Short communications/Technical notes/Letters to the Editor in every field of pharmaceutical sciences.

The publication language of the journal is English.

The Turkish Journal of Pharmaceutical Sciences does not charge any article submission or processing charges.

A manuscript will be considered only with the understanding that it is an original contribution that has not been published elsewhere.

The Journal should be abbreviated as "Turk J Pharm Sci" when referenced.

The scientific and ethical liability of the manuscripts belongs to the authors and the copyright of the manuscripts belongs to the Journal. Authors are responsible for the contents of the manuscript and accuracy of the references. All manuscripts submitted for publication must be accompanied by the Copyright Transfer Form [copyright transfer]. Once this form, signed by all the authors, has been submitted, it is understood that neither the manuscript nor the data it contains have been submitted elsewhere or previously published and authors declare the statement of scientific contributions and responsibilities of all authors.

Experimental, clinical and drug studies requiring approval by an ethics committee must be submitted to the JOURNAL with an ethics committee approval report including approval number confirming that the study was conducted in accordance with international agreements and the Declaration of Helsinki (revised 2013) (http://www.wma.net/en/30publications/10policies/b3/). The approval of the ethics committee and the fact that informed consent was given by the patients should be indicated in the Materials and Methods section. In experimental animal studies, the authors should indicate that the procedures followed were in accordance with animal rights as per the Guide for the Care and Use of Laboratory Animals (http://oacu.od.nih.gov/regs/guide/guide.pdf) and they should obtain animal ethics committee approval.

Authors must provide disclosure/acknowledgment of financial or material support, if any was received, for the current study.

If the article includes any direct or indirect commercial links or if any institution provided material support to the study, authors must state in the cover letter that they have no relationship with the commercial product, drug, pharmaceutical company, etc. concerned; or specify the type of relationship (consultant, other agreements), if any.

Authors must provide a statement on the absence of conflicts of interest among the authors and provide authorship contributions.

All manuscripts submitted to the journal are screened for plagiarism using the 'iThenticate' software. Results indicating plagiarism may result in manuscripts being returned or rejected.

The Review Process

This is an independent international journal based on double-blind peer-review principles. The manuscript is assigned to the Editor-in-Chief, who reviews the manuscript and makes an initial decision based on manuscript quality and editorial priorities. Manuscripts that pass initial evaluation are sent for external peer review, and the Editor-in-Chief assigns an Associate Editor. The Associate Editor sends the manuscript to at least two reviewers (internal and/or external reviewers). The Associate Editor recommends a decision based on the reviewers' recommendations and returns the manuscript to the Editor-in-Chief. The Editor-in-Chief makes a final decision based on editorial priorities, manuscript quality, and reviewer recommendations. If there are any conflicting recommendations from reviewers, the Editor-in-Chief can assign a new reviewer.

The scientific board guiding the selection of the papers to be published in the Journal consists of elected experts of the Journal and if necessary, selected from national and international authorities. The Editor-in-Chief, Associate Editors may make minor corrections to accepted manuscripts that do not change the main text of the paper.

In case of any suspicion or claim regarding scientific shortcomings or ethical infringement, the Journal reserves the right to submit the manuscript to the supporting institutions or other authorities for investigation. The Journal accepts the responsibility of initiating action but does not undertake any responsibility for an actual investigation or any power of decision.

The Editorial Policies and General Guidelines for manuscript preparation specified below are based on "Recommendations for the Conduct, Reporting, Editing, and Publication of Scholarly Work in Medical Journals (ICMJE Recommendations)" by the International Committee of Medical Journal Editors (2013, archived at http://www.icmje.org/).

Preparation of research articles, systematic reviews and meta-analyses must comply with study design guidelines:

CONSORT statement for randomized controlled trials (Moher D, Schultz KF, Altman D, for the CONSORT Group. The CONSORT statement revised recommendations for improving the quality of reports of parallel group randomized trials. JAMA 2001; 285: 1987-91) (http://www.consort-statement.org/);

PRISMA statement of preferred reporting items for systematic reviews and meta-analyses (Moher D, Liberati A, Tetzlaff J, Altman DG, The PRISMA Group. Preferred Reporting Items for Systematic Reviews and Meta-Analyses: The PRISMA Statement. PLoS Med 2009; 6(7): e1000097.) (http://www.prisma-statement.org/);

STARD checklist for the reporting of studies of diagnostic accuracy (Bossuyt PM, Reitsma JB, Bruns DE, Gatsonis CA, Glasziou PP, Irwig LM, et al., for the STARD Group. Towards complete and accurate reporting of studies of diagnostic accuracy: the STARD initiative. Ann Intern Med 2003;138:40-4.) (http://www.stard-statement.org/);

STROBE statement, a checklist of items that should be included in reports of observational studies (http://www.strobe-statement.org/);

MOOSE guidelines for meta-analysis and systemic reviews of observational studies (Stroup DF, Berlin JA, Morton SC, et al. Meta-analysis of observational studies in epidemiology: a proposal for reporting Meta-analysis of observational Studies in Epidemiology (MOOSE) group. JAMA 2000; 283: 2008-12).

GENERAL GUIDELINES

Manuscripts can only be submitted electronically through the Journal Agent website (http://journalagent.com/tjps/) after creating an account. This system allows online submission and review.

TURKISH
JOURNAL OF PHARMACEUTICAL SCIENCES

INSTRUCTIONS TO AUTHORS

Format: Manuscripts should be prepared using Microsoft Word, size A4 with 2.5 cm margins on all sides, 12 pt Arial font and 1.5 line spacing.

Abbreviations: Abbreviations should be defined at first mention and used consistently thereafter. Internationally accepted abbreviations should be used; refer to scientific writing guides as necessary.

Cover letter: The cover letter should include statements about manuscript type, single-Journal submission affirmation, conflict of interest statement, sources of outside funding, equipment (if applicable), for original research articles.

ETHICS COMMITTEE APPROVAL

The editorial board and our reviewers systematically ask for ethics committee approval from every research manuscript submitted to the Turkish Journal of Pharmaceutical Sciences. If a submitted manuscript does not have ethical approval, which is necessary for every human or animal experiment as stated in international ethical guidelines, it must be rejected on the first evaluation.

Research involving animals should be conducted with the same rigor as research in humans; the Turkish Journal of Pharmaceutical Sciences asks original approval document to show implements the 3Rs principles. If a study does not have ethics committee approval or authors claim that their study does not need approval, the study is consulted to and evaluated by the editorial board for approval.

SIMILARITY

The Turkish Journal of Pharmaceutical Sciences is routinely looking for similarity index score from every manuscript submitted before evaluation by the editorial board and reviewers. The journal uses iThenticate plagiarism checker software to verify the originality of written work. There is no acceptable similarity index; but, exceptions are made for similarities less than 15 %.

REFERENCES

Authors are solely responsible for the accuracy of all references.

In-text citations: References should be indicated as a superscript immediately after the period/full stop of the relevant sentence. If the author(s) of a reference is/are indicated at the beginning of the sentence, this reference should be written as a superscript immediately after the author's name. If relevant research has been conducted in Turkey or by Turkish investigators, these studies should be given priority while citing the literature.

Presentations presented in congresses, unpublished manuscripts, theses, Internet addresses, and personal interviews or experiences should not be indicated as references. If such references are used, they should be indicated in parentheses at the end of the relevant sentence in the text, without reference number and written in full, in order to clarify their nature.

References section: References should be numbered consecutively in the order in which they are first mentioned in the text. All authors should be listed regardless of number. The titles of Journals should be abbreviated according to the style used in the Index Medicus.

Reference Format

Journal: Last name(s) of the author(s) and initials, article title, publication title and its original abbreviation, publication date, volume, the inclusive page numbers. Example: Collin JR, Rathbun JE. Involutional entropion: a review with evaluation of a procedure. Arch Ophthalmol. 1978;96:1058-1064.

Book: Last name(s) of the author(s) and initials, book title, edition, place of publication, date of publication and inclusive page numbers of the extract cited.

Example: Herbert L. The Infectious Diseases (1st ed). Philadelphia; Mosby Harcourt; 1999:11;1-8.

Book Chapter: Last name(s) of the author(s) and initials, chapter title, book editors, book title, edition, place of publication, date of publication and inclusive page numbers of the cited piece.

Example: O'Brien TP, Green WR. Periocular Infections. In: Feigin RD, Cherry JD, eds. Textbook of Pediatric Infectious Diseases (4th ed). Philadelphia; W.B. Saunders Company;1998:1273-1278.

Books in which the editor and author are the same person: Last name(s) of the author(s) and initials, chapter title, book editors, book title, edition, place of publication, date of publication and inclusive page numbers of the cited piece. Example: Solcia E, Capella C, Kloppel G. Tumors of the exocrine pancreas. In: Solcia E, Capella C, Kloppel G, eds. Tumors of the Pancreas. 2nd ed. Washington: Armed Forces Institute of Pathology; 1997:145-210.

TABLES, GRAPHICS, FIGURES, AND IMAGES

All visual materials together with their legends should be located on separate pages that follow the main text.

Images: Images (pictures) should be numbered and include a brief title. Permission to reproduce pictures that were published elsewhere must be included. All pictures should be of the highest quality possible, in

JPEG format, and at a minimum resolution of 300 dpi.

Tables, Graphics, Figures: All tables, graphics or figures should be enumerated according to their sequence within the text and a brief descriptive caption should be written. Any abbreviations used should be defined in the accompanying legend. Tables in particular should be explanatory and facilitate readers' understanding of the manuscript, and should not repeat data presented in the main text.

MANUSCRIPT TYPES

Original Articles

Clinical research should comprise clinical observation, new techniques or laboratories studies. Original research articles should include title, structured abstract, key words relevant to the content of the article, introduction, materials and methods, results, discussion, study limitations, conclusion references, tables/figures/images and acknowledgement sections. Title, abstract and key words should be written in both Turkish and English. The manuscript should be formatted in accordance with the above-mentioned guidelines and should not exceed 16 A4 pages.

Title Page: This page should include the title of the manuscript, short title, name(s) of the authors and author information. The following descriptions should be stated in the given order:

TURKISH
JOURNAL OF PHARMACEUTICAL SCIENCES

INSTRUCTIONS TO AUTHORS

1. Title of the manuscript (Turkish and English), as concise and explanatory as possible, including no abbreviations, up to 135 characters

2. Short title (Turkish and English), up to 60 characters

3. Name(s) and surname(s) of the author(s) (without abbreviations and academic titles) and affiliations

4. Name, address, e-mail, phone and fax number of the corresponding author

5. The place and date of scientific meeting in which the manuscript was presented and its abstract published in the abstract book, if applicable

Abstract: A summary of the manuscript should be written in both Turkish and English. References should not be cited in the abstract. Use of abbreviations should be avoided as much as possible; if any abbreviations are used, they must be taken into consideration independently of the abbreviations used in the text. For original articles, the structured abstract should include the following sub-headings:

Objectives: The aim of the study should be clearly stated.

Materials and Methods: The study and standard criteria used should be defined; it should also be indicated whether the study is randomized or not, whether it is retrospective or prospective, and the statistical methods applied should be indicated, if applicable.

Results: The detailed results of the study should be given and the statistical significance level should be indicated.

Conclusion: Should summarize the results of the study, the clinical applicability of the results should be defined, and the favorable and unfavorable aspects should be declared.

Keywords: A list of minimum 3, but no more than 5 key words must follow the abstract. Key words in English should be consistent with "Medical Subject Headings (MESH)" (www.nlm.nih.gov/mesh/MBrowser.html). Turkish key words should be direct translations of the terms in MESH.

Original research articles should have the following sections:

Introduction: Should consist of a brief explanation of the topic and indicate the objective of the study, supported by information from the literature.

Materials and Methods: The study plan should be clearly described, indicating whether the study is randomized or not, whether it is retrospective or prospective, the number of trials, the characteristics, and the statistical methods used.

Results: The results of the study should be stated, with tables/figures given in numerical order; the results should be evaluated according to the statistical analysis methods applied. See General Guidelines for details about the preparation of visual material.

Discussion: The study results should be discussed in terms of their favorable and unfavorable aspects and they should be compared with the literature. The conclusion of the study should be highlighted.

Study Limitations: Limitations of the study should be discussed. In addition, an evaluation of the implications of the obtained findings/results for future research should be outlined.

Conclusion: The conclusion of the study should be highlighted.

Acknowledgements: Any technical or financial support or editorial contributions (statistical analysis, English/Turkish evaluation) towards the study should appear at the end of the article.

References: Authors are responsible for the accuracy of the references. See General Guidelines for details about the usage and formatting required.

Review Articles

Review articles can address any aspect of clinical or laboratory pharmaceuticals. Review articles must provide critical analyses of contemporary evidence and provide directions of or future research. Most review articles are commissioned, but other review submissions are also welcome. Before sending a review, discussion with the editor is recommended.

Reviews articles analyze topics in depth, independently and objectively. The first chapter should include the title in Turkish and English, an unstructured summary and key words. Source of all citations should be indicated. The entire text should not exceed 25 pages (A4, formatted as specified above).

TURKISH
JOURNAL OF PHARMACEUTICAL SCIENCES

CONTENTS

TURKISH
JOURNAL OF PHARMACEUTICAL SCIENCES

CONTENTS

PUBLICATION NAME	Turkish Journal of Pharmaceutical Sciences
TYPE OF PUBLICATION	Vernacular Publication
PERIOD AND LANGUAGE	Bimonthly-English
OWNER	Erdoğan ÇOLAK on behalf of the Turkish Pharmacists' Association
EDITOR-IN-CHIEF	Prof.Terken BAYDAR, Ph.D.
ADDRESS OF PUBLICATION	Turkish Pharmacists' Association, Mustafa Kemal Mah 2147.Sok No:3 06510 Çankaya/ Ankara, TURKEY

TURKISH
JOURNAL OF PHARMACEUTICAL
SCIENCES

Volume: 17, No: 3, Year: 2020

CONTENTS

Turk J Pharm Sci 2020;17(3):242-248
DOI: 10.4274/tjps.galenos.2020.72325

ORIGINAL ARTICLE

Knowledge and Attitudes Among Hospital Pharmacists About COVID-19

Hastane Eczacılarının COVID-19 Konusunda Bilgi ve Tutumları

Emre KARA[1]*, Kutay DEMİRKAN[1], Serhat ÜNAL[2]

[1]Hacettepe University Faculty of Pharmacy, Department of Clinical Pharmacy, Ankara, Turkey
[2]Hacettepe University Faculty of Medicine, Department of Infectious Diseases and Clinical Microbiology, Ankara, Turkey

ABSTRACT

Objectives: Coronavirus (COVID-19) cases and deaths related to the virus have been reported all over the world. Pharmacists play an important role in conveying accurate information about COVID-19 to the community. The aim of this study was to evaluate the knowledge and attitudes among hospital pharmacists about COVID-19.

Materials and Methods: A questionnaire was distributed to pharmacists participating in the 7th National Hospital and Institution Pharmacists Congress. The questions included in this questionnaire were created using the Turkish COVID-19 Scientific Committee guideline (COVID-19 Guideline).

Results: Analysis of 237 questionnaires (72.6% completed by women) showed that the media (television, newspaper), internet (nonscientific resources), internet (scientific resources), and social media were the most popular sources of information (60.3%, 53.6%, 53.2%, and 41.4%, respectively). The participants' age and the source of information that they used had an important influence on their knowledge of and attitudes towards COVID-19 infection. The majority of the participants (72.6%) stated that they were not wearing any kind of mask. Transmission of the disease by airborne route was well known by the participants (91.1%), as well as the main symptoms such as fever (92.4%), cough (84.4%), and dyspnea (60.3%). The participants were aware of the risk groups for COVID-19 infection such as advanced age (84.8%) and having comorbidities (80.2%). Washing hands with soap (92.0%), using hand disinfectants (80.6%), and avoiding contact with sick people (81.9%) were popular answers for protection from the disease, but wearing an N95 mask was also mentioned by 59.1% of the participants. Prevention of the disease by rinsing the nose with saline solution was believed in by 43.9% of the participants.

Conclusion: Classical media and social media affect the attitudes of both the public and health professionals. Using media tools for accurate information is one of the basic conditions for preventing and controlling the spread of the disease.

Key words: COVID-19, hospital pharmacists, knowledge, attitudes

ÖZ

Amaç: Tüm dünyada Koronavirüs (COVID-19), olguları ve bu hastalığa bağlı ölümler bildirilmiştir. Bir sağlık uzmanı olarak eczacılar COVID-19 hakkında doğru bilgilerin topluma iletilmesinde önemli rol üstlenmektedir. Bu çalışmada hastane eczacılarının COVID-19 hakkındaki bilgi ve tutumlarının değerlendirilmesi amaçlanmıştır.

Gereç ve Yöntemler: Çalışma kapsamında 7. Ulusal Hastane ve Kurum Eczacıları Kongresi'ne katılan hastane eczacılarına bir anket uygulandı. Bu ankette yer alan sorular, Türkiye COVID-19 Bilim Kurulu Kılavuzu (COVID-19 Kılavuzu) kullanılarak oluşturulmuştur.

Bulgular: Çalışmada %72,6'sı kadın olmak üzere toplam 237 katılımcıya ait anket değerlendirilmiştir. Katılımcıların sırasıyla %60,3, %53,6, %53,2 ve %41,4'ünün bilgi kaynağı olarak en çok medyayı (televizyon, gazete), internet (bilimsel kaynaklar), interneti (bilimsel olmayan kaynaklar) ve sosyal medyayı kullandığı saptanmıştır. Katılımcıların COVID-19 ile ilgili bilgi ve tutumlarında yaşın ve kullandıkları bilgi kaynaklarının önemli etkisinin olduğu belirlenmiştir. Katılımcıların %72,6'sı korunma amaçlı cerrahi maske kullanmadığını bildirmiştir. Katılımcıların, hastalığın damlacıkla bulaştığı (%91,1) ve hastalığın genel semptomları (ateş; %92,4, öksürük; %84,4, solunum güçlüğü %60,3) konularında bilgi sahibi oldukları görülmüştür. Katılımcıların geneli tarafından, ileri yaşın (%84,8) ve eşlik eden hastalıkların (%80,2) COVID-19 için risk faktörü olduğunun bilindiği saptanmıştır. Hastalıktan korunmak için ellerin sabunla yıkanması (%92,0), el dezenfektanı kullanılması (%80,6), hasta kişilerle temasın önlenmesi (%81,9) sıklıkla belirtilen cevaplar arasında yer alsa da, katılımcıların %59,1'i N95 maske kullanımının da gerekli olduğunu belirtmiştir. Katılımcıların %43,9'unun tuzlu su ile burnu yıkamanın, hastalığı önlemede etkili olduğuna inandığı görülmüştür.

Sonuç: Klasik medya ve sosyal medya toplumun ve sağlık profesyonellerinin tutumlarını etkilemektedir. Doğru bilginin sağlanması için medya araçlarını kullanmak, hastalığın yayılmasını önlemek ve kontrol etmek için önemlidir.

Anahtar kelimeler: COVID-19, hastane eczacıları, bilgi, tutum

*Correspondence: **E-mail:** emrekara@hacettepe.edu.tr, **Phone:** +90 506 051 24 43 **ORCID-ID:** orcid.org/0000-0002-7034-4787
Received: 04.04.2020, **Accepted:** 13.04.2020

INTRODUCTION

In December 2019, a new, severe pneumonia outbreak occurred in Wuhan, China and a new coronavirus was identified as the pathogen responsible. First, this virus was named 2019 Novel Coronavirus and later Severe Acute Respiratory Syndrome - Coronavirus-2 (SARS-COV-2), and the disease caused by this virus has been named Coronavirus Disease 2019 (COVID-19).[1]

Positive cases of COVID-19 and deaths due to this virus have been reported in almost every country in the world.[2] Coronaviruses are a family of viruses that can cause mild diseases, such as the common cold, and more serious diseases, such as Middle East Respiratory syndrome (MERS) - COV or SARS-COV. SARS-COV-2, which is currently the cause of a pandemic and was the subject of this survey, is a virus from this family. Coronaviruses are mainly zoonotic and can cause disease in humans as a result of transmission from animals.[3]

The most common symptoms of infection are fever, cough, and dyspnea. In more serious cases pneumonia, severe acute respiratory syndrome, kidney failure, and death may develop.[4] The available data show that the rate of fatal cases is not very high in the young population.[5] However, older people (over 60 years) and people with comorbidities (such as diabetes and heart disease) may be more vulnerable and mortality can be high in this population.[3]

So far, there is no specific, effective, proven, pharmacological treatment or prophylaxis. Although no vaccine or drug has been developed for this infection, it has been suggested that some existing drugs can be used for treatment.[6]

As healthcare professionals, pharmacists play an important role in conveying accurate information about COVID-19 to the community. The aim of the present study was to evaluate the knowledge and attitudes among hospital pharmacists about COVID-19.

MATERIALS AND METHODS

A two-page self-structured questionnaire consisting of 22 multiple-choice and/or open-ended questions was distributed to pharmacists participating in the 7th National Hospital and Institution Pharmacists Congress held between 4 and 7 March 2020 in Turkey. The first positive COVID-19 case in Turkey was identified on 10 March 2020, and therefore no known COVID-19 case existed in Turkey during the period of the study. Moreover, none of the presentations at the congress were related to COVID-19 infection. There are 2747 hospital pharmacists in Turkey.[7] The sample size for this study was calculated as 155 people with an 80% confidence level and a 5% margin of error. The questionnaire was distributed to the participants who attended the first session on the 2nd day of the congress. At the end of the session, the questionnaires were collected from the participants.

The questions included in this questionnaire were created using the guideline (COVID-19 Guideline) created by the Turkish COVID-19 Scientific Committee and the COVID-19 information on the Ministry of Health website (https://hsgm.saglik.gov.tr/tr/bulasici-hastaliklar/2019-n-cov.html).

The questionnaire did not include the first name or surname of the participants, and the data were obtained anonymously. Age, sex, duration (years) of work in the profession, and job title were collected as demographic data. The participants' flu vaccination status was enquired about to evaluate their attitudes on protection from infection. The names of the two coronaviruses that had previously caused significant outbreaks were asked about to understand their interest in the issue (open-ended questions with no options). Fifteen other multiple-choice questions were asked about sources of information, knowledge, thoughts, and attitudes about COVID-19. The participants were instructed to choose only one answer for some of the questions (n=4) and more than one answer for the others (n=8). There were also 5 true/false questions. "Other" was provided as a choice for each question and an explanation was expected if this option was marked. Answers to the other options are given in brackets in the results.

Statistical analysis

The results obtained were analyzed using IBM SPSS Statistics for MacOS, version 23.0 (IBM Corp., Armonk, NY, USA). Percentage, average and standard deviation, median, and minimum-maximum were used for the descriptive data. A chi-square test was used to compare categorical variables. A 95% confidence interval was applied to examine the change in data and $p<0.05$ was considered statistically significant for all tests.

RESULTS

A total of 550 pharmacists participated in the congress and 440 (80%) of them were hospital pharmacists. Approximately 300 questionnaires were distributed to participants during the session. The questionnaire was filled out by 268 participants. Thirty one questionnaires were excluded because either the participants were not pharmacists (n=2) or not hospital pharmacists (n=24) or due to incomplete data (n=5). Thus the analysis was performed with a total of 237 questionnaires.

Table 1. Demographic characteristics of the participants

Parameters		n (%)
Sex	Female	172 (72.6)
	Male	65 (27.4)
Age	20-29 years	80 (33.8)
	30-39 years	79 (33.3)
	40-49 years	54 (22.8)
	50-59 years	18 (7.6)
	≥60 years	6 (2.5)
How many years have you been working?	<5 years	74 (31.2)
	5-10 years	48 (20.3)
	11-20 years	62 (26.2)
	20 years and older	53 (22.4)

The majority of the participants were women (n=172, 72.6%) and between the ages of 20 and 39 (n=159, 67.8%) (Table 1). Only 6.8% (n=16) of the participants stated that they were vaccinated for influenza every year and 5.1% (n=12) stated that they had been vaccinated for influenza this year.

SARS-CoV was given as an answer by 157 (66.2%) participants and MERS-CoV by 99 (41.8%) to the question "What are the two coronaviruses that previously caused important epidemics?" Other answers were H1N1 (swine flu) (n=33, 13.9%), H5N1 (bird flu) (n=13, 5.5%), Ebola (n=11, 4.6%), Influenza (n=3, 1.3%), HCoV-229E (n=2, 0.8%), HCoV-OC43 (n=1, 0.4%), and H2N2 (n=1, 0.4%). The majority of the participants (139 out of 232, 59.9%) stated that they had a fear of being infected with SARS-CoV-2. Only 43 out of 216 (18.1%) participants reported that there is an effective antiviral drug against COVID-19 disease.

The answers given by participants to the COVID-19 questionnaire are given in Tables 2, 3, and 4.

Participants' knowledge and attitudes towards COVID-19 infection were compared according to the source of information from which they learned about COVID-19 infection and statistically significant findings were detected only regarding the issues given below.

When the attitudes of 'the participants that obtained information through social media' and 'those that did not' were compared, statistically significant differences were determined in the following:

- Their behavior regarding wearing a mask in crowded environments (14.5% and 5.3%, respectively; p=0.016);
- Their knowledge about transmission of the disease through kissing (61.2% and 43.9%, respectively; p=0.012) and through blood (19.4% and 8.6%, respectively; p=0.019);
- Their knowledge of prevention of the disease by rinsing the nose with saline solution (54.1% and 36.7%, respectively; p=0.011) and eating mulberry molasses (7.1% and 1.4%, respectively; p=0.035);
- Their belief in protection from the disease by wearing N95 masks (69.4% and 51.8%, respectively; p=0.007), protective eyeglasses (32.7% and 18.0%, respectively; p=0.015), and medical gloves (48.0% and 31.7%, respectively; p=0.014).

When the attitudes of 'the participants that used the internet (scientific resources) as an information source' and 'those that did not' were compared, statistically significant differences were detected in the following:

- Their belief in transmission of COVID-19 by shipments from China (42.7% and 58.9%, respectively; p=0.021);
- Their behavior in protection from the disease by washing hands more than before (91.3% and 77.5%, respectively; p=0.004), wearing a mask on public transport (11.9% and 2.7%, respectively; p=0.012), wearing a mask while traveling (14.3% and 5.4%, respectively; p=0.030), and wearing a mask in crowded environments (15.9% and 1.8%, respectively; p<0.001). However, respectively 62.7% and 83.8% of the participants stated that they were not wearing a mask at all (p<0.001).

Table 2. Questions on knowledge about COVID-19 disease

Questions	Answers*	n (%)
When will the outbreak end? (n=222)	When the air temperature rises	87 (39.2)
	Within 1-2 months	34 (15.3)
	6 months to 1 year	66 (29.7)
	Within 1-2 years	18 (8.1)
	Within 2-5 years	10 (4.5)
	Within 5-10 years	1 (0.5)
	After 10 years	3 (1.4)
	Other (it will not end)	3 (1.4)
What is the first source of the infection? (n=212)	It is not known clearly	112 (52.8)
	Bats	78 (36.8)
	Pangolins	19 (9.0)
	Humans	3 (1.4)
	Camels	0 (0.0)
How long is the incubation period of the disease? (n=220)	<2 days	2 (0.9)
	2-14 days	176 (80.0)
	15-28 days	41 (18.6)
	>28 days	1 (0.5)
What is the mortality rate from COVID-19? (n=209)	0-1%	21 (10.0)
	1.1-5%	127 (60.8)
	5.1-10%	45 (21.5)
	10.1-25%	13 (6.1)
	>25%	3 (1.4)

*: Only one option was chosen, COVID: Coronavirus Disease

Table 3. The approach of the participants to true/false knowledge questions about COVID-19

Proposal	True, n (%)	False, n (%)
Coronaviruses are zoonotic viruses, mainly causing infection in animals (n=228)	161 (70.6)	67 (29.4)
COVID-19 is a vaccine-preventable disease (n=226)	102 (45.1)	124 (54.9)
COVID-19 can be treated with antiretroviral drugs (n=223)	109 (48.9)	114 (51.1)
In this country, the necessary facilities are available to diagnose COVID-19 (n=229)	160 (69.9)	69 (30.1)
There is a possibility of SARS-COV-2 infection from packages or products from China (n=230)	89 (38.7)	141 (61.3)

COVID: Coronavirus Disease, SARS-COV-2: Severe Acute Respiratory Syndrome Coronavirus-2

Table 4. Questions on knowledge and attitudes about COVID-19 disease

Questions	Answers*	n (%)
From which source(s) did you learn about COVID-19?	Media (TV, newspaper)	143 (60.3)
	Internet (nonscientific resources)	127 (53.6)
	Internet (scientific resources)	126 (53.2)
	Social media	98 (41.4)
	Educational/scientific meeting	66 (27.8)
	Friends/family	30 (12.7)
	Courses	2 (0.8)
	I did not get information	1 (0.4)
	Other (ministry announcements)	1 (0.4)
Do you wear a mask for COVID-19?	I do not	172 (72.6)
	While traveling	24 (10.1)
	In crowded environments	22 (9.3)
	In the workplace	21 (8.9)
	On public transport	18 (7.6)
	While walking in the streets	1 (0.4)
	I always wear one	1 (0.4)
	Every time I leave home	0 (0.0)
In which way(s) is COVID-19 transmitted?	It is transmitted by airborne route	216 (91.1)
	Kissing	121 (51.1)
	Shaking hands	89 (37.6)
	It is transmitted by blood	31 (13.1)
	By sexual intercourse	23 (9.7)
	From mother to baby during childbirth	21 (8.9)
What is the symptom(s) of the infection?	Fever	219 (92.4)
	Cough	200 (84.4)
	Dyspnea	143 (60.3)
	Pneumonia	91 (38.4)
	Runny nose	64 (27.0)
	Sudden loss of consciousness	24 (10.1)
	Diarrhea	15 (6.3)
	Kidney failure	10 (4.2)
	Bleeding	4 (1.7)
	Other (nausea)	1 (0.4)
Who is more affected by COVID-19?	Elderly	201 (84.8)
	People with comorbidities such as asthma, diabetes, and heart disease	190 (80.2)
	Children	70 (29.5)
	Pregnant women	48 (20.3)
	Young adults	7 (3.0)
	Other (immunocompromised individuals)	2 (0.8)
Which should be applied to protect from COVID-19?	Washing hands with soap	218 (92.0)
	Avoiding contact with sick people	194 (81.9)
	Using hand disinfectant	191 (80.6)
	Wearing an N95 mask	140 (59.1)
	Wearing medical gloves	91 (38.4)
	Wearing a surgical mask	89 (37.6)
	Covering the nose and mouth with tissue paper	82 (34.6)
	Wearing protective eyeglasses	58 (24.5)
	Wearing protective clothing	58 (24.5)
Which can prevent COVID-19?	Rinsing the nose with saline solution	104 (43.9)
	Using vinegar	51 (21.5)
	Using ginger	24 (10.1)
	Using turmeric	23 (9.7)
	Using echinacea	22 (9.3)
	Eating mulberry molasses	9 (3.8)
	Using pomegranate peel	7 (3.0)
	Other (alkaline disinfectants, vaccination, vitamin C, drinking plenty of liquid, ethanol, drinking warm water, black elderberry, sheep's head and foot soup, cologne, propolis)	12 (5.1)
What actions do you perform to protect against COVID-19?	I wash my hands more than before	201 (84.8)
	I try to touch less frequently where other people touch	172 (72.6)
	I try to stay away from people coughing	153 (64.6)
	I go to shopping malls less	113 (47.7)
	I reduce my use of public transportation	106 (44.7)
	I participate less in indoor activities such as theater and cinema	84 (35.4)
	I cancel meetings and activities with my friends	40 (16.9)

*: More than one option was chosen, COVID: Coronavirus Disease

Statistically significant differences were also detected in the comparison of the attitudes and knowledge of 'the participants that obtained information from family/friends' and 'those that did not' in some points such as:

- Their knowledge about prevention of the disease by eating mulberry molasses (13.3% and 2.4%, respectively; p=0.017);
- Their knowledge on the protective role of wearing a surgical mask (66.7% and 33.3%, respectively; p=0.001), protective eyeglasses (40.0% and 22.2%, respectively; p=0.042), and protective clothing (50.0% and 20.8%, respectively; p=0.001).

When the attitudes of 'the participants that obtained information from educational/scientific meetings' and 'those that did not' were compared, statistically significant differences were detected in their knowledge about the protective role of washing hands (98.5% and 89.5%, respectively; p=0.029) and wearing a surgical mask (51.5% and 32.2%, respectively; p=0.007).

When attitudes of 'the participants that used the Internet (nonscientific resources) to obtain information about COVID-19' and 'those that did not' were compared, statistically significant differences were determined in their knowledge on transmission of the disease through kissing (57.5% and 43.6%, respectively; p=0.038).

When the attitudes of 'the participants under the age of 40 years' and 'the participants over the age of 40 years' were compared, statistically significant differences were detected in some points such as their belief in the protective role of echinacea (13.2% and 1.3%, respectively; p=0.002), sexual transmission of the infection (13.8% and 1.3%, respectively; p=0.002), and transmission of the infection from mother to baby at birth (13.2% and 0%, respectively; p<0.001).

When the attitudes of 'the participants that believe COVID-19 is transmitted by airborne route' and 'those that do not' were compared, statistically significant differences were determined only in the following:

- Their belief in protection from the disease by washing hands with soap (96.8% and 42.9%, respectively; p<0.001), using hand disinfectants (84.3% and 42.9%, respectively; p<0.001), avoiding contact with sick people (86.1% and 38.2%, respectively; p<0.001), wearing an N95 mask (64.8% and 0%, respectively; p<0.001), wearing medical gloves (41.7% and 4.8%, respectively; p=0.001), and wearing protective clothing (26.4% and 4.8%, respectively; p=0.031);
- Their knowledge on prevention of the disease by rinsing the nose with saline solution (46.8% and 14.3%, respectively; p=0.005);
- Their actions that they implemented to protect against COVID-19 infection such as
  - canceling meetings and activities with friends (18.5% and 0%, respectively; p=0.029),
  - reducing public transportation use (47.7% and 14.3%, respectively; p=0.005),
  - minimizing shopping mall visits (51.4% and 9.5%, respectively; p<0.001),
  - minimizing indoor activities such as theater and cinema (38.4% and 4.8%, respectively; p=0.001),
  - trying to stay away from people coughing (68.5% and 23.8%, respectively; p<0.001),
  - trying to touch less frequently where other people touch (76.9% and 28.6%, respectively; p<0.001),
  - washing hands more than before (89.8% and 33.3%, respectively; p<0.001).

DISCUSSION

Providing information about drugs to patients, caregivers, and healthcare professionals is one of the main responsibilities of all pharmacists.[8] These days, as the number of positive cases of COVID-19 continues to increase in this country, healthcare professionals must have accurate and reliable information to be able inform the public properly. Health professionals have important roles in reducing the sense of panic in the community, encouraging individuals to take measures without panic, and convincing them to continue their lives by taking precautions.[9]

At the end of January, a survey was conducted to evaluate the knowledge, attitudes, and practices among the public in China. More than half of the participants included in that study were living in the Hubei region, where the disease first appeared. Correct answers were given to 70.2% to 98.6% of the questions about COVID-19. People between the ages of 30 and 49, those with higher educational status (master's degree and above), and students gave more right answers to the questions. The rate of wearing a mask and level of knowledge were significantly higher in participants living in Hubei.[10] By the time the survey was conducted, many people in China had been diagnosed with COVID-19 infection and many had died from it. However, when the questionnaire was applied in our study, no positive COVID-19 case had been diagnosed in Turkey. The first positive case was detected 5 days later and then more educational/informational programs organized by the Ministry of Health were shown in the media for public awareness.

According to available data, close contacts, droplets, and aerosol were defined as transmission routes of COVID-19.[11] In our study, almost all of the participants stated that it was transmitted by airborne route. Some common traditional behaviors in Turkish society such as hugging and kissing (on the cheeks or the hands of the elderly) are risky sources of close contact and can cause disease transmission.[12] The participants also mentioned handshaking and kissing as transmission routes.

In the present study, the participants generally used the media, Internet, and social media as resources. The source of information that the participants used to learn about COVID-19 infection had an important influence on their knowledge of and attitudes towards COVID-19 infection. The participants that used the Internet (scientific resources) as an information source had the right approaches especially in actions for protection from the disease (such as washing hands more than ever and wearing a mask on public transport, while traveling, and in crowded environments). The participants that obtained information from educational/scientific meetings also had the right approaches concerning protection from the disease (such as washing hands and wearing a surgical mask). However, those that obtained information from family/friends had the wrong approaches mainly regarding prevention of the disease (such as eating mulberry molasses) and protection from the disease (such as wearing protective eyeglasses and protective clothing). The participants that received information through social media had incorrect approaches, especially concerning the transmission of the disease (such as through blood), prevention of the disease (such as rinsing the nose with saline and eating mulberry molasses), and protection from the disease (such as wearing an N95 mask, protective eyeglasses, and medical gloves). It is recommended that an N95 mask be worn

by healthcare workers and surgical/medical masks should be worn by patients with respiratory symptoms in public.[11]

Some misleading information such as rinsing the nose with saline or consumption of some foods or products (e.g., vinegar, echinacea, and mulberry molasses) has been proposed by either some physicians or some prominent people on TV programs in Turkey. Even though these statements were criticized and corrected by other physicians and experts, some of the participants' preference for these methods (especially rinsing the nose with saline solution) reveals the strong influence of the media.

In the present study, it was detected that age is another factor that influences the participants' knowledge of and attitudes towards COVID-19 infection. The participants under the age of 40 had the wrong approaches especially regarding the protective role of echinacea and transmission routes of the disease (such as sexually and from mother to baby at birth).

SARS-CoV and MERS-CoV diseases were known about by approximately half of the participants, meaning that half of the participants were not interested in this issue. The majority of the participants believed that the pandemic would end when the air temperature rose or within 6 months to 1 year. In the study by Zhong et al.[10], 91% of the participants indicated that COVID-19 would be successfully controlled. In the studies conducted in the SARS-CoV epidemic, most of the participants (70.1-88.9%) stated that the epidemic would be successfully controlled. The fact that rapid restrictive measures were taken in the SARS-CoV epidemic and COVID-19 pandemic in China may be the source of this trust. While it is often thought that the first source of infection is unknown, bats was the answer given most by the participants. In our study, the incubation period was known correctly by almost all of the participants as stated by Chinese guidelines (average 7 days, ranging from 2 to 14 days).[13]

Although mortality rates vary between countries, almost all the respondents stated a mortality rate of 1-10% in the present study, which is generally correct. The case-fatality rate was found to be 2.3% in a wide-ranging assessment in China.[14] The average mortality rate is thought to be between 2% and 5%. Coronaviruses are zoonotic viruses and, in the present study, 70% of the participants answered this question correctly.[15] Although no vaccine has been discovered yet, many vaccine studies are ongoing and COVID-19 is expected to become a vaccine-preventable disease.[16,17] Even though no vaccine is currently available, nearly half of the participants in the present study stated that COVID-19 is a vaccine-preventable disease, which might be due to extrapolation of the knowledge of other flu-like viral infections. Many drugs are being tried for the treatment of COVID-19, and the effectiveness of these drugs has been demonstrated by some observational studies.[16,18] Some of these drugs are antiretroviral drugs. In the present study, almost half of the participants were aware of this information.

In the study by Zhong et al.[10], almost all of the participants stayed away from crowded places (96.4%) and they always wore masks (98.0%) when they went out. Because no positive COVID-19 cases had been diagnosed in Turkey at the time of our study, 72.6% of the participants stated that they were not wearing a mask.

The present study has some limitations. As it was conducted during a congress, it was limited to the congress participants and most of the participants were women. However, one of the strengths of the study is that the people attending the congress came from many different cities in Turkey and their age distribution was homogeneous. Another limitation is that attitudes and beliefs have not been evaluated in a standardized way and adequately, and in-depth interviews and multidimensional measurements may be required for this assessment.

CONCLUSION

It is important for pharmacists to have correct information about COVID-19 and to convey this knowledge to the public. Classical media and social media affect the attitudes of both society and health professionals. In addition, the high level of knowledge of individuals also positively affects their attitudes. Using media tools for accurate information is one of the basic conditions for preventing and controlling the spread of the disease. In this regard, studies evaluating the knowledge, beliefs, and attitudes of other healthcare professionals and other segments of society are required.

Conflicts of interest: No conflict of interest was declared by the authors. The authors alone are responsible for the content and writing of the paper.

REFERENCES

1. Zhu N, Zhang D, Wang W, Li X, Yang B, Song J, Song J, Zhao X, Huang B, Shi W, Lu R, Niu P, Zhan F, Ma X, Wang D, Xu W, Wu G, Gao GB, Tan W, Novel C. A Novel Coronavirus from Patients with Pneumonia in China, 2019. N Engl J Med. 2020;382:727-733.
2. World Health Organisation. Weekly Surveillance Report. Available at: http://www.euro.who.int/en/health-topics/health-emergencies/coronavirus-covid-19/weekly-surveillance-report. Accessed: April 2, 2020.
3. Lu R, Zhao X, Li J, Niu P, Yang B, Wu H, Wang W, Song H5, Huang B, Zhu N, Bi Y,Ma X, Zhan F, Wang L, Hu T, Zhou H, Zhenhong Hu, Zhou W, Zhao L, Chen J, Meng Y, Wang J, Lin Y, Yuan J, Xie Z, Ma J, Liu WJ, Wang D, Xu W, Holmes EC, Gao GF, Wu G, Chen W, Shi W, Tan W. Genomic characterisation and epidemiology of 2019 novel coronavirus: implications for virus origins and receptor binding. Lancet. 2020;395:565-574.
4. Huang C, Wang Y, Li X, Ren L, Zhao J, Hu Y, Zhang L, Fan G, Xu J, Gu X, Cheng Z, Yu T, Xia J, Wei Y, Wu W, Xie X, Yin W, Li H, Liu M, Xiao Y, Gao H, Guo L, Xie J,Wang G, Jiang R, Gao Z, Jin Q, Wang J, Cao B. Clinical features of patients infected with 2019 novel coronavirus in Wuhan, China. Lancet. 2020;395:497-506.
5. Wu Z, McGoogan JM. Characteristics of and Important Lessons From the Coronavirus Disease 2019 (COVID-19) Outbreak in China: Summary of a Report of 72314 Cases From the Chinese Center for Disease Control and Prevention. JAMA. 2020.
6. Lim J, Jeon S, Shin HY, Kim MJ, Seong YM, Lee WJ, Choe KW, Kang YM, Lee B, Park SJ. Case of the Index Patient Who Caused Tertiary

Transmission of COVID-19 Infection in Korea: the Application of Lopinavir/Ritonavir for the Treatment of COVID-19 Infected Pneumonia Monitored by Quantitative RT-PCR. J Korean Med Sci. 2020;35:e79.

7. T.C. Sağlık Bakanlığı Sağlık Bilgi Sistamleri Genel Müdürlüğü. Ankara; Sağlık İstatistikleri Yıllığı 2018; 2019.
8. Ghaibi S, Ipema H, Gabay M, American Society of Health System Pharmacists. ASHP guidelines on the pharmacist's role in providing drug information. Am J Health Syst Pharm. 2015;72:573-577.
9. Woods C, West C, Buettner P, Usher K. "Out of our control": living through Cyclone Yasi. Int J Qual Stud Health Well-being. 2014;9:19821.
10. Zhong BL, Luo W, Li HM, Zhang QQ, Liu XG, Li WT, Li Y. Knowledge, attitudes, and practices towards COVID-19 among Chinese residents during the rapid rise period of the COVID-19 outbreak: a quick online cross-sectional survey. Int J Biol Sci. 2020;16:1745-1752.
11. Adhikari SP, Meng S, Wu YJ, Mao YP, Ye RX, Wang QZ, Sun C, Sylvia S, Rozelle S, Raat H, Zhou HI. Epidemiology, causes, clinical manifestation and diagnosis, prevention and control of coronavirus disease (COVID-19) during the early outbreak period: a scoping review. Infect Dis Poverty. 2020;9:29.
12. Marchiori BE, Carraher CE, Stiles K. Understanding and overcoming business etiquette differences in Japan, Turkey, and the United States of America. Journal of Technology Management in China. 2014;9:274-288.
13. National Health Commission of People's Republic of China. Prevent guideline of 2019-nCoV. 2020. Available at: http://www.nhc.gov.cn/xcs/yqfkdt/202001/bc661e49b5bc487dba182f5c49ac445b.shtml. Accessed April 1, 2020.
14. Epidemiology Working Group for NCIP Epidemic Response, Chinese Center for Disease Control and Prevention. The epidemiological characteristics of an outbreak of 2019 novel coronavirus diseases (COVID-19) in China]. Zhonghua Liu Xing Bing Xue Za Zhi. 2020;41:145-151.
15. Wu YC, Chen CS, Chan YJ. The outbreak of COVID-19: An overview. J Chin Med Assoc. 2020;83:217-220.
16. Li H, Zhou Y, Zhang M, Wang H, Zhao Q, Liu J. Updated approaches against SARS-CoV-2. Antimicrob Agents Chemother. 2020;64:483.
17. Ahmed SF, Quadeer AA, McKay MR. Preliminary Identification of Potential Vaccine Targets for the COVID-19 Coronavirus (SARS-CoV-2) Based on SARS-CoV Immunological Studies. Viruses. 2020;12:254.
18. Sarma P, Prajapat M, Avti P, Kaur H, Kumar S, Medhi B. Therapeutic options for the treatment of 2019-novel coronavirus: An evidence-based approach. Indian J Pharmacol. 2020;52:1-5.

Turk J Pharm Sci 2020;17(3):249-253
DOI: 10.4274/tjps.galenos.2019.38278

ORIGINAL ARTICLE

Investigation of the Compressibility Characteristics of Paracetamol using "Compaction Simulator"

"Compaction Simulator" Kullanılarak Parasetamolün Basılabilirlik Özelliklerinin İncelenmesi

Yıldız ÖZALP*, Joseph Turemi CHUNU, Nailla JIWA

Near East University Faculty of Pharmacy, Department of Pharmaceutical Technology, Nicosia, Cypus

ABSTRACT

Objectives: This study was performed to understand the behavior of poorly compressible paracetamol powder using a compaction simulator (CS), equipment that records data during the compaction process. The aim was to investigate the compressibility of paracetamol tablets using a dry granulation (slugging) process, with different formulation compositions.

Materials and Methods: Formulations were prepared to observe the effect on compressibility with two different lactose-based fillers, Flowlac®100 and Granulac®70, and a binder, Kollidon® K90. In each combination, a total of four formulations were prepared with paracetamol to filler ratios of 1:1 and 0.8:1. Tablets were produced by single punch (11.28 mm) CS at six different pressures (152, 210, 263, 316, 400, and 452 MPa). During compression, upper punch displacement and force data were produced by the CS equipment. The compressed tablets were tested for hardness, thickness, and weight variation and compared with each other.

Results: All formulations reached maximum tensile strength at compaction pressures between 263 and 316 MPa. In the formulations without binder, those containing Granulac®70 had higher tensile strength than those containing Flowlac®100 at both filler ratios. The results obtained indicated that the addition of binder to the formulations (F-45-1, F-45-2, F-50-3, and F-50-4) improved the compressibility of paracetamol. Formulation F-45-2, containing Flowlac®100 and binder, showed better compressibility at 2.9 MPa tensile strength. Data from the CS were used to compare Young's modulus and work of compaction on selected formulations (F-45-1 and F-45-2).

Conclusion: The proposed lactose-based filler, Flowlac®100, with low pressure can be successfully applied for improving the compressibility of paracetamol. An optimum formulation can be designed with smaller amounts of materials using a compaction simulator.

Key words: Compaction simulator, tableting, compactibility, paracetamol, alpha-lactose

ÖZ

Amaç: Bu çalışmada basım sırasında verileri kaydeden "Compaction Simulator (CS)" cihazı kullanılarak sıkışabilirlik özellikleri zayıf olan toz parasetamolün basılabilirlik davranışları incelendi. Çalışmanın amacı, kuru granülasyon (slugging) yöntemi ile hazırlanan farklı formülasyonlardaki parasetamol tabletlerin basılabilirlik özelliklerinin incelenmesidir.

Gereç ve Yöntemler: Laktoz bazlı iki değişik dolgu maddesi olarak Flowlac®100 ve Granulac®70 ile bağlayıcı olarak Kollidon®K90 kullanılarak hazırlanan farklı formülasyonların basılabilirliği üzerine bu maddelerin etkisi gözlendi. Her kombinasyon için parasetamol: yardımcı madde oranı 1:1 ve 0.8:1 olan toplam 4 formülasyon hazırlandı. Tabletler tek zımbalı (11,28 mm) CS'de altı farklı basınçta (152, 210, 263, 316, 400, 452 MPa) üretildi. Sıkıştırma sırasında üst zımba ötelemesi ve zımba kuvvet verileri CS cihazı çıktılarıdır. Basılan tabletleride sertlik, kalınlık ve ağırlık sapması testleri yapıldı ve sonuçlar birbirleri ile mukayese edildi.

Bulgular: Bütün formülasyonlar en büyük gerilme direncine 263-316 MPa sıkıştırma aralığındaki basınçta ulaştılar. Bağlayıcı olmayan ve aynı oranda dolgu maddesi içeren formülasyonlarda Granulac®70 içerenler, Flowlac®100 içerenlere göre daha yüksek gerilme direnci göstermiştir. Sonuçlara göre, formülasyonlara bağlayıcı ilavesi (F-45-1, F-45-2, F-50-3 ve F-50-4), parasetamolün basılabilirliğini iyileştirmiştir. Flowlac®100 ve bağlayıcı içeren F-45-2 formülasyonu 2,9 MPa basınçta daha iyi bir basılabilirlik göstermiştir. CS verileri belli formülasyonlarda (F-45-1 ve F-45-2) Young modülleri ve basım çalışmaları sonuçlarını karşılaştırmada kullanılmıştır.

Sonuç: Parasetamolün düşük basınçta basılabilirliği laktoz bazlı dolgu maddesi olan Flowlac®100 ile başarıyla sağlanabilmiştir.

Anahtar kelimeler: Compaction simulator, tablet hazırlama, sıkışabilirlik, parasetamol, alfa-laktoz

*Correspondence: **E-mail:** yildiz.ozalp@neu.edu.tr, **Phone:** 0532 463 00 08 **ORCID-ID:** orcid.org/0000-0001-7928-1666
Received: 14.02.2019, **Accepted:** 21.03.2019

INTRODUCTION

During the manufacture of pharmaceutical tablets, there are certain problems that may arise, such as poor flowability, mixing, compactibility, and compressibility, and inconsistent die filling. The need to avert such problems in manufacturing may include the use of different tableting methods such as granulation.[1,2]

Slugging, an old conventional method, is chosen for research purposes in respect to the roller compactor, which is a more modern and efficient method used for dry granulation (DG).

The effect of DG often results in decreased tensile strength in tablets in comparison to other processes. This outcome is due to the loss of binding potential, which occurs after the first compression.[3,4,5]

The ability to transform powder into tablets involves certain factors and these factors, such as compactibility (tensile strength vs pressure) and other tableting measures, give a perspective on powder tableting characteristics.[1,6]

In the tableting process, three important stages are paramount for understanding the characteristics of powders. The stages are die filling (powder blends are loaded into the die under gravity, which applies to powder flowability), compaction (where compression is applied between two punches), and ejection (when the tablet is ejected from the die). These three stages determine the powder behavior and tableting parameters.[7]

The compaction behavior can be assessed using stress strain graphs to obtain Young's modulus, which gives insight into the plastic, elastic, or brittle nature of powders. Data obtained from measurements of macroscopic dimensional variations during the compaction cycle give information about the compressibility and compactibility of powder material.[8]

In formulating a poorly compressible active ingredient, the choice of excipient is important for the outcome. Therefore, finding the best tableting parameters is essential for further production and can also be used as an outline in fixing production problems.

To understand and characterize the compaction behavior and tableting parameters, instrumented single stations and multistations have been widely used. As observed, powders with good performance in a laboratory tablet press sometimes perform differently, with problems during scale up. However, with a compaction simulator these problems can be predicted with data used to analyze the compaction behavior of pharmaceutical materials. A compaction simulator provided advantages, limitations, and modifications by using methods such as F-D curve, tensile strength, and hardness measurement to improve the design and development of solid dosage forms.[9,10]

The use of a compaction simulator as a mimicking machine that emulates scale-up production gives real time data on every tablet pressed. These data can be analyzed and powder behavior and characteristics can be observed.[11]

In the present study, data obtained from a compaction simulator were used from an industrial perspective to determine and evaluate the tableting parameters to obtain improved compactibility of poorly compressible paracetamol.

MATERIALS AND METHODS

Materials

Paracetamol was used as the model drug in the present study, USP grade (Kimetsan). Two types of lactose-based fillers from Meggle, milled alpha-lactose monohydrate (Granulac® 70) and spray dried lactose (Flowlac®100), were used in the formulation at different concentrations to understand the effect of fillers on tableting parameters using the slugging process. Stearic acid (Kimetsan) was used as lubricant; it was kept at a constant concentration of 2% in every formulation.

The reason for addition of a binder from BASF (Kollidon® K90) to specific formulations was to further understand certain variables that may influence tablet behavior during compaction.

Methods

Slugging

Tablets (slugs) were made containing API, filler, and lubricant mixture, with ratios 1:1 and 0.8:1 (paracetamol to filler loading). The slugs were made with a mixture of paracetamol powder and filler (both Flowlac® 100 and Granulac® 70, at different ratios) with the addition of 1% of the lubricants to the mixture (Tables 1a and 1b).

The slugs were produced using an 18 mm single punch (Korsch XP1), milled using an Erweka oscillating mill granulator, and passed through a sieve with sieve size of 0.68 mm.

Mixing

The granules obtained from the DG slugging process were mixed with the binder and the remaining 1% lubricant (w/w) (according to each concentration variation in different formulation composition and ratio).

Tableting

Formulations were compressed at different compaction pressures: 152, 210, 263, 316, 400, and 452 MPa. Tablets were produced with a flat-faced Euro B punch of 11.28 mm diameter using a compaction simulator (Stylcam 200R). Tablets of eight different formulation mixtures were pressed to understand and characterize formulations of each compaction force.

For die filling, each powder was weighed individually using a Mettler Toledo AB 104-S/PH analytic balance and hand-filled in the die for compaction. From the tablets pressed, tablets from each formulation and batch were selected randomly and immediately characterized for weight variation and thickness.

Tensile strength

Tensile strength was calculated from crushing force (TBH 225; Erweka) and thickness.

Tensile strength was calculated using the following equation:

$$TS = \frac{2F}{\pi Dt}$$

where F is the crushing force in N; D the diameter and t the thickness of the tablet, both in mm.

Table 1a. Formulation composition with paracetamol to filler ratio 0.8:1

Formulation	Paracetamol	Flowlac® 100	Granulac® 70	Kollidon® K90	Stearic acid
F-45-1	45%	-	51%	2%	2%
F-45-2	45%	51%	-	2%	2%
F-45-3	45%	-	53%	-	2%
F-45-4	45%	53%	-	-	2%

Table 1b. Formulation composition with paracetamol to filler ratio 1:1

Formulation	Paracetamol	Flowlac® 100	Granulac® 70	Kollidon® K90	Stearic acid
F-50-1	50%	-	48%	-	2%
F-50-2	50%	48%	-	-	2%
F-50-3	50%	-	46%	2%	2%
F-50-4	50%	46%	-	2%	2%

Stress-strain graph

A graph was obtained using both upper and lower punch displacement data derived from the compaction simulator. Young's modulus was obtained from slope of the line of the stress-strain graph.

F-D curve

Compression force vs punch displacement profiles (F-D curve) can be obtained in order to assess the compaction behavior of materials and to calculate the work involved during tablet compaction.

Statistical analysis

Analysis of variance was applied for prediction using a one-way ANOVA model. The software package IBM SPSS Statistics v26 was used for calculation. The level of significance was defined as $p<0.05$.

RESULTS

Figure 1 shows the tensile strength for the set of formulations with different filler types at different ratios (1:1 and 0.8:1).[11,12,13] The formulations containing Granulac® 70 (F-45-3 and F-50-1) gave higher tensile strength in comparison to those containing Flowlac® 100. The effect of the filler ratio is seen in Figure 1, with formulations F-45-3 and F-45-4 showing better compressibility than formulations F-50-1 and F-50-2, respectively. Granulac® 70-containing formulations improved the compressibility of paracetamol more than Flowlac® 100-containing formulations at both ratios. Analysis of variance indicated that both filler ratio and filler type exert statistical significance ($p<0.05$).

Figure 2 shows the effect of binder on the tensile strength of the formulations. There was an increase in the tensile strength of all different formulation compositions. Formulation F-45-2 containing Flowlac® 100 had a higher tensile strength at lower compaction pressure than F-45-1 containing Granulac® 70 at a similar filler ratio (0.8:1). Flowlac® 100 had more improved tensile strength with addition of binder in comparison to Figure 1. The significant difference ($p<0.05$) with a confidence level of 95% indicates clear variation with the addition of binder.

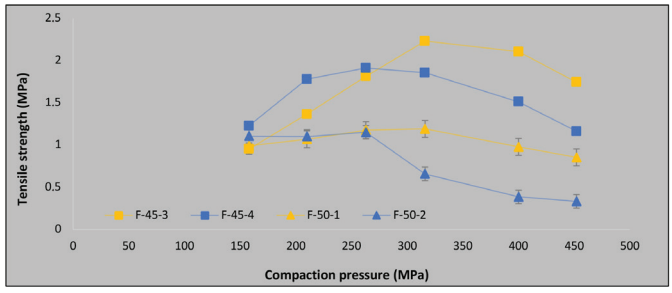

Figure 1. Effect of Flowlac® 100 and Granulac® 70 in different ratios on tensile strength (n=3)

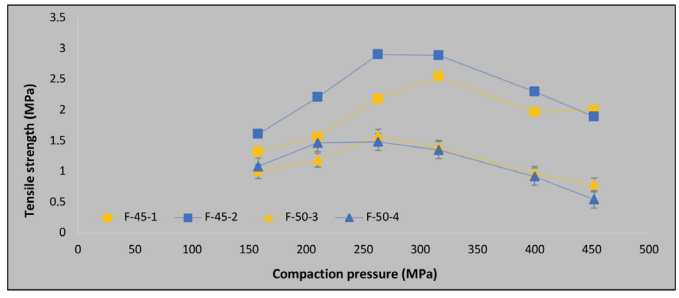

Figure 2. Effect of Flowlac® 100 and Granulac® 70 composition with binder (Kollidon® K90) on tensile strength (n=3)

In Figure 3, both tablets' results are derived from similar compaction conditions, having been selected from tensile strength resulting data to be the optimum tablets from different filler type formulation compositions. Figure 3 shows the variation in stress-strain for F-45-1 and F-45-2. There was a linear increase in F-45-2, but a different result was observed in F-45-1, which takes more loading capacity to see a significant change in the strain of F-45-1. The Young's modulus results were given at 60 for F-45-1 and 98 for F-45-2. As calculated from Figure 3, Young's modulus for F-45-1 is lower than that for F-45-2, indicating that F-45-1 has greater elastic recovery.

Figure 4 shows the total of work compaction for the selected formulations. The area under the curve shows the energy required during the compaction process. F-45-2 is seen to require more energy in comparison to F-45-1.

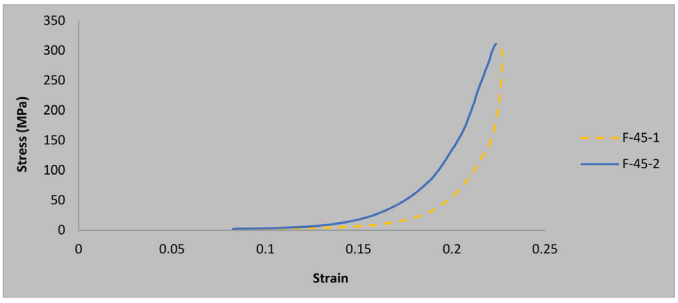

Figure 3. Stress vs strain for selected formulations (F-45-1 and F-45-2)

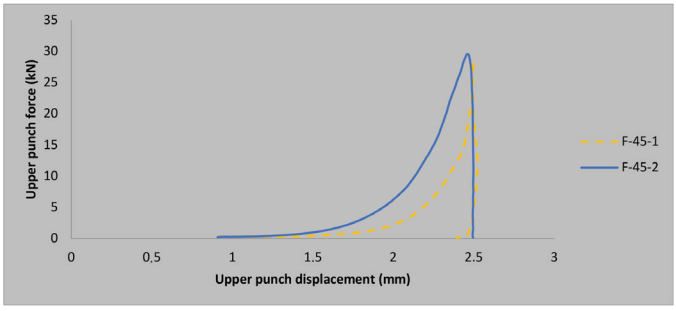

Figure 4. Determination of energy for selected formulations (F-45-1 and F-45-2)

DISCUSSION

As seen in the results in Figure 1, Granulac® 70 displayed better loading capacity than Flowlac® 100. In both filler ratios, Granulac® 70-containing formulations performed better under higher compaction pressure. However, Flowlac® 100 had better tensile strength at lower pressures. The particle structure and size difference of filler affects the bonding and may show different results under identical compaction conditions.[14,15,16] All formulations had a significant decline in tensile strength as compaction pressures increased above 316 MPa.

Figure 2 shows the change in formulation composition with the addition of binder. From the tensile strength results, both filler types at ratios 1:1 and 0.8:1 improved in compressibility when compared with the results in Figure 1. It is seen that binder effect has a more significant impact in Flowlac® 100 than in Granulac® 70. Formulation F-50-3 containing Granulac® 70 maintained a slightly better higher tensile strength than formulation F-50-4 containing Flowlac® 100. This indicates the need for higher filler loading ratio for Flowlac® 100 to exhibit proper bonding, increasing the tensile strength. Granulac® 70, however, has more compactibility at different loading ratios. It was observed that with the addition of binder and tensile strength increase, the tableting behavior of all formulations at different filler ratios and formulation compositions had a distinctive pattern in respect to compaction pressure. These results suggest that lactose-based fillers may have unpredictable compression behavior, giving more deviations when lubricated.[16,17]

As seen in the stress-strain curve, the variation in deformation of both formulations with similar tableting parameters may have many reasons. A factor that may give rise to these variations is density distribution in the tablets as a result of stress transmission, which is dependent on internal friction, contact powder, and lubrication.[18,19,20] The relationship between Young's modulus and tablet strength is that the higher the elastic recovery, the lower the tablet strength.[21,22] This can be further supported by the results that F-45-1 has lower tensile strength than F-45-2 because of its greater elastic recovery, shown by higher Young's modulus. Flowlac® 100-containing formulations showed lower elastic recovery because of its spray-dried property, which results in harder tablets.[23]

Results from the F-D curve show that the work of compaction gives a detailed assessment of the characteristics of tableting parameters due to differences in packing characteristics of individual formulation powders.[10,24] Powders with different plastic and elastic deformational properties and different packing characteristics will absorb varying amounts of energy,[25] as seen by differences in compaction energy between formulations F-45-1 and F-45-2.

CONCLUSION

With a compaction simulator it is possible to obtain:

- the mechanical properties of powders,
- optimum tabletability profile for designed formulations,
- compaction data such as stress strain and F-D curves, which can help in optimizing a formulation.

Granulac® 70 is seen to have better loading capacity than Flowlac® 100. However, it needs more pressure during the compaction process. The addition of binder has more effect on Flowlac® 100 in improving the compressibility of paracetamol at lower compaction pressure.

The most robust formulation, F-45-2, is selected from the set of formulations due to its superior compaction characteristics. Based on the information obtained from the compaction simulator, large-scale manufacturing can be reproduced.

Conflicts of interest: No conflict of interest was declared by the authors. The authors alone are responsible for the content and writing of the paper.

REFERENCES

1. Sun CC, Kleinebudde P. Mini review: Mechanisms to the loss of tabletability by dry granulation. Eur J Pharm Biopharm. 2016;106:9-14.
2. Mosig J, Kleinebudde P. Critical evaluation of root causes of the reduced compactability after roll compaction/dry granulation. J Pharm Sci. 2015;104:1108-1118.
3. Herting MG, Kleinebudde P. Roll compaction/dry granulation: effect of raw material particle size on granule and tablet properties. Int J Pharm. 2007;338:110-118.
4. Kochhar SK, Rubinstein MH, Barnes D. The effects of slugging and recompression on pharmaceutical excipients. Int J Pharm. 1995;115:35-43.
5. Herting MG, Kleinebudde P. Studies on the reduction of tensile strength of tablets after roll compaction/dry granulation. Eur J Pharm Biopharm. 2008;70:372-379.
6. Bozic DZ, Dreu R, Vrecer F. Influence of dry granulation on compactibility and capping tendency of macrolide antibiotic formulation. Int J Pharm. 2008;357:44-54.

7. Wu CY, Ruddy OM, Bentham AC, Hancock BC, Best SM, Elliott JA. Modelling the mechanical behaviour of pharmaceutical powders during compaction. Powder Technology. 2005;152:107-117.
8. Freitag F, Kleinebudde P. How do roll compaction/dry granulation affect the tableting behaviour of inorganic materials? Comparison of four magnesium carbonates. Eur J Pharm Sci. 2003;19:281-289.
9. Sun CC. Dependence of ejection force on tableting speed-A compaction simulation study. Powder Technology. 2015;279:123-126.
10. Çelik M. Overview of compaction data analysis techniques. Drug Dev Ind Pharm. 1992;18:767-810.
11. Çelik M, Marshall K. Use of a compaction simulator system in tabletting research. Drug Dev Ind Pharm. 1989;15:759-800.
12. Kawashima Y, Takeuchi H, Hino T, Niwa T, Lin TL, Sekigawa F, Kawahara K. Preparation of a sustained-release matrix tablet of acetaminophen with pulverized low-substituted hydroxypropylcellulose via dry granulation. Chemical Pharm Bull (Tokyo). 1993;41:1827-1831.
13. Khan KA, Musikabhumma P. Effect of slugging pressure on the properties of granules and tablets prepared from potassium phenethicillin. J Pharm Pharmacol. 1981;33:627-631.
14. Jain S. Mechanical properties of powders for compaction and tableting: an overview. Pharm Sci Technolo Today. 1999;2:20-31.
15. Sun CC, Himmelspach MW. Reduced tabletability of roller compacted granules as a result of granule size enlargement. J Pharm Sci. 2006;95:200-206.
16. Haware RV, Tho I, Bauer-Brandl A. Multivariate analysis of relationships between material properties, process parameters and tablet tensile strength for α-lactose monohydrates. Eur J Pharm Biopharm. 2009;73:424-431.
17. Boschini F, Delaval V, Traina K, Vandewalle N, Lumay G. Linking flowability and granulometry of lactose powders. Int J Pharm. 2015;494:312-320.
18. Kadiri MS, Michrafy A. The effect of punch's shape on die compaction of pharmaceutical powders. Powder Technology. 2013;239:467-477.
19. Michrafy A, Ringenbacher D, Tchoreloff P. Modelling the compaction behaviour of powders: application to pharmaceutical powders. Powder Technology. 2002;127:257-266.
20. Michrafy A, Dodds JA, Kadiri MS. Wall friction in the compaction of pharmaceutical powders: measurement and effect on the density distribution. Powder Technology. 2004;148:53-55.
21. Han LH, Elliott JA, Bentham AC, Mills A, Amidon GE, Hancock BC. A modified Drucker-Prager Cap model for die compaction simulation of pharmaceutical powders. Int J Solids Struct. 2008;45:3088-3106.
22. Malamataris S, Hatjichristos T, Rees JE. Apparent compressive elastic modulus and strength isotropy of compacts formed from binary powder mixes. Int J Pharm. 1996;141:101-108.
23. Vromans H, Bolhuis GK, Lerk CF, Van de Biggelaar H, Bosch H. Studies on tableting properties of lactose. VII. The effect of variations in primary particle size and percentage of amorphous lactose in spray dried lactose products. Int J Pharm. 1987;35:29-37.
24. Krycer I, Pope DG, Hersey JA. An evaluation of the techniques employed to investigate powder compaction behaviour. Int J Pharm. 1982;12:113-134.
25. Fell JT, Newton JM. Assessment of compression characteristics of powders. J Pharm Sci. 1971;60:1428-1429.

Turk J Pharm Sci 2020;17(3):254-258
DOI: 10.4274/tjps.galenos.2019.46873

ORIGINAL ARTICLE

Method Validation of Contact and Immersion TLC-bioautography for Determination of Streptomycin Sulfate in Shrimp

Karideste Streptomisin Sülfat Tayini için Kontak ve İmmersiyon İTK-biyootografi Yönteminin Validasyonu

Febri ANNURYANTI, Isnaeni ISNAENI*, Asri DARMAWATI, Iftitahatur ROSYIDAH, Aprelita Nurelli DWIANA

Airlangga University, Department of Pharmaceutical Chemistry, Surabaya, Indonesia

ABSTRACT

Objectives: Contact and immersion thin layer chromatography (TLC)-bioautography were developed for identification and quantification of streptomycin sulfate in shrimp.

Materials and Methods: TLC of streptomycin sulfate standard solution was carried out using silica gel F_{254} and 7.5% of KH_2PO_4 solution as stationary and mobile phase, respectively.

Results: The retardation factor of the streptomycin sulfate standard was 0.51 and the selectivity of streptomycin sulfate was 4.1 with the presence of kanamycin sulfate in the shrimp. The bioautography was performed with *Escherichia coli* ATCC 8739 as a test bacterium. The limit of detection of streptomycin sulfate obtained by contact and immersion TLC-bioautography was 0.24 µg and 0.16 µg, respectively. Both methods showed good linearity with an r value greater than 0.999 and a Vxo value less than 2%. The accuracy of the contact and immersion TLC-bioautography was tested by standard addition method and the obtained percentage recovery was 86.93±1.60% and 96.42±0.65%, respectively. The coefficient of variation of the contact and immersion TLC-bioautography was 2.39±1.79% and 0.53±0.17%, respectively.

Conclusion: The immersion TLC-bioautography was more sensitive with better recovery than the contact TLC-bioautography. In addition, immersion TLC-bioautography was successfully employed for determination of streptomycin sulfate in shrimp.

Key words: Streptomycin sulfate, contact TLC-bioautography, immersion TLC- bioautography, shrimp

ÖZ

Amaç: Kontak ve immersiyon ince tabaka kromatografisi (İTK)-biyootografi, karideslerde streptomisin sülfatın tanımlanması ve miktarının belirlenmesi için geliştirilmiştir.

Gereç ve Yöntemler: İTK, streptomisin sülfat standart çözeltisi, sabit ve hareketli faz olarak sırasıyla silika jel F_{254} ve %7,5 KH_2PO_4 çözeltisi kullanılarak gerçekleştirilmiştir.

Bulgular: Streptomisin sülfat standardının alıkonma zamanı 0,51 olarak bulunmuştur ve karideste kanamisin sülfat varlığında streptomisin sülfatın seçiciliği 4,1 olarak tespit edilmiştir. Biyootografi, bir test bakterisi olan *Escherichia coli* ATCC 8739 kullanılarak yapılmıştır. Kontak ve immersiyon İTK-biyootografi ile elde edilen streptomisin sülfat tayini için sınır değerler, sırasıyla 0,24 µg ve 0,16 µg olarak bulunmuştur. Her iki yöntem de r değeri 0,999'dan büyük ve Vxo değeri %2'den düşük olan iyi doğrusallık göstermiştir. Kontak ve immersiyon İTK-biyootografinin doğruluğu standart ekleme yöntemi ile test edildi ve elde edilen yüzde geri kazanım sırasıyla %86,93±1,60 ve %96,42±0,65 olarak bulunmuştur. Kontak ve immersiyon İTK-biyootografinin varyasyon katsayısı sırasıyla %2,39±1,79 ve %0,53±0,17'dir.

Sonuç: İmmersiyon İTK-biyootografi, geri kazanımının daha iyi olması nedeniyle kontak İTK -biyootografiden daha hassas olduğu sonucuna varılmıştır. Ek olarak, immersiyon İTK-biyootografi, karideslerde streptomisin sülfatın belirlenmesi için başarıyla kullanılmıştır.

Anahtar kelimeler: Streptomisin sülfat, kontak İTK-biyootografi, immersiyon İTK-biyootografi, karides

*Correspondence: **E-mail:** isna.yudi@gmail.com, **Phone:** +6281331021303 **ORCID-ID:** orcid.org/0000-0003-4502-2433
Received: 30.01.2019, **Accepted:** 21.03.2019

INTRODUCTION

Shrimp is one of Indonesia's export commodities with a significant impact on its economy. High export demand sometimes results in uncontrolled cultivation because farmers generally use antibiotics to prevent fish diseases.[1,2] As regulated by the Minister of Maritime Affairs and Fisheries in the PER regulation number 02/MEN/2007,[3] fishery products must be free from drug residues, chemicals, biological materials, and other contaminants. One of the antibiotics used by farmers for disease prevention is streptomycin. Streptomycin is an aminoglycoside used for treatment of infections caused by aerobic gram-negative bacteria and is also effective against gram-positive bacteria such as *Staphylococcus aureus*.[4] In Indonesia, streptomycin is usually used for treating bacterial diseases in shrimp and ornamental fish.[5] According to the Codex Alimentarius, the maximum residue limit for streptomycin is 600 µg/kg.[6] Antibiotic residues in food can be a risk to human health because they can contribute to antibiotic resistance through the food chain.[7] Therefore, a fast and perfect analysis method is needed to detect antibiotic residues, especially streptomycin sulfate in shrimp.

Thin layer chromatography (TLC)-bioautography is used for determination of the level of antibiotics in complex samples based on microbiological activities. In TLC-bioautography, determination of antimicrobial levels is initiated by applying antimicrobial analytes to the TLC plate followed by elution with a suitable mobile phase. Contact TLC-bioautography was performed by putting the TLC chromatogram plate on the surface of the agar medium inoculated with the test bacterium and it was left in contact with the agar medium for a certain time for the diffusion process.[8] Subsequently, the chromatogram plate was removed and incubated for 16-24 h for the growth range, but this can be reduced to 5-6 h by spraying 2,6-dichlorophenol-indofenol or 2,3,5-tetrazoliumchloride on the surface of the test medium. The antimicrobial activity was determined from the inhibitory zone around the reservoir hole on the surface agar medium or the spot position on the TLC-bioautogram plate, corresponding to the spots on the TLC chromatogram plate.[9]

Immersion bioautography is a combination of direct and contact bioautography. The chromatograms are sprayed until the plate is covered by test medium containing the test bacterium at a temperature of 45 °C. The plate is then cooled to condense and allow the diffusion process. Furthermore, the plate is incubated at a certain temperature for a certain time, and then sprayed with tetrazolium salt to visualize the inhibitory zone.

Antibiotic analysis in the shrimp matrix of kanamycin,[10] oxytetracycline,[11] and streptomycin sulfate[12] with the TLC-bioautography contact method has been reported. However, comparison of contact and immersion TLC-bioautography methods in determining the levels of streptomycin in frozen shrimp has never been reported, and so it is necessary to conduct research to select a more effective method and provide results that meet the validation parameters.

MATERIALS AND METHODS

Chemicals

Streptomycin sulfate and kanamycin sulfate obtained from PT Meiji, shrimp obtained from a local market, *Escherichia coli* ATCC 8739, KH_2PO_4, nutrient broth and nutrient agar (Oxoid), sodium chloride p.a., methanol p.a., TLC silica gel plate GF_{254} (Merck), methyl thiazole tetrazolium (Sigma Aldrich), distilled water (Otsuka), a microliter syringe (Hamilton), a chromatographic vessel (10x10x6 cm^3), an incubator (Memmert), calipers (Tricle brand), an autoclave (Huxley HV-340 Speedy), a spectrophotometer (Genesis 20), and a shaker incubator (Thermo Fisher Scientific) were used in this study. Ethic committee approval and patient informed consent were not required.

Preparation of growth medium

Eighteen grams of agar, 8 g of nutrient broth powder, and 1000 mL of distilled water were mixed and heated until dissolved and homogeneous. The liquid medium was poured into a test tube (10, 15, and 20 mL) and then covered with cotton. The medium was sterilized by autoclaving at 121 °C for 15 min.[13]

Preparation of bacterial test

Escherichia coli ATCC 8739 was inoculated on agar slant medium and incubated at 35-37 °C for 24-48 h. The bacterial suspension was prepared by adding 10 mL of sterile saline (NaCl 0.9%) solution to a 24 h culture and shaking by vortex until the entire colony was removed from the surface of the agar medium. A 25% transmittance of bacteria was measured by spectrophotometer at a wavelength of 580 nm.

Loss on drying of shrimp samples

Loss on drying was determined according to Indonesian Pharmacope 5th edition.[14] Sample containers were heated at 105 °C for 30 min. The container was weighed until it reached constant weight. One gram of each sample was weighed carefully and put into the constant container. The samples were then put in an oven with an open lid. Samples and the lid were heated at 105 °C until constant weight was obtained. Loss on drying was calculated using the equation below:

Loss on drying=(initial sample weight-final sample weight)/ initial sample weight x100%

Validation method of contact and immersion TLC-bioautography

The methods of analysis were validated for the parameters of selectivity, limit of detection, linearity, accuracy, and precision. The accuracy was determined using the standard addition method.

Analysis using contact TLC-bioautography

First, 8 µL of test solution was applied to the silica gel TLC plate F_{254} and then it was eluted with 7.5% KH_2PO_4 solution as the mobile phase. Subsequently, the TLC plate was dried and attached to the surface of agar inoculated with *Escherichia coli* in a sterile petri dish. The TLC plate was then stored in the fridge for 1 h to allow the diffusion and stain process of the compound to the medium. Marks were made on the side of the

plate followed by incubation of the TLC plate at 37 ˚C for 24 h. Finally, the inhibitory zone was observed and its diameter was measured.

Analysis using immersion TLC-bioautography

First, 8 µL of test solution was applied to the silica gel TLC plate F_{254} and then it was eluted with 7.5% KH_2PO_4 solution as the mobile phase, followed by drying of the TLC plate and it was coated with 15 mL of inoculated *Escherichia coli* medium until a thin layer was formed. The TLC plate was stored in a sterile petri dish and then incubated at 37 ˚C for 16-18 h. The plates were sprayed with methyl thiazoletetrazolium (2.5 mg/mL) and finally a white-yellow inhibitory zone was observed.[15]

Statistical analysis

The analytical characteristics of the TLC-bioautography were validated to ensure conformity to the analytical requirements and the reliability of the results.

All the data analysis was carried out in triplicate and standard deviation and coefficient variation values were calculated.

RESULTS AND DISCUSSION

The mobile phase, 7.5% KH_2PO_4 solution, used to eluate streptomycin sulfate was based on previous research.[13] The (retardation factor) Rf results of the contact TLC-bioautography of streptomycin are presented in Table 1. The Rf values met the requirement range of 0.2-0.8. The loss on drying of the shrimp was 9.44±1.85% (Table 2).

The selectivity was tested by spotting of streptomycin sulfate, kanamycin sulfate standard solution, and shrimp on the F_{254} silica gel TLC plate. The elution was carried out by 7.5% KH_2PO_4 solution. The selectivity test results of the contact TLC-bioautography method are depicted in Figure 1 and Table 3. The data showed the Rf and resolution (Rs) values of streptomycin and kanamycin sulfate analyzed simultaneously using the contact TLC-bioautography method. The Rs value was 4.1 (Rs≥1.5), which means that both analytes can separate well.

The detection limit was determined by the antibiotic concentration in which activity was still seen. The minimum inhibitory concentration (MIC) of streptomycin sulfate analyzed using contact TLC-bioautography was 30.4 mg/L with 8 µL of sample solution (equivalent to 0.24 µg of streptomycin), whereas the MIC of the streptomycin analyzed by immersion TLC-bioautography was 20.3 mg/L (equivalent to 0.16 µg of streptomycin) (Table 4).

The linearity test of streptomycin in contact and immersion TLC-bioautography was carried out in the concentration range 100-250 mg/L. The linearity of the streptomycin analyzed using contact and immersion TLC-bioautography was y=14.7212x-23.2398 (r value=0.9992) and y=12.6655x-18.5557 (r value=0.9994), respectively (Figures 2 and 3).

Accuracy and precision were tested by spotting three different concentrations of streptomycin sulfate. The accuracy and

Table 1. Retardation factor of streptomycin sulfate standard analyzed by contact TLC-bioautography

Mobile phase	Concentration of streptomycin sulfate (mg/L)	Rf
7.5% KH_2PO_4 solution	50.75	0.53
	101.50	0.51
	152.25	0.50
	203.00	0.50
	253.75	0.53
Mean of Rf		0.51

Rf: Retardation factor, TLC: Thin layer chromatography

Table 2. Loss on drying of shrimp

Sample name	Replicate	Initial weight (g)	Final weight (g)	LOD (%)	Mean of LOD (%)
Shrimp	1	1.0134	0.9187	9.34	9.44±1.85
	2	1.0187	0.9204	9.65	
	3	1.0172	0.9240	9.32	

LOD: Loss on drying

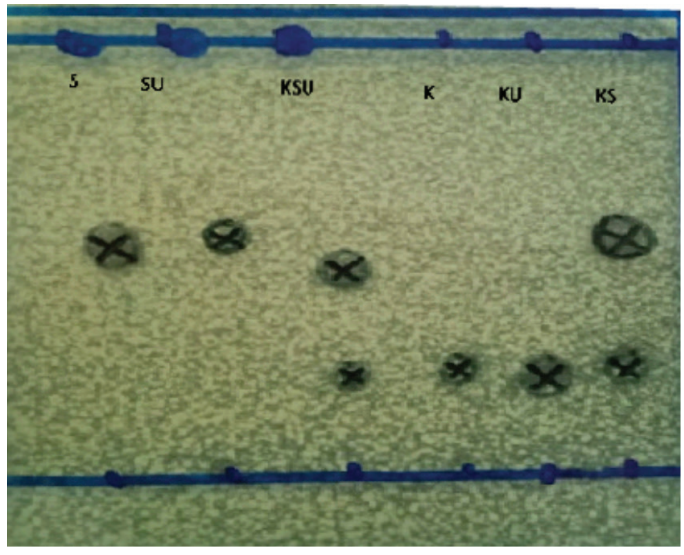

Figure 1. The retardation factor (Rf) of streptomycin sulfate (S) and kanamycin sulfate (K) in shrimp (U) for the determination of resolution (Rs) value

Table 3. Resolution value of streptomycin (s), kanamycin (k), and shrimp (u)

Compound name	Rf (S)	Rf (K)	Rs
Streptomycin sulfate	0.51	-	-
Streptomycin + shrimp	0.52	-	-
Kanamycin + streptomycin + shrimp (K+S+U)	**0.50**	**0.21**	**4.1**
Kanamycin	-	0.24	-
Kanamycin + shrimp	-	0.22	-
Kanamycin + streptomycin	0.52	0.24	3.9

Rs: Resolution, Rf: Retardation factor, S: Streptomycin sulfate, K: Kanamycin

Table 4. Detection limit of streptomycin analyzed using contact and immersion TLC-bioautography method

Method of TLC-bioautography	Concentration (mg/L)	Inhibitory zone	Diameter of inhibitory zone (mm)
Contact	20.3	-	-
	30.4[a]	**+**	**4.90**
	40.6	+	6.10
	50.8	+	6.70
	60.9	+	8.10
Immersion	5.1	-	-
	10.2	-	-
	15.2	-	-
	20.3[b]	**+**	**3.50**
	30.4	+	4.60

[a]: Detection limit of streptomycin sulfate in contact TLC-bioautography, [b]: detection limit of streptomycin sulfate in immersion TLC-bioautography, TLC: Thin layer chromatography

precision results of streptomycin sulfate analyzed by the two methods of TLC-bioautography are shown in Tables 5 and 6, respectively.

The contact and immersion TLC-bioautography methods developed for the determination of streptomycin sulfate and kanamycin sulfate were precise and reliable by only using a single, cheap, and hazardless solvent. Based on the TLC-bioautogram, the regression linear equation is capable of reliably predicting analyte concentration in the range of 5-100 mg/mL and 0.1-100 mg/mL for streptomycin sulfate and kanamycin sulfate, respectively.

CONCLUSION

The method was validated successfully and can be used to simultaneously determine streptomycin sulfate and kanamycin sulfate in a common market frozen shrimp. Those simple methods are recommended for monitoring antibiotic abuse in frozen foods, especially for streptomycin at the concentration of 0.16 µg in the presence of kanamycin sulfate.

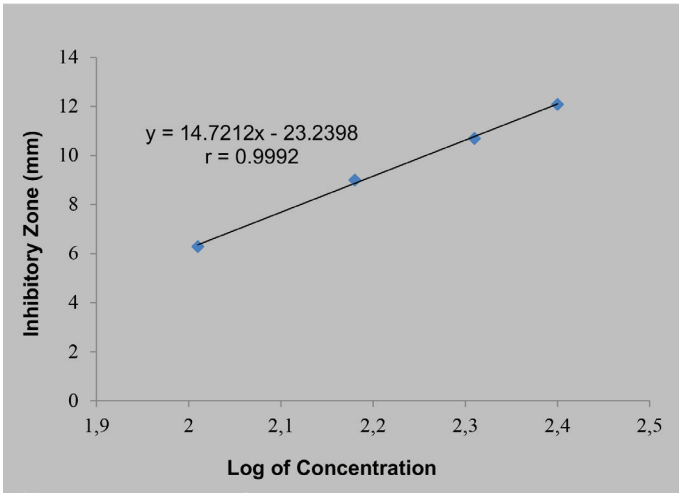

Figure 2. Linear regression of streptomycin sulfate analyzed using contact TLC-bioautography

TLC: Thin layer chromatography

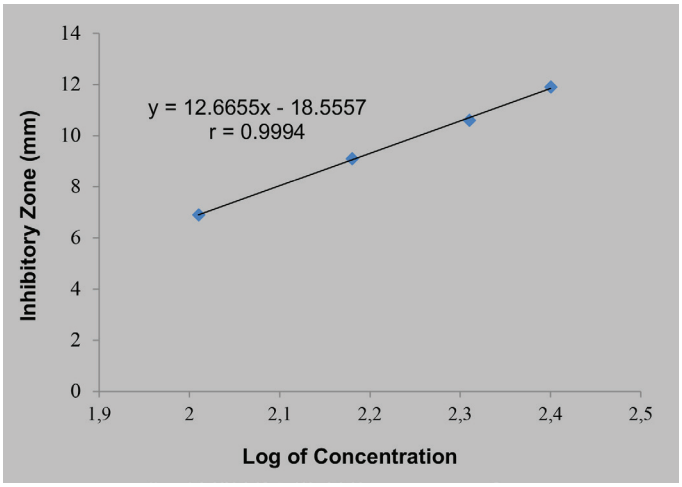

Figure 3. Linear regression of streptomycin sulfate analyzed using immersion TLC-bioautography

TLC: Thin layer chromatography

Table 5. Accuracy of streptomycin sulfate analyzed by contact and immersion TLC-bioautography

Method	Replicate	Added amount (µg)	Inhibitory zone (mm)	Obtained amount (µg)	% Recovery	Mean of % recovery (± SD)
Contact TLC-bioautography	I	1.2992	8.50	1.1459	88.20	86.93±1.60
	II	1.4616	9.20	1.2785	87.47	
	III	1.6240	9.70	1.3825	85.13	
Immersion TLC-Bioautography	I	1.2992	9.20	1.2432	95.69	96.42±0.65
	II	1.4616	9.90	1.4119	96.60	
	III	1.6240	10.50	1.5746	96.96	

SD: Standard deviation, TLC: Thin layer chromatography

Table 6. Precision of streptomycin sulfate analyzed by contact and immersion TLC-bioautography

Method	Conc (µg)	Inhibitory zone (mm)			% CV	Mean of % CV
		I	II	III		
Contact TLC-bioautography	121.8	5.70	6.10	6.20	4.41	2.39
	162.4	8.30	8.60	8.45	1.78	
	203.0	10.10	10.30	10.20	0.98	
Immersion TLC-bioautography	160.0	8.25	8.20	8.30	1.24	0.53
	180.0	8.60	8.65	8.65	1.41	
	200.0	9.10	9.00	9.10	1.57	

% CV: Percent coefficient of variation, TLC: Thin layer chromatography

ACKNOWLEDGEMENT

The current research was funded by Directorate General of the Ministry of Research and Technology.

Conflicts of interest: No conflict of interest was declared by the authors. The authors alone are responsible for the content and writing of this article.

REFERENCES

1. Serrano PH. Responsible use of antibiotics in aquaculture (1st ed). Rome; FAO;2005:469.
2. Irwandaru D, Ajie W. Peningkatan Daya Saing Produk Lokal Dalam Upaya Standardisasi Memasuki Pasar Global (Standardisasi Mutu dan Kualitas Udang Windu). UG Journal. 2013;6:9-15.
3. Minister of Marine and Fisheries of The Republic of Indonesia. Control of Fish Drug Residues, Chemicals, and Contaminants in Consumption of Fish Cultivation Activities. Regulation of The Minister of Marine and Fisheries of The Republic of Indonesia. 2015;1:1-19. Available from: https://www.google.com/url?sa=t&source=web&rct=j&url=http://jdih.kkp.go.id/peraturan/per-02-men-2007.pdf&ved=2ahUKEwiHz-Sa7uvpAhVwZhUIHfe3AN0QFjAAegQIARAC&usg=AOvVaw3U-T8wCcsjXKbKzv5sqinU
4. United States of Pharmacopeia. Aminoglycosides. Drugs for Animal Use. Veterinary-Systemic. United States of Pharmacopeia Convention. 2007:1-30. Available from: https://www.google.com/url?sa=t&source=web&rct=j&url=https://cdn.ymaws.com/www.aavpt.org/resource/resmgr/imported/aminoglycosides.pdf&ved=2ahUKEwjLtYXb7evpAhXdTRUIHTBmASEQFjAAegQIBBAB&usg=AOvVaw2vLeMHyRoysJa ZGjZDNmRa
5. Holmström K, Gräslund S, Wahlström A, Poungshompoo S, Bengtsson BE, Kautsky N. Antibiotic use in shrimp farming and implications for environmental impacts and human health. J Food Sci Technol. 2003;38:255-266.
6. World Health Organization. Dihydrostreptomycin/Sterptomyicin. In: Maximum Residue Limits (MRLs) and Risk Management Recommendations (RMRs) for Residues of Veterinary Drugs in Foods, 2nd ed. USA: FAO: 2018;2:18.
7. Okocha RC, Olatoye IO, Adedeji OB. Food safety impacts of antimicrobial use and their residues in aquaculture. Public Health Rev. 2018;39:21.
8. Choma IM, Grzelak EM. Bioautography detection in thin-layer chromatography. J Chromatogr A. 2011;1218:2684-2691.
9. Dewanjee S, Gangopadhyay M, Bhattacharya N, Khanra R, Dua TK. Bioautography and its scope in the field of natural product chemistry. J Pharm Anal. 2015;5:75-84.
10. Mufida FA. Perbandingan Metode KLT-Densitometri Dan Bioautografi Untuk Penetapan Kadar Kanamisin Dalam Matriks Udang. Final Report. 2010.
11. Anggraeni FY. Perbandingan Validasi Metode KLT-Densitometri dan KLT-Bioautografi untuk Penetapan Kadar Oksitetrasiklin dalam Udang. Final Report. 2010.
12. Jahanbakhshi A. Determination some engineering properties of snake melon (Cucumis melo var. flexuosus) fruit Agric Eng Int CIGR J. 2018;20:171-176.
13. Astuti A. Validasi Metode Bioautografi untuk Determinasi Streptomisin Sulfat. Final Report. 2006.
14. Anonim. Penetapan Susut Pengeringan In: Farmakope Indonesia V. Jakarta: Departemen Kese hatan RI. 2014:1043-1044. Avail able from: https://www.google.com/url?sa=t&source=web&rct=j&url=https://www.academia.edu/35210175/Farmakope_Indonesia_V.pdf&ved=2ahUKEwjQjvi38OvpAhWDUhUIHYmKBpEQFjADegQIARAB&usg=AOvVaw0qdSY3ugzGReN_CB2ImOeO
15. Kusumaningtyas E, Astuti E, Darmono D. Sensitivitas metode bioautografi kontak dan agar overlay dalam penentuan senyawa antikapang. J Ilmu Kefarmasian Indonesia. 2008;6:75-79.

Turk J Pharm Sci 2020;17(3):259-264
DOI: 10.4274/tjps.galenos.2019.75537

ORIGINAL ARTICLE

Microemulsion Based Gel of Sulconazole Nitrate for Topical Application

Topikal Uygulama İçin Mikroemülsiyon Esaslı Sulkonazol Nitrat Jeli

Sumedha Prashanth PAYYAL, Narayana Charyulu ROMPICHERLA*, Sandeep Divate SATHYANARAYANA, Ravi Gundadka SHRIRAM, Anoop Narayanan VADAKKEPUSHPAKATH

Nitte Gulabi Shetty Memorial Institute of Pharmaceutical Sciences, Nitte (Deemed to be University), Department of Pharmaceutics, Mangaluru, Karnataka, India

ABSTRACT

Objectives: Sulconazole is a broad spectrum antifungal agent of the imidazole class used against dermatophytes and other fungi to treat skin infections. The aim of the present work was to formulate and evaluate a microemulsion-based topical sulconazole gel.

Materials and Methods: Microemulsion formulation of sulconazole nitrate was prepared by using oil, surfactant, cosurfactant and water at different ratios. This was then subjected to clarity and particle size analysis, a centrifugation test, a dilution test, and freeze thawing.

Results: The zeta potential of formulation F1 was -41.3 and stable. The pH of the microemulsion formulation was within the range of pH of skin. F1 showed a higher percentage amount of drug as compared with the other formulations. The viscosity showed that F1 was optimum. The freezing and thawing results showed there was no phase separation and the formulation was stable. *In vitro* drug release showed that the drug release from the microemulsion of F1 was higher when compared to the other formulations. It revealed F1 had the highest drug content of 95.88±0.3% and % cumulative drug release was 88.75% release in 8 h. The *in vivo* skin irritation study on rats confirmed that formulation was nontoxic and nonirritant.

Conclusion: The present study confirmed the safety of the formulated sulconazole loaded microemulsion gel for topical application.

Key words: Microemulsion, sulconazole nitrate, *in vitro* release, fungal infection

ÖZ

Amaç: Sulkonazol, dermatofitler ve diğer mantarlara karşı deri enfeksiyonlarını tedavi etmek için kullanılan imidazol sınıfının geniş spektrumlu bir antifungal ajanıdır. Mevcut çalışmanın amacı, mikroemülsiyon esaslı topikal sulkonazol jeli formüle etmek ve değerlendirmektir.

Gereç ve Yöntemler: Sulkonazol nitratın mikroemülsiyon formülasyonu, farklı oranlarda yağ, yüzey aktif madde, yardımcı yüzey aktif madde ve su kullanılarak hazırlandı. Formülasyon daha sonra berraklık ve parçacık boyutu analizine, santrifüj testine, seyreltme testine ve donma çözünme testine tabi tutuldu.

Bulgular: Formülasyon F1'in zeta potansiyeli değerinin -41,3 ve kararlı olduğu tespit edildi. Mikroemülsiyon formülasyonunun pH değeri cildin pH aralığı dahilindeydi. F1 formülasyonunun, diğer formülasyonlara kıyasla daha yüksek oranda ilaç yüzdesine sahip olduğu bulundu. Viskozite sonuçları, F1'in optimum olduğunu gösterdi. Donma ve çözünme sonuçları, faz ayrılmasının olmadığını ve formülasyonun stabil olduğunu gösterdi. *İn vitro* ilaç salımı çalışmaları, F1 mikroemülsiyonundan ilaç salımının, diğer formülasyonlara kıyasla daha yüksek olduğunu gösterdi. Bu çalışma ayrıca, F1'in en yüksek ilaç içeriğine sahip olduğunu (% 95,88±%0,3) ve % kümülatif ilaç salımının 8 saat içinde %88,75 olduğunu ortaya koydu. Sıçanlar üzerinde yapılan *in vivo* deri irritasyon çalışması, formülasyonun toksik ve tahriş edici olmadığını doğruladı.

Sonuç: Bu çalışma, formüle edilen sulkonazol yüklü mikroemülsiyon jelin topikal uygulama için güvenirliğini doğrulamıştır.

Anahtar kelimeler: Mikroemülsiyon, sulkonazol nitrat, *in vitro* salım, mantar enfeksiyonu

*Correspondence: E-mail: narayana@nitte.edu.in, Phone: +919448164750 ORCID-ID: orcid.org/0000-0002-4404-0296
Received: 12.09.2018, Accepted: 17.01.2019

INTRODUCTION

Novel drug delivery systems are meant to attain and maintain sufficient therapeutic levels of drug at the target site. In order to overcome the problems connected with traditional modes of drug administration, topical drug delivery was started. For local dermatological disorders topical drug delivery is the effective way for drug administration. Drug delivery through the skin has attracted attention because it avoids the first pass effects, gastrointestinal irritation, and metabolic degradation associated with oral administration. The topical route of administration is also utilized to produce systemic drug effects in some instances. Major attention needs to be paid to new topical formulations to ensure adequate localization of drug within the skin to enhance the local effect or to increase the penetration. Drugs applied topically, mainly for local action, include antifungal, anti-inflammatory, and antiseptic agents as well as skin emollients for protective effects, while this route can also be used for systemic drug delivery.[1]

Microemulsions are thermodynamically stable multicomponent fluids consisting of oil, water, and surfactant. The droplets of microemulsions are in the range of 10-100 nm in diameter. Since the dispersed particles have diameters less than one-fourth of the wavelength of visible light, they do not refract light and that is the reason microemulsions are transparent to the eye.[2,3]

A microemulsion when applied to the skin is expected to penetrate the stratum corneum and to exist intact in the horny layer, resulting in alteration of both the lipid and the polar pathways. The lipophilic domain of the microemulsion interacts with the stratum corneum in a different way. A drug that gets dissolved in the lipid domain of the microemulsion can directly partition into lipid of the stratum corneum.[4]

Sulconazole is a broad spectrum antifungal agent of the imidazole class used against dermatophytes and other fungi to treat skin infections such as ringworm and athlete's foot. It is lipophilic in nature and can be effortlessly formulated for topical delivery by using a microemulsion as topical vehicle for an antifungal effect with several advantages such as ease of preparation, thermodynamic stability, transparent and elegant appearance, increased drug loading, enhanced penetration into the biological membrane, and increased bioavailability compared to conventional dosage form likes cream. Hence, in the present study we developed a sulconazole loaded microemulsion gel for topical delivery and investigated it in terms of physicochemical characterization, drug content, *in vitro* drug release and kinetic studies, and *in vivo* skin irritation.[5]

MATERIALS AND METHODS

Materials

Sulconazole nitrate was received as a gift sample from Ranbaxy Laboratory, New Delhi, India. Olive oil, Tween 20, and PEG 400 were purchased from HiMedia, Mumbai, India. Propylene glycol and Carbopol 934 were procured from Lobachemie Pvt. Ltd, Mumbai, India. Triethanolamine was purchased from Rankem Fine Chemicals Ltd., New Delhi, India. All the chemicals and reagents were used of analytical grade.

Methods

Fourier transform infrared (FTIR) spectroscopy

FTIR spectroscopy was carried out to check the compatibility between the drug and polymer. Using an IR spectrophotometer (Spectrum one model, Alpha-Bruker, Germany) IR spectra of sulconazole nitrate, Carbopol 934, and physical mixture of sulconazole nitrate and Carbopol were obtained and compared to check the interactions.

Preparation of microemulsion

Sulconazole nitrate containing o/w microemulsion was formulated by water titration method involving the following steps. First, surfactant and cosurfactant were added in fixed ratios to oil followed by sulconazole nitrate. Then bath sonication was performed for 5 min followed by heating. Later the required quantity of water was added dropwise with constant stirring until the formation of a clear and transparent liquid. A series of microemulsion formulations were prepared using Tween 20 and PEG 400 as the surfactant and cosurfactant and olive oil as the oil. In all these formulations, the amount of sulconazole nitrate was kept constant (50 mg) and the amounts of surfactant, cosurfactant, oil, and cosolvent were varied (Table 1).

Characterization of sulconazole nitrate microemulsion formulations

Globule size determination

One drop of the sample was taken on a microscopic glass slide and a cover slip was placed over it and it was observed at 45x resolution under a microscope (Zeiss, Germany). The particle size was measured using BIOVIS software.[6]

Dilution test

The formulated microemulsions were diluted with distilled water to confirm the type of emulsion and miscibility with the aqueous phase.

Centrifugation test

This is used to specify the stability of the microemulsion as to whether it is monophasic or not. Samples were centrifuged using a cold centrifuge (CM8plus, Remi Lab World, Mumbai,

Table 1. Composition of different microemulsion formulations

Formulation code	Sulconazole nitrate	Olive oil (% v/v)	S:Cos ratio	Tween 20/PEG 400 (%)	Water (%)
F1	2 g	5.0	3:1	55	40.0
F2	2 g	5.0	3:1	60	35.0
F3	2 g	7.5	3:1	45	47.5
F4	2 g	7.5	3:1	50	42.5
F5	2 g	10	3:1	55	35.0
F6	2 g	10	3:1	60	30.0

India) at 10.000 rpm for 30 min and then were examined for whether the system was monophasic or biphasic.[7]

Zeta potential determination

A Malvern Zeta Sizer (Malvern Instruments, UK) was used to measure the zeta potential of the globules on the electrophoresis and electrical conductivity of the microemulsion. Measurements were performed using small volume zeta cells.[7]

Determination of pH

The pH of the microemulsion formulations was measured using a digital pH meter (Systronics 335, Ahmedabad, India).

Determination of viscosity

The viscosity of the formulated microemulsions was determined by Brookfield viscometer DV-II model using spindle number 92 at 20, 30, 50, 60, and 100 rpm.[7]

Freeze thawing

Freeze thawing was employed to evaluate the stability of the microemulsion formulations. The microemulsion preconcentrates of various formulations were subjected to 3 to 4 freeze thaw cycles, which included freezing at -10 °C for 24 h followed by thawing at 40 °C for 24 h. The various formulations were then subjected to centrifugation at 3000 rpm for 5 min. The formulations were then visually observed for phase separation.[8]

Preparation of drug loaded microemulsion gel

The polymers Carbopol 934P and propylene glycol were used to prepare blank gel. Among them Carbopol 934P 1% gel was optimized for its transparency and its consistency for application on skin. Carbopol 934P (1%) and propylene glycol (5%) (as humectants) were added to the required quantity of water with constant stirring and left for hydration for 4-5 h. The microemulsion was in the gel phase and it was left overnight. Finally the required quantity of triethanolamine was added to adjust the pH.[9]

Evaluation of microemulsion gel

The prepared drug-containing gel formulations were evaluated for pH and drug content. For drug content determination, microemulsion gel (1 g) was weighed and dissolved in a mixture of ethanol:phosphate buffer pH 7.4 (2:3). From this, 2 mL of the solution was diluted to 50 mL with the same medium and absorbance was measured at λ_{max} 227 nm. Blank solution was prepared in the same manner by taking gel without drug. For determination of pH, 1 g of microemulsion gel was dissolved in 100 mL of distilled water and stored for 2 h and pH was measured using a digital pH meter (Systronics 335, Ahmedabad, India).[10]

In vitro drug release and kinetic studies

The *in vitro* drug release study of drug from formulations was carried out using an artificial semipermeable membrane (Cellophane) with a Franz diffusion cell. The receptor compartment consisted of 50 mL of ethanol:phosphate buffer pH 7.4 (2:3), temperature was maintained at 37±2 °C and it was stirred using a magnetic stirrer. The microemulsion gel (~10 mg sulconazole nitrate) was placed on an artificial semipermeable membrane tied to one end of an open ended glass cylinder that was then dipped into the receptor medium on a magnetic stirrer. Samples were taken from the receptor medium over 12 h at different time intervals and replaced immediately with the buffer. All the samples were analyzed at 227 nm and the cumulative amount of drug release was calculated. In order to describe the kinetics of the release process of drug in the different formulations, zero order, first order, Higuchi, and Korsmeyer and Peppas models were fitted to the dissolution data of selected formulations using linear regression analysis.[11]

In vivo skin irritation study

The skin irritation test was carried out on healthy male albino rats (200-250 g) obtained from NUCARE-Nitte (Deemed to be University) with ethical approval from the ethical committee and the document no: is NGSMIPS/IAEC/May-2016/9. The experiments were performed in accordance with the CPCSEA guidelines. The preparation was applied to the properly shaved skin of rats and secured with adhesive tape, and its adverse effects like change in color and skin morphology were checked over 72 h. Two sets of 6 rats were used for the study. Among these 6 were used as the placebo group and the other 6 as the treatment group. The animals were observed for any sign of erythema and edema over different time intervals.[12,13]

RESULTS

Fourier transform infrared spectroscopy

The IR spectra of pure drug sulconazole nitrate (Figure 1), Carbopol 940P (Figure 2), and a physical mixture of sulconazole nitrate with Carbopol 940P (Figure 3) were obtained and interpreted for spectral data comparison for (Figure 1).

Microemulsion formulations of sulconazole nitrate were prepared by water titration. According to the definition, a microemulsion must be clear and transparent in nature. All the formulations were transparent and clear and without any precipitation, which indicated the formation of good microemulsions.

Evaluation of microemulsion of sulconazole nitrate

Globule size determination

Microemulsions are thermodynamically stable, transparent systems having particle size <100 nm. Globule size is a very important evaluation parameter because the therapeutic effectiveness of a microemulsion depends on its globule size. The formulated microemulsions showed globule size between 243.8±0.02 µm and 679.2±0.01 µm. Formulation F1, with the highest proportions of surfactant and cosurfactant with a fixed amount of oil, showed the lowest mean particle diameter, whereas formulation F6, with the highest proportion of surfactant and a fixed amount of oil, showed the highest mean particle diameter.

Dilution test

The dilution test is based on the fact that an emulsion is only miscible with the liquid that forms the continuous phase.

Centrifugation test

The data for the formulations for stability for monophasic nature are shown in Table 2.

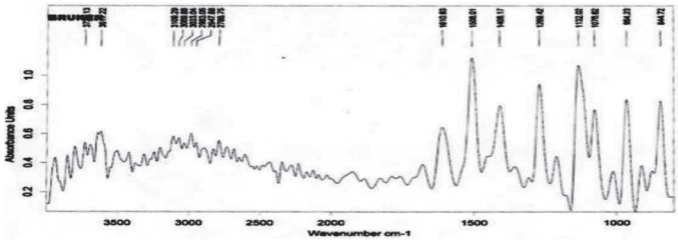

Figure 1. IR spectra of pure sulconazole nitrate
IR: Infrared spectroscopy

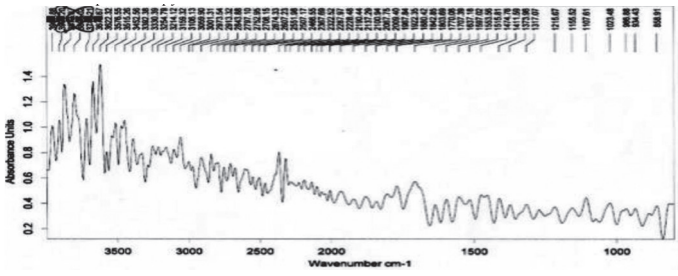

Figure 2. IR spectra of Carbopol 940P
IR: Infrared spectroscopy

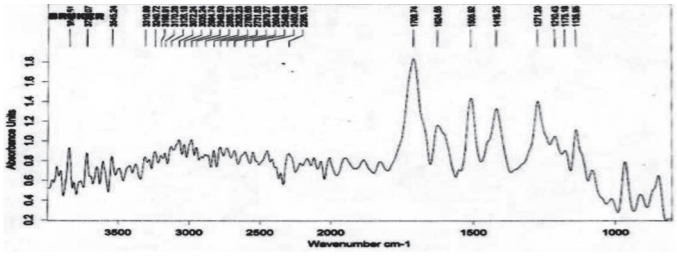

Figure 3. IR spectra of a physical mixture of sulconazole nitrate and Carbopol 934P
IR: Infrared spectroscopy

Table 2. Evaluation of the centrifugation test

Formulation code	Centrifugation
F1	Monophasic, stable
F2	Not stable
F3	Monophasic, stable
F4	Monophasic, stable
F5	Not stable
F6	Not stable

Table 3. Results of freeze thawing test

Formulation code	Freeze thawing
F1	Stable and no separation
F3	Stable and no separation
F4	Stable and no separation

Freeze thawing test

This test checks the stability and phase separation of formulations if found (Table 3).

Determination of zeta potential

The zeta potential value depends on the type and composition of the carrier used in the formulation. The zeta potential of F1 was -33.5, which indicates good stability (Table 4).

Determination of pH

F1, F3, and F4 were in the pH range of 6.32-7.0, which is within the specified range for topical formulations (Table 4).

Drug content

The percentage drug content of F1, F3, and F4 was 93.05%-95.88%. This shows that the drug is uniformly distributed throughout the microemulsion. The maximum drug content was obtained for F1 (Table 4).

Table 4. Zeta potential, pH, and drug content of F1, F3, and F4

Formulation code	Zeta potential (mV)	pH	Drug content (%)
F1	-33.5±2.3	7.0±0.01	95.88±0.3%
F3	-41.2±3.4	6.32±0.03	91.42±0.2%
F4	-38.3±2.7	6.89±0.02	93.05±0.4%

*Mean ± SD (n=3), SD: Standard deviation

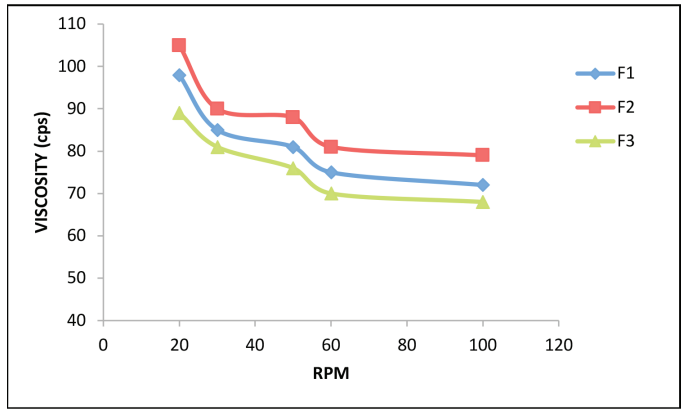

Figure 4. Rheology of sulconazole microemulsions for F1, F3, and F4

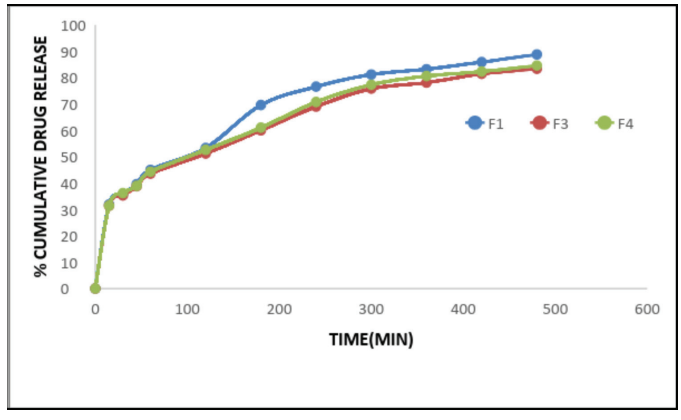

Figure 5. *In vitro* drug release profile of F1, F3, and F4 microemulsion gel formulations

Determination of viscosity

The viscosity of F1, F2, and F3 microemulsion formulations at 20, 30, 50, 60, and 100 rpm was measured using spindle number 92 at room temperature. The viscosity curve was plotted by taking shear rate (rpm) on the x-axis and viscosity on the y-axis (Figure 4) with the data obtained (Table 5).

Preparation of drug loaded microemulsion gel

Sulconazole nitrate microemulsion (F1, F3, and F4) containing Carbopol appeared to be transparent, clear, and smooth textured. These drug-containing gel formulations were further evaluated for pH and drug content.

Evaluation of microemulsion gel

Drug content values were in the range of 91.5-95.5% and pH ranged between 7.2 and 7.8 (Table 6).

In vitro drug release and kinetic studies

Three microemulsion gel formulations (F1, F3, and F4) were selected for the *in vitro* drug release study. The % cumulative drug release was 83.32-88.75 at the end of 8 h (Figure 5). The mechanism of drug release was calculated by fitting the dissolution data to different models like Higuchi's and Korsmeyer-Peppas. The best model was selected based on the highest regression value (Figure 6).

In vivo skin irritation study

The skin irritation study was carried out on six rats, of which three were treated with placebo and three with F1. They were observed for 72 h to check for signs of erythema and edema on the skin surface (Figure 7).

DISCUSSION

From the FTIR study, the peaks that appeared for the physical mixture indicated that the drug and the gelling agents are compatible with each other.

Table 5. Viscosity of F1, F2, and F3 at different rpm

rpm	Viscosity (cps)*		
	F1	F2	F3
20	98±0.01	105±0.01	89±0.01
30	85±0.07	90±0.01	81±0.01
50	81±0.02	88±0.02	76±0.03
60	75±0.03	81±0.03	70±0.01
100	72±0.02	79±0.01	68±0.01

*Values are mean ± SD (n=3), SD: Standard deviation

Table 6. Drug content and pH of F1 microemulsion

Test	Drug loaded microemulsion gel		
	F1	F3	F4
Drug content	95.5±0.34%	91.5±0.26%	92.5±0.36%
pH	7.21±0.01	7.72 ±0.02	7.81 ±0.02

*Values are mean ± SD (n=3), SD: Standard deviation

From the results of globe size analysis, it was observed that an increase in the ratio of the oil phase resulted in an increase in the particle size because of the decrease in the surfactant/cosurfactant proportion. An increase in the surfactant/cosurfactant ratio and decrease in oil ratio led to a decrease in mean particle size.

The dilution test showed that after dilution of microemulsion with water the microemulsions remained clear, indicating the good miscibility of microemulsions with water, which was used as the continuous phase.

From the centrifugation test, it was observed that F1, F3 and F4 were stable and monophasic liquids and they were further evaluated for pH, drug content, and zeta potential.

The freeze thawing results also confirmed that all three formulations were stable and there was no phase separation.

The zeta potential of formulation F1 was found to be good and was optimized as the best formulation. The pH of the formulated microemulsions was within the specified skin range.

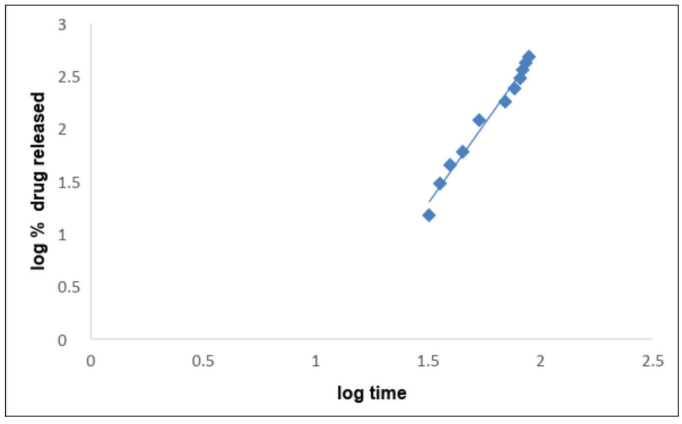

Figure 6. Korsmeyer-Peppas model for F1 microemulsion

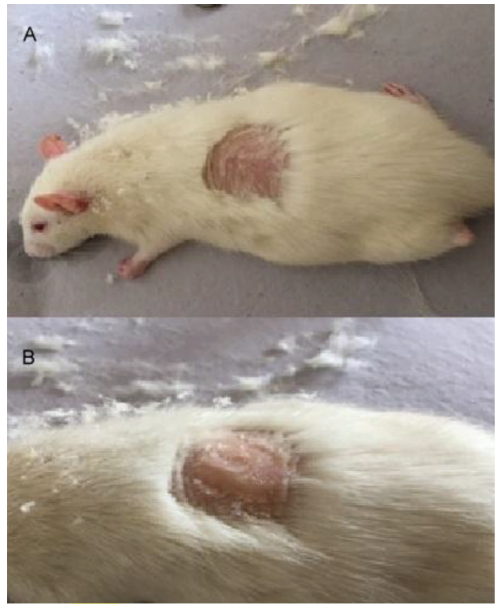

Figure 7. *In vivo* skin irritation test for F1 microemulsion: (A) before application, (B) after application

From the viscosity study, all three formulations showed pseudoplastic non-newtonian flow and viscosity values decreased as the shear rates increased.

From the drug release data F1 was found to show a higher percentage of drug release in comparison to F3 and F4. This may be because spontaneous formation of microemulsion with small particle size permitted a faster rate of drug release. Thus greater permeability of the dissolved sulconazole nitrate from the microemulsion gel formulation, which can lead to higher absorption through the skin, can be expected.

F1 followed the Korsmeyer-Peppas model since the regression coefficient value was higher.

The *in vivo* skin irritation study showed that there was no sign of erythema or edema after 72 h of application of the gel and F1 was found to be safe, nontoxic, and nonirritant for application on the skin.

CONCLUSION

The microemulsion based gel of sulconazole nitrate was successfully formulated for topical delivery to treat fungal infections. The formulated gel possessed good physicochemical properties, high drug content, and sustained drug release. It was also confirmed that the formulated gel is safer for topical delivery by the *in vivo* studies. Based on these results, it can be concluded that a microemulsion based gel of sulconazole nitrate is promising for topical delivery against fungal infections.

ACKNOWLEDGEMENTS

The authors are thankful to Ranbaxy Laboratory, New Delhi, for providing sulconazole nitrate as a gift sample and N.G.S.M. Institute of Pharmaceutical Sciences, Nitte (Deemed to be University), Mangaluru, for providing the necessary facilities to carry out this work.

Conflicts of interest: No conflict of interest was declared by the authors. The authors alone are responsible for the content and writing of this article.

REFERENCES

1. Kikwai L, Babu RJ, Prado R, Kolot A, Armstrong CA, Ansel JC, Singh M. *In vitro* and *In vivo* evaluation of topical formulation of spantide II. AAPS Pharm Sci Tech. 2005;6:565-572.
2. Kumar R, Katare OP, Lecithin organogels as a potential phospholipid structured for topical drug delivery, a review. AAPS Pharm Sci Tech. 2005;6:298-310.
3. Chein YW. Transdermal therapeutic systems. In: Robinson JR, Lee VHL, eds.Text book of Controlled drug delivery: fundamentals and application, 2nd ed. New York: Marcel Dekker Inc; 1987:524-549.
4. Chen H, Chang X, Du D, Li J, Xu H, Yang X. Microemulsion based hydrogel formulation of ibuprofen for topical delivery. Int J Pharm. 2006;315:52-58.
5. Benjamin EJ, Lee M, Tom J, Lin LY, Hanesian M, Wu D. Stabilization of sulconazole nitrate in topical powder formulation. Int J Pharma. 1983;14:209-211.
6. Badawi AA, Nour SA, Sakran WS, El-Mancy SMS. Preparation and evaluation of microemulsion systems containing salicylic acid. AAPS Pharm Sci Tech. 2009;10:1081-1084.
7. Brime B, Moreno MA, Frutos G, Ballesteros MP, Frutos P. Amphotericin B in oil in water Lecithin-based microemulsions: Formulation and toxicity evaluation. J Pharm Sci. 2002;91:1178-1185.
8. Karasulu YH, Karabulut B, Göker E, Güneri T, Gabor F. Controlled release of Methotrexate from w/o microemulsion and its *in vitro* antitumor activity. Drug Deliv. 2007;14:225-233.
9. Bajpai M, Sharma PK, Mittal A. A study of oleic acid base for the tropical delivery of dexamethasone microemulsion formulations. Asian J Pharm. 2009;208-214.
10. Dhamankar AK, Manwar JV, Kumbhar DD. The novel formulation design of o/w microemulsion of ketoprofen for improving transdermal absorption. Int J Pharm. 2009;1:1449-1457.
11. Bansal K, Rawat MK, Jain A, Rajput A, Chaturvedi TP. Development of satranidazole mucoadhesive gel for the treatment of periodontitis. AAPS Pharm Sci Tech. 2009;10(3):716-723.
12. Basha NB, Prakasam K, Goli D. Formulation and evaluation of gel containing fluconazole-antifungal agent. Int J Drug Dev Res. 2011;3:109-128.
13. Kumar A, Kushwaha VS, Sharma P. Pharmaceutical microemulsion: Formulation, characterization and drug deliveries across skin. Int J Drug Dev Res. 2014;6:1-21.

Turk J Pharm Sci 2020;17(3):265-270
DOI: 10.4274/tjps.galenos.2019.05658

ORIGINAL ARTICLE

Obtaining Stem Cell Spheroids from Foreskin Tissue and the Effect of *Corchorus olitorius* L. on Spheroid Proliferation

Sünnet Derisinden Kök Hücre Sferoidlerinin Elde Edilmesi ve *Corchorus olitorius* L.'nin Sferoid Proliferasyonuna Etkisi

Eda BECER[1], Günsu SOYKUT[2]*, Hilal KABADAYI[3], Emil MAMMADOV[4], İhsan ÇALIŞ[5], Seda VATANSEVER[3]

[1]Near East University Faculty of Pharmacy, Department of Biochemistry, Nicosia, North Cyprus
[2]Near East University Faculty of Health Sciences, Department of Nutrition and Dietetics, Nicosia, North Cyprus
[3]Manisa Celal Bayar University Faculty of Medicine, Department of Histology and Embryology, Manisa, Turkey
[4]Near East University, Faculty of Medicine, Department of Pediatric Surgery, Nicosia, North Cyprus
[5]Near East University Faculty of Pharmacy, Department of Pharmacognosy, Nicosia, North Cyprus

ABSTRACT

Objectives: Mesenchymal stem cells are self-renewing stem cells. The human foreskin has potential to be used as a source of stem cells. The aim of the study was to obtain spheroid formation of human foreskin cells (hnFSSCs) isolated from newborn human foreskin tissue. In addition, the apoptotic and proliferative effects of a traditional plant, *Corchorus olitorius* L. (*C. olitorius*), on hnFSSC spheroids were investigated.

Materials and Methods: After a routine circumcision procedure the cells were isolated and cultured in suitable medium. The plant leaves was extracted with ethanol and their composition was analyzed by liquid chromatography coupled with mass spectrometry (LC-MS/MS). The foreskin stem cells were characterized immunocytochemically by CD45, CD34, and CD90 antibodies. hnFSSC spheroids were formed using the hanging drop technique. Immunofluorescence staining was used on the obtained spheroids to determine the distribution of caspase-3 and Ki-67 after being treated with *C. olitorius* extract for 48 h.

Results: Immunostaining analysis showed that hnFSSCs were positive for CD45 and CD34 and negative for CD90. According to LC-MS/MS *C. olitorius* was rich in flavanols and hydrocinnamic acid derivatives. Although the spheroids obtained were loose and floating, the cells interacted with each other. Caspase-3 activity was higher in the control group than in the extract-treated group and Ki-67 was higher in the extract-treated group than in the control group, suggesting that the plant might have the capacity to increase stem cell proliferation due to its rich polyphenolic content.

Conclusion: The results suggest that hnFSSCs and spheroids might be used in stem cell generation, tissue repair and renewal as human foreskin tissue has potential to be used as a stem cell source. *C. olitorius* also increased proliferation of hnFSSCs, showing that polyphenols might increase proliferation of stem cells.

Key words: *Corchorus olitorius*, spheroid, human foreskin, stem cell

ÖZ

Amaç: Mezenkimal kök hücreler kendi kendini yenileyebilme özelliğine sahiptir. Sünnet derisinin kök hücre kaynağı olarak kullanılma potansiyeli vardır. Çalışmanın amacı, yeni doğmuş insan sünnet derisi izole hücrelerinden (hnFSSCs) sferoid oluşumunu elde etmektir. Buna ek olarak, Kıbrıs'a özgü geleneksel bir bitki olan *Corchorus olitorius* L. (*C. olitorius*) bitkisinin hnFSSCs sferoidleri üzerindeki apoptotik ve proliferatif etkileri de araştırılmıştır.

Gereç ve Yöntemler: Rutin sünnet prosedüründen sonra hücreler izole edildi ve uygun besi yeri ortamında kültüre edildi. Bitki yaprakları etanol ile ekstre edildi ve içerik analizi sıvı kromatografi-kütle spektrometresi (LC-MS/MS) yöntemi ile yapıldı. Sünnet derisi kök hücreleri CD45, CD34, CD90 antikorları kullanılarak immünositokimyasal olarak karakterize edilmiştir. hnFSSC sferoidleri asılı damla tekniği kullanılarak oluşturuldu. Elde edilen sferoidler daha sonra *C. olitorius* ekstraktı ile 48 saat süre muamele edildikten sonra kaspaz-3 ve Ki-67'nin dağıtımı için immünofloresan boyama yöntemiyle boyandı.

*Correspondence: E-mail: gunsusoykut@gmail.com, Phone: +90542 866 08 80 ORCID-ID: orcid.org/0000-0002-8479-1457
Received: 28.09.2018, Accepted: 07.03.2019

Bulgular: İmmünoboyama analiz sonuçları, hnFSSC'lerin CD45, CD34 için pozitif fakat CD90 için negatif olduğunu gösterdi. LC-MS/MS sonuçlarına göre *C. olitorius* bitkisinin, flavanoller ve hidro-sinnamik asit türevleri içerdiği saptanmıştır. Elde edilen sferoidler gevşek ve yüzer vaziyette olmalarına rağmen hücreler birbirleri ile etkileşim halindeydi. Kaspaz-3 aktivitesi kontrol grubunda ekstrakt grubuna göre daha yüksekti ve ekstraksiyon uygulanan grupta Ki-67 aktivitesi kontrol grubuna göre daha yüksek bulundu. Bu sonuçlar, bitkinin polifenol içeriğinden dolayı kök hücre proliferasyonunu artırma kapasitesine sahip olabileceğini göstermektedir.

Sonuç: hnFSSC'lerin ve sferoidlerin kök hücre üretimi ve doku onarımı ve yenilenmesinin bir parçası olarak kullanılabilme potansiyeli, sünnet derisinin kök hücre kaynağı olarak kullanılması durumunda mevcuttur. *C. olitorius* içerdiği polifenollerinden dolayı kök hücrelerin proliferasyonunu artıran etki göstermeyi başarmıştır.

Anahtar kelimeler: *Corchorus olitorius*, sferoid, sünnet derisi, kök hücre

INTRODUCTION

Mesenchymal stem cells (MSCs) are multipotent, self-renewing adult stem cells that are isolated from multiple tissues such as adipose tissue, bone, umbilical cords, dental pulp, and skin. MSCs are fibroblast-like cells and *in vitro* studies have shown that they have the potential to differentiate into adipocytes, osteoblasts, and chondrocytes.[1] According to the International Society of Cellular Therapy criteria, human MSCs are defined by positive expression for cell surface markers including CD29, CD44, CD90, CD49a-f, CD51, CD73 (SH3), CD105 (SH2), CD106, CD166, and Stro-1 and lack of expression of CD45, CD34, CD14 or CD11b, CD79a or CD19, and HLA-DR surface molecules.[2] Because of their easy isolation and lack of ethical issues, MSCs are among the first stem cell types to be used in the treatment of various conditions, including autoimmune diseases, orthopedic injuries, and liver and cardiovascular diseases.[3]

Skin is the largest organ of the human body and a source of multipotent mesenchymal cells with the capacity for multipotential differentiation. Human newborn foreskin tissue is part of the skin that is obtained by noninvasive techniques and can proliferate without cell differentiation over a long period.[4] Recent studies reported that human foreskin isolated cells (hnFSSCs) have stem cell properties and multipotent and pluripotent abilities. Skrzypczyk et al.[5] showed that storage of hnFSSCs and newborn foreskin tissue might be very beneficial in terms of disease development potentials and treatment actions.

Spheroids are 3D cell culture models to be used as *in vitro* models for screening new anticancer therapeutics. There are multiple methods for spheroid creation, namely hanging drop, spinner culture, nonadhesive hydrogel micromolds, pellet culture, liquid overlay, rotating wall vessel, external force, cell sheets, and microfluidics.[6] 3D spheroids models have been shown to be advantageous compared to traditional two dimensional (2D) cell culture. 2D monolayer culture mostly focuses on cell growth conditions, cell proliferation, and gene and protein expression profiles. However, 3D spheroids are able to accurately mimic some properties of normal or tumor tissue structure, such as their micro-environments, spatial architecture, physiological responses, signaling cascades, gene expression patterns, and drug resistance mechanisms. Thus, the behavior of 3D cultured cells is more reflective of *in vivo* cellular responses.[7]

Corchorus olitorius L. (*C. olitorius*) is a plant that is commonly consumed in Eastern Mediterranean and Middle Eastern countries. The plant is known to have medicinal properties, showing anti-inflammatory, anticancer, antibacterial, and antioxidant effects.[8-11] It is also known that the plant content is rich in polyphenols, antioxidant vitamins, and minerals that are part of endogenous antioxidant systems.[8,9,12] *C. olitorius* contains quercetin and its derivatives and chlorogenic acid derivatives, which are thought to provide the plant with its medicinal properties.[9,12,13] Polyphenols also tend to improve proliferation and have the potential to increase stem cell viability due to differentiation in stem cells.[14,15]

The aim of the present study was to obtain spheroid formation of hnFSSCs isolated from newborn human foreskin tissue. Furthermore, the proliferative and apoptotic effects of *C. olitorius* on hnFSSC spheroids were assessed.

MATERIALS AND METHODS

Isolation and culture of human foreskin stem cells

Human newborn foreskin tissue was obtained following routine circumcisions. Foreskin samples were obtained from donors 4 to 40 weeks of age at Near East University Hospital after informed consent was obtained from their parents. The study was approved by Near East University Health Sciences Ethics Committee (YDU/2018/62-658). The mucosa part of the foreskin was collected. The mucosa was digested enzymatically with 1 mg/mL collagenase type 1 (Sigma, C0130) for 1 h at 37 °C and 5% CO_2. Cells were collected and centrifuged to remove collagenase. The hnFSSCs were cultured in DMEM-F12 medium supplemented with 10% fetal bovine serum, 1% penicillin-streptomycin, and 25 µg/mL amphotericin B in a humidified atmosphere at 37 °C and 5% CO_2. When the cultured cells reached 80% confluence state, they were subcultured using 0.25% trypsin-EDTA solution (Biochrom, L 2143) for further studies.

Characterization of human foreskin stem cells

hnFSSCs were characterized immunocytochemically for distribution of CD45, CD34, and CD90 (Thy-1 glycoprotein). The hnFSSCs were fixed with 4% paraformaldehyde in phosphate buffered saline (PBS) at 4 °C for 30 min. For permeabilization, 0.1% Tween 20 (Sigma-Aldrich) was added for 15 min on ice. The cells were washed with PBS and endogenous peroxidase activity was quenched by incubation with 3% H_2O_2 for 5 min at room temperature. After the cells were washed with PBS three times for 5 min, primary antibodies anti-CD45 (sc-1178), anti-CD34 (sc-74499), and anti-CD90 (Thy-1 glycoprotein) (sc-19614) were added, followed by incubation overnight at 4 °C.

Biotinylated secondary antibody and streptavidin-peroxidase (Histostain-Plus, IHC Kit, HRP, 859043, Thermo Fischer) were added and each secondary antibody was incubated for 30 min followed by PBS wash (×3) for 5 min. Cells were then stained with diaminobenzidine for 5 min for enhancement of immunolabeling. After being washed with distilled water, they were counterstained with Mayer's hematoxylin for 5 min and mounted with mounting medium (Merck Millipore, 107961, Germany). All specimens were examined under a light microscope (Olympus BX40, Tokyo, Japan).

Plant material and extraction

Mature *C. olitorius* leaves were collected from Kyrenia, Cyprus. The collected plant sample was registered with the Near East Herbarium at Near East University under the Herbarium number 6904. The dry leaves of *C. olitorius* (100 g) were powdered (Waring Commercial Blender, USA) and extracted with 80% ethanol during incubation overnight at room temperature with occasional stirring. The extract was vacuum filtered and concentrated to 200 mL by rotary evaporator (BUCHI Rotavapor R-210). The extract was evaporated and lyophilized (Christ Alpha 1-4 LD Plus, Germany) to yield 14.8 g of crude extract.

Liquid chromatography-mass spectrometry (LC-MS/MS) analysis of C. olitorius leaf extract

The extract composition of *C. olitorius* leaves was investigated by LC/MS-MS analysis. LC separation was performed using an Agilent 1200 high performance LC (HPLC) system (Agilent, USA) equipped with an automatic degasser, a quaternary pump, and an autosampler. Chromatographic separation was carried out on a Waters SunFire™ C18 column (150 mm×4.6 mm, 5 m) at 40 ˚C. The flow rate of the mobile phase was maintained at 0.5 mL/min. The mobile phases were (A) acetonitrile:water:formic acid (10:89:1, v/v/v) and (B) acetonitrile:water:formic acid (89:10:1, v/v/v). The HPLC system was connected to a 3200 Q TRAP LC/MS/MS system with a hybrid triple quadrupole/LIT (linear ion trap) mass spectrometer equipped with an ESI ion source (Applied Biosystems/MDS Sciex, USA). The instrument control and data acquisition were carried out by the software Analyst 1.6.

Cell viability and growth assay

The extract was dissolved with dimethyl sulfoxide [(DMSO), Sigma-Aldrich)] to 100 mg/mL. It was further diluted in culture medium (5 µg/mL, 10 µg/mL, 20 µg/mL, 50 µg/mL, and 100 µg/mL). The final concentration of DMSO in cell lines was less than 0.05%. hnFSSCs were collected, suspended in medium, and seeded in 96 well culture dishes at a density of 5×10^4/mL cells in each well with 100 µL of medium. The hnFSSCs were incubated for 24 h and 48 h.

Cell viability was estimated by MTT assay. MTT solution (Biotium, #30006) was heated to 37 ˚C and then 10 µL was added to each well. After 4 h incubation at 37 ˚C in 5% CO_2, 200 µL of DMSO was added to dissolve the formazan salts. The absorbance was measured at 570 nm with a spectrophotometer (Versa Max, Molecular Device, Sunnyvale, CA, USA).

Preparation of the 3D spheroid model and determination of the effects of C. olitorius leaf extract

hnFSSC spheroids were formed using the hanging drop technique with 600 cells per 20 µL droplet (Y5, Fermenne 2013). The cells were incubated in a humidified atmosphere at 37 ˚C in 5% CO_2 for 36 h and 72 h. Two different culture time spheroids were collected and transferred in two different 24 well plates and all of them were incubated with 50 µg/mL *C. olitorius* extract for 48 h.

Immunofluorescence of 3D spheroids

The spheroids were fixed with 4% paraformaldehyde at room temperature for 30 min and then washed three times with PBS. The spheroids were then embedded in OCT compound (Jung, 0201-08926) and cross-sectioned with a cryostat at 8 µm thickness. Sections were kept at -20 ˚C until the staining procedure. The sections were warmed at room temperature overnight and washed with PBS for 2×30 min at 37 ˚C. The sections were traced around with a PAP pen (Diagnostic BioSystems, K039). The blocking solution [10% sheep serum (sc-2488) in PBS with 0.05% Triton X-100)] was added, followed by incubation for 1 h. The blocking solution was aspirated and primary antibodies [rabbit polyclonal anti-caspase-3 (sc-98785) and mouse monoclonal anti-Ki-67 (BioGenex mv370-uc)] diluted in 2% sheep serum in PBS with 0.05% Triton X-100 were added overnight in a humidified chamber at 4 ˚C. The cells were then incubated with secondary antibodies (goat anti-rabbit TRITC sc-2091, goat anti-mouse FITC Millipore AP308F) for 2 h after washing with PBS with 0.05% Triton X-100. They were then washed and stained with DAPI (Applichem A1001-0025) for 2 min. All sections were covered with mounting media (JA1750) and then evaluated under a fluorescence microscope (Olympus IX71, Tokyo, Japan).

Staining of Ki-67 and caspase-3 was also graded semiquantitatively using the intensity of staining with a value of 1, 2, or 3 (mild, moderate, or strong, respectively).

Statistical analysis

The results were analyzed using GraphPad Prism 7 software. The results were expressed as mean ± standard deviation and standard error where appropriate.

RESULTS

Cell morphology

Fibroblast-like and spindle-formed cells were isolated from the mucosal part of human newborn foreskin tissue. After 4 days, fibroblast-homologous, spindle-formed morphology cells were visible and it had been observed that the cells covered the surface after 7 days. After subculture of the cells, the proliferation rate was triggered and accelerated (Figure 1).

Immunocytochemical characterization of human foreskin stem cells

Immunostaining analysis showed that the hnFSSCs were positive for CD45 and CD34 and negative for CD90. Mucosa-derived foreskin fibroblast-like stromal cells expressed MSC surface markers at passage 1 (Figure 2).

LC-MS/MS Analysis of C. olitorius extract

The extract of *C. olitorius* was analyzed by LC-MS/MS. Caffeoyl glucose, 3-caffeoylquinic acid, quercetin glucoside, quercetin acetylglucoside, 3,5-dicaffeoylquinic acid, 1,3-dicaffeoylquinic acid, luteolin, and/or kaempferol acetylglucoside were identified in *C. olitorius* extract (Table 1).

Cell viability and cytotoxicity

The hnFSSCs were treated with different concentrations (5-100 µg/mL) of *C. olitorius* extract for 24 and 48 h. None of the dilutions showed any cytotoxic effects on the hnFSSCs and 50 µg/mL concentration at 48 h incubation period was optimal as cell viability was 100% (Figure 3).

Effects of C. olitorius extract on the 3D culture hnFSSC spheroids model

The cells started to aggregate after 24 h (Figure 4). After 36 and 72 h, two different groups of spheroids were collected and placed in 6 well plates. The clumps increased in size with time until day 7 and started to disintegrate after 7 days of incubation. Day 7 was therefore chosen as the time for collecting the spheroids for assays.

Immunoreactivity of caspase-3 was detected in both the control and extract-treated groups. However, the intensity of caspase-3 was less in the extract-treated group than in the control group (Table 2). Immunoreactivity of caspase-3 was higher in the 36-h-incubated control group than in the extract-treated spheroid group (Figure 5). Immunostaining intensity

Table 1. Main identified components of *Corchorus olitorius* extract

Rt	$(M-H)^-$	MS^2	Identified as
4.1	341	179, 161	Caffeoyl glucose
4.7	353	191, 179	3-Caffeoylquinic acid
9.9	463	299, 271, 255	Quercetin glucoside
10.9	505	299, 271, 255	Quercetin acetylglucoside
11.5	515	353, 191, 179, 173	3,5-Dicaffeoylquinic acid
12.1	515	353, 191, 179, 135	1,3-Dicaffeoylquinic acid
12.6	489	284, 255, 227	Luteolin/kaempferol acetylglucoside

Table 2. The intensity of caspase-3 and Ki-67 immunolabeling in hnFSSC spheroids treated with *Corchorus olitorius* extract at 50 µg/mL concentration for 36 and 72 h

	Corchorus olitorius extract group		Control group	
	36 h	72 h	36 h	72 h
Caspase-3	+	++	++	++
Ki-67	++	+++	+	-

hnFSSC: Human newborn foreskin stem cell

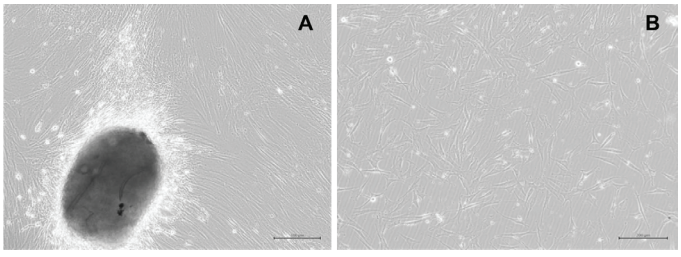

Figure 1. hnFSSCs. (A) Basal photomicrographic representation of cells on day 4 of isolation. (B) Mucosa-derived hnFSSC morphologies at passage 1. scale bars=200 µM

hnFSSCs: Human newborn foreskin stem cells

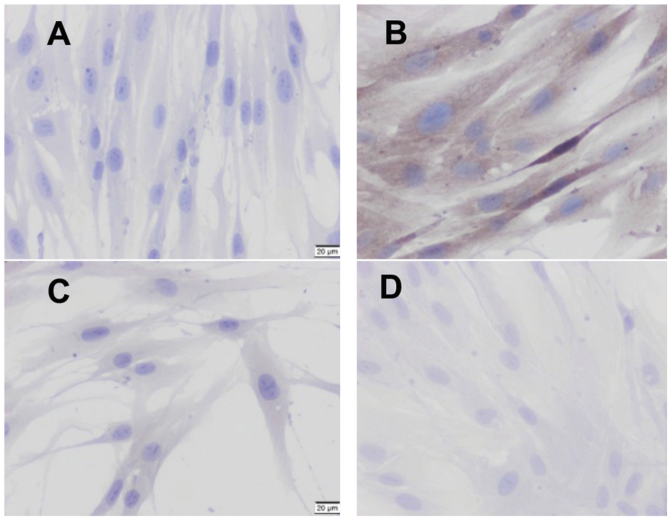

Figure 2. Immunochemical staining indicated the positive mesenchymal stem cell surface markers CD45 and CD34 and negative for CD90. Negative control (A), CD45 (B), CD34 (C), CD90 (D). Scale bars=20 µM

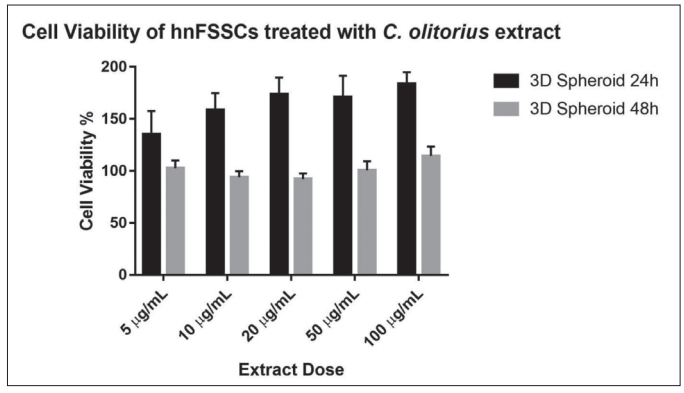

Figure 3. Effect of *Corchorus olitorius* extract on cell viability of hnFSSCs. The data are given as mean ± standard deviation

hnFSSCs: Human newborn foreskin stem cells

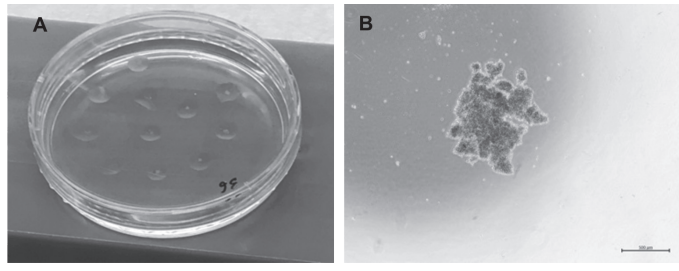

Figure 4. (A) Hanging drops (600 cells/20 µL) on the lid of a petri dish, (B) 7 day incubated spheroid. Scale bars=500 µM

for Ki-67 was moderate to strong for spheroids treated with extracts for 36 and 72 h (Table 2). As shown in Figure 6, Ki-67 immunoreactivity was weak or negative in the control groups (Figure 6).

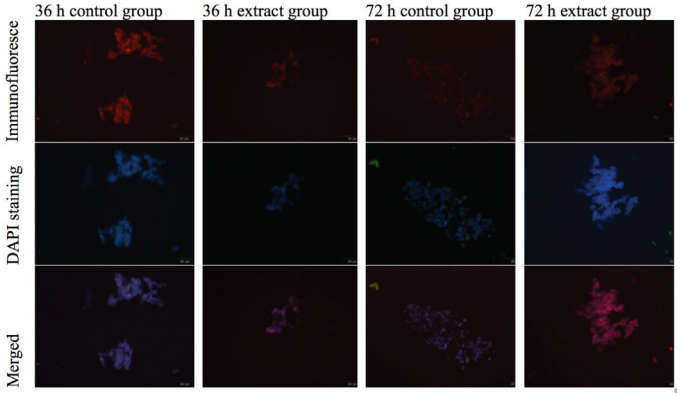

Figure 5. Immunofluorescence, DAPI staining, and merged photomicrographs of caspase-3 in 36 and 72 h hnFSSC spheroids treated with 50 µg/mL *Corchorus olitorius* extract for 48 h. Scale bars=50 µM
hnFSSC: Human newborn foreskin stem cell

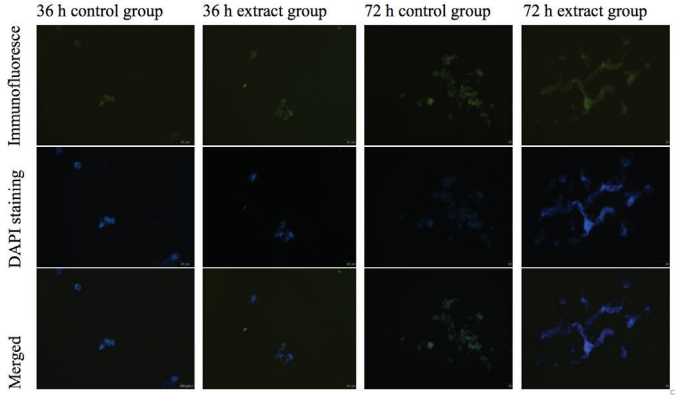

Figure 6. Immunofluorescence, DAPI staining, and merged photomicrographs of Ki-67 in 36 and 72 h hnFSSC spheroids treated with 50 µg/mL *Corchorus olitorius* extract for 48 h. Scale bars=50 µM
hnFSSC: Human newborn foreskin stem cell

DISCUSSION

Circumcision is a ritual that has been performed for centuries for medical, cultural, or religious reasons. The foreskin removed after surgery is usually discarded. It has been thought that the foreskin tissue might have the potential to be used as a source of stem cells, especially if the procedure is performed in early infancy and the tissue is collected from newborns.[4] The foreskin is usually more easily accessible than other tissues used for stem cell generation. In addition, as the tissue is usually discarded straight after the procedure, subjection to ethical issues might be negligible in terms of stem cell collection. If the collected foreskin tissue is from newborns, the differentiation rate and capacity are higher than in adults and nearly as high as in bone marrow.[4] Most studies' results suggested that hnFSSCs therapy is more beneficial than adult and embryonic stem cell therapies. The fact that positive markers were shown for hemopoietic and neural stem cells is also an indication that foreskin stem cells might be used in treatments for blood cancers, Parkinson's and Alzheimer's.[1] A very similar study found that hnFSSCs can also differentiate in myogenic cells.[3] In parallel to these studies, our results also revealed that hnFSSCs expressed MSC markers. In the current study, hnFSSCs positively expressed CD45 and CD34, which are known to be MSC surface markers. However, CD90 expression was negative. This might have been due to the hnFSSCs collected having originated from mucosal cells. Our results suggested that hnFSSCs are capable of differentiating into MSCs and have potential to be used in tissue renewal and repair.

MSCs play an important role in repairing damaged tissue through their anti-inflammatory properties. Recent studies showed that 3D spheroids of MSCs have high differentiation ability and cell survival when compared with 2D culture. Moreover, 3D MSCs' spheroid structure increases the anti-inflammatory proteins from immune cells.[15] MSC spheroids are widely used in oncology research as they synthesize more extracellular matrix than 2D culture. 3D culture also increases the therapeutic effects of intervention when compared with 2D formation.[12] MSC spheroids are solid aggregates due to upregulated cadherin expression.[16] In our study, hnFSSC spheroids were formed using the hanging drop technique. Our results showed that spheroids collected from hnFSSCs were not as compact as MSC spheroids. We obtained more loose and floating spheroids from hnFSSCs. However, even though the spheroid structure was loose, the cells were intact and interacted with each other.

In the current study, the apoptotic and proliferative effects of the plant *C. olitorius* on spheroids were studied. Caspase-3 is known as an executioner caspase and its trigger induces apoptosis, programmed cell death.[17] On the other hand, expression of Ki-67 is an indication of cell proliferation.[18] Caspase-3 immunostaining was observed in both cell groups, but this was expected in spheroid structures as the center is more compact and the nutrients are harder to diffuse to the center. However, caspase-3 staining intensity was less in extract-treated cells, which shows the plant might prevent stem cell apoptosis. In contrast to these results, Ki-67 immunostaining was higher in extract-treated cells than in the control group in both incubation periods, which indicates that *C. olitorius* might have the capacity to increase stem cell proliferation. The LC-MS/MS results indicated that *C. olitorius* contains polyphenolic compounds including quercetin and caffeoylquinic acid and their derivatives. Other studies also showed similar results, showing that the plant is rich in flavonols and hydroxycinnamic acids.[9,10] A 50 µg/mL dose was regarded as the treatment and optimal dose for further immunofluorescence analysis. In addition, other studies also stated that the plant has apoptotic effects in cancer cell lines via caspase-3 activation.[19] On the other hand, quercetin glucuronide has been shown to increase neural stem cell proliferation and promote migration.[20] Another study showed that quercetin enhanced bone marrow MSC proliferation and osteogenic differentiation.[21] This indicates that *C. olitorius* has the potential to increase stem cell proliferation by its rich polyphenolic content, which might be supportive for stem cell differentiation and better for mimicking *in vivo* structures and further tissue repair.

Study limitations

Flow cytometry could help in the identification of stem cell sources. In addition, the use of Western blotting could enhance Ki-67 and caspase-3 immunofluorescence staining results in terms of identification of protein expression of the antibodies.

CONCLUSION

In summary, the results indicate that hnFSSCs have great potential in stem cell differentiation and potential to be used in stem cell therapy. Moreover, spheroids were obtained from hnFSSCs and *C. olitorius* extract has the potential for enhancing their proliferation activity. All of these indicate that hnFSSCs and using spheroids may be used as a part of future clinical applications. These *in vitro* results also need to be evaluated with animal studies for further progression of hnFSSC spheroids in clinical applications.

ACKNOWLEDGEMENTS

The authors would like to thank the Experimental Health Research Center of Health Sciences laboratory.

Conflicts of interest: No conflict of interest was declared by the authors. The authors alone are responsible for the content and writing of the paper.

REFERENCES

1. Pittenger MF, Mackay AM, Beck SC, Jaiswal RK, Douglas R, Mosca JD, Moorman MA, Simonetti DW, Craig S, Marshak DR. Multilineage potential of adult human mesenchymal stem cells. Science. 1999;284:143-147.
2. Dominici M, Le Blanc K, Mueller I, Slaper-Cortenbach I, Marini FC, Krause DS, Deans RJ, Keating A, Prockop DJ, Horwitz EM. Minimal criteria for defining multipotent mesenchymal stromal cells. The International Society for Cellular Therapy position statement. Cytotherapy. 2006;8:315-317.
3. Squillaro T, Peluso G, Galderisi U. Clinical Trials With Mesenchymal Stem Cells: An Update. Cell Transplant. 2016;25:829-848.
4. Somuncu ÖS, Taşlı PN, Şişli HB, Somuncu S, Şahin F. Characterization and Differentiation of Stem Cells Isolated from Human Newborn Foreskin Tissue. Appl Biochem Biotechnol. 2015;177:1040-1054.
5. Skrzypczyk A, Giri S, Bader A. Generation of induced pluripotent stem cell line from foreskin fibroblasts. Stem Cell Res. 2016;17:572-575.
6. Foty R. A Simple Hanging Drop Cell Culture Protocol for Generation of 3D Spheroids. J Vis Exp. 2011:2720.
7. Ong CS, Zhou X, Han J, Huang CY, Nashed A, Khatri S, Mattson G, Fukunishi T, Zhang H, Hibino N. *In vivo* therapeutic applications of cell spheroids. Biotechnol Adv. 2018;36:494-505.
8. Zeghichi S, Kallithraka S, Simopoulos AP. Nutritional Composition of Molokhiya (Corchorus olitorius) and Stamnagathi (Cichorium spinosum). In: Simopoulos AP, Gopalan C, eds. Karger: World Rev Nutr Diet; 2003:1-21.
9. Handoussa H, Hanafi R, Eddiasty I, El-Gendy ME, Khatib AE, Linscheid M, Mahran L, Ayoub N. Anti-inflammatory and cytotoxic activities of dietary phenolics isolated from Corchorus olitorius and Vitis vinifera. J Funct Foods. 2013;5:1204-1216.
10. Ihan S, Savaroğlu F, Çolak F. Antibacterial and Antifungal Activity of Corchours olitorius L. (Molokhia) Extracts. Int J Nat Eng Sci. 2007;1:59-61.
11. Soykut G, Becer E, Calis I, Yucecan S, Vatansever S. Apoptotic effects of Corchorus olitorius L. leaf extracts in colon adenocarcinoma cell lines. Prog Nutr. 2018;20:689-698.
12. Azuma K, Nakayama M, Koshioka M, Ippoushi K, Yamaguchi Y, Kohata K, Yamauchi Y, Ito H, Higashio H. Phenolic antioxidants from the leaves of Corchous Olitorius L. J Agric Food Chem 1999;47:3963-3966.
13. Darcansoy İşeri Ö, Yurtcu E, Sahin FI, Haberal M. Corchorus olitorius (jute) extract induced cytotoxicity and genotoxicity on human multiple myeloma cells (ARH-77). Pharm Biol. 2013;51:766-770.
14. Yagi H, Tan J, Tuan RS. Polyphenols suppress hydrogen peroxide-induced oxidative stress in human bone-marrow derived mesenchymal stem cells. J Cell Biochem. 2013;114:1163-1173.
15. Safaeinejad Z, Kazeminasab F, Kiani-Esfahani A, Ghaedi K, Nasr-Esfahani MH. Multi-effects of Resveratrol on stem cell characteristics: Effective dose, time, cell culture conditions and cell type-specific responses of stem cells to Resveratrol. Eur J Med Chem. 2018;155:651-657.
16. Lin RZ, Chou LF, Chien CCM, Chang HY. Dynamic analysis of hepatoma spheroid formation: Roles of E-cadherin and beta1-integrin. Cell Tissue Res. 2006;324:411-422.
17. Huerta S, Goulet EJ, Livingston EH. Colon cancer and apoptosis. Am J Surg. 2006;191:517-526.
18. Scholzen T, Gerdes J. The Ki-67 protein: from the known and the unknown. J Cell Physiol. 2000;182:311-322.
19. Li CJ, Huang SY, Wu MY, Chen YC, Tsang SF, Chyuan JH, Hsu HY. Induction of apoptosis by ethanolic extract of Corchorus olitorius leaf in human hepatocellular carcinoma (HepG2) cells via a mitochondria-dependent pathway. Molecules. 2012;17:9348-9360.
20. Baral S, Pariyar R, Kim J, Lee HS, Seo J. Quercetin-3-O-glucuronide promotes the proliferation and migration of neural stem cells. Neurobiol Aging. 2017;52:39-52.
21. Pang X, Cong Y, Bao NR, Li YG, Zhao JN. Quercetin stimulates bone marrow mesenchymal Stem Cell Differentiation through an Estrogen Receptor-Mediated Pathway. Biomed Res Int 2018:1-11.

Turk J Pharm Sci 2020;17(3):271-279
DOI: 10.4274/tjps.galenos.2019.69875

ORIGINAL ARTICLE

In Vitro Studies of *Jatropha curcas* L. Latex Spray Formulation for Wound Healing Applications

Yara İyileşmesine Yönelik *İn Vitro Jatropha curcas* L. Lateks Sprey Formülasyonu Çalışmaları

Kittiya TINPUN[1], Titpawan NAKPHENG[1], Alwar Ramanujam PADMAVATHI[1], Teerapol SRICHANA[1,2]*

[1]Prince of Songkla University, Drug Delivery System Excellence Center, Songkhla, Thailand
[2]Prince of Songkla University Faculty of Pharmaceutical Sciences, Department of Pharmaceutical Technology, Songkhla, Thailand

ABSTRACT

Objectives: There is an increasing demand for wound healing products of natural origin. Our objective was to develop a spray formulation from *Jatropha curcas* (*J. curcas*) L. latex extracts for wound healing applications.

Materials and Methods: *J. curcas* L. latex was subjected to solvent extraction. The phytochemical structure was elucidated by ^{1}H-NMR and confirmed by liquid chromatography-mass spectrometer spectrometry. A topical spray formulation prepared from *J. curcas* latex extracts was evaluated in terms of its antimicrobial activity and radical scavenging activity. The toxicity of the formulation on fibroblast cell lines, collagen production, and wound healing activities were tested.

Results: The ^{1}H-NMR and mass spectrometric analyses revealed the pure compound as curcacycline A. The *J. curcas* latex extract formulation had radical scavenging and antibacterial activities. Moreover, the formulation was not toxic to the human fibroblast cells and it stimulated collagen production and healed cell injury in 24 h.

Conclusion: The *J. curcas* latex extract promoted wound healing after cell injury. Our findings indicate the possibility of utilizing the *J. curcas* latex extract spray formulation as a potential antibacterial, antioxidant, and wound healing product from nature.

Key words: *Jatropha curcas* L. latex, wound healing, spray formulation, collagen production, antioxidant

ÖZ

Amaç: Doğal kaynaklı yara iyileştirici ürünlere olan talep giderek artmaktadır. Amacımız, yara iyileşmesinde etkili *Jatropha curcas* (*J. curcas*) L. lateks ekstrelerinden bir sprey formülasyonu geliştirmektir.

Gereç ve Yöntemler: *J. curcas* L. lateks solvan ekstraksiyonuna tabi tutuldu. Fitokimyasal yapı, ^{1}H-NMR ile aydınlatıldı ve LC-MS spektrometrisi ile doğrulandı. *J. curcas* lateks ekstrelerinden hazırlanan topikal bir sprey formülasyonu, antimikrobiyal aktivitesi ve radikal süpürücü aktivitesi açısından değerlendirildi. Formülasyonun, fibroblast hücre hatları üzerindeki toksisitesi, kollajen üretimine etkisi ve yara iyileştirme aktivitesi test edildi.

Bulgular: ^{1}H-NMR ve kütle spektrometrisi analizleri, saf bileşiğin kurkasiklin A olduğunu ortaya koydu. *J. curcas* lateks ekstraktı formülasyonunun radikal temizleyici ve antibakteriyel aktiviteleri vardı. Ayrıca, formülasyonun insan fibroblast hücrelerinde toksik etki göstermediği ve 24 saat içinde kollajen üretimini uyardığı *ve* hücre hasarını iyileştirdiği tespit edildi.

Sonuç: *J. curcas* lateks özütünün, hücre hasarından sonra yara iyileşmesini desteklediği gösterildi. Bulgularımız, *J. curcas* lateks ekstraktının sprey formülasyonunun doğal potansiyel bir antibakteriyel, antioksidan ve yara iyileştirici ürün olarak kullanılma olasılığı olduğunu göstermiştir.

Anahtar kelimeler: *Jatropha curcas* L. lateks, yara iyileşmesi, sprey formülasyonu, kollajen üretimi, antioksidan

***Correspondence: E-mail:** teerapol.s@psu.ac.th, **Phone:** +66 74288979 **ORCID-ID:** orcid.org/0000-0002-4772-2276
Received: 08.11.2018, **Accepted:** 14.02.2019

INTRODUCTION

A wound is the result of an injury that damages the dermis of the skin. It may vary from a simple, acute wound to a chronic wound. Naturally, the human body possesses the potential to initiate wound healing to replace the damaged cellular structures and tissue layers. Wound healing is a complex process orchestrated by sequential events arising from homeostasis, inflammation, and proliferation/granulation to remodeling/maturation.[1] Wound care is a million-dollar industry and encompasses simple topical treatments for deep seated tissue regeneration using stem cell therapy.[2] Wound care determines the appropriate treatment to promote wound healing with minimal infections. Despite medical advancements, there is a mounting demand for alternative treatments from the clinical and economic perspective to treat wounds. In ancient times, tribal healers used plant parts to cure wounds. Even now, plants are considered an enormous repository of novel bioactive agents. It has been determined that at present there are more than 450 plant species being exploited for their wound healing ability,[3] yet the search for novel wound healing agents from natural resources with minimal scar formation is incessant. In this context, *Jatropha curcas* (*J. curcas*) L., a plant used for wound healing in folk medicine, was evaluated for its wound healing ability *in vitro* to substantiate its traditional use. In addition, the present study attempted to utilize the Thai traditional knowledge by formulating the *J. curcas* extract as a spray suitable for modern day use. It has been used in folk medicine to treat burns, dermatitis, syphilis, inflammation, rash, rheumatism, scabies, and sores, and its latex is known to possess wound healing activity.[4,5] In addition to its enormous applications in folk medicine, the natural binding ability of latex powder in tablets has also been demonstrated.[6] Fagbenro Beyioku et al.[7] and coworkers reported the antiparasitic activity of *J. curcas* sap and proposed it as an effective malaria vector control agent. Preliminary evaluation of the anti-HIV activity of *J. curcas* leaf extract was also reported.[8] *J. curcas* latex reduced the blood clotting time[9] and *in vitro* studies of latex extracts have clearly demonstrated wound healing activity.[10] Although *J. curcas* latex has been used in traditional wound healing, studies have revealed that pure undiluted latex caused caustic lesions in mouse models.[11] The sap was also found to be highly toxic to mice when administered orally or intraperitoneally.[7] Against this backdrop, the present study aimed to evaluate the bioactivity of a spray formulation containing pure compound from *J. curcas* latex and evaluate its *in vitro* antimicrobial, antioxidant, and wound healing potential.

MATERIALS AND METHODS

Apparatus, cell lines, microbial species, and reagents

The normal phase and reversed phase for thin layer chromatography (TLC) and silica gel for column chromatography were purchased from Merck (Merck, Darmstadt, Germany). The ^{1}H-NMR spectrum was characterized by Varian fourier transform-NMR spectrometer (Varian, Palo Alto, CA, USA). The molecular weight and fragmentation pattern of purified samples were further analyzed by electrospray ionization (ESI)-liquid chromatograph mass spectrometer (Micromass LCT, Altrincham, UK). The solvent content in the formulation after spraying was detected by gas chromatograph-mass spectrometer (MS) (Trace GC Ultra, Thermo Scientific, Inc., TX, USA) using an AT-WasMS capillary column (30 mmx0.25 mm; 0.25-µm film thickness). High performance liquid chromatography [(HPLC), Waters, Milford, MA, USA] was used to investigate the physical stability of the spray formulation. Scanning electron microscopy [(SEM)-Quanta; FEI Quanta 400, model: 1450 EP, Carl Zeiss Micro-Imaging, Inc., Thornwood, NY, USA] was used to obtain information about the morphology and film thickness of the spray formulation. The antibacterial activity was evaluated using gram-positive bacteria including *Staphylococcus aureus* ATCC 25925 (*S. aureus*) and *Staphylococcus epidermidis* ATCC35983 (*S. epidermidis*) and gram-negative bacteria including *Escherichia coli* ATCC 25922 (*E. coli*) and *Pseudomonas aeruginosa* ATCC 27853 (*P. aeruginosa*) that were compared with clinical isolates of *S. aureus*, *S. epidermidis*, *E. coli*, and *P. aeruginosa* (derived from clinical infections from Songkla Nagarind Hospital, Hat Yai, Thailand). The bacteria were maintained in brain heart infusion (BHI) broth (Becton, Dickinson and Company, NJ, USA). The cytotoxicity test was evaluated by a cell proliferation and viability assay using the human keratinocyte cell line (HaCaT) (Cell Lines Service GmbH, Eppelheim, Germany) and the human fibroblast cell line (BJ) (ATCC, Manassas, VA, USA). Dulbecco's modified eagle medium (DMEM), Eagle's minimum essential medium (EMEM), fetal bovine serum (FBS), and antibiotics (penicillin and streptomycin) were purchased from Gibco (Grand Island, NY, USA). The Sircol® collagen assay kit was purchased from Biocolor Life Science Assays (Belfast, Northern Ireland, UK). The epidermal growth factor Proteoglycan positive control (IPC) standard was bought from Ichimaru Pharcos (Ichimaru Pharcos Co. Ltd., Tokyo, Japan). A phase-contrast microscope (Olympus CK2, Tokyo, Japan) was used to photograph the monolayer of cells and the distance between the scratches was analyzed using an image processing program, Image J1.42q (Wayne Rasband, National Institute of Health, Bethesda, MD, USA). All other reagents were of analytical grade and used without further purification.

Collection of Jatropha latex

J. curcas L. is a shrub belonging to the family Euphorbiaceae. It is originally native to the tropical areas of the Americas from Mexico to Argentina, and has spread throughout the world in tropical and subtropical regions. *J. curcas* is 2-5 m tall and produces a watery latex.[12] In the present work, the latex was collected from *J. curcas* (specimen voucher number: SKP 071100301) plants at the botanical garden maintained by the Department of Pharmaceutical Botany and Pharmacognosy, Prince of Songkla University, Hat Yai, Thailand. The latex was obtained by cutting the leaf stalk and the collected latex was immediately stored at 4 ˚C until further use.

Extraction, isolation, and purification

Latex (100 mL, 107.8 g) was diluted with 20 mL of distilled

water and the mixture was extracted with *n*-hexane (200 mLx3 replications). The solvent phase was separated and the aqueous phase was further extracted with ethyl acetate (200 mLx3 replications) followed by butanol (200 mLx3 replications). The remaining aqueous phase was allowed to dry and the other solvent extracts were evaporated using a rotary evaporator. All the test extracts were primarily isolated by TLC using normal and reverse phase precoated silica plates. The mobile phase was optimized using various solvents such as hexane, ethyl acetate, acetone, dichloromethane, chloroform, acetonitrile, and methanol for the normal phase, whereas different ratios of methanol and water were used to optimize the mobile phase for the reverse phase TLC. The TLC plates were sprayed with 20% H_2SO_4 and developed on a hot plate (100 ˚C for 90 s). The solvent mixture that yielded better separation in TLC was used as a mobile phase for column chromatography using silica gel (230-400 mesh). Dried butanol extract (3 g) was loaded on the silica column (6x32 cm) and sequentially eluted with various ratios of chloroform:ethyl acetate:methanol (7:2:1, 6:3:1, and 5:4:1). Fractions were collected, concentrated, and tested for purity by TLC. Purified fractions were subjected to ^{1}H-NMR in deuterated dimethyl sulfoxide (DMSO)-d_7 and the spectra were recorded at 500 MHz. The spectrum was processed using vnmr software running on the Solaris operating system. The molecular weight and fragmentation patterns were analyzed by ESI-liquid chromatography- (LC) MS. The ESI-LC-MS instrument was operated using an ESI source (positive ion mode), with a source voltage of 4.0 kV, spray current of 100.0 µA, and a desolvation temperature of 130 ˚C (source temperature: 120 ˚C; acquisition mode: scan 100-1500 m/z). Nitrogen gas was used for desolvation and as tube lens gas.

Preparation of the spray formulation

Half a percent *J. curcas* latex extract (butanol extract) or curcacycline A was dissolved in ethanol and acetone as a co-solvent (80:20 v/v). One percent sorbitan monooleate (Span® 80) was used as a wetting and lubricating agent. The mixture was stirred overnight until a clear solution formed. The clear solution (4 g) was put into a spray canister and 8 g of hydrofluoroalkane propellant (HFA134a) was added and then it was sealed. These formulations are henceforth referred to as *J. curcas* latex extract formulation (JcF) and curcacycline A formulation (CAF).

Stability tests

The physical stability of JcF was observed for 3 months during storage by monitoring the pH, weight, color change, and appearance of the sediment. The curcacycline A was resolved by HPLC in a C18 reverse phase analytical column (150x4.6 mm; 5 µm) using a methanol and water isocratic system (50:50). The sample (15 µL) was automatically injected and elution was performed for 15 min. The results were detected at the optimum wavelength of optical density $(OD)_{266}$ nm. The LC was performed using the Waters Alliance 2690 liquid chromatography system C_{18} column (2.1x100 mm; 3.5 µm).

Gas chromatography (GC)-mass spectrometry (MS) of the spray formulation

GC-MS was employed to detect acetone in case it was left as a residue after spraying. The JcF was analyzed by GC-MS to trace the solvent level of the final product after application. JcF was sprayed 10 times in a glass beaker from a distance of 10 cm and briefly dried at ambient temperature. The dried content was reconstituted in acetonitrile and subjected to GC-MS analysis with an AT-WaxMS capillary column (30 m×0.25 mm; 0.25-µm film thickness) using the following conditions: column oven temperature: initial 50 ˚C, hold for 9 min; ramp to 120 ˚C at 2 ˚C min^{-1}; ramp to 200 ˚C at 25 ˚C min^{-1}, hold for 5 min; injection temperature: 150 ˚C; injection mode: splitless; sampling time: 1.00 min; constant flow: 1 mL min^{-1}; ionization mode: electron ionization; acquisition mode: scan, 30-500 amu; ion source temperature: 230 ˚C. The chromatogram obtained was identified by comparison with the mass spectral database (NIST and Wiley Library, 2005).

The scanning electron microscopy analysis

SEM-Quanta was used to obtain information on the morphology and film thickness of the spray formulation. The spray formulation was sprayed on stubs and coated with gold/palladium (20 nm). The specimens were viewed under a Zeiss EVO LS10 microscope using high-vacuum mode at 10 kV.

Antioxidant activity

The antioxidant activity was quantitatively investigated. In the 2,2-diphenyl-1-picrylhydrazyl (DPPH) radical scavenging activity test, various concentrations (7.75, 15, 31, 62, and 124 µg/mL) of *J. curcas* latex extract, JcF, or CAF were tested for their free radical scavenging activity using DPPH.[13] A blank sample (ethanol:acetone (80:20 v/v), 1% sorbitan monooleate Span® 80) was used as a negative control. The DPPH solution (0.2 mM) was freshly prepared by dissolving 7.89 µg of DPPH in 100 mL of methanol. Test extracts (1 mL) were mixed with 2 mL of DPPH solution and incubated in the dark for 30 min. After incubation, the OD was read at 517 nm. The DPPH solution was mixed with 1 mL of DMSO as a negative control and ascorbic acid as a positive control. The antioxidant activity was calculated using the following formula:

$$\text{Antioxidant activity (\%)} = \frac{OD_{517} \text{ of negative control} - OD_{517} \text{ of sample}}{OD_{517} \text{ of negative control}} \times 100$$

Antibacterial activity

Antibacterial activity was tested using two strains of gram-positive bacteria, *S. aureus* and *S. epidermidis*, and gram-negative bacteria, *E. coli* and *P. aeruginosa*. The bacteria were maintained in BHI broth at 37 ˚C by the cylinder cup diffusion method and the clear zone of *J. curcas* latex extract, JcF, and CAF was screened. The stock solution of all extract was prepared at 500 mg/mL and then the extract solution was loaded into the cylinder cup to obtain a final concentration of 10 mg/cup. After incubation at 35 ˚C for 24 h, the inhibition zones (mm) were measured by vernier caliper, recorded, and considered an indication of antibacterial activity.

Broth microdilution was employed to obtain the minimum inhibitory concentrations (MICs) and minimum bactericidal concentrations (MBCs). ATCC strains and clinical isolate strains of *S. aureus*, *S. epidermidis*, *E. coli*, and *P. aeruginosa* were used in this assay. The assay was performed in 96 well polystyrene plates. Wells containing 100 µL of BHI broth with formulation were inoculated with 10 µL of bacterial suspension containing 10^5 CFU/mL. The plate was incubated at 37 ˚C for 18 h. After incubation, 30 µL of resazurin (0.02% w/v) was added to each well and the plate was further incubated for 5 h. The MIC was determined as the lowest concentration of test extract in which pink coloration was not observed. Vancomycin and gentamicin were used as positive controls. For the determination of the MBC, the agar dilution method was employed.[14] A blank sample (ethanol:acetone (80:20 v/v), 1% sorbitan monooleate Span® 80) was used as a negative control.

Evaluation of cytotoxicity

The HaCaT and the human fibroblast cell line (BJ) were maintained in DMEM and EMEM, respectively, supplemented with 10% FBS and antibiotics (100 U penicillin and 100 U/mL streptomycin) at 37 ˚C with 5% CO_2. The cytotoxicity test was evaluated by a cell proliferation and viability assay using the HaCaT and BJ cell lines.[15] The cells ($2x10^4$ cells/mL) were seeded into the wells of a 96 well plate with their respective medium. Various concentrations (7.75, 15, 31, 62, and 124 µg/mL) of *J. curcas* latex extract, JcF, and CAF were added to the wells, followed by incubation at 37 ˚C for 24 h with 5% CO_2. Cells without tested samples served as a control. In addition, a blank sample (ethanol:acetone (80:20 v/v), 1% sorbitan monooleate Span® 80) was used as a negative control. After incubation, the media were removed and the cells were rinsed with sterile phosphate buffered saline (PBS). The wells were supplemented with 100 µL of fresh media and 10 µL of 3-(4, 5-dimethylthiazol-2-yl)-2, 5-diphenyltetrazoliumbromide (MTT, 5 mg/mL) and incubated at 37 ˚C for 4 h. After incubation, the contents of the wells were removed and the formazan crystals formed were dissolved by adding 200 µL of DMSO and measured at 540 nm. The percentage of cell viability was calculated using the following formula:

$$\text{Viability (\%)} = \frac{\text{Control OD}_{540} - \text{Treated OD}_{540}}{\text{Treated OD}_{540}} \times 100$$

Estimation of the soluble collagen produced by human fibroblast cells

For estimation of the soluble collagen produced by human fibroblast cells, the soluble collagen produced by the BJ cell line was determined.[16] BJ cells were seeded into the wells of a 96 well plate at an initial concentration of $2x10^4$ cells/mL in EMEM supplemented with 10% FBS. Various concentrations (7.75, 15, 31, 62, and 124 µg/mL) of extracts, *J. curcas* latex extract, JcF, and CAF, were added to the cells and incubated at 37 ˚C for 24 h in a 5% CO_2 atmosphere. Proteoglycan IPC was extracted from nasal cartilage of *Oncorhynchus keta* (salmon) having a property like epidermal growth factor. It was used as a positive control. BJ cells alone served as a control. After incubation, 100 µL of supernatants were collected separately and the total soluble collagen (type 1) was quantified using 1 mL of a Sircol® collagen assay kit. The mixture was incubated at room temperature for 30 min and then subjected to centrifugation at 15.000 rpm for 10 min. The collagen was obtained as a pellet and dissolved in 1 mL of an alkaline reagent (0.5 M NaOH). The solution was transferred to a 96 well plate and the optical density was measured at 540 nm. A standard curve was prepared using standard bovine skin collagen type 1 obtained from American disease-free animals. The soluble collagen produced by BJ cells in the presence and absence of JcF was calculated based on the standard curve. A blank sample (ethanol:acetone (80:20 v/v), 1% sorbitan monooleate Span® 80) was used as a negative control.

Assay for the cell culture wound closure

The wound closure assay in cultured cells was performed to assess the *in vitro* wound healing ability of JcF in the HaCat and BJ cell lines.[16] The wells of a 6 well plate were seeded with $5x10^4$ cells/mL with appropriate culture medium and allowed to grow as a confluent monolayer. A linear scratch was then created using a sterile tip and the wells were washed with sterile PBS to remove cell debris. Culture medium (2 mL) was added to the wells with (treated, 31 µg/mL) or without JcF (blank sample) as a negative control. This was considered day 0 and photographs of the monolayer were acquired at 100x magnification using a phase-contrast microscope. The plates were incubated at 37 ˚C for 24 h in a 5% CO_2 atmosphere. After incubation, the cells were again photographed on day 1. These images were examined using an image processing program and the distance between the scratches was measured and the cell migration rate was calculated using the following formula:

$$\text{Migration rate (\%)} = \frac{\text{Distance between scratches (day 0)-Distance on day 1}}{\text{Distance on day 0}} \times 100$$

Statistical analysis

Assays were performed in triplicate and the values were expressed as mean ± standard deviation. One-way ANOVA was carried out using SPSS version 17.0. The significance was set at $p \leq 0.05$.

Ethics Committee approval and patient informed consent were not required as the experiment did not involve animal or human studies.

RESULTS

Extraction, isolation, and purification

Solvent extraction (hexane, ethyl acetate, butanol, and water extracts) of the *J. curcas* latex (107.8 g) yielded a total of 10.81 g that comprised the extracts from hexane (5 g; 19%), ethyl acetate (5 g; 19%) butanol (4.81 g; 30%) and water (5.36 g; 33%). All the test extracts were subjected to TLC using normal and reverse phase precoated silica plates and it was found that the hexane, ethyl acetate, butanol, and water fractions had similar TLC profiles (data not shown), but a few additional bands were observed in the butanol fraction. Thus, the butanol fraction was chosen for further purification with the silica

gel open column chromatography. Hence, the butanol fraction (3 g) was subjected to further fractionation by open column chromatography. Among the 200 fractions collected, we found that fractions 9 and 10 yielded a single abundant band in the TLC with a retention factor of 0.29. Then the pure compound from fractions 9 and 10 was further identified by ^{1}H-NMR and found to be curcacycline A (pure compound), which is a major constituent of *J. curcas* latex (Table 1). Curcacycline A was further confirmed by mass spectrometric analysis corresponding to $C_{37}H_{67}N_8O_9^+Na^+$ (Figure 1).

Spray formulation

J. curcas JcF was prepared from the butanol extract fraction employing various compositions (Table 2) and it was found that the formulation with *J. curcas* extract (0.5%), ethanol (78.5%), acetone (20%), and Span® 80 (1%) had preserved its bioactivity. JcF (pH: 7) exhibited a clear solution (Figure 2). In addition, CAF was also prepared in the same conditions with JcF and it was seen that the formulation with curcacycline A (0.5%), ethanol (78.5%), acetone (20%), and Span® 80 (1%) showed a clear solution without precipitation (data not shown). We collected both formulations for further investigation of bioactivity.

Table 1. Comparison of ^{1}H-NMR of pure compound with reported curcacycline A[17]

	Pure compound	Curcacycline A
	δ (ppm), *J* coupling constants (Hz), Integration proton, (500 MHz, DMSO-d_6)	δ (ppm), *J* coupling constants (Hz), Integration proton (400 MHz, DMSO-d_6
1.	8.521 (brs., 1H)	8.67 (t, *J*=5.7 Hz, 1H)
2.	8.46-8.32 (brs., 1H, 1H)	8.63-8.54 (m, 1H)
3.	-	8.51 (s, 1H)
4.	8.16 (d, *J*=7.5 Hz, 1H)	8.17 (d, *J*=8.5 Hz, 1H)
5.	8.04 (brs., 1H)	8.03 (s, 1H)
6.	7.80 (d, *J*=8 Hz, 1H)	7.73 (d, *J*=7.5 Hz, 1H)
7.	7.59 (brs., 1H, 1H)	7.53 (d, *J*=8.9 Hz, 1H)
8.	-	7.39 (d, *J*=9.9 Hz, 1H)
9.	5.30 (d, *J*=10.5 Hz, 1H)	5.34 (d, *J*=10.8 Hz, 1H)
10.	4.67 (d, *J*=7.5 Hz, 1H)	4.76 (dd, *J*=9.9, 3.7 Hz, 1H)
11.	4.49 (brs., 1H)	4.60 (dd, *J*=14.2, 8.3 Hz, 1H)
12.	4.30-4.26 (m, 2H)	4.37-4.22 (m, 2H)
13.	4.11-4.09 (dd, *J*=8 Hz, 4.5 Hz, 1H)	4.12-4.05 (m, 1H)
14.	3.96-3.86 (dd, dd, (*J*=14 Hz, 7.5 Hz), (*J*=17 Hz, 7 Hz), 4H)	3.96-3.79 (m, 4H)
15.	3.46 (d, *J*=17 Hz, 1H)	3.45 (d, *J*=5.2 Hz, 1H)
16.	3.43 (dd, *J*=11.5 Hz, 5.5 Hz, 1H)	3.40 (d, *J*=4.9 Hz, 1H)
17.	2.32-2.26 (m, 1H)	3.15 (d, *J*=5.2 Hz, 1H)
18.	1.96-1.89 (m, 1H)	2.50-2.46 (m, 1H)
19.	1.79 (d, *J*=13.5, 1H)	2.32 (td, *J*=13.8, 6.9 Hz, 1H)
20.	1.64-1.40 (m, 13H)	1.69-1.18 (m, 13H)
21.	0.90-0.80 (m, 32H)	1.08-0.69 (m, 32H)

NH

NH

s: Singlet, d: Doublet, dd: Doublet of doublets, m: Multiplet, brs: Broad singlet, DMSO: Dimethyl sulfoxide

Chemical and physical stability tests

Storage did not affect the stability, pH, weight, color, or homogeneity of JcF. HPLC analysis of JcF revealed a major peak eluted at 1.98 min with 81% recovery. LC-MS analysis and the ESI-MS spectra fragmentation pattern revealed the major constituent as curcacycline A. The GC-MS analysis revealed the presence of 7.4% ethanol (data not shown) but acetone residue was not detected due to quick evaporation. The 10.000x micrographs of the spray formulation from SEM are shown in Figure 3. Figure 3A displayed the film on the stub with interspersed droplets and small particles observed on the surface. Furthermore, cross-section SEM revealed that the formulation formed a thin film after spraying on the stub (Figure 3B). Furthermore, curcacycline A was used to formulate the CAF using the same excipient, which revealed similar physical properties to JcF (data not shown).

Antioxidant activity and antibacterial activity

The antioxidant activity of *J. curcas* latex extract, JcF, and CAF is illustrated in Figure 4. The results showed that *J. curcas* latex extract and JcF significantly increased antioxidant activity in a concentration-dependent manner, but CAF did not. In addition, the inhibition zone of antimicrobial activity is given in Table 3. The results revealed that both *J. curcas* latex extract and JcF possessed antibacterial activity with MIC and MBC at 5 mg/mL against both gram-negative and gram-positive bacteria and their clinical isolates, whereas vancomycin and gentamicin exhibited MIC at 1 and 4 µg/mL against gram-positive and gram-negative bacteria, respectively. Notably, an inhibition zone of antimicrobial activity of CAF was not observed against either type of bacteria.

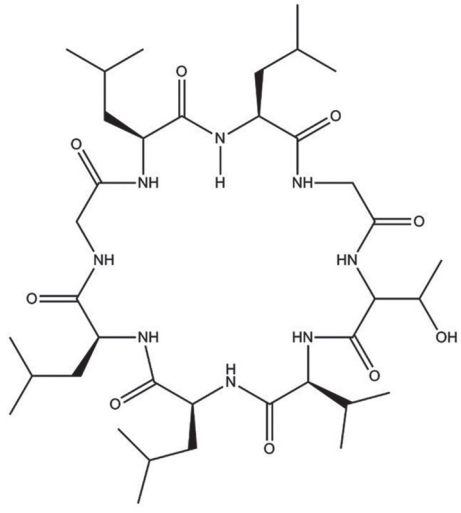

Figure 1. The molecular structure of curcacycline A

Table 2. *Jatropha curcas* extract spray formulation design

Ingredients	Compositions % (w/w)								
	F1	F2	F3	F4	F5	F6	F7	F8	F9
Jatropha curcas extract	0.5	0.5	0.5	0.5	0.5	0.5	0.5	0.5	0.5
Ethanol	78.5	78.5	77.5	75.5	76.9	78	76.5	75.4	78.5
Acetone	20	20	20	20	20	20	20	20	20
PEG 400	-	0.5	1	2	0.5	0.5	1	2	-
Span 80	1	0.5	0.2	1	0.5	0.1	1	0.5	-
Eudragit® E100	-	0.1	0.5	1	0.1	0.5	1	0.1	0.5
Kollidon® VA 64	-	0.1	0.5	1	0.1	0.5	1	0.1	0.5
Kolliphor P	-	1	0.5	0.2	1	0.5	0.2	1	0.5
Test results	✓	x	x	x	x	x	x	x	x

✓: No precipitation, x: Precipitation

Figure 2. Formulation of *Jatropha curcas* latex extract filled in metered dose spray canister

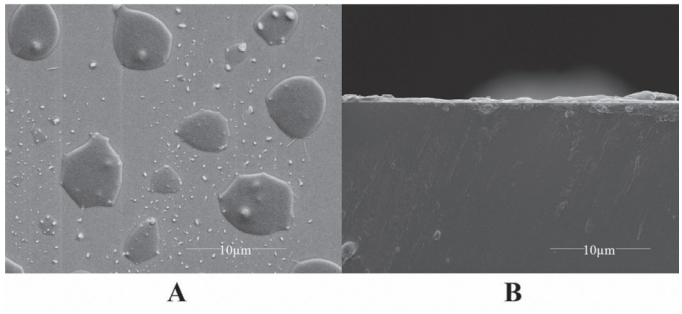

Figure 3. The surface morphology of JcF spray droplets (A) and thin film micrographs of JcF (B)
JcF: *Jatropha curcas* latex extract formulation

Cytotoxicity

The cytotoxicity of *J. curcas* latex extract, JcF, and CAF in HaCat and BJ cells was evaluated by MTT assay. The results revealed that cell viability of HaCat cells was higher than 80% at all concentrations of all tested samples (Figure 5A). However,

Table 3. Antibacterial activity of *Jatropha curcas* extract and JcF against reference and clinical isolates of gram-positive and -negative bacteria. Notably, antibacterial activity of CAF is not shown in this table due to inability to measure its inhibition zone

Pathogen	Strain	Zone of inhibition (mm)	
		J. curcas latex extract	JcF
S. aureus	ATCC25925	23±0.2	25±0.5
	Clinical isolate	15±0.3	14±0.5
S. epidermidis	ATCC35983	23±0.2	27±0.2
	Clinical isolate	20±0.2	20±0.1
E. coli	ATCC25922	23±0.2	21±0.1
	Clinical isolate	12±0.5	12±0.2
P. aeruginosa	ATCC27853	22±0.1	20±0.2
	Clinical isolate	14±0.1	12±0.2

JcF: *Jatropha curcas curcas* latex extract formulation, CAF: Curcacycline A formulation

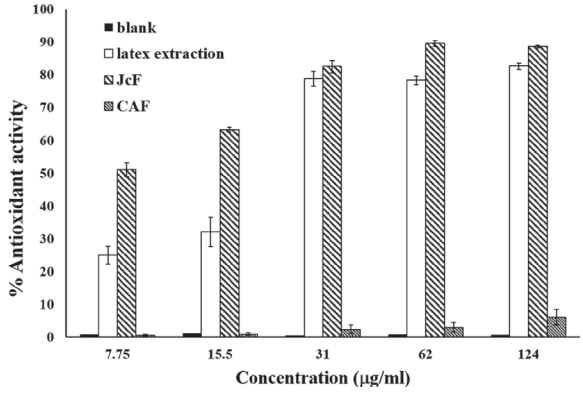

Figure 4. Antioxidant activity of *Jatropha curcas* latex extract, JcF, and CAF. Various concentrations of tested samples were tested for their free radical scavenging activity using 2,2-diphenyl-1-picrylhydrazyl (DPPH). A blank sample (ethanol:acetone (80: 20 v/v), 1% sorbitan monooleate Span® 80) was used as a negative control
JcF: *Jatropha curcas* latex extract formulation, CAF: Curcacycline A formulation

the concentration of 62 and 124 µg/mL *J. curcas* latex extract significantly decreased cell viability of BJ cells while JcF- and CAF-treated BJ cells were not toxic (>80%) (Figure 5B). Notably, JcF- and CAF-treated HaCat and BJ cells displayed more than 80% cell viability at all concentrations (Figure 5).

Collagen production and wound healing

The collagen production after treatment with *J. curcas* latex extract, JcF, and CAF in human fibroblast BJ cells was determined by Sircol assay. The results showed that *J. curcas* latex extract and JcF promoted collagen production in BJ cells in a concentration-dependent manner, whereas collagen production was not observed in CAF-treated cells (Figure 6). In fact, *J. curcas* latex extract slightly promoted collagen production (47-198 pg/mL), while JcF prominently promoted it (179-335 pg/mL). These results revealed that JcF exhibited good collagen production activity and was nontoxic to both cells, but this was not the case for *J. curcas* latex extract or CAF. Thus, we selected JcF for further investigation of wound healing activity. The wound healing in HaCat and BJ cells was also determined using a scratch assay, and the proteoglycan IPC (1 µg/mL) was used as a positive control. In the present study, we used a concentration of 31 µg/mL JcF for wound healing. The results after treatment for 24 h showed that JcF completely promoted wound healing in HaCat and BJ cells (Figures 7A and 7B). Indeed, the wound healing of JcF-treated HaCat cells was more rapid than that of proteoglycan IPC, but was similar in BJ cells.

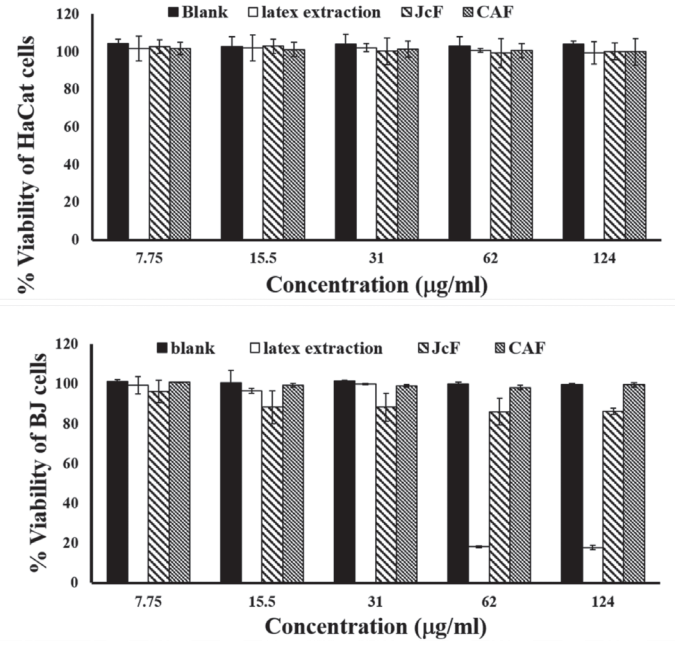

Figure 5. Cytotoxicity evaluation of *Jatropha curcas* latex extract, JcF, and CAF using HaCaT cells (A) and BJ cells (B). A blank sample (ethanol:acetone (80:20 v/v), 1% sorbitan monooleate Span® 80) was used as a negative control

JcF: *Jatropha curcas* latex extract formulation, CAF: Curcacycline A formulation, HaCaT: human keratinocyte cell line, BJ: Human fibroblast cell line

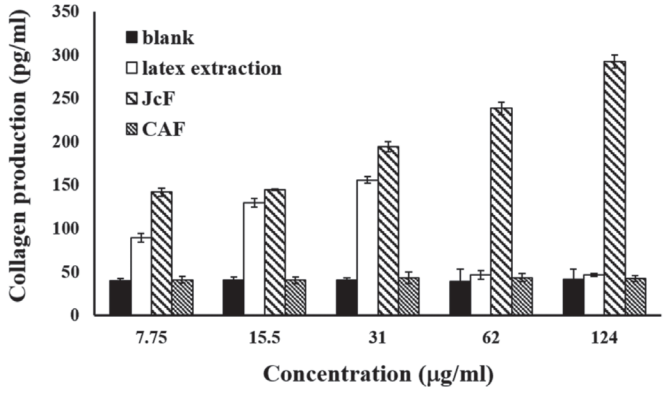

Figure 6. Collagen production by BJ cells treated with various concentrations of *Jatropha curcas* latex extract, JcF, and CAF. A blank sample (ethanol:acetone (80:20 v/v), 1% sorbitan monooleate Span® 80) was used as a negative control

BJ: Human fibroblast cell line, CAF: Curcacycline A formulation, JcF: *Jatropha curcas* latex extract formulation

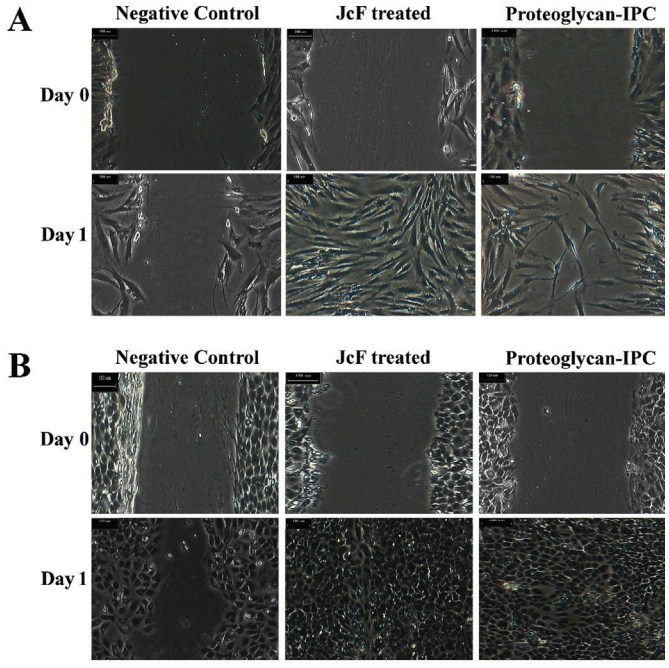

Figure 7. (A) *In vitro* wound closure assay of BJ cells with (JcF and proteoglycan IPC) and without (negative control) treatment. (B) *In vitro* wound closure assay of HaCaT cells with (JcF and proteoglycan IPC) and without (negative control) treatment. Scale bar indicates 100 µm

BJ: Human fibroblast cell line, JcF: *Jatropha curcas* latex extract formulation, IPC: Positive control, HaCaT: Human keratinocyte cell line

DISCUSSION

In the structure elucidation of pure compound from *J. curcas* latex extracts, 1H-NMR revealed eight positions of chemical shifts at 8.52, 8.46, 8.32, 8.16, 8.04, 7.80, and 7.59 ppm (Table 1). This characteristic of ^{1}H-NMR indicates the protons of amino acid residues in curcacycline A, a cyclic octapeptide, which has been reported in various parts of *J. curcas*.[17] In addition, the ESI-MS displayed 789.5 m/z corresponding to $C_{37}H_{67}N_8O_9^+Na^+$ and a

similarity search in the mass spectral database revealed a close match as curcacycline A.[18] The data from ^{1}H-NMR and ESI-MS together supported that pure compound was curcacycline A.

Next, *J. curcas* latex extract and curcacycline A were used to formulate the JcF and CAF using ethanol, acetone, Span® 80, and propellants as excipient. The results revealed that formulations retained properties including pH, weight, color, and homogeneity of the formulation, suggesting this formulation was stable at room temperature. In addition, LC-MS analysis of the JcF revealed that curcacycline A was stable in this formulation. Furthermore, the GC-MS results detected a low amount of ethanol residue due to quick evaporation. The concentration of ethanol in JcF is also less than that of typical antiseptic alcohol, which contains >70% ethanol. The absence of acetone guaranteed the safety of JcF for wounds. In addition, the film thickness of JcF from SEM data suggested that the spray formulation formed a uniform film containing some particles on a film surface. Moreover, cross-section SEM showed that JcF formed a thin layer of film after spraying onto a stub with a thickness of 1-2 µm. For CAF, the physical and chemical properties of this formulation were similar to those of JcF.

In the biological activity studies, *J. curcas* latex extract and JcF had high antioxidant potency, but CAF did not. A similar phenomenon was observed for antimicrobial activity in the microbial tests on gram-positive and -negative bacteria in which *J. curcas* latex extract and JcF showed significant antimicrobial activities, but CAF did not. These suggested that curcacycline A is not an active compound for that biological activity. Most antioxidants are likely to promote wound healing.[19] The *J. curcas* extract illustrated its potential to possess antimicrobial and antioxidant activities. Thus, JcF with antioxidant activity could promote wound healing while preventing reactive oxygen species mediated further cellular damage at the wound site. Most wound infections are colonized by polymicrobial infections consisting of both gram-positive and gram-negative bacteria but many classes of antibiotics are effective against them. Although broad spectrum antibiotics can be administered to control wound infections, this could cause an increase in the incidence of antibiotic resistance in clinical use.[20] In addition, there will be a requirement for the administration of wound healing products. The ability of *J. curcas* extract to control both gram-positive and gram-negative bacteria and its wound healing potential assure its perpetual applications in wound care products. The ability of *J. curcas* latex ointments in controlling pathogens was also proven, which is consistent with the present study.[21,22]

The *in vitro* cytotoxic activity of *J. curcas* latex extract, JcF, and CAF in human keratinocyte and human fibroblast cell lines was investigated. All concentrations of JcF and CAF were not toxic and stimulated cell growth in both cells, but this was not the case for *J. curcas* latex extract in BJ cells, suggesting that JcF and CAF are safer than *J. curcas* latex crude extract. Furthermore, JcF increased collagen production and so will have a positive impact on improving wound healing, but CAF did not. This suggested that curcacycline A is not an active compound for collagen production. Collagen is known to play a major role in wound healing and re-epithelialization, which is crucial for wound closure. It acts as a reinforcing factor by increasing the strength of the wound, which helps to restore the functionality of the skin.[1] Previous studies with *J. curcas* latex revealed its toxicity towards fibroblasts.[23] However, in our studies JcF promoted wound healing potential without inducing any toxicity to fibroblast cells. In the scratch assay, 'expanding' mode of human keratinocytes was enhanced in the presence of JcF and the results were significantly better than the positive control of proteoglycan IPC, suggesting a potentially high wound healing property. This expanding mode may activate wound closure and switch back to a 'balanced' mode that will maintain homeostasis.[24] JcF reduced the time required for wound re-epithelialization, which also hastened the wound healing process, which is already evident from studies carried out with *J. curcas* plant exudates,[25] leaf extract,[26] and ointment prepared from it.[27] The ointment prepared from *J. curcas* was proven to be safe for albino rats as histopathology of liver and kidney were found to be unaltered.[28] The rate of re-epithelialization is important to avoid scarring, which is considered a social stigma. The efficiency of the spray formulation in increasing the natural healing process will aid in the development of better wound care products. Wound healing is a complex process orchestrated by various cellular events from cell migration and proliferation to remodeling. Several studies have shown that the accumulation of oxidative stress hampers the healing process and advised the use of locally applied antioxidants to reduce hypoxia and to promote wound healing.[29,30] Previous research has revealed the active ingredient responsible for wound healing as curcain.[31,32] However, in our study we did not detect curcain in the extraction process.

CONCLUSION

The present study for the first time reports the formulation of a spray from *J. curcas* latex extract with potential applications in wound healing. The formulation of a spray from curcacycline A had no such applications. The study also found that the latex extract formulation preserved bioactive potentials such as antimicrobial, antioxidant, and wound healing without any loss in function. Development of a spray product for treating wounds has advantages over other formulations like ointment or creams that alter the healing process. The ability to induce collagen and prevent microbial infections, and the antioxidant property of JcF greatly enhance its wound healing potentials.

ACKNOWLEDGEMENTS

The authors acknowledge the financial assistance provided by Prince of Songkla University (grant no. PHA570862S). Instrumentation facility provided by the Drug Delivery System Excellence Center, Faculty of Pharmaceutical Sciences, is also thankfully acknowledged. Thanks to Dr. Brian Hodgson for assistance with the English.

Conflicts of interest: No conflict of interest was declared by the authors. The authors alone are responsible for the content and writing of this article.

REFERENCES

1. Kirsner RS, Eaglstein WH. The wound healing processes. Dermatol Clin. 1993;11:629-640.
2. Hu MS, Leavitt T, Malhotra S, Duscher D, Pollhammer MS, Walmsley GG, Maan ZN, Cheung ATM, Schmidt M, Huemer GM, Longaker MT, Lorenz HP. Stem cell-based therapeutics to improve wound healing. Plast Surg Int. 2015:2015.
3. Ghosh PK, Gaba A. Phyto-extracts in wound healing. J Pharm Pharm Sci. 2015;16:760-820.
4. Watt JM, Breyer-Brandwijk MG. The medicinal and poisonous plants of southern and eastern Africa: being an account of their medicinal and other uses, chemical composition, pharmacological effects and toxicology in man and animal. E S. Livingstone. 1962.
5. Balqis U, Darmawi, Iskandar CD, Salim MN. Angiogenesis activity of *Jatropha curcas* L. latex in cream formulation on wound healing in mice. Vet World. 2018;11:939-943.
6. Ghatage S, Patil S, Patrakar R, Patil S. Formulation and Evaluation of Tablet using Latex Powder of *Jatropha curcas* as a Natural Binder. J Appl Pharm Sci. 2015;5:77-81.
7. Fagbenro-Beyioku AF, Oyibo WA, Anuforom BC. Disinfectant/ antiparasitic activities of Jatropha curcas. East Afr Med J. 1998;75:508-511.
8. Dahake R, Roy S, Patil D, Rajopadhye S, Chowdhary A, Deshmukh RA. Potential anti-HIV activity of *Jatropha curcas* Linn. leaf extracts. J Antivir Antiretrovir. 2013;5:160-165.
9. Osoniyi O, Onajobi F. Coagulant and anticoagulant activities in *Jatropha curcas* latex. J Ethnopharmacol. 2003;89:101-105.
10. Villegas LF, Fernandez ID, Maldonado H, Torres R, Zavaleta A, Vaisberg AJ, Hammond GB. Evaluation of the wound-healing activity of selected traditional medicinal plants from Perú. J Ethnopharmacol. 1997;55:193-200.
11. Salas J, Tello V, Zavaleta A, Villegas L, Salas M, Fernández I, Vaisberg A. [Cicatrization effect of *Jatropha curcas* latex (Angiospermae: Euforbiaceae)]. Rev Biol Trop. 1994;42:323-326.
12. Heller J. Physic nut, *Jatropha curcas* L. 1st ed. Rome; IPGRI; 1996:1-66.
13. Balekar N, Katkam NG, Nakpheng T, Jehtae K, Srichana T. Evaluation of the wound healing potential of Wedelia trilobata (L.) leaves. J. Ethnopharmacol. 2012;141:817-824.
14. Mostafa AA, Al-Askar AA, Almaary KS, Dawoud TM, Sholkamy EN, Bakric MM. Antimicrobial activity of some plant extracts against bacterial strains causing food poisoning diseases. Saudi J Biol Sci. 2018;25:361-366.
15. Balekar N, Nakpheng T, Katkam NG, Srichana T. Wound healing activity of ent-kaura-9(11), 16-dien-19-oic acid isolated from *Wedelia trilobata* (L.) leaves. Phytomedicine. 2012;19:1178-1184.
16. Aramwit P, Kanokpanont S, De-Eknamkul W, Kamei K, Srichana T. The effect of sericin with variable amino-acid content from different silk strains on the production of collagen and nitric oxide. J Biomater Sci Polym Ed. 2009;20:1295-1306.
17. Van den Berg AJ, Horsten SF, Kettenes-van den Bosch JJ, Kroes BH, Beukelman CJ, Leeflang BR, Labadie RP. Curcacycline A--a novel cyclic octapeptide isolated from the latex of *Jatropha curcas* L. FEBS Lett. 1995;358:215-218.
18. Insanu M, Anggadiredja J, Kayser O. Curcacycline A and B - new pharmacological insights to an old drug. Int J Appl Res Nat Prod. 2012;5:26-34.
19. Kefayati Z, Motamed SM, Shojaii A, Noori M, Ghods R. Antioxidant activity and phenolic and flavonoid contents of the extract and subfractions of euphorbia *Splendida Mobayen*. Pharmacognosy Res. 2017;9:362-365.
20. Dohmen PM. Antibiotic resistance in common pathogens reinforces the need to minimise surgical site infections. J Hosp Infect. 2008;70(Suppl 2):15-20.
21. Oyi RA, Onaolapo JA, Haruna KA. Evaluation of *Jatropha curcas* latex ointment formulations *in vitro* and *in vivo*. J Pharm Bioresour. 2005;2:5-12.
22. Arekemase MO, Kayode RMO, Ajiboye AE. Antimicrobial activity and phytochemical analysis of *Jatropha Curcas* plant against some selected microorganisms. Int J Biol 2011;3:52-59.
23. Siregar F, Akbar SMS. Cytotoxicity of *Jatropha curcas* (Euphorbiaceae) latex on fibroblast by MTT assay. Med J Indones. 2000;23:143-148.
24. Roshan A, Murai K, Fowler J, Simons BD, Nikolaidou-Neokosmidou V, Jones PH. Human keratinocytes have two interconvertible modes of proliferation. Nat Cell Biol. 2016;18:145-156.
25. Ligha AE, Fawehimi HB. Histopathological observations of the wound healing properties of plant exudates of *Jatropha curcas* Linn. J Exp Clin Anat. 2009;7:17-21.
26. Odoh UE, Ezugwe CO, Menkiti C, Ezejiofo M. Chromotographic and wound healing studies of *Jatropha curcas* (Euphorbiacea). J Pharm Allied Sci. 2011;7:2.
27. Esimone CO, Nworu CS, Jackson CL. Cutaneous wound healing activity of a herbal ointment containing the leaf extract of *Jatropha curcas* L. (Euphorbiaceae). Int J App Res Nat Prod. 2008;14:1-4.
28. Nwala, Omeni C, Akaninwor JO, Monanu MO. Use of extracts of *Jatropha Curcas* leaf formulated in a simple ointment base in wound healing activities: how safe is it? International Journal of Engineering Science Invention. 2013;2:53-57.
29. Sen CK, Khanna S, Gordillo G, Bagchi D, Bagchi M, Roy S. Oxygen, oxidants, and antioxidants in wound healing: an emerging paradigm. Ann N Y Acad Sci. 2002;957:239-249.
30. Fitzmaurice SD, Sivamani RK, Isseroff RR. Antioxidant therapies for wound healing: A clinical guide to currently commercially available products. Skin Pharmacol Physiol. 2011;24:113-126.
31. Nath LK, Dutta SK. Extraction and purification of curcain, a protease from the latex of *Jatropha curcas* Linn. J Pharm Pharmacol. 1991;43:111-114.
32. Nath LK, Dutta SK. Wound healing responses of the proteolytic enzyme curcain. Indian J Pharmacol. 1992;24:114-115.

Turk J Pharm Sci 2020;17(3):280-284
DOI: 10.4274/tjps.galenos.2019.30633

ORIGINAL ARTICLE

Pyrophen Isolated from the Endophytic Fungus *Aspergillus fumigatus* Strain KARSV04 Synergizes the Effect of Doxorubicin in Killing MCF7 but not T47D Cells

Endofitik Mantar *Aspergillus fumigatus* KARSV04 Suşundan İzole Edilen Pirofen Doksorubisinin MCF7 Hücrelerini Öldürme Etkisini Sinerjize Etmiş T47D Hücreleri Üzerindeki Etkisini Değiştirmemiştir

Puji ASTUTI[1]*, Ika Buana JANUARTI[2], Naelaz Zukhruf Wakhidatul KIROMAH[3], Hidayah Anisa FITRI[4], Wahyono WAHYONO[1], Subagus WAHYUONO[1]

[1]Universitas Gadjah Mada Faculty of Pharmacy, Department of Pharmaceutical Biology, Yogyakarta, Indonesia
[2]Sultan Agung Islamic University Faculty of Medicine, Pharmacy College, Semarang, Indonesia
[3]Stikes Muhammadiyah Gombong, Kebumen, Indonesia
[4]Universitas Muhammadiyah Purwokerto Faculty of Pharmacy, Banyumas, Indonesia

ABSTRACT

Objectives: Pyrophen, an amino acid-pyrone derivative isolated from *Aspergillus fumigatus* strain KARSV04 has been reported to have an anticancer effect on T47D cells by inhibiting the growth of cells and modulating the cell cycle in the S phase. In the present study, the effect of pyrophen in doxorubicin (Dox) chemotherapy in an *in vitro* model of breast cancers was studied.

Materials and Methods: The cytotoxicity of pyrophen and Dox separately and in combination were evaluated in T47D and MCF-7 cells by 3-(4,5-dimethylthiazol-2-yl)-2,5-diphenyltetrazolium bromide assay. Modulation of cell cycle distribution and apoptosis was examined by flow cytometry.

Results: Our findings showed that pyrophen did not significantly potentiate Dox-induced cytotoxicity in T47D cells. Adding Dox-treated T47D cells with pyrophen at a concentration of 9.20 µg/mL induced a slight increase in the S-phase cell population. This compound induced cytotoxicity of MCF-7 cells with IC_{50} of 70.57 µg/mL. Co-treatment of pyrophen and Dox in MCF-7 cells increased cytotoxicity relative to Dox alone, which was suggested in part to be due to modulation of the cell cycle in the G2/M phase and apoptosis.

Conclusion: The data suggest different mechanisms of regulation in promoting cell death by two different cell lines in response to administration of pyrophen.

Key words: *Aspergillus fumigatus*, pyrophen, doxorubicin, T47D, MCF-7

ÖZ

Amaç: *Aspergillus fumigatus* KARSV04 suşundan izole edilen amino asit-piron türevi olan pirofenin, hücrelerin büyümesini engelleyerek ve S fazındaki hücre döngüsünü modüle ederek T47D hücreleri üzerinde antikanser etki gösterdiği rapor edilmiştir. Bu çalışmada, pirofenin doksorubisin (Dox) kemoterapisindeki olası etkisi *in vitro* meme kanseri modelinde incelenmiştir.

Gereç ve Yöntemler: Pirofen ve Dox için ayrı ayrı ve kombinasyon halinde T47D ve MCF-7 hücrelerinde 3-(4,5- dimetil tiyazol -2-yl)-2,5- difenil tetrazolium bromür ile sitotoksisite deneyi yapılmıştır. Hücre döngüsünün modülasyonu ve apoptozis akış sitometrisi ile incelendi.

Bulgular: Bulgularımız, pirofenin T47D hücrelerinde Dox kaynaklı sitotoksisiteyi önemli ölçüde artırmadığını gösterdi. Dox ile muamele edilmiş T47D hücrelerine, 9,20 µg/mL konsantrasyonunda pirofen eklenmesi, S-faz hücre popülasyonunda hafif bir artışa neden oldu. Bu bileşik, MCF-7 hücrelerinde

*Correspondence: E-mail: puji_astuti@ugm.ac.id, Phone: +62274543120 ORCID-ID: orcid.org/0000-0003-3316-6149
Received: 16.01.2019, Accepted: 21.02.2019

sitotoksisiteyi indüklemiştir (IC_{50} 70,57 µg/mL). MCF-7 hücrelerine pirofen ve Dox'un birlikte uygulanması, tek başına Dox ile karşılaştırıldığında sitotoksisiteyi arttırmıştır; bunun kısmen hücre döngüsünün G2/M fazında modülasyonu ve apoptoz kaynaklı olduğu düşünülmüştür.

Sonuç: Veriler, pirofen uygulamasına yanıt olarak iki farklı hücre hattında indüklenen hücre ölümünün farklı düzenleme mekanizmaları olduğunu düşündürmektedir.

Anahtar kelimeler: *Aspergillus fumigatus*, pirofen, doksorubisin, T47D, MCF-7

INTRODUCTION

Breast cancer is one of the most common cancers, affecting women all around the world, and the risk factor increases are influenced by age.[1,2] Doxorubicin (Dox), an anthracycline antibiotic, is one of the most widely used chemotherapeutic agents for breast cancer treatment.[3] It exhibits anticancer activity by intercalation with DNA and inhibits topoisomerase II as well as generation of reactive oxygen species, resulting in apoptosis of tumor cells.[4-6] In spite of the widely used Dox to treat cancer, its side effects, including cardiotoxicity, and the development of drug resistance limit its clinical application in cancer therapy.[7-9] Many strategies have been developed to minimize its side effects and improve its chemotherapeutic effect, one of which involved combining Dox with some sensitizing agents.[10-12] A proteasome inhibitor, carfilzomib, was reported to increase Dox-induced cytotoxic effects and apoptosis in various subtypes of breast cancer.[10] Similarly, a phosphodiesterase-5 inhibitor, sildenafil, was shown to enhance Dox-induced apoptosis in PC-3 and DU145 prostate cancer cells. A flavonoid, luteolin-7-O-β-D-glucopyranoside, isolated from *Dracocephalum tanguticum* exhibited protective activity against Dox-induced toxicity in H9c2 cardiomyocytes.[12]

Pyrophen is an amino acid-pyrone derivative isolated from various organisms including *Aspergillus niger* and *Alternaria alternata*.[13,14] Recently, Reber and Burdge[15] reported that this compound was able to be synthesized using commercially available *N*-Boc amino acids. Investigations on its potential as an anticancer agent are limited. Previous findings demonstrated that pyrophen isolated from *Aspergillus* sp. endophytic fungi modulated the T47D cell cycle.[16] The aim of the present study was to examine whether pyrophen enhanced the chemotherapeutic effect of Dox in T47D as well as in another type of cells, MCF-7.

MATERIALS AND METHODS

Materials

Pyrophen was isolated from the culture of endophytic fungus *Aspergillus fumigatus* strain KARSV04 (culture collection of Pharmaceutical Biology Department, Faculty of Pharmacy, UGM).[16] RPMI 1640, fetal bovine serum (FBS), penicillin/streptomycin, Fungizone, and sodium bicarbonate were supplied by Gibco. 4-(2-Hydroxyethyl)-1- piperazine ethane sulfonic acid was obtained from Invitrogen. Phosphate-buffered saline (PBS), propidium iodide (PI), Annexin-V-FLUOS staining kit, 3-(4,5-dimethylthiazol-2-yl)-2,5-diphenyltetrazolium bromide (MTT), RNAse, and Dox were purchased from Sigma-Aldrich.

Cell culture

T47D and MCF-7 breast cancer cells were grown in RPMI and DMEM media, respectively. Each medium was supplemented with 10% heat inactivated FBS, 1% penicillin/streptomycin, and 1 µg/mL Fungizone. The cultures were incubated in a humidified incubator at 37 ˚C with 5% CO_2.

Cytotoxicity assay

The cell cytotoxicity assay was conducted by modified MTT assay.[17] Briefly, 100 µL of media containing 10^4 cells was added to a 96-well plate followed by incubation for 24 h. The cells were further grown alone or treated with just pyrophen or in combination with Dox for another 24 h. The treated cells were gently washed with prewarmed 1X PBS, and 100 µL of media containing 0.5 mg/mL MTT was added to the wells. The cells were incubated for 4 h at 37 ˚C. Then 100 µL of 10% sodium dodecyl sulfate was added to the cells and they were incubated overnight at room temperature in the dark. The absorbance in each well was measured using a microplate reader (Bio-Rad) at 595 nm. The data generated were used to plot a cell viability curve. Each experiment was conducted in triplicate.

Cell cycle distribution and apoptotic cell analysis

Cell cycle distribution and percentage of apoptotic cells were examined using flow cytometry. Briefly, $1.5x10^5$ cells were inoculated in 6 well plates and grown for 24 h at 37 ˚C. For the cell cycle analysis, following treatment with pyrophen alone or in combination with Dox, the cells were harvested and fixed with cold ethanol. After washing with PBS, the cells were resuspended in buffer containing 1 mg/mL PI and 10 mg/mL RNAse, incubated for 5 min, and subjected to flow cytometry analysis. For the apoptotic cell analysis, following the addition of pyrophen alone or in combination with Dox, Annexin-V and PI were added to the cells, followed by incubation in the dark for 15 min at 4 ˚C and analysis by flow cytometry.

This article contains experimental studies that do not require approval by an ethics committee.

Statistical analysis

The results are expressed as mean ± standard error of the mean. Normal distribution was analyzed by Shapiro-Wilk test. $p>0.05$ indicated normal distribution. The difference in the averages of cell viability between groups was analyzed by one-way ANOVA using SPSS version 23.00. $P<0.05$ indicated a significant difference.

RESULTS

Pyrophen modulates the growth of MCF-7 cells

A previous study reported the cytotoxic effect *in vitro* of pyrophen on T47D breast cancer cells.[16] In order to assess the anticancer activity of this compound on other molecular subtypes of breast cancer, the MCF-7 cell line was used. MCF-7 cells were treated

with pyrophen at concentrations of 11.25-90.00 µg/mL, and the cell viability was determined by MTT assay. The results showed that pyrophen reduced the viability of MCF-7 cells in a dose-dependent manner and this was confirmed by morphological changes in the cells following 24 h treatment (Figure 1). The IC_{50} of pyrophen on MCF-7 cells was observed at 70.57 µg/mL.

The effect of pyrophen on Dox-treated T47D and MCF-7 cells

In order to study its potential as an adjuvant to existing chemotherapeutic agents, T47D and MCF-7 cells were treated with the tested compounds individually or in combination. In the present study, pyrophen at the concentrations used did not reduce the viability of Dox-treated T47D cells (Figure 2). Adding the Dox-treated cells with pyrophen up to 6.25 µg/mL also did not affect the cell cycle distribution. However, when the pyrophen concentration was raised to the IC_{50} value (9.2 µg/mL), there was a shift in the synthesis (S) phase cell population from 17.16% to 22.15% (Figure 3). It was interesting to note that there was a decrease in MCF-7 cell viability when the cells were treated with a combination of pyrophen and Dox compared to Dox alone. The effect was obvious when the cells were treated with pyrophen at a higher concentration (45 µg/mL) and this was observed in all concentrations of Dox-treated cells. Cell cycle analysis of Dox-treated MCF-7 cells administered together with pyrophen showed a decrease in the G0/G1 phase population and increased number of cells in the G2/mitotic (M) phase. Addition of a higher concentration of pyrophen up to 90 µg/mL increased the sub-G1 phase population from 3.5% (Dox-treated MCF-7 cells) to 20% (Dox-treated MCF-7 cells + pyrophen 90 µg/mL) (Figure 3). Further observation using Annexin-V in combination with PI staining showed that the number of apoptotic cells increased from 11.60% (Dox-treated MCF-7 cells) to 26.67% (Dox-treated MCF-7 cells + pyrophen 90 µg/mL) (Figure 4).

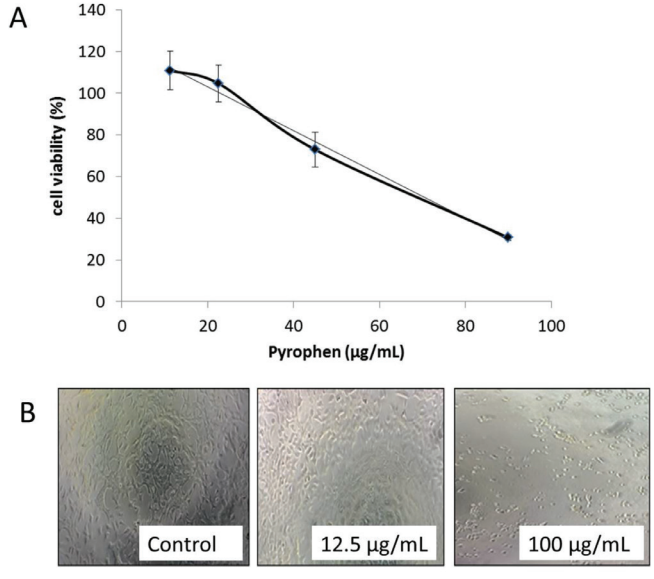

Figure 1. Cell viability and cell cycle profile of MCF-7 cells treated with pyrophen. Dose-viability curve response (A) and morphological changes in MCF-7 cells treated with pyrophen at various concentrations (B)

DISCUSSION

A previous study reported that pyrophen isolated from the endophytic fungus *Aspergillus fumigatus* KARSV04 showed toxicity towards p53 defective breast cancer cell line T47D.[16] Its potency to kill other breast cancer cells was further explored

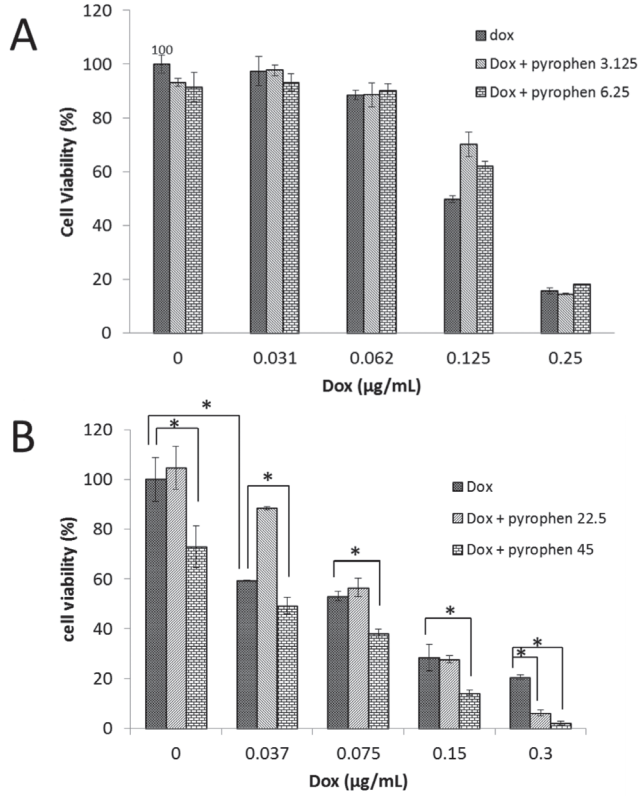

Figure 2. Viability of T47D cells (A) and MCF-7 cells (B) treated with Dox in combination with pyrophen. *p<0.05 compared with the value obtained for Dox alone

Dox: Doxorubicin

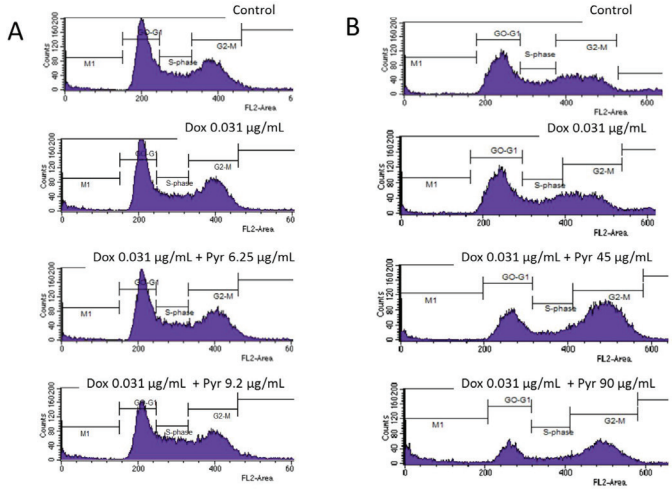

Figure 3. Cell cycle distribution of T47D (A) and MCF-7 (B) cells treated with Dox alone and in combination with pyrophen. Cells were inoculated in a 6-well plate followed by 16 h incubation with Dox alone or in combination with pyrophen in a humidified incubator at 37 °C, 5% CO_2. The cells were analyzed for cell cycle distribution by flow cytometry

Dox: Doxorubicin

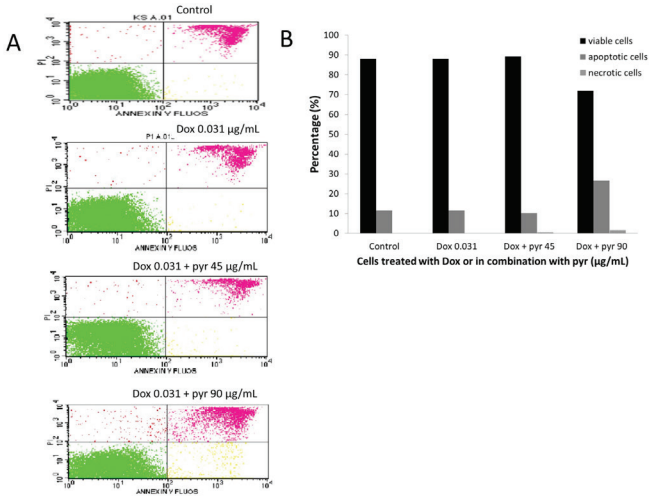

Figure 4. The effect of pyrophen on Dox-treated MCF-7 cells. Flow cytometry profiles (A) and apoptotic and necrotic cell distribution (B)
Dox: Doxorubicin

by observing its toxicity towards p53 competent MCF-7 cells. In the present study we found that pyrophen showed cytotoxicity towards MCF-7 cells. It inhibits the growth of MCF-7 cells in a concentration-dependent manner. However, its IC_{50} value is higher than that of T47D.

Further examination of its potential as an adjuvant to the existing conventional anticancer drug Dox was conducted. Adjuvant therapy of Dox with novel or bioactive compounds is reportedly a promising approach to increase the efficacy of this drug in breast cancer.[18-20] In the present study we found that although pyrophen is more toxic to T47D cells than to MCF-7 cells, combining this compound with Dox-treated cells demonstrated different effects. Pyrophen did not significantly affect the viability of Dox-treated T47D cells, while a synergistic effect was seen on Dox-treated MCF-7 cells in combination with pyrophen. It was interesting to note that adding pyrophen at 9.2 µg/mL to Dox-treated cells increased the S phase population of T47D cells, indicating that this compound may interfere with cell cycle progression though S phase modulation. A similar finding was obtained upon treating T47D with this compound alone.[16] On the other hand, it is indicated that pyrophen increased the G2/M population of MCF-7 cells. Combination of Dox with higher concentrations of pyrophen caused an increase in cell death as shown by an increase in the sub-G1 population and apoptotic cells. The decrease in the number of MCF-7 cells in the G2/M phase may contribute to a shift of the cell population to the sub-G1 phase.

The difference in response upon treatment of T47D and MCF-7 cells with pyrophen might be explained by the fact that these two breast cancer cell lines have different characteristics in that T47D cells are p53 defective mutants while MCF-7 bear p53 wild type.[21] The accumulation of T47D cells in the S phase may be in part due to the inability of cells to promote p53-dependent cell death and rely on S phase arrest following pyrophen treatment. Tumor cells that have a mutation on p53 have been reported to be resistant to DNA-damaging agents and diminish response to apoptosis-inducing agents.[22,23] MCF-7 cells, however, arrest at the G2/M phase upon treatment with Dox and further promote G2/M arrest upon combination with pyrophen. The functional p53 in MCF-7 cells may contribute to the additional increase in the G2/M cell population. Upon DNA damage, ATM and/or ATR kinase are activated, which then phosphorylate Chk1/Chk2, causing the inactivation of cdc25 phosphatase and thus preventing entry into mitosis. The ATM/ATR also phosphorylates p53 on S15, leading to increased transcription of $p21^{Waf/Cip1}$, GADD45, and 14-3-3, proteins, which are suggested to be responsible for maintaining G2 arrest.[24,25] Adding a higher concentration of pyrophen to the Dox-treated MCF-7 cells, however, led to cell death, which suggested that p53 may shift its function from promoting arrest to induction of apoptosis. Further research is needed to examine the effect of pyrophen in regulating apoptosis.

CONCLUSION

Pyrophen induced cytotoxicity towards MCF-7 cells and this effect was synergistic upon treatment with Dox. This compound induced accumulation of Dox-treated MCF-7 cells in the G2/M phase. Dox-treated T47D cells accumulated in the S phase upon treatment with pyrophen, suggesting a different mechanism in regulating cell cycle progression in these two cell lines.

ACKNOWLEDGEMENTS

The authors thank the Indonesian Ministry of Research, Technology and Higher Education under Universitas Gadjah Mada PUPT Grant 2016-2017 for providing funding for this study.

Conflicts of interest: No conflict of interest was declared by the authors. The authors alone are responsible for the content and writing of the paper.

REFERENCES

1. Ferlay J, Soerjomataram I, Dikshit R, Eser S, Mathers C, Rebelo M, Parkin DM, Forman D, Bray F. Cancer incidence and mortality worldwide: sources, methods and major patterns in GLOBOCAN 2012. Int J Cancer. 2015;136:359-386.
2. Siegel R, Naishadham D, Jemal A. Cancer statistics, 2013. CA Cancer J Clin. 2013;63:11-30.
3. Moretti E, Oakman C, Di Leo A. Predicting anthra-cycline benefit: have we made any progress? Curr Opin Oncol. 2009;21:507-515.
4. Roca-Alonso L, Pellegrino L, Castellano L, Stebbing J. Breast cancer treatment and adverse cardiac events: what are the molecular mechanisms? Cardiology. 2012;122:253-259.
5. Kugawa F, Ueno A. Profiles of caspase activation and gene expression in human breast cancer cell line MCF-7, after cyclophosphamide, doxorubicin, 5-fluorouracil (CDF) multi-drug administration. J Health Sci. 2010;56:81-87.
6. Hussein MA. Preclinical rationale, mechanisms of action, and clinical activity of anthracyclines in myeloma. Clin Lymphoma Myeloma. Clin Lymphoma Myeloma. 2007;7(Suppl 4):145-149.

7. Xu F, Wang F, Yang T, Sheng Y, Zhong T, Chen Y. Differential drug resistance acquisition to doxorubicin and paclitaxel in breast cancer cells. Cancer Cell Int. 2014;14:142.
8. Neilan TG, Blake SL, Ichinose F, Raher MJ, Buys ES, Jassal DS, Furutani E, Perez-Sanz TM, Graveline A, Janssens SP, Picard MH, Scherrer-Crosbie M, Bloch KD. Disruption of nitric oxide synthase 3 protects against the cardiac injury, dysfunction, and mortality induced by doxorubicin. Circulation. 2007;116:506-514.
9. Swain SM, Whaley FS, Ewer MS. Congestive heart failure in patients treated with doxorubicin: a retrospective analysis of three trials. Cancer. 2003;97:2869-2879.
10. Shi Y, Yu Y, Wang Z, Wang H, Bieerkehazhi S, Zhao Y, Suzuk L, Zhang H. Second-generation proteasome inhibitor carfilzomib enhances doxorubicin-induced cytotoxicity and apoptosis in breast cancer cells. Oncotarget. 2016;7:73697-73710.
11. Das A, Durrant D, Mitchell C, Mayton E, Hoke NN, Salloum FN, Park MA, Qureshi I, Lee R, Dent P, Kukreja RC. Sildenafil increases chemotherapeutic efficacy of doxorubicin in prostate cancer and ameliorates cardiac dysfunction. Proc Natl Acad Sci USA. 2010;107:18202-18207.
12. Wang SQ, Han XZ, Li X, Ren DM, Wang XN, Lou HX. Flavonoids from *Dracocephalum tanguticum* and their cardioprotective effects against doxorubicin-induced toxicity in H9c2 cells. Bioorg Med Chem Lett. 2010;20:6411-6415.
13. Shaaban M, Shaaban KA, Abdel-Aziz MS. Seven naphtho-γ-pyrones from the marine-derived fungus Alternaria alternata: structure elucidation and biological properties. Org Med Chem Lett. 2012;2:6.
14. Barnes CL, Steiner JR, Torres E, Pachecho R, Marquez H. Structure and absolute configuration of pyrophen, a novel pryrone derivative of L-phenylalanine from Aspergillus niger. Int J Peptide Protein Res. 1990;36:292-296.
15. Reber KP, Burdge HE. Total Synthesis of Pyrophen and Campyrones A-C. J Nat Prod. 2018;81:292-297.
16. Astuti P, Eden W, Wahyono, Wahyuono S, Hertiani T. Pyrophen produced by endophytic fungi *Aspergillus* sp isolated from Piper crocatum Ruiz and Pav exhibited cytotoxic activity and induced S phase arrest in T47D brest Canver cells. Asian Pac J Cancer Prev. 2016;17:615-618.
17. Bahuguna A, Khan I, Bajpai VK, Kang SC. MTT assay to evaluate the cytotoxic potential of a drug. Bangladesh J Pharmacol. 2017;12:115-118.
18. Putri H, Jenie RI, Handayani S, Kastian RF, Meiyanto E. Combination of Potassium Pentagamavunon-0 and Doxorubicin Induces Apoptosis and Cell Cycle Arrest and Inhibits Metastasis in Breast Cancer Cells. Asian Pac J Cancer Prev. 2016;17:2683-2688.
19. Li S, Yuan S, Zhao Q, Wang B, Wang X, Li K. Quercetin enhances chemotherapeutic effect of doxorubicin against human breast cancer cells while reducing toxic side effects of it. Biomed Pharmacother. 2018;100:441-447.
20. Khaki-Khatibi F, Ghorbani M, Sabzichi M, Ramezani F, Mohammadian J. Adjuvant therapy with stattic enriches the anti-proliferative effect of doxorubicin in human ZR-75-1 breast cancer cells via arresting cell cycle and inducing apoptosis. Biomed Pharmacother. 2019;109:1240-1248.
21. Crawford KW, Bowen WD. Sigma-2 receptor agonists activate a novel apoptotic pathway and potentiate antineoplastic drugs in breast tumor cell lines. Cancer Res. 2002;62:313-322.
22. Wallace-Brodeur RR, Lowe SW. Clinical implications of p53 mutations. Cell Mol Life Sci. 1999;55:64-75.
23. Ryan KM, Vousden KH. Characterization of structural p53 mutants which show selective defects in apoptosis but not cell cycle arrest. Mol Cell Biol. 1998;18:3692-3698.
24. Sancar A, Lindsey-Boltz LA, Unsal-Kacmaz K, Linn S. Molecular mechanisms of mammalian DNA repair and the DNA damage checkpoints. Annu Rev Biochem. 2004;73:39-85.
25. Sun M, Zhang N, Wang X, Cai C, Cun J, Li Y, Lv S, Yang Q. Nitidine chloride induces apoptosis, cell cycle arrest, and synergistic cytotoxicity with doxorubicin in breast cancer cells. Tumour Biol. 2014;35:10201-10212.

Turk J Pharm Sci 2020;17(3):285-292
DOI: 10.4274/tjps.galenos.2019.15428

ORIGINAL ARTICLE

Sun Protective Potential and Physical Stability of Herbal Sunscreen Developed from Afghan Medicinal Plants

Afgan Tıbbi Bitkilerinden Geliştirilen Bitkisel Güneş Koruyucunun Güneş Koruyucu Potansiyeli ve Fiziksel Stabilitesi

Amina AHMADY[1]*, Mohammad Humayoon AMINI[2], Aqa Mohammad ZHAKFAR[1], Gulalai BABAK[1], Mohammad Nasim SEDIQI[2]

[1]Kabul University Faculty of Pharmacy, Department of Pharmaceutics, Kabul, Afghanistan
[2]Kabul University Faculty of Pharmacy, Department of Pharmacognosy, Kabul, Afghanistan

ABSTRACT

Objectives: The aim of this study was to develop an herbal topical sunscreen formulation based on some fixed oils in combination with some medicinal plants.

Materials and Methods: The crude and purified extracts were screened for their phytochemical profile and their sun protection potentials. Based on our results, *Elaeagnus angustifolia* purified extract (EAPE), sesame oil, and sea buckthorn oil were selected for the development of the sunscreen formulation. The developed sunscreen formulations containing different concentration of EAPE were evaluated for their different physicochemical properties and stability.

Results: The results of the phytochemical analysis revealed the presence of phenolic compounds and flavonoids in all tested extracts. EAPE, sesame oil, and sea buckthorn oil showed the highest absorption in the ultraviolet region. The sun protection factor (SPF) value of the developed formulations containing different concentration of EAPE was in the range of 6.37±0.14 to 21.05±0.85. The sunscreen formulation containing 6% EAPE was stable for 8 weeks in an oven (40 ˚C) and refrigerator (4 ˚C).

Conclusion: The findings of this study revealed a higher sun protection capacity of EAPE than the other plant extracts. Sunscreen formulations containing 6% EAPE showed promising SPF values. However, further *in vivo* studies are highly recommended to prove further the safety and efficacy of our developed sunscreen formulation.

Key words: Sunscreen, UV filter, emulgel, *Elaeagnus angustifolia*

ÖZ

Amaç: Bu çalışmanın amacı, bazı tıbbi bitkiler ve sabit yağlar kullanılarak bir bitkisel güneş koruyucu geliştirmektir.

Gereç ve Yöntemler: Sabit yağların ham ve saflaştırılmış ekstreleri, fitokimyasal profilleri ve güneş koruma potansiyelleri açısından taranmıştır. Elde edilen sonuçlara dayanarak, güneş koruyucu formülasyonunun geliştirilmesi için *Elaeagnus angustifolia* saflaştırılmış ekstresi (EAPE), susam yağı ve yabani iğde yağı seçilmiştir. Farklı EAPE konsantrasyonları içeren geliştirilmiş güneş koruyucu formülasyonlar, farklı fizikokimyasal özellikleri ve stabiliteleri açısından değerlendirilmiştir.

Bulgular: Fitokimyasal analizler, test edilen tüm ekstrelerde fenolik bileşiklerin ve flavonoitlerin varlığını göstermiştir. EAPE, susam yağı ve yabani iğde yağı, ultraviyole bölgede en yüksek absorbsiyon göstermiştir. Farklı EAPE konsantrasyonları içeren geliştirilmiş formülasyonların güneş koruma faktörü (SPF) değerlerinin, 6,37±0.14 ile 21,05±0,85 aralığında olduğu bulunmuştur. Geliştirilen 6% EAPE içeren güneş koruyucu formülasyonunun kurutma fırınında (40 ˚C) ve buzdolabında (4 ˚C) 8 hafta süresince stabil olduğu tespit edilmiştir.

Sonuç: Bu çalışmanın bulguları, EAPE'nin diğer bitki ekstrelerden daha yüksek güneş koruma kapasitesine sahip olduğunu göstermiştir. %6 EAPE içeren güneş koruyucu formülasyonun umut verici bir SPF değerine sahip olduğu bulunmuştur. Bununla birlikte sonuçlara göre geliştirdiğimiz güneş koruyucu formülasyonun güvenilirliğini ve etkinliğini kanıtlamak için ek *in vivo* çalışmaların yapılması oldukça önemlidir.

Anahtar kelimeler: Güneş koruyucu, UV filtresi, emulgel, *Elaeagnus angustifolia*

*Correspondence: **E-mail:** amina.ahmady@yahoo.com, **Phone:** +93747228758 **ORCID-ID:** orcid.org/0000-0001-6493-381X
Received: 19.11.2018, **Accepted:** 21.03.2019

INTRODUCTION

Exposure to solar ultraviolet (UV) radiation for a long time causes a variety of skin damage. Sunburn, skin pigmentation, premature aging, and photocarcinogenesis are some examples of skin damage due to UV radiation.[1,2] The main mechanism of skin damage by UV radiation is the formation of reactive oxygen species (ROS) that interact with proteins and lipids and subsequently alter them.[3] UVC (200-280 nm), UVB (280-320 nm), and UVA (320-400 nm) are three subcategories of the UV region. UVB and to a lesser extent UVA are responsible for inducing skin damage.[4,5]

Although sunscreens have shown efficacy in prevention of sunburn, several studies indicate that they are not effective in prevention of skin carcinoma and premature aging.[6,7] Currently it is very well understood that ROS are the main cause of skin damage such as skin cancer, actinic keratosis, and photoaging that happen due to chronic exposure to sunlight. Thus, the incorporation of antioxidants in addition to UV filters in formulations of sunscreens can improve the performance of sunscreens in the prevention of skin cancer and photoaging.[5,8,9]

Herbal extracts and oils have complex compositions, resulting in the exhibition of different effects, such as antioxidant, sun blocking, anti-inflammatory, and immunomodulatory.[10,11] Moreover, the efficacy of herbal extracts in improving skin appearance and treatment of various skin diseases is very well understood. Plants due to their antioxidant potential are known as an attractive option to be used in sunscreen formulations for the prevention of skin damage due to solar radiation.[5,8,9,12]

Afghanistan is a mountainous country with a rich plant flora encompassing valuable nutritional and medicinal plants. The Afghan plant flora is estimated to be composed of around 3500 species (with 25-30% endemics).[13] The present work was designed in order to evaluate the sun protective potential of extracts and fixed oils extracted from some medicinal as well as nutritional plants growing in Afghanistan. In this research, sea buckthorn [*Hippophae rhamnoides* L. (*H. rhamnoide*)] ripe fruit oil, olive (*Olea europaea*) fruit oil, and sesame (*Sesamum indicum*) seed oil were tested by *in vitro* method for their sun protective potential. Similarly, *Alhagi pseudalhagi* (*A. pseudalhagi*) herbs and *Elaeagnus angustifolia* (*E. angustifolia*) leaf extracts were screened for their phytochemical profile and sun protective potential. According to the results obtained from the preliminary studies on the sun protection potential of the aforementioned plants and fixed oils, a topical sunscreen formulation was developed.

MATERIALS AND METHODS

Chemicals

Different solvents such as methanol (MeOH) (Merck), ethanol (Merck), ethyl acetate, hexane (Sigma-Aldrich), petroleum ether (Sigma-Aldrich), and diethyl ether (Riedel-deHaen) were used in different steps of the extraction processes. Cetostearyl alcohol (CDH), butylated hydroxy toluene (BDH), sodium lauryl sulfate (BDH), propylene glycol (CDH), methyl paraben (BDH), propyl paraben (BDH), and xanthan gum (BDH) were used for preparation of the emulgel formulation.

Collection and identification of plant materials

Mature fruits of *H. rhamnoides* were collected from Kapisa Province, located north of Kabul. Fresh leaves of *E. angustifolia* (family Elaeagnaceae) were collected from Paghman, a western district of Kabul Province. Aerial parts of *A. pseudalhagi* at blooming time were collected from the campus of Kabul University. The olive and sesame oils were procured from local markets in Jalalabad and Jowzjan, respectively.

All of the collected plants were botanically identified in the Pharmacognosy Dept., Kabul University (KU) by Prof. M.N. Sediqi. Prepared herbarium sheets of identified plants were kept as further reference in the herbarium of the Pharmacy Faculty, KU. The plant parts, after being shade dried, were ground into coarse powder and passed through mesh no: 1400, and then were used in further experiments.

Preparation of crude extracts of the plants

Twenty grams of powdered *A. pseudalhagi* herb and powdered *E. angustifolia* leaves were extracted in a Soxhlet extractor at 70 °C, and 70% MeOH was used as solvent. The obtained MeOH extracts were filtered through filter paper (Whatman Number 1), and then were subjected to concentration at 40 °C under reduced pressure to get the crude semisolid extracts. For complete drying of the semisolid extracts, a drying oven (Yamato DX601) adjusted to 60 °C was used. Similarly, 20 g of dried powdered fruits of *H. rhamnoides* was extracted by n-hexane at 70 °C using a Soxhlet extractor. The obtained extract was concentrated at 30 °C under reduced pressure in a Rotavapor to get *H. rhamnoides* fixed oil (HRO). The obtained orange colored HRO was further dried in an oven (60 °C) to ensure complete removal of n-hexane (used as solvent) and constant weight of the HRO.

Purification of the methanolic extracts

The crude methanolic extracts of *A. pseudalhagi* purified extract (APCE) and *E. angustifolia* crud extract (EACE) were separately subjected to further purification by slightly modifying a method previously described by Jarzycka et al.[14] Methanolic solutions of EACE and APCE were separately prepared in aqueous MeOH (70%), which were then extracted by their equal volume of petroleum ether (4 times). The methanolic fractions of both extracts were dried and then their aqueous solutions in hot distilled water were prepared. Ascorbic acid was added to the aqueous extracts (0.5 mg/g) and the obtained mixtures were kept for 24 h in the refrigerator. Then the mixtures were washed with diethyl ether (5 times). Next, ethyl acetate (5 times) was used in extraction of the aqueous phases. The obtained ethyl acetate fractions of each plant's extracts were concentrated and dried to obtain purified extract of *E. angustifolia* (EAPE) and purified extract of *A. pseudalhagi* (APPE).

Dried extracts were separately dissolved in hot distilled water, followed by the addition of ascorbic acid (0.5 mg/g). The mixtures were kept in the refrigerator for 24 h and then were extracted with diethyl ether (5 times). Next, the aqueous fractions were extracted with ethyl acetate (5 times). The ethyl acetate fractions of each plant's extracts were dried and labeled as APPE and EAPE, which were used in further studies.

Qualitative phytochemical screening of the extracts

Stock solutions of EACE, EAPE, APCE, and APPE were separately prepared in MeOH (2 mg/mL) and were subjected to qualitative phytochemical tests as per prescribed methods[15-18] for detection of the phytochemical classes present in the test extracts. The results of the qualitative phytochemical screening are presented in Table 1.

Detection of alkaloids

The following qualitative tests were performed for assessing the presence of alkaloids in the test extracts:

Dragendorff's test: Two milliliters of sample solution placed in a test tube was treated with 3 drops of Dragendorff's reagent. Formation of an orange red/brown precipitate indicates the presence of alkaloids.[15]

Hagers' test: Three drops of picric acid saturated solution were dropped on 2 mL of sample solution in a test tube. Appearance of yellow-whitish precipitate is proof of detection of alkaloids.[15]

Mayer's test: Three drops of potassium mercuric iodide solution were added to a test tube containing 2 mL of the sample solution. Appearance of a creamy or yellow precipitate shows the existence of alkaloids in test solution.[15]

Wagner's test: Three drops of solution of iodine were dropped on 2 mL of test solution in a clean test tube, and was observed for the formation of a brown or reddish-brown precipitate.[15]

Detection of phenols

$FeCl_3$ test: Three drops of solution of 1% $FeCl_3$ were dropped onto 2 mL of sample solution in a clean test tube. Appearance of an intense greenish-black color shows the existence of phenolic compounds in the test sample.[16]

Lead acetated test: One milliliter of 10% solution of lead acetate was added to a test tube containing 2 mL of extract solution and was observed for the appearance of a bulky white precipitate.[17]

Detection of flavonoids

Alkali reagent test: About 3 drops of aqueous solution of NaOH (1 N) were added dropwise to 2 mL of extract solution, and it was observed for the appearance of a yellow-orange color gradually increasing by addition of alkali drops. Adding some drops of diluted hydrochloric acid will diminish the intensity of the color produced.[15,18]

Ammonia test: A strip of filter paper impregnated with the test solution while dried was subjected to ammonia vapor. If an orange-red or yellow color appears on this strip, it shows the presence of flavonoids in the test extract.[15]

Shinoda test: Three drops of concentrated hydrochloric acid were added to 3 mL of test solution containing a small quantity of magnesium turnings, and it was left for completion of the reaction. If a pinkish color appears, it shows the existence of flavonoids in the test solution.[15]

Detection of tannins

Gelatin assay: About 2 mL of an aqueous solution containing 1% gelatin and 10% NaCl was mixed with 2 mL of sample solution in a clean test tube. If a whitish precipitate or a milky color forms, it shows that tannins are present in the test solution.[19]

Measuring the UV spectrum of the extracts and fixed oils

Methanolic solutions (100 µg/mL) of the extracts were separately prepared and were screened for their absorbance spectra in the range of 290 to 400 nm, using a UV spectrophotometer (Shimadzu UV mini 1240).[20] Similarly, hexane solutions of the fixed oils (1:100) were separately prepared and their absorbances in the range of 290 to 400 nm were recorded.[21] The UV spectrum of extracts and fixed oils are shown in Figure 1 and Figure 2 respectively.

Preparation of sunscreen emulgel

The sunscreen formulation was developed from sesame oil, HR oil, and EAPE, which had shown the highest sun blocking properties in preliminary studies. The components of the emulgel base are presented in Table 2. The sunscreen was prepared by adding different concentrations of the EAPE (where x=2%, 4%, 6%, and 8%) to the formulation. The procedure for the preparation of emulgel involved the preparation of a gel phase by dissolving xanthan gum in a portion of purified hot water (80 °C) containing the appropriate amount of polyphenol fraction. Then it was left for 1 h to form a homogeneous gel. The oil and aqueous phases were heated separately to about 60 °C and then the aqueous phase was added to the oil phase with

Table 1. Results of phytochemical screening of plant extracts

No.	Phytochemicals	EACE	EAPE	APCE	APPE
1	Alkaloid	-	-	-	-
2	Phenols				
	$FeCl_3$ test	+	+	+	+
	Lead acetate test	+	+	+	+
3	Flavonoids				
	Alkali R. test	+	+	+	+
	Ammonia test	+	+	+	+
	Shinoda test	+	+	+	+
4	Tannin				
	Gelatin test	+	-	+	-

EACE: *Elaeagnus angustifolia* crud extract, EAPE: *Elaeagnus angustifolia* purified extract, APCE: *Alhagi pseudalhagi* crud extract, APPE: *Alhagi pseudalhagi* purified extract

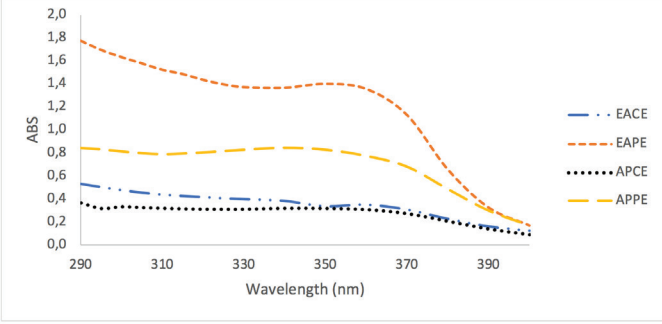

Figure 1. UV spectrum of methanolic solution of plant extracts at final concentration of 100 µg/mL

UV: Ultraviolet, EACE: *Elaeagnus angustifolia* crud extract, EAPE: *Elaeagnus angustifolia* purified extract, APCE: *Alhagi pseudalhagi* crud extract, APPE: *Alhagi pseudalhagi* purified extract, ABS: Absorbance of sunscreen product

continuous stirring. Afterward, the gel phase was added to the mixture and the formulation was mixed vigorously to cool the emulgel to room temperature.

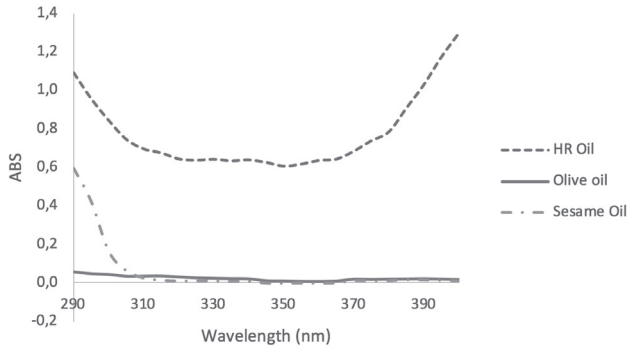

Figure 2. UV spectrum of *Hippophae rhamnoides* oil, olive oil, and sesame oil diluted 1:100 in hexane
UV: Ultraviolet, HR: *Hippophae rhamnoides*

Table 2. Ingredients included in emulgel formulation

Ingredients	Weight %
Phase A (oil phase)	
Sesame oil	14.5
Hippophae rhamnoides oil	0.5
Cetostearyl alcohol	5
Butylated hydroxy toluene	0.05
Phase B (aqueous phase)	
Sodium lauryl sulfate	0.55
Propylene glycol	5
Methyl paraben	0.2
Propyl paraben	0.1
Purified water	qsp
Phase C (gel phase)	
Xanthan gum	0.5
EAPE	x
Purified water	qsp

EAPE: *Elaeagnus angustifolia* purified extract

Physicochemical evaluation of the developed sunscreen formulations

Formulations containing different concentrations of EAPE were evaluated in terms of emulsion type, color, spreadability on the skin, precipitate, pH, and sun protective factor (SPF).

Determination of pH

To measure the pH of the sunscreen formulation, 1 g of the sample was weighed and diluted with distilled water up to 10 mL. The diluted sample was homogenized and then the pH of the sample solution was measured using a HM-25G model pH meter.[22] The pH values of formulations containing different concentrations of EAPE are shown in Table 3.

Determination of precipitation

The centrifugation test provides information very quickly regarding the physical stability of the emulsion based system. To perform this test, 1 g of sample was weighed and centrifuged for 30 min at 3000 rpm. Then the weight of supernatant (separated phase) was measured.[22]

In vitro determination of the sun protective factor of the developed sunscreen formulations

Usually the SPF is used to express the sun protective capacity of sunscreens.[23] There are many various *in vivo* and *in vitro* methods for determination of the SPF of sunscreen formulations. In the current work, the *in vitro* spectrophotometric method that was developed by Mansur et al.[24,25] was used to measure the SPF of the sunscreen formulations containing different concentrations of EAPE. Ethanolic solutions of sunscreen formulations at the final concentration of 2 µL/mL were prepared. The absorption of samples was recorded in the range of 290-320 nm, every 5 nm using a UV-visible spectrophotometer (Shimadzu UV mini 1240). The SPF of the sunscreen formulations was calculated using the Mansur equation. Measurements were performed in triplicate and the results were shown as mean ± standard deviation (SD).

$$SPF = CF \sum_{290}^{320} EE(\lambda)\ I(\lambda)\ ABS(\lambda),$$

where CF: Correction factor (=10), ABS (λ): Absorbance of sunscreen product, EE (λ): Erythemal effect spectrum, and I (λ): Solar intensity spectrum. The values of EE×I are constant, predetermined, and presented in Table 4.[26]

Table 3. Physical characteristics and SPF of emulgel formulation containing different concentrations of EAPE

	Blank	SUNF 2%	SUNF 4%	SUNF 6%	SUNF 8%
Color	Light yellow	Yellow	Yellowish brown	Brown	Brown
Emulsion type	O/W	O/W	O/W	O/W	O/W
Spreadability on the skin	Suitable	Suitable	Suitable	Suitable	Suitable
pH	8.04±0.16	7.75±0.12	7.32±0.12	6.86±0.09	6.39±0.06
Precipitation	-	-	-	-	-
SPF	0.27±0.08	6.37±0.14	11.59±0.11	16.03±0.12	21.05±0.85

EAPE: *Elaeagnus angustifolia* purified extract, SPF: Sun protective factor, SUNF: Sunscreen formulation

Physical stability evaluation of sunscreen formulation

Pharmaceutical or cosmetic products should be stable during their shelf life. Since the formulation containing 6% extract had higher SPF and at the same time did not produce any color on the skin, it was selected for conducting physical stability studies. The stability studies were conducted in two storage conditions (oven at 40±2 ˚C and refrigerator at 4±2 ˚C) for 8 weeks. The formulation was packaged in glass containers. The pH, SPF, precipitation, and organoleptic properties of samples were checked 7, 14, 21, 28, and 56 days after preparation. Each test was performed in triplicate and the results were recorded as mean ± SD, as shown in Tables 5 and 6 and Figures 3 and 4.

Statistical analysis

All measurements were conducted in triplicate and the results are presented as mean ± SD. MS Excel 2016 was used for the statistical analysis. To assess the difference between different variables, one-way ANOVA and Student's t-test were used. All analysis was performed at the 5% significance level ($p<0.05$).

Table 4. Value of EE×I used in the calculation of SPF[26]

EE×I	Wavelength (nm)
0.015	290
0.0817	295
0.2874	300
0.3278	305
0.1864	310
0.0839	315
0.018	320

EE: Erythemal effect spectrum, I: Solar intensity spectrum

RESULTS AND DISCUSSION

Phytochemical screening of the plant extracts

The phytochemical screening involved the detection of flavonoids, phenolic compounds, tannins, and alkaloids in the extracts. The results are shown in Table 3. The result of the alkaloids test was negative. Based on our findings, all extracts contain flavonoids and phenolic compounds, while the purified

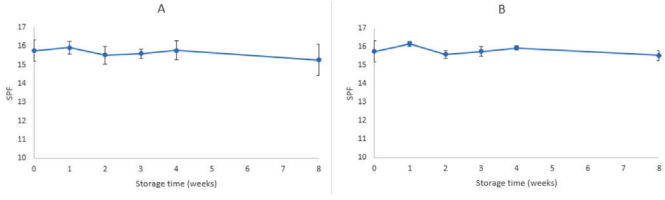

Figure 3. SPF changes in formulation containing 6% EAPE during 8 weeks' storage at 40 °C (A) and 4 °C (B)
SPF: Sun protective factor, EAPE: *Elaeagnus angustifolia* purified extract

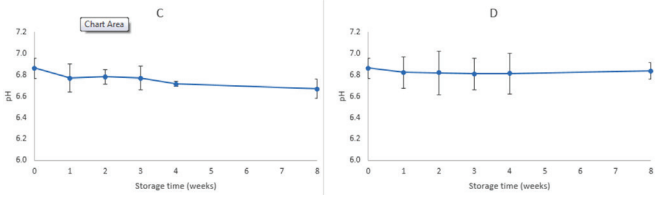

Figure 4. pH changes in formulation containing 6% EAPE during 8 weeks' storage at 40 °C (C) and 4 °C (D)
EAPE: *Elaeagnus angustifolia* purified extract

Table 5. SPF and physical characteristics of emulgel formulation during 8 weeks' storage in the oven (40 ˚C)

Oven (40 ˚C)					
	Week 1	Week 2	Week 3	Week 4	Week 8
SPF	15.92±0.34	15.53±0.48	15.60±0.25	15.77±0.51	15.26±0.84
pH	6.77±0.13	6.78±0.07	6.77±0.11	6.72±0.03	6.67±0.09
Precipitation	0±0	0±0	0±0	0±0	0±0
Phase separation	-	-	-	-	-
Color change	SLD	SLD	SLD	SLD	SLD

SPF: Sun protective factor, SLD: Slightly darker than the sample at the time of preparation

Table 6. SPF and physical characteristics of emulgel formulation during 8 weeks' storage in the refrigerator (4 ˚C)

Refrigerator (4 ˚C)					
	Week 1	Week 2	Week 3	Week 4	Week 8
SPF	16.17±0.15	15.60±0.21	15.77±0.26	15.95±0.11	15.54±0.26
pH	6.82±0.15	6.82±0.2	6.81±0.15	6.81±0.19	6.84±0.08
Precipitation	0±0	0±0	0±0	0±0	0±0
Phase separation	-	-	-	-	-
Color change	-	-	-	-	-

SPF: Sun protective factor

extracts (EAPE and APPE) were free of tannins. This may have been due to the low solubility of tannins in ethyl acetate.

Sun protective capacity of extracts and fixed oils

The UV spectra of the EACE, EAPE, APCE, and APPE are presented in Figure 1. The UV spectra of all plant extracts indicated that they have sun protective capacity in both the UVA and UVB regions. For nearly all extracts, the absorption was constant in the range of 290 to 370 nm and it decreased after 370 nm. The order of UV absorption of the tested extracts was EAPE > APPE > EACE > APCE. The purified extracts had higher absorption than the crude (methanolic) extracts. In the present research work the extracts were purified by the method previously developed by Wolski et al.[26] for extraction of polyphenolic fractions.[14,27] Polyphenols and flavonoids have been reported as sun protective agents in many published articles.[20,28-30] Thus the increased UV absorption by the methanolic solution of EAPE and APPE may be due to the higher concentrations of polyphenol and flavonoid compounds in the purified extracts. The UV spectra profile of the oil component including olive oil, sesame oil, and HRO is presented in Figure 2. Sesame oil and olive oil have negligible absorption compared with HRO. Olive oil has nearly the same absorption profile in both the UVA and UVB regions, but sesame oil showed more absorption in the range of 290 to 310 nm. Therefore, sesame oil can provide better protection in the UVB region than olive oil can. Thus sesame oil was selected for use in the formulation. HRO showed very interesting absorption in both the UVA and UVB regions. In the present research work the oil of full dried fruit (seed and pulp) was extracted using hexane. This oil showed much higher absorption than the oil that was obtained from HR seeds by other researchers.[31] The oil obtained from the full dried fruit (seed and pulp) had a strong orange color, which limited its use in high concentration in topical formulations.

Physicochemical properties and SPF of the sunscreen formulations

The physicochemical evaluation and SPF results of formulations containing different concentrations of EAPE are shown in Table 3. Incorporation of different percentages of the extract into the base cream caused some changes in the organoleptic properties of the emulgel formulations. The color of formulations ranged from light yellow for blank to brown for sunscreen formulation containing 8% EAPE (SUNF 8%). Following the administration on the skin, with the exception of SUNF 8%, none of them produced any color on the skin. Therefore, the sunscreen formulation containing 6% EAPE (SUNF 6%) was selected for conducting stability studies, because it possessed higher SPF and did not color the skin. All formulations showed suitable viscosity and they easily were spread on the skin. The addition of extract into the base cream did not cause any visible change in the apparent viscosity or spreadability of the formulations. However, the formulations containing the extracts seemed to be less greasy. The pH of the formulations was in the range of 8.03 to 6.39. In the sunscreen formulations as the extract concentration increased, the pH value of the formulations decreased. There was a negative linear correlation (R^2=0.993) between the pH and concentration of extract in the sunscreen formulation. Our result is in agreement with other researchers' work.[20,22] The pH value of the skin is in the range of 5 to 5.5.[32] In an ideal situation, especially in the case of topical formulations that are used frequently, the pH of a topical formulation should be slightly acidic in the range of 5 to 5.5. However, in practice, a pH range of 5-7 is acceptable for topical formulations.[33,34] Thus, SUNF 6% and SUNF 8% have a pH in the range 5-7, which is acceptable for topical formulations. The SPF of formulations varied from 0.27±0.08 for the base emulgel to 21.05±0.85 for the formulation containing 8% EAPE, as shown in Table 3. The SPF of the base emulgel was negligible (0.27±0.08), but the addition of extracts to the base cream caused a considerable increase in the SPF value of the emulgel formulations. There was a positive linear correlation (R^2=0.999) between the SPF and concentration of the extract in the sunscreen formulations.

Physical stability of the sunscreen formulations

Tables 5 and 6 summarize the physical characteristics of the sunscreen formulations stored in the oven at 40 °C and in the refrigerator at 4 °C, respectively. The following parameters were assessed for monitoring the physical stability during the 8 week storage period: SPF, pH, precipitation, occurrence of phase separation, and color change. These characteristics were observed at 40 °C (oven) and 4 °C (refrigerator) for 8 weeks. The centrifugation test provides fast and reliable information regarding the stability properties of formulations.[16] There was no phase separation in the samples during storage in either condition. Even after the centrifugation, no phase separation was observed. There were minor changes in SPF values of formulations during storage at 40 °C (oven) and 4 °C (refrigerator). Figure 3 shows the changes in the SPF of the sunscreen formulation containing 6% EAPE. We can say that there were no significant differences between the SPF of formulations over 8 weeks and the SPF values were stable. The pH of a topical formulation is an important characteristic that should be compatible with the formulation's other components and with the application site to avoid irritation. Thus measuring the pH of the formulation is necessary to ensure that the pH is stable during storage. pH changes in the sunscreen formulation containing 6% EAPE are presented in Figure 4. The pH value changes were in the range of 6.86±0.13 to 6.67±0.09 and from 6.86±0.13 to 6.84±0.08 for samples stored in the oven and refrigerator, respectively. There were no significant differences in the pH of the formulation over 8 weeks. It was observed that the pH of the formulation was stable for 8 weeks in the two storage conditions. It was observed that during the storage time (oven and refrigerator) the organoleptic properties of the formulation were stable. The only change was related to a negligible color change in the sample that was kept in the oven. The color of the formulation seemed to be darker. This change was observed after 1 week.

CONCLUSION

In the present era, sunscreens are extensively used to prevent UV-induced skin damage including sunburn, early aging,

and skin cancers. Recent research revealed that most of the synthetic sunscreens produce unwanted effects either in the short or long term of their application on the skin. Thus, there is an enormous need for effective and safe UV-filters around the world, particularly of natural origin. Fortunately, natural or herbal sunscreens are preferred because of being enriched with natural and safe compounds as compared with synthetic products. Based on the findings in the current work, the EAPE, which is rich in both flavonoids and polyphenols, exhibited high sun protective capacity. In the present work, the topical herbal sunscreen formulation containing sesame oil, HRO, and 6% EAPE showed an SPF value of 16.03 and was stable during 8 weeks' storage in the refrigerator at 4 ˚C and oven at 40 ˚C. However, further *in vivo* studies are highly recommended to further prove the safety and efficacy of the developed sunscreen formulation.

ACKNOWLEDGEMENT

This research work was funded by Family Health International under Cooperative Agreement no: AID-306-A-13-00009-00 funded by USAID. The publication's content does not generally reflect the view, analysis, or policies of FHI 360 nor does any mention of commercial products, organizations, or tradename indicate endorsement by FHI 360 or USAID. The authors are very grateful to the Afghan Ministry of Higher Education for providing all facilities and support to conduct this research work.

Conflicts of interest: No conflict of interest was declared by the authors. The authors alone are responsible for the content and writing of the paper.

REFERENCES

1. Lakhdar H, Zouhair K, Khadir K, Essari A, Ricard A, Seite S, Rougier A. Evaluation of the effectiveness of a broad-spectrum sunscreen in the prevention of chloasma in pregnant women. J Eur Acad Dermatol Venereol. 2007;21:738-742.
2. Wolf R, Tüzün B, Tüzün Y. Sunscreens. Dermatol Ther. 2001;14:208-214.
3. Imam S, Azhar I, Mahmood ZA. In-vitro evaluation of sun protection factor of a cream formulation prepared from extracts of musa accuminata (L.), psidium gujava (L.) And pyrus communis (L.). Asian J Pharm Clin Res. 2015;8:234-237.
4. Chanchal D, Swarnlata S. Herbal Photoprotective Formulation and their Evaluation. Ope Nat Prod J. 2009;2:71-76.
5. Afaq F, Mukhtar H. Botanical Antioxidant in the Prevention of Photocarcinogenesis and Photoaging. Exp Dermatol. 2006;15:678-684.
6. Gasparro FP. Sunscreen, Skin Photobiology, and skin cancer: The Need for UVA Protection and Evaluation of Efficacy. Environ Health Perspect. 2000;108:71-78.
7. Vainio H, Miller AB, Bianchini F. An International Evaluation of the Cancer Preventive Potentioal of Sunscreens. Int J Cancer. 2000;88:838-842.
8. Afaq F, Mukhtar H. Photochemoprevention by Botaanical Antioxidants. Skin Pharmacol Appl Skin Physiol. 2002;15:297-306.
9. Chermahini SH, Majid FAA, Sarmadi MR. Casmeceutical Value of herbal extracts as natural ingredient and novel technologies in anti aging. J Med Plants Res. 2011;5:3074-3077.
10. Psotova J, Svobodova A, Kolarova H, Walterova D. Photoprotective properties of Prunella vulgaris and rosmarinic acid on human keratinocytes. J Photochem Photobiol B. 2006;84:167-174.
11. Aquino R, Morelli S, Tomaino A, Pellegrino M, Saija A, Grumetto L, Puglia C, Ventura D, Bonina F. Antioxidant and photoprotective activity of a crude extract of Culcitium reflexum H.B.K. leaves and their major flavonoids. J Ethnopharmacol. 2002;79:183-191.
12. Korac RR, Khambholja KM. Potential of herbs in skin protection from ultraviolet radiation. Pharmacogn Rev. 2011;5:164-173.
13. Breckle SW, Rafiqpoor MD. Field Guide Afghanistan: Flora and Vegetation. Germary: Scientia Bonnensi; 2010:430
14. Jarzycka A, Lewinska A, Gancarz R, A wilk K. Assessment of extracts of Helichrysum arenarium, Crataegus monogyna, Sambucus nigra in photoprotective UVA and UVB; photostability in cosmetic emulsions. J Photochem Photobiol B. 2013;128:50-57.
15. Shah B, Seth AK. textbook of pharmacognosy and phytochemistry (1st ed). Haryana: Elsevier; 2010:189;234-236.
16. Harborne A. Phytochemical Methods: A guide to modern techniques of plant analysis (3rd ed). Springer. 1998:31-110.
17. Banu KS, Cathrine L. General Techniques involved in Phytochemical Analysis. Int J Adv Res Chem Sci. 2015;2:25-32.
18. Bhandary SK, Kumari N.S, Bhat VS, Sharmila KP, Bekal MP. Preliminary phytochemical screening of various extracts of Punica granatum peel, whole fruit and seeds. NUJHS 2012;2:34-38.
19. Evans WC. Trease and Evans Pharmacognosy (16th ed). London; SAUNDERS; 2009;136:616.
20. Tabrizi H, Mortazavi SA, Kamalinejad M. An in vitro evaluation of rosa damascena flower extracts as a natural antisolar agent. Int J Cosmet Sci. 2003;25:259-265.
21. Oomaha D, Ladet S, Godfrey DV, Liang J. Girard B. Characteristics of raspberry (Rubus idaeus L.) seed oil. Food Chemistry. 2000;69:187-193.
22. Kim SH, Jung EY, Kang DH, Chang UJ, Hong YH, Suh HJ. Physical stability, antioxidative properties, and photoprotective effects of a functionalized formulation containing black garlic extract. J Photochem Photobiol B. 2012;117:104-110.
23. Salvador A, Chisvert A. Analysis of Cosmetic Product, Amsterdam: Elsvire; 2007:94
24. Mansur JDS, Breder MNR, Mansur MCA, Azulay RD. Determinação do fator de proteção solar por espectrofotometria. An Bras Dermatol. 1986;61:121-124.
25. Santos EP, Freitas ZM, Souza KR, Garcia S, Vergnanini A. *In vitro* and *in vivo* determinations of sun protection factors of sunscreen lotions with octylmethoxycinnamate. Int J Cosmet Sci. 1999;21:1-5.
26. Wolski T, Ludwiczuk A, Baj T, Glowniak K. Genus Panax taxonomy chemical composition pharmacological effects medicinal application and phytochemical analysis of aerial and underground parts of american ginseng (Panax quinquefolium L.). Method of extraction and determination of phenolic compounds. Postepy Fitoterapii. 2008;4: 206-223.
27. Dutra AE, Oliveria, AGC, Kedor-Hackmann ERM, Santoro Miritello IRM. Determination of sun protection factor (SPF) of sunscreen by ultraviolet spectrophotometry. Braz J Pharm Sci. 2004;40:381-385.

28. Ebrahimzadeha MA, Enayatifard R, Khalilia M, Ghaffarloo M, Saeedi M, Charati JY. Correlation between Sun Protection Factor and Antioxidant Activity, Phenol and Flavonoid Contents of some Medicinal Plants. Iran J Pharm Res. 2014;13:1041-1047.

29. Baliga MS, Katiyar SK. Chemoprevention of photocarcinogenisis by selected dietary botanicals. Photochem Photobiol Sci. 2006;5:245-253.

30. Bonina F Lanza M, Montenegro L, Puglisi C, Tomaino A, Trombetta D, Castelli F, Saija A. Flavonoids as potential protective agents against photo-oxidative skin damage. Int J Pharm. 1996;145:87-94.

31. Beveridge T, Li TSC. Oomah BD, Smith A. Sea Buckthorn Products: Manufacture and Composition. J Agric Food Chem. 1999;47:3480-3488.

32. Betz G. Aeppli A, Menshutina N, Leuenberger H. *In vivo* comparison of various liposome formulations for cosmetic application. Int J Pharm. 2005;296:44-54.

33. Benson HAE, Watkinson AC. Transdermal and Topical Drug Delivery: Principles and Paractice. New Jersey: John Wiley & Sons; 2012:268.

34. Wiechers JW, Solutions JW. Formulating at pH 4-5: How Lower pH Benefits the Skin and Formulations. Cosmetics Toileters. 2013.

Turk J Pharm Sci 2020;17(3):293-298
DOI: 10.4274/tjps.galenos.2019.94210

ORIGINAL ARTICLE

A Synbiotic Mixture Augmented the Efficacy of Doxepin, Venlafaxine, and Fluvoxamine in a Mouse Model of Depression

Sinbiyotik Karışım, Fare Depresyon Modelinde Doksepin, Venlafaksin ve Fluvoksaminin Etkinliğini Artırdı

Azadeh MESRIPOUR[1]*, Andiya MESHKATI[1], Valiollah HAJHASHEMI[2]

[1]Isfahan University of Medical Sciences, School of Pharmacy and Pharmaceutical Sciences, Department of Pharmacology and Toxicology, Isfahan, Iran
[2]Isfahan University of Medical Sciences, School of Pharmacy and Pharmaceutical Sciences, Isfahan Pharmaceutical Sciences Research Center, Isfahan, Iran

ABSTRACT

Objectives: Currently available antidepressant drugs have notable downsides; in addition to their side effects and slow onset of action their moderate efficacy in some individuals may influence compliance. Previous literature has shown that probiotics may have antidepressant effects. Introducing complementary medicine in order to augment the efficacy of therapeutic doses of antidepressant drugs appears to be very important. Therefore, the effect of adding a synbiotic mixture to drinking water was assessed in a mouse model of depression following the administration of three antidepressant drugs belonging to different classes.

Materials and Methods: The marble burying test (MBT) and forced swimming test (FST) were used as animal models of obsessive behavior and despair. The synbiotic mixture was administered to the mice's drinking water ($6.25x10^6$ CFU) for 14 days and the tests were performed 30 min after the injection of the lowest dose of doxepin (1 mg/kg), venlafaxine (15 mg/kg), and fluvoxamine (15 mg/kg) on days 7 and 14.

Results: After 7 days of ingestion of the synbiotic mixture, immobility time decreased in the FST for doxepin (92±5.5 s) and venlafaxine (17.3±2.5 s) compared to the control group (drinking water), but fluvoxamine decreased immobility time after 14 days of ingestion of the synbiotic mixture (70±7.5 s). Preadministration of the synbiotic mixture improved the MBT test response for venlafaxine, while it did not change the results for the other two drugs.

Conclusion: Adding the synbiotic mixture to drinking water improved the efficacy of discrete antidepressant drugs particularly during the FST. Probiotics could be a useful complementary medicine for drug-resistant depressed individuals.

Key words: Probiotic, synbiotic, depression, antidepressant, forced swimming test, complementary medicine

ÖZ

Amaç: Günümüzde temin edilebilen antidepresan ilaçların belirgin dezavantajları vardır; yan etkilerine ve yavaş etki etmelerine ek olarak, orta derecedeki etkinlikleri bazı kişilerde hasta uyuncunu etkileyebilir. Daha önceki literatür bilgileri probiyotiklerin antidepresan etkilere sahip olabileceğini göstermiştir. Antidepresan ilaçların terapötik dozlarının etkinliğini artırmak için tamamlayıcı tıbbın etkisinin çok önemli olduğu düşünülmektedir. Burdan hareketle, bu çalışmada içme suyuna sinbiyotik bir karışımın eklenmesinin etkisi, farklı sınıflara ait üç antidepresan ilacın uygulanmasını takiben fare depresyon modelinde değerlendirilmiştir.

Gereç ve Yöntemler: Obsesif davranış ve umutsuzluğun hayvan modeli olarak misket gömme testi (MBT) ve zorunlu yüzme testi (FST) kullanılmıştır. Sinbiyotik karışım, farelerin içme suyuna ($6,25x10^6$ CFU) 14 gün boyunca uygulanmış ve testler, 7. ve 14. günlerde en düşük dozda doksepin (1 mg/kg), venlafaksin (15 mg/kg) ve fluvoksamin (15 mg/kg) enjeksiyonundan 30 dakika sonra yapılmıştır.

Bulgular: Sinbiyotik karışımın 7 gün süreyle uygulanmasından sonra, doksepin (92±5,5 s) ve venlafaksin (17,3±2,5 s) için FST'de kontrol grubuna (içme suyu) kıyasla hareketsizlik süresi azalmış, ancak fluvoksamin ile, sinbiyotik karışımın 14 gün süreyle uygulanmasından (70±7,5 s) sonra hareketsizlik süresi azalmıştır. Sinbiyotik karışımın önceden uygulanması venlafaksin için MBT test yanıtını geliştirmiş, diğer iki ilacın sonuçlarını değiştirmemiştir.

Sonuç: Sinbiyotik karışımın içme suyuna eklenmesi, özellikle FST sırasında ayrı antidepresan ilaçların etkinliğini arttırmıştır. Probiyotikler, ilaca dirençli depresif bireyler için yararlı bir tamamlayıcı olabilir.

Anahtar kelimeler: Probiyotik, sinbiyotik, depresyon, antidepresan, zorunlu yüzme testi, tamamlayıcı tıp

*Correspondence: **E-mail:** a_mesripour@yahoo.com, **Phone:** +00983137927089 **ORCID-ID:** orcid.org/0000-0003-3150-5581
Received: 04.02.2019, **Accepted:** 07.03.2019

INTRODUCTION

Probiotics are live organisms that when chronically ingested in adequate amounts could induce beneficial effects in the host.[1] Single strain probiotics or their combinations are useful for a variety of diseases, including gastrointestinal (GI) disorders such as inflammatory bowel disease, diarrhea, Irritable Bowel syndrome (IBS), and allergies.[2] This is now even being extended to some ailments of the central nervous system (CNS).[3,4] Gut bacterial microorganisms have two dominant genera, *Bacteroidetes* and *Firmicutes*, while other types have lower abundance, for instance *Proteobacteria*, *Actinobacteria*, and *Fusobacteria*.[5] Evidently, the brain-gut axis is a bidirectional homeostatic route and so its aberration may cause important pathophysiological results.[3] The high risk of co-existing psychiatric symptoms such as anxiety with GI disorders, for instance IBS, provides further evidence of the importance of this axis.[6] The brain-gut axis is connected not only by complex systems including the vagus nerve, endocrine, immune, and humoral links but also the gut microbiota in order to maintain GI stability and to connect cognitive and emotional areas of the brain with GI functions.[7]

Major depressive disorder is the most common mood disorder, affecting 5% of the population each year.[8] Several mechanisms are involved in its pathogenesis, such as altered monoaminergic (serotonergic, noradrenergic, and dopaminergic) and glutamatergic systems, increased inflammation, hypothalamic-pituitary-adrenal (HPA) axis aberrations, and decreased neuroplasticity.[9] Probiotics have shown antidepressant effects in animal models of depression. Species of the genus *Lactobacillus* are particularly characterized as antidepressants.[10] A probiotic mixture of *Lactobacillus* strains (*L. rhamnosus* and *L. helveticus*) ameliorated depression by regulating corticosterone levels in rat pups.[11] Likewise, chronic ingestion of a *L. rhamnosus* strain (JB-1) in mice alleviated depressive behavior and caused regional alteration in GABA receptor expression and since these changes were not observed in vagotomized mice the vagus nerve was considered critical for the brain-gut axis.[12] *Bifidobacterium* species also induce physiologic changes in favor of antidepressants effects in animal studies; for instance, *B. infantis* ameliorated depressive behavior in the maternal separation model.[13] In a systematic review regarding the effects of probiotics on depression in humans most of the studies found positive results on all values of depressive symptoms, but there were wide differences in the strain of probiotic, the dosing, and the duration of treatment.[14] The possible mechanisms that were considered for antidepressant effects of *B. infantis* by use in a rat model were reduction of pro-inflammatory cytokines, alteration of tryptophan metabolism, and CNS neurotransmitters.[15] The combination of *Lactobacilli* and *Bifidobacteria* was tested in depression following post-myocardial infarction (MI) in rats. Administration of *L. helveticus* and *B. longum* together had positive effects on post-MI depression through reduction of pro-inflammatory cytokines (for instance IL-4) and intestinal permeability restoration.[16,17] In addition, prebiotics such as oligosaccharides that stimulate the growth of nonpathogenic intestinal microflora such as *Lactobacilli* and *Bifidobacteria* also have neurotropic effects.[18]

Although drug therapy of depression is usually safe and effective, it is still not ideal because the latency time for clinical results is quite long (about 3-5 weeks) and there are still concerns regarding side effects such as loss of libido and weight gain. Additionally, there are a significant number of patients that do not respond well to antidepressant drugs, psychotherapy, and electroconvulsive therapy.[19] Thus the aim of the present study was to first observe the effect of a synbiotic (probiotic + prebiotic) mixture on behavior in an animal model of depression. Since it has been previously shown[11-15] that the probiotics *Lactobacilli* and *Bifidobacteria* have antidepressant effects in animal studies, a manufactured premixed product was chosen that comprised these genus and also a prebiotic, fructooligosaccharides. Second, in order to observe the effect of the synbiotic mixture on the efficacy of antidepressant drugs from different classes, subthreshold doses of doxepin [a tricyclic antidepressant (TCA)], venlafaxine [a serotonin-norepinephrine reuptake inhibitor (SNRI)), and fluvoxamine (a selective serotonin reuptake inhibitor (SSRI)] were chosen.

MATERIALS AND METHODS

Animals

Male Swiss mice weighing 23-26 g were housed at 21±2 ºC in a 12-h light/dark cycle with the lights on in the day time 6 am-6 pm. Tap water or the synbiotic mixture and standard food pellets were available *ad libitum*. For each experiment 6 mice were used and they were housed 3 per cage. Tests were performed in the behavior laboratory 24 h after the mice had become acclimatized to the environment. In order to minimize the influence of circadian rhythm, all experiments were performed between 8 am and 1 pm in the pharmacology laboratory. All animal procedures were approved by the Ethics Committee of Isfahan University of Medical Science and performed in accordance with the National Institutes of Health Guide for the Care and Use of Laboratory Animals (Ethical no: IR.MUI.REC.1395.3.864).

The synbiotic mixture and drug therapy

The synbiotic mixture comprised 10^9 CFU [*Lactobacillus casei*, *L. acidophilus*, *L. rhamnosus*, *L. bulgaricus*, *Bifidobacterium breve*, *B. infantis*, *Streptococcus thermophilus*, fructooligosaccharides (a prebiotic); a product of Zist Takhmir, Iran]. The animals had free access to the synbiotic mixture solution in drinking water that was prepared freshly each day in three concentrations: 6.25, 12.5, and $25x10^6$ CFU (based on pilot studies); the control animals had tap water *ad libitum*. The amounts of the synbiotic mixture solution or normal drinking water ingested by the animals were measured daily. The therapy continued for 14 days and the tests were performed on days 7 and 14.

The antidepressants were first administered intraperitoneally alone 30 min before starting the first test. Two doses were applied for each drug according to previous studies[20] and finally the lowest effective dose (data not shown) was chosen to be

applied following the synbiotic mixture administration. The selected antidepressants were doxepin 1 mg/kg (Razak, Iran), venlafaxine 15 mg/kg (Sigma-Aldrich, India), and fluvoxamine 15 mg/kg (Sigma-Aldrich, India). All the drugs were freshly prepared in normal saline solution and injections were adjusted for a volume of 10 mL/kg mouse body weight. The selected dose of each antidepressant drug was administered on days 7 and 14 following the synbiotic therapy (6.25x10^6 CFU), 30 min before the tests were performed.

Marble burying test (MBT)

The first test was the MBT. This is a method used to evaluate anxiety behavior and obsessive compulsive behavior. With minor modification to the method presented by Njung'e and Handley[21], the mice were separately placed in plastic cages (42x24x12 cm) containing 12 opaque glass marbles (1 cm diameter) that were distributed evenly over 5 cm of deep sawdust without food or water for 30 min. The number of marbles at least two-thirds buried (MB) was counted after 30 min.[22]

Forced swimming test (FST)

After performing the MBT each mouse was subjected to the FST. With some modifications[23] the mice were forced to swim in a glass beaker (diameter 14 cm) containing 25 ºC water for 6 min. The depth was about 15 cm to prevent the mice from escaping or touching the bottom of the glass beaker with their paws or tail. After 2 min of adaptation the total immobility time was measured by a chronometer in the last 4 min of the trial. Immobility is defined as the time the animal was floating and staying still when no additional activity was observed other than that required to keep the animal's head above water. Finally the mice were dried carefully and returned to their home cage.

Data processing and statistical analysis

The results were expressed as group mean ± standard error of the mean. The results were analyzed by One-Way ANOVA, followed by Tukey's multiple comparison tests and p values less than 0.05 were considered significant. The software programs used for data analysis and making graphs were Excel 2010 and the GraphPad Prism 6.

RESULTS

Daily drinking intake

According to Table 1, daily measurements of the synbiotic mixture ingestion showed that approximately a dose of 2.4-9.2x10^6 CFU/g body weight of synbiotic was ingested.

Effect of the synbiotic mixture on the MBT and FST

The number of marbles buried during the MBT showed that consuming 12.5x10^6 CFU synbiotic after 7 days or 14 days reduced obsessive behavior in the mice (Figure 1A). The percentage of marbles buried after 30 min on days 7 and 14 of ingesting the middle concentration of the synbiotic mixture was 25% and 41%, respectively, which was significantly ($p<0.05$) different from the corresponding control group (50% and 58.3% on days 7 and 14, respectively; $p<0.05$). The lowest synbiotic concentration only reduced MB to a significant amount on day 7 compared to the control animals (33.3% vs 50%; $p<0.05$). However, consuming the highest synbiotic concentration showed opposite results on MB behavior, since the animals buried more marbles measured after 7 (87%, $p<0.001$ vs control) and 14 days of therapy. During the FST the animals that ingested the synbiotic showed antidepressant behavior as presented in Figure 1B. After the mice had ingested the synbiotic mixture for

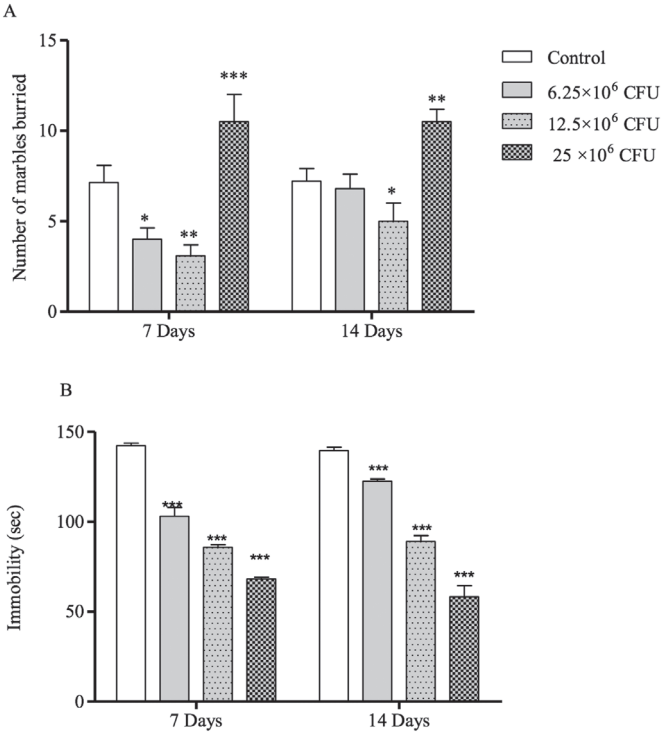

Figure 1. The effect of 3 concentrations of the synbiotic cocktail ingestion for 14 days on mouse behavior. A) The MBT the number of marbles at least two-thirds buried after 30 min, and B) the total immobility time during the last 4 min in the FST. The tests took place on days 7 and 14; each animal was first subjected to the MBT and then the FST. Number of animals in each group was 6; the control animals drank tap water. Results are expressed as group mean ± SEM and analyzed by One-Way ANOVA, followed by Tukey's post-hoc test. * $p<0.05$, ** $p<0.01$, and *** $p<0.001$ compared with the control group

MBT: Marble burring test, FST: Forced swimming test, SEM: Standard error of the mean

Table 1. Daily liquid intake

Synbiotic mixture CFU	6.25x10^6	12.5x10^6	25x10^6	0 (Tap water)
Daily intake mL/g body weight	0.38	0.37	0.37	0.39
Daily dose CFU/g body weight	2.375x10^6	4.625x10^6	9.25x10^6	0

The synbiotic mixture comprised *Lactobacillus casei*, *L. acidophilus*, *L. rhamnosus*, *L. bulgaricus*, *Bifidobacterium breve*, *B. longum*, *Streptococcus thermophilus*, fructooligosaccharides (a prebiotic)

a week the immobility time measured during the FST decreased in a dose-dependent manner since the highest mixture concentration (25x10^6 CFU) caused the lowest immobility time (68.1±2.5 s vs 142.3±4.3 s, p<0.001). After 14 days of synbiotic ingestion, the animals dose-dependently showed a shorter immobility time compared with the control animals (139.6±5.4 s); the animals that had ingested the highest concentration of the synbiotic mixture had the shortest immobility time (58.3±15 s, p<0.001).

Effect of the synbiotic mixture pretreatment on mouse response to antidepressants during the MBT and FST

The lowest concentration of the synbiotic mixture (6.25x10^6 CFU) was chosen to observe the animals' behavior during the MBT and FST on days 7 and 14 after injection of the lowest dose of each antidepressant drug (Figure 2). The antidepressant drugs all significantly reduced the number of MB compared to the control group (Figure 2A, p<0.05). Synbiotic ingestion significantly influenced the effects of venlafaxine on MB behavior since the animals significantly buried fewer marbles compared to those that had drunk water (percentage of MB decreased from 25% to 7%). However, consumption of the synbiotic mixture did not have any considerable effect on the MB behavior of animals injected with doxepin or fluvoxamine. On the other hand, drinking the synbiotic mixture increased the antidepressant effects of the lowest dose of each of the drugs (Figure 2B). The immobility time decreased dramatically in the animals that had drunk the synbiotic mixture either for 7 days (17.3±2.5 s) or for 14 days (60±16 s) prior to the administration of venlafaxine (p<0.001, vs the venlafaxine alone group 146±1 s). The results for synbiotic drinking prior to doxepin injection followed the same trend; after 7 days the immobility time was 92±5.5 s and after 14 days it was 70±7.4 s, which was decreased significantly compared to the doxepin alone group, 100±19 s (p<0.001). The synbiotic effect on fluvoxamine was slightly different as only after 14 days immobility time decreased significantly compared to the drug administered alone (70±7.5 s vs 100±9 s, p<0.001).

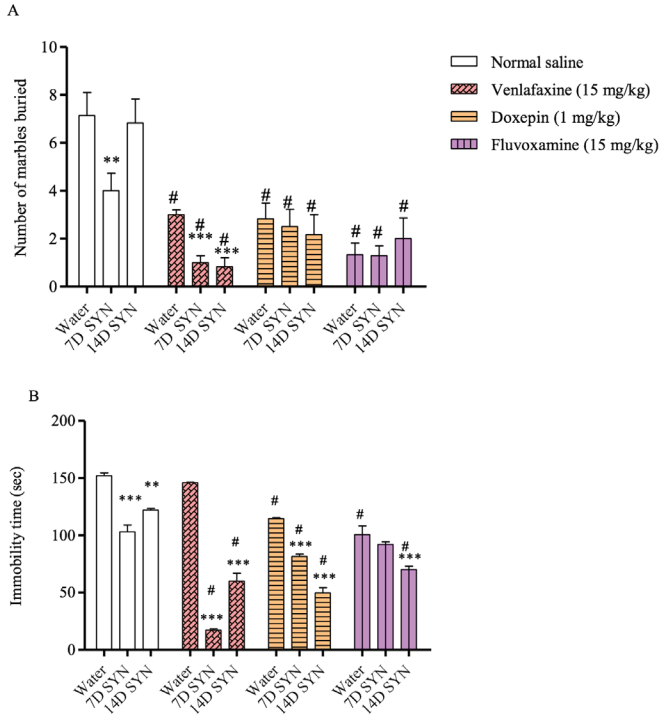

Figure 2. The effect of drinking the synbiotic mixture and the lowest dose of antidepressants on mouse behavior. A) The MBT the number of marbles at least two-thirds buried after 30 min are presented, and B) the total immobility time during the last 4 min in the FST. Number of animals in each of the groups was 6; animals ingested the synbiotic mixture (SYN; 6.25x10^6) for 14 days; the control group ingested tap water. The drugs were injected IP 30 min before testing; each animal was first subjected to the MBT and then the FST. Results are expressed as group mean ± SEM and analyzed by One-Way ANOVA followed by Tukey's post-hoc test. ** p<0.01 and *** p<0.001 compared with the probiotic free group. # p<0.01 compared with the corresponding control groups (the plane bars)

IP: Intraperitoneally, MBT: Marble burying test, FST: Forced swimming test, SYN: Synbiotic, SEM: Standard error of the mean

DISCUSSION

Our results showed that the synbiotic mixture could mitigate the immobility time in the FST, which denotes its possible antidepressant effects. Interestingly, only after a week of ingesting the synbiotic mixture did response to the lowest dose of the antidepressants increase dramatically. However, the MB behavior showed variable results. The MB behavior appears to be just a form of digging, but the behavior in mice has been used as a model of anxiety disorders including obsessive compulsive disorder (OCD).[24] This method is also useful for evaluating the mechanisms of action of drugs.[25] Venlafaxine (SNRI), doxepin (TCA), and fluvoxamine (SSRI) in our set of experiment clearly reduced the number of marbles buried, which was parallel with previous literature.[22,25] The FST is a reliable tool for drug discovery in industrial settings where high quantity screening of new compounds is necessary, as well as in research regarding complementary medicine.[23] By leaving the mouse in the water container it gradually loses hope to escape the stressful environment, and thus the immobility time reflects a measure of "behavioral despair". In the same trend as previous results, all antidepressant drugs of different classes that were tested in our study presented antidepressant effects in mice by reducing the immobility time.[22]

The daily preparation of the synbiotic mixture in the mice's drinking water was based on previous literature that *B. infantis* was administered by dissolving a powder containing 10^{10} bacterial cells in 100 mL of the rats' drinking water every morning.[26] There is also evidence that dead probiotic bacteria or just integral components of the bacterial cell such as peptidoglycan fragments or DNA would also be effective.[27] Therefore, although survivability of the mixture was not assessed before the new batch the next morning the research showed that the content remained effective. The synbiotic mixture dose-dependently reduced the immobility time during the FST, which obviously denotes its antidepressant-like effect in mice. However, a dose-dependent effect on obsessive behavior was not observed during the MBT; although lower doses of the synbiotic mixture reduced the MB behavior, this was not observed with the higher dose. A high dose of the synbiotic mixture had opposite effects

on the MBT. The different effects of the synbiotic mixture on the FST and MBT could be because of the different mechanisms involved in each test. Earlier research has proven that although the MBT and FST are invaluable predictive tests of OCD and antidepressant action, each assay appears to engage completely distinct neurochemical systems.[28] While the FST is more susceptible to compounds that are effective by altering activity in the noradrenergic system, the MBT mostly depends on modulation of the serotonergic system.[28] The downside of our research was that we did not measure the monoamine neurotransmitters, but this has been proven earlier.[29,30] Reports have shown that chronic gavage of *L. plantarum* in mice reduced stress-induced depression-like behaviors, normalized the HPA axis and immune systems, and modulated the changes in the dopamine and serotonin system in the prefrontal cortex.[29] Additionally, probiotics changed behavior and the CNS function in naïve adult animals.[30] The consumption of a fermented milk product containing *B. aimalis*, *S. thermophilus*, *L. bulgaricus*, and *L. lactis* in healthy women without psychiatric symptoms as observed by functional magnetic resonance imaging induced robust alterations in the activity of brain regions that control the central processing of emotions and sensations.[31]

Pretreatment with the synbiotic mixture before the administration of venlafaxine (SNRI) had a synergistic effect on the MBT, but this synergistic effect was not observed with doxepin or fluvoxamine. Previous studies on rat models of depression have reported that the ingestion of probiotics has a role in restoring the monoamine levels in important brain regions.[4,13] Therefore, it is possible that restoring the monoamine level improved the efficacy of venlafaxine in the MBT. On the other hand, the synbiotic mixture had a synergistic antidepressant-like effect on venlafaxine and doxepin (TCA); the antidepressant efficacy of fluvoxamine (SSRI) only increased after 14 days of synbiotic ingestion. Several studies have supported the argument that probiotics can exert psychotropic potential and this effect could be mediated by alterations in the monoamines. For instance, it has been shown that *B. infantis* reverses maternal separation-induced depressive-like behavior in rats during the FST,[13] and at least part of this antidepressant effect is due to elevation of tryptophan.[15] Previous findings suggest that in naïve mice the probiotic *L. plantarum* could modulate both serotonergic and dopaminergic systems,[29] and interestingly the probiotic increased dopamine, 3,4-dihydroxyphenylaceticacid, and homovanillicacid but there was no change in the dopamine turnover rate.[29] Earlier literature advocates that the vagus mediates the behavioral and neurochemical effects of probiotics.[7,12] Nevertheless, the antidepressant effects of the probiotic mixture may arise independently of any changes to the monoamine systems; for instance, it may be caused by attenuation of pro-inflammatory immune responses.[15]

The results of the present research were not only parallel with the previous literature regarding the antidepressant effects of probiotics but also extended it in several ways: first, the synbiotic mixture could decrease MB behavior. Second, the cocktail ingested by animals augmented the efficacy of the SNRI antidepressant venlafaxine during the MBT. Finally, after 7 days of the synbiotic drink it had a synergistic antidepressant-like effect on venlafaxine and doxepin, and it increased fluvoxamine efficacy after 14 days. Previous results proved that fluoxetine and escitalopram have antimicrobial activity *in vitro*, and psychotropic medications differentially influence the composition of gut microbiota *in vivo*.[32] Therefore, adding probiotics may help to improve the gut microbial composition in patient receiving antidepressant therapies.

CONCLUSION

Since extrapolating animal results to humans must be done with caution, further clinical research is warranted regarding adding synbiotics to drug-resistant patients and adding synbiotics in order to reduce antidepressant drug dosage and side effects mainly when SNRI or TCA are administered.

ACKNOWLEDGEMENT

This work was supported by the School of Pharmacy and Pharmaceutical Sciences Research Council (grant number: 395864, 12/05/2016), Isfahan University of Medical Sciences.

Conflict of Interest: Authors confirm that there is no conflict of interest in relation to this article.

REFERENCES

1. Sherman PM, Ossa JC, Johnson-Henry K. Unraveling mechanisms of action of probiotics. Nutr Clin Pract. 2009;24:10-14.
2. Floch MH, Walker WA, Guandalini S, Hibberd P, Gorbach S, Surawicz C, Sanders ME, Garcia-Tsao G, Quigley EM, Isolauri E, Fedorak RN, Dieleman LA. Recommendations for probiotic use--2008. J Clin Gastroenterol. 2008;42(Suppl 2):104-108.
3. Dinan TG, Cryan JF. Melancholic microbes: a link between gut microbiota and depression? Neurogastroenterol Motil. 2013;25:713-719.
4. Cerdó T, Ruíz A, Suárez A, Campoy C. Probiotic, prebiotic, and brain Development. Nutrients. 2017;9:1247.
5. Lankelma JM, Nieuwdorp M, de Vos WM, Wiersinga WJ. The gut microbiota in internal medicine: implications for health and disease. Neth J Med. 2015;73:61-68.
6. Kennedy PJ, Clarke G, Quigley EMM, Groeger JA, Dinan TG, Cryan JF. Gut memories: towards a cognitive neurobiology of irritable bowel syndrome. Neurosci Biobehav Rev. 2012;36:310-340.
7. Carabotti M, Scirocco A, Maselli MA, Severi C. The gut-brain axis: interactions between enteric microbiota, central and enteric nervous systems. Ann Gastroenterol. 2015;28:203-209.
8. Kessler RC, Wang PS. The descriptive epidemiology of commonly occurring mental disorders in the United States. Ann Rev Public Health. 2008;29:115-129.
9. Dean J, Keshavan M. The neurobiology of depression: An integrated view. Asian J Psychiatr. 2017;27:101-111.
10. Wang Y, Kasper LH. The role of microbiome in central nervous system disorders. Brain Behav Immun. 2014;38:1-12.
11. Gareau MG, Jury J, MacQueen G, Sherman PM, Perdue MH. Probiotic treatment of rat pups normalises corticosterone release and ameliorates colonic dysfunction induced by maternal separation. Gut. 2007;56:1522-1528.

12. Bravo JA, Forsythe P, Chew MV, Escaravage E, Savignac HM, Dinan TG, Bienenstock J, Cryan JF. Ingestion of Lactobacillus strain regulates emotional behavior and central GABA receptor expression in a mouse via the vagus nerve. Proc Natl Acad Sci U S A. 2011;108:16050-16055.

13. Desbonnet L, Garrett L, Clarke G, Kiely B, Cryan JF, Dinan TG. Effects of the probiotic Bifidobacterium infantis in the maternal separation model of depression. Neuroscience. 2010;170:1179-1188.

14. Wallace CJK, Milev R. The effects of probiotics on depressive symptoms in humans: a systematic review. Ann Gen Psychiatry. 2017;16:14.

15. Desbonnet L, Garrett L, Clarke G, Bienenstock J, Dinan TG. The probiotic *Bifidobacteria infantis*: an assessment of potential antidepressant properties in the rat. J Psychiatr Res. 2008;43:164-174.

16. Arseneault-Breard J, Rondeau I, Gilbert K, Girard SA, Tompkins TA, Godbout R, Rousseau G. Combination of Lactobacillus helveticus R0052 and Bifidobacterium longum R0175 reduces post-myocardial infarction depression symptoms and restores intestinal permeability in a rat model. Brit J Nutr. 2012;107:1793-1799.

17. Gilbert K, Arseneault-Breard J, Flores Monaco F, Beaudoin A, Bah TM, Tompkins TA, Godbout R, Rousseau G. Attenuation of postmyocardial infarction depression in rats by n-3 fatty acids or probiotics starting after the onset of reperfusion. Brit J Nutr. 2013;109:50-56.

18. Savignac HM, Corona G, Mills H, Chen L, Spencer JPE, Tzortzis G, Burnet PWJ. Prebiotic feeding elevates central brain derived neurotrophic factor, N-methyl-d-aspartate receptor subunits and d-serine. Neurochem Int. 2013;63:756-764.

19. Berton O, Nestler EJ. New approaches to antidepressant drug discovery: beyond monoamines. Nat Rev Neurosci. 2006;7:137-151.

20. Kulkarni SK, Dhir A. Effect of various classes of antidepressants in behavioral paradigms of despair. Prog Neuropsychopharmacol Biol Psychiatry. 2007;31;1248-1254.

21. Njung'e K, Handley SL. Evaluation of marble-burying behavior as a model of anxiety. Pharmacol Biochem Behav. 1991;38:63-67.

22. Mesripour A, Hajhashemi V, Kuchak A. Effect of concomitant administration of three different antidepressants with vitamin B6 on depression and obsessive compulsive disorder in mice models. Res Pharm Sci. 2017;12:46-52.

23. Yankelevitch-Yahav R, Franko M, Huly A, Doron R. The forced swim test as a model of depressive-like behavior. J Vis Exp. 2015;97:52587.

24. Hedlund PB, Sutcliffe JG. The 5-HT7 receptor influences stereotypic behavior in a model of obsessive-compulsive disorder. Neurosci Lett. 2007;414:247-251.

25. Harasawa T, Ago Y, Itoh S, Baba A, Matsuda T. Role of serotonin type 1A receptors in fluvoxamine-induced inhibition of marble-burying behavior in mice. Behav Pharmacol. 2006;17:637-640.

26. Desbonnet L, Garrett L, Clarke G, Kiely B, Cryan JF, Dinan TG. Effects of the probiotic *bifidobacterium infantis* in the maternal separation model of depression. Neuroscience. 2010;170:1179-1188.

27. Oelschlaeger TA. Mechanisms of probiotic actions - A review. Int J Med Microbiol. 2010;300:57-62.

28. Kobayashi T, Hayashi E, Shimamura M, Kinoshita M, Murphy NP. Neurochemical responses to antidepressants in the prefrontal cortex of mice and their efficacy in preclinical models of anxiety-like and depression-like behavior: a comparative and correlational study. Psychopharmacology (Berl). 2008;197:567-580.

29. Liu YW, Liu WH, Wu CC, Juan YC, Wu YC, Tsai HP, Wang S, Tsai YC. Psychotropic effects of Lactobacillus plantarum PS128 in early life-stressed and naïve adult mice. Brain Res. 2016;1631:1-12.

30. Moloney RD, Desbonnet L, Clarke G, Dinan TG, Cryan JF. The microbiome: stress, health and disease. Mamm Genome. 2014;25:49-74.

31. Tillisch K, Labus J, Kilpatrick L, Jiang Z, Stains J, Ebrat B, Guyonnet D, Legrain-Raspaud S, Trotin B, Naliboff B, Mayer EA. Consumption of fermented milk product with probiotic modulates brain activity. Gastroenterology. 2013;144:1394-1401.

32. Cussotto S, Strain CR, Fouhy F, Strain RG, Peterson VL, Clarke G, Stanton C, Dinan TG, Cryan JF. Differential effects of psychotropic drugs on microbiome composition and gastrointestinal function. Psychopharmacology (Berl). 2019;236:1671-1685.

Turk J Pharm Sci 2020;17(3):299-306
DOI: 10.4274/tjps.galenos.2019.94103

ORIGINAL ARTICLE

In Vitro Antimicrobial and Antioxidant Activity of Biogenically Synthesized Palladium and Platinum Nanoparticles Using *Botryococcus braunii*

Botryococcus braunii Kullanarak Biyojenik Olarak Sentezlenmiş Paladyum ve Platin Nanopartiküllerin *İn Vitro* Antimikrobiyal ve Antioksidan Aktiviteleri

Anju ARYA, Khushbu GUPTA, Tejpal Singh CHUNDAWAT*

The North Cap University, Department of Applied Sciences, Haryana, India

ABSTRACT

Objectives: The spread of infectious diseases and the increase in drug resistance among microbes has forced researchers to synthesize biologically active nanoparticles. Ecofriendly procedures for the synthesis of nanoparticles are improving day by day in the field of nanobiotechnology. In the present study we used extract of the green alga *Botryococcus braunii* for the synthesis of palladium and platinum nanoparticles and evaluated their antimicrobial and antioxidant activity.

Materials and Methods: Green alga was collected from Udaisagar Lake, Udaipur (Rajasthan, India) and isolated by serial dilution method and grown on Chu-13 nutrient medium. The characterization of alga synthesized palladium and platinum nanoparticles was carried out using X-ray diffraction and scanning electron spectroscopy. The zone of inhibition was measured by agar well plate method and minimum inhibitory concentration was determined by agar dilution assay for antimicrobial activity. The antioxidant activity of the nanoparticles was also studied by 1,1-diphenyl-2-picrylhydrazyl method.

Results: Stable palladium and platinum nanoparticles were successfully produced using green alga. The XRD pattern revealed the crystalline nature and scanning electron micrographs showed the morphology of biogenically synthesized metal nanoparticles. Fourier transform infrared measurements showed all functional groups having control over stabilization and reduction of the nanoparticles. The green synthesized nanoparticles exhibited antimicrobial activity against gram-positive and gram-negative bacterial strains, antifungal activity against a fungus, and antioxidant activity.

Conclusion: The biogenic synthesis of metal nanoparticles can be a promising process for the production of other transition metal nanoparticles and new nanocatalysts will revolutionize the synthesis of organic heterocycles.

Key words: Palladium, platinum, nanoparticles, antimicrobial, antioxidant, biogenic

ÖZ

Amaç: Bulaşıcı hastalıkların yayılması ve mikroplar arasında gözlenen ilaç direncindeki artış, araştırmacıları biyolojik olarak aktif nanopartikülleri sentezlemeye zorladı. Nanopartiküllerin sentezine yönelik çevre dostu prosedürler, nanobiyoteknoloji alanında her geçen gün gelişmektedir. Bu çalışmada palladyum ve platin nanopartiküllerin sentezi için yeşil bir alg olan *Botryococcus braunii* ekstraktını kullandık ve nanopartiküllerin antimikrobiyal ve antioksidan aktivitelerini değerlendirdik.

Gereç ve Yöntemler: Udaisagar Gölü, Udaipur'dan (Rajasthan, Hindistan) yeşil alg toplandı ve seri seyreltme yöntemiyle izole edildi ve Chu-13 besi yerinde büyütüldü. Alg tarafından sentezlenmiş paladyum ve platin nanopartiküllerinin karakterizasyonu, X-ışını kırınımı ve taramalı elektron spektroskopisi kullanılarak gerçekleştirildi. İnhibisyon alanı, agar difüzyon tekniği kullanılarak ölçüldü ve minimum inhibitör konsantrasyonu, antimikrobiyal aktivite için agar seyreltme deneyi ile belirlendi. Nanopartiküllerin antioksidan aktivitesi de 1,1- difenil-2-picrylhydrazyl yöntemi ile belirlendi.

Bulgular: Kararlı paladyum ve platin nanoparçacıklar yeşil alg kullanılarak başarılı bir şekilde üretildi. XRD paterni, kristalin yapıyı doğruladı ve taramalı elektron mikroskobu mikrografları, biyolojik olarak sentezlenen metal nanoparçacıkların morfolojisini gösterdi. fourier dönüşümü

*Correspondence: E-mail: chundawatchem@yahoo.co.in, Phone: +91-9910436314 ORCID-ID: orcid.org/0000-0001-8666-4403
Received: 18.12.2018, Accepted: 07.03.2019

kızılötesi sonuçları, nanopartiküllerin stabilizasyonu ve indirgenmesi üzerinde etkisi olan tüm fonksiyonel grupları göstermiştir. Yeşil sentezlenmiş nanopartiküller, Gram-pozitif ve Gram-negatif bakteriyel suşlara karşı antimikrobiyal aktivite, bir mantara karşı antifungal aktivite ve antioksidan aktivite gösterdi.

Sonuç: Metal nanoparçacıkların biyojenik sentezi, diğer geçiş metali nanoparçacıklarının üretimi için umut verici bir süreç olabilir ve yeni nanokatalizörler organik heterosikliklerin sentezinde devrim yaratacaktır.

Anahtar kelimeler: Paladyum, platin, nanopartiküller, antimikrobiyal, antioksidan, biyojenik

INTRODUCTION

The green synthesis of metal nanoparticles has three qualifying characteristics: as an environmentally safe solvent system, particle-stabilizing capping agents, and ecofriendly reducing agents.[1] Biological synthesis using algae is one of the green approaches for the synthesis of d-block metal nanoparticles. Algae are eukaryotic, photoautotrophic, aquatic, and oxygenic organisms.[2,3] Algae have more information in their genetic material to encode various reducing stabilizing agents that mediate the biogenic synthesis of metal nanoparticles. Algae acquire energy from sunlight through photosynthesis and convert inorganic carbon into organic material for their growth. Since algae are sustainable bioresources, they can be used largely in the greener synthesis of metal nanoparticles.[4] Biogenic synthesis is the alternate route for synthesizing biocompatible metal nanoparticles to other synthesis processes such as chemical and physical.[5] It is the newest possible way of linking nanotechnology and biotechnology in the developing field of nanobiotechnology.[6]

Transition metal nanoparticles are regarded as important because of their biocompatibility, greener approach, ecofriendly adoptable nature, and photosynthesizing properties.[7] Many metal nanoparticles like Cu, Ag, Pt, Au, and Pd were used in different fields such as catalysts, labeling biological substances, optoelectronics, photothermal therapy, and biological activities against microbes. In particular, the biogenic synthesis of palladium and platinum nanoparticles has attracted the attention of researchers because it is cost effective, sustainable, and ecofriendly. Palladium and platinum nanoparticles are broadly used as heterogeneous and homogeneous catalysts,[8] drug carriers, and drugs; in many medical diagnoses without damaging the DNA structure[9] and in cancer treatment; as nanocatalysts in environment remediation scavenging dyes from the textile industry; in Suzuki coupling reactions;[10] and they have demonstrated antimicrobial activities[11] and been assessed in other disciplines of biological sciences.[12] There is a parallel increase in the use of methods for estimating the efficiency of such nanoparticles as antioxidants.[13,14] One such method that is currently popular is based upon the use of the stable free radical 1,1-diphenyl-2-picrylhydrazyl (DPPH).[14]

Our aim in the present contribution was to synthesize and characterize palladium and platinum nanoparticles from aqueous extract of the green alga *Botryococcus braunii* (*B. braunii*) and to evaluate their antimicrobial potential against bacterial and fungal species and antioxidant efficacy. Our study can be considered the first report on the synthesis of palladium and platinum nanoparticles using this green alga. The methods used are elucidated and the synthesized palladium and platinum nanoparticles were characterized using different techniques including ultraviolet (UV) visible spectroscopy, fourier transform infrared (FTIR) spectroscopy, scanning electron microscopy, and X-ray diffraction.

MATERIALS AND METHODS

Chemicals and test strains

B. braunii was collected from Udaisagar Lake, Udaipur (Rajasthan, India). The reagents agar-agar, palladium acetate [Pd $(OAc)_2$], and hexachloroplatinic acid (H_2PtCl_6) were of analytical grade and were purchased from Sigma Aldrich. Bacterial strains like *Pseudomonas aeruginosa* (MTCC 441), *Escherichia coli* (MTCC 442), *Klebsiella pneumoniae* (MTCC 109), and *Staphylococcus aureus* (MTCC 96) and a fungal strain, *Fusarium oxysporum*

Fusarium oxysporum (MTCC 2087) were purchased from Microbial Type Collection, Chandigarh (India).

Isolation and culturing of B. braunii

This green alga was isolated by serial dilution and grown on Chu-13 nutrient medium solidified by 1.5% agar-agar. The composition of the Chu-13 medium was $CaNO_3$ (0.300 g/L), $MgSO_4.7H_2O$ (0.025 g/L), $CaCl_2.2H_2O$ (0.027 g/L), K_2HPO_4 (0.010 g/L), ferric citrate (0.0035 g/L), citric acid (0.0035 g/L), Na_2CO_3 (0.02 g/L), $Na_2SiO_3.5H_2O$ (0.044 g/L), and some micronutrients.[15] Algal colonies appearing after 3 weeks of incubation were isolated and inoculated into liquid medium. For growth experiments algal species was grown for algal biomass in an incubator at 27±1 °C, 1.2±0.2 klux light intensity, and 16:8 h light:dark cycle in nutrient medium. After standardization of optimal culture conditions in Chu-13 medium the best results of growth of green alga were found.

Preparation of algal extract

The grown algal biomass was centrifuged, shade dried, and 5 g of algal biomass was taken in a 250 mL Erlenmeyer flask along with 100 mL of distilled water. Then the mixture was autoclaved for 15 min and filtered through Whatman No. 1 filter paper. The filtered extract was centrifuged and the supernatant was used as reducing agent for preparing metal nanoparticles. The prepared algal extract was kept at 4 °C in a refrigerator for further experimental use.[16]

Synthesis of palladium and platinum nanoparticles

The nanoparticles were synthesized using the following processes.

Palladium nanoparticles: 20 mL of algal extract was mixed with 80 mL of 1 mM Pd $(OAc)_2$ aqueous solution in a 250 mL Erlenmeyer flask at pH 6-7 and put on a magnetic stirrer at 60 °C for 3 h. Simultaneously, a positive control of Pd $(OAc)_2$ aqueous solution and algal extract and a negative control containing only Pd $(OAc)_2$ aqueous solution were maintained under the same conditions. The progress of the process was regularly monitored by observing color change. In the positive control the initial pale yellow solution turned dark brown, indicating formation of palladium nanoparticles, but in the negative control no change in color was observed. After the formation of palladium nanoparticles, the solution was centrifuged for 30 min and the obtained nanoparticles were washed with deionized water to remove impurities. This process of centrifugation and washing was carried out three times to achieve better separation of nanoparticles. The obtained palladium nanoparticles were oven dried at 70 °C.[17]

Platinum nanoparticles: 90 mL of 1 mM aqueous solution of H_2PtCl_6 was added with 10 mL of algal extract to a 250 mL Erlenmeyer flask at pH 6-7. The mixture was put on a magnetic stirrer at 95 °C for 4 h. Simultaneously, a positive control of H_2PtCl_6 aqueous solution and algal extract and a negative control containing only H_2PtCl_6 aqueous solution were maintained under the same conditions. In the positive control the initial light yellow solution turned brown and finally black, consistent with the formation of platinum nanoparticles, but in the negative control no change was observed. The synthesized platinum nanoparticles were separated from the mixture by centrifugation for 30 min and then washed with deionized water. This process of centrifugation and washing was repeated three times and finally the obtained platinum nanoparticles were oven dried at 58 °C for 4 h.[11]

Characterization of metal nanoparticles

FTIR analyses were carried out on a Perkin-Elmer instrument in the range of 4000-450 cm^{-1} using dried powders of the metal nanoparticles. Samples for analysis were prepared under ambient conditions and mixed with KBr. X-ray diffraction measurements were carried out on a Philips Xpert Pro XRD system (DY 1650) for determining the size of the synthesized metal nanoparticles. Images were obtained with the help of a scanning electron microscope (SEM) (Model-FEI Quanta 200) for analyzing the morphology of the nanoparticles.

Evaluation of antimicrobial activity

Test microorganisms

The antimicrobial activity of the platinum and palladium nanoparticles was studied against two Gram-negative bacterial strains *Pseudomonas aeruginosa* (MTCC 441) and *Escherichia coli* (MTCC 442), two Gram-positive bacterial strains *Klebsiella pneumoniae* (MTCC 109) and *Staphylococcus aureus* (MTCC 96) and a fungal strain *Fusarium oxysporum* (MTCC 2087). The antibacterial and antifungal potential of the nanoparticles was assessed in terms of zone of inhibition of microbial growth by agar well plate method and minimum inhibitory concentration was determined by agar dilution assay.

Agar well plate method

Bacterial cultures were maintained in petri plates containing nutrient agar medium at 37 °C. The medium was prepared containing 10 g of beef extract, 2 g of yeast extract, 5 g of peptone, 5 g of NaCl, and 15 g of agar in 1 L of distilled water. The fungus *F. oxysporum* was maintained on potato dextrose agar at 25 °C. The nutrient agar and potato dextrose agar were autoclaved at 121 °C at 15 psi for 15 min and poured onto sterile petri plates to a uniform depth of approximately 4 mm. Once the medium solidified the culture was spread onto the petri plates with the help of an L-spreader. With a sterilized 5 mm cork borer, wells were introduced into the agar and 20 µL of both platinum and palladium was added to the wells. Untreated algal extract and salt of platinum and palladium were used as negative control. The plates were incubated at 37 °C and 25 °C overnight as per requirements. The experiments were carried out in triplicate. The antimicrobial activity was evaluated by measuring the size of the clear zone around each well.[18]

Agar dilution method

The minimum inhibitory concentration (MIC) of these nanoparticles was determined by agar dilution technique where stocks of 50 mg/mL of the synthesized nanoparticles were resuspended in 10% dimethyl sulfoxide to produce two-fold dilutions in the range of 25-30 mg/mL and so on. Each dilution of nanoparticles was put into the melted agar. The agar was poured into petri plates and allowed to solidify. After this, bacteria prepared to a standard concentration were added as a spot to each plate, with 10^4 colony forming units per spot. These dilution plates were then incubated at 37 °C with a control plate having no antimicrobial agent. After incubation the growth of the microbial isolates on the agar plate was assessed. The lowest concentration of nanoparticles that prevents microbial growth was considered to be the MIC value of those nanoparticles against that microorganism.[18,19]

DPPH radical scavenging activity

The free radical scavenging activity of all the extracts was evaluated by DPPH according to the method previously reported by Blois[20] in 1958. Briefly, a 0.1 mM solution of DPPH in ethyl alcohol was prepared and 1 mL of this solution was added to 3 mL of the solution of all extracts in methanol at different concentrations (5, 10, 15, 20, and 25 µg/mL). The mixtures were shaken vigorously and allowed to stand at room temperature for 30 min. Then the absorbance was measured at 541 nm using a UV-Vis spectrophotometer. Ascorbic acid was used as the reference. Lower absorbance values of the reaction mixture indicate higher free radical scavenging activity. The capability of scavenging the DPPH radical was calculated using the following formula:

DPPH scavenging effect (% inhibition)={(A0-A1)/A0)×100},

where A0 is the absorbance of the control reaction and A1 is the absorbance in the presence of all of the extract samples and reference. All the tests were performed in triplicate and the results were averaged.

RESULTS AND DISCUSSION

In the present study, we synthesized palladium and platinum nanoparticles by the use of extract of the green alga *B. braunii*. Algal extract appears to be a potential source of reducing and stabilizing agent without using any chemical as reducing agent. The complete process of formation of metal nanoparticles was initially confirmed by visual observation as shown in Figure 1. In Figure 1a the change in color from pale yellow to dark brown and in Figure 1b from light yellow to black of the reaction mixture provide a convenient sign to indicate the formation of palladium and platinum nanoparticles, respectively.[15,16]

Fourier transform infrared spectroscopy

The FTIR spectrum of experimental samples revealed two types of vibrations, stretching and bending, in the wavelength range of 4000-450 cm^{-1}. The FTIR spectrum measurements were demonstrated to identify the major functional groups present in *B. braunii* to examine their possible involvement in the synthesis of palladium and platinum nanoparticles. Different peaks were seen at 3435.88, 2923.49, 2852.33, 1637.82, 1559.61, 1414.42, 1384.79, 1069.01, 1056.17, 837.53, 781.32, 714.25, 695.06, 657, 618.16, and 532.74 cm^{-1} in the FTIR spectrum of algal extract of *B. braunii*. The peak at 3435.88 was due to N-H and O-H stretching vibrations,[21,22] while the 2923.49 and 2852.33 cm^{-1} bands arose due to asymmetrical C-H stretching vibrations of $-CH_2$ and $-CH_3$.[22] The 1637.82 cm^{-1} peak is characteristic of N-H bending vibrations in amide of protein as a capping agent.[23,24] The peak at 1559.61 cm^{-1} showed the presence of a carboxyl group and the weak band at 1414.42 and 618.16 cm^{-1} was due to COO^- in amino acid residue of protein.[25] The peak observed around 1384.79 cm^{-1} can be assigned to C-N stretching vibrations of amine. C-H bending vibrations by carbohydrates (glucose residue by C-OH bond) showed a peak at 1037.17 cm^{-1}.[26] The 873.53, 781.32, 695.06, and 532.74 cm^{-1} bands were demonstrated due to O-C=O bending vibrations of CO_3^{-2}, C-H rocking of lipids, and N-H wagging of amine and alkyl halide, respectively. The results of the present study have shown that hydroxyl groups have a strong ability to interact with nanoparticles. The main peaks existing in the spectrum of the alga are also present in the spectrum of the palladium and platinum nanoparticles synthesized with lower intensities and slight shift. Therefore, it may be evidenced that proteins, polysaccharides, amides, and long chain fatty acids are the biomolecules responsible for bioreduction and act as capping and stabilizing agents.[27,28]

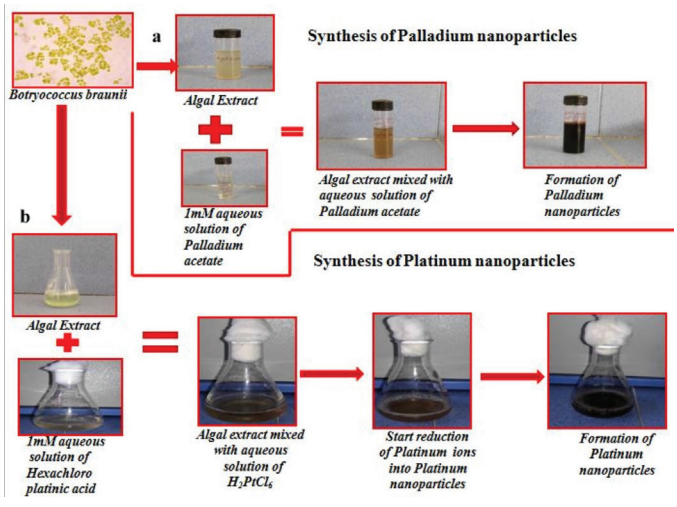

Figure 1. Biogenic synthesis of metal nanoparticles: (a) palladium nanoparticles, (b) platinum nanoparticles
H_2PtCl_6: Hexachloroplatinic acid

Scanning electron microscopy

The shape and size of the biogenically synthesized nanoparticles were elucidated with the help of SEM (Figures 2a and 2b). SEM showed that cubical, spherical, and truncated triangular palladium and platinum nanoparticles were synthesized.[29,30] The size distribution histogram shows that the average size of synthesized nanoparticles was 4.89 nm and 86.96 nm for

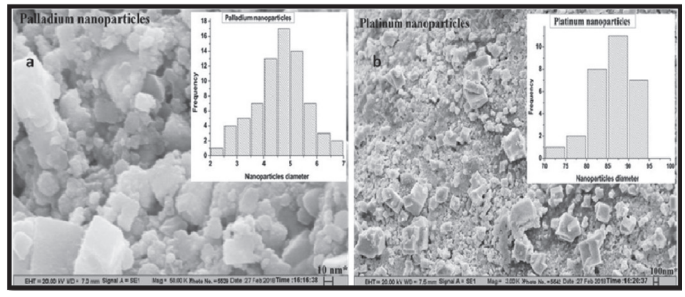

Figure 2. SEM images of green synthesized (a) palladium nanoparticles, (b) platinum nanoparticles
SEM: Scanning electron microscope

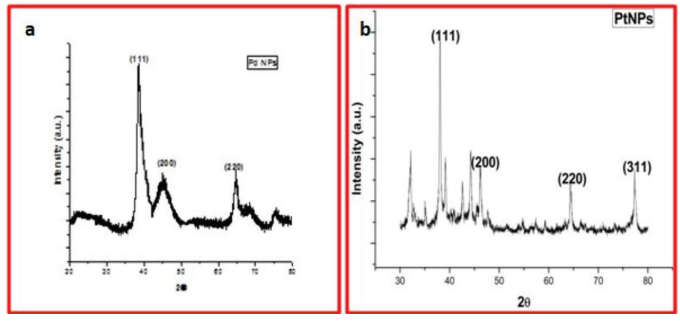

Figure 3. XRD patterns of biogenically synthesized (a) palladium nanoparticles and (b) platinum nanoparticles

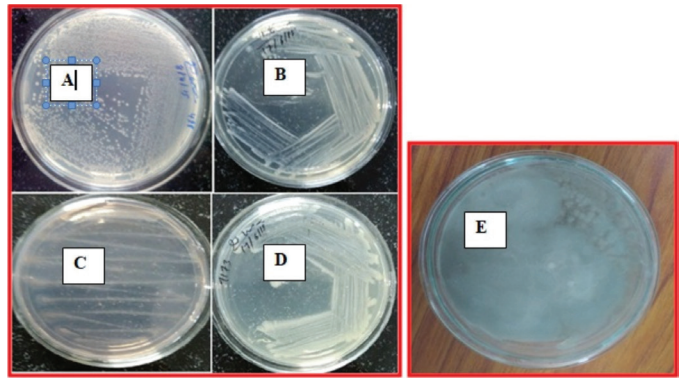

Figure 4. Revived culture of (A) *Klebsiella pneumoniae*, (B) *Staphylococcus aureus*, (C) *Pseudomona aeruginosa*, (D) *Escherichia coli*, and (E) *Fusarium oxysporum*

palladium and platinum nanoparticles, respectively. From the SEM images the number of nanoparticles (total 50 particles for each sample) was counted by ImageJ software. The following equation was used for calculating statistical properties of nanoparticles named as number average diameter (D_n), weight-average diameter (D_w), and polydispersity index (PDI).

$$D_n = \frac{\Sigma d_i}{n}$$

$$D_w = \frac{(\Sigma d_i)^4}{\Sigma (d_i)^3}$$

$$PDI = \frac{D_w}{D_n}$$

Here d_i is the diameter of microspheres and n represents the number of nanoparticles.

The PDI values of 0.198 for platinum nanoparticles and 0.862 for palladium nanoparticles were calculated and these values showed uniform size of synthesized nanoparticles. The PDI values were used as an indicator for the size distribution of the synthesized nanoparticles.[31]

X-ray diffraction

The synthesized metal nanoparticles were further evidenced by XRD measurements. The XRD analysis of green synthesized palladium nanoparticles in Figure 3a showed major diffraction peaks at 2θ of 40.1°, 46.6°, and 68.0°, corresponding to (111), (200), and (220) planes of the face-centered cubic structure of palladium nanoparticles (JCPDS no. 05-0681). The crystallite size of palladium nanoparticles was calculated from the (111) plane of face-centered cubic (fcc) palladium using the Scherrer equation. The crystallite size of the synthesized palladium nanoparticles was calculated to be around 5 nm.[32,33]

Furthermore, in Figure 3b the diffraction lines at about 2θ of 38.10, 46.60, 64.70, and 77.40 matched the (111), (200), (220), and (311) planes of the fcc crystal lattice of platinum (JCPDS No. 88-2343). The crystallite size of platinum nanoparticles was calculated from the (111) plane of fcc using the Scherrer equation. The crystallite size of the synthesized platinum nanoparticles was found to be 87 nm.[34,35]

Antimicrobial activity of synthesized palladium and platinum nanoparticles

Revived bacterial strains were maintained on nutrient agar medium as shown in Figure 4 and the fungal strain was maintained on potato dextrose agar as also shown.

Assay of biological activity

The biological activity of the algal extract and synthesized nanoparticles was tested against both bacteria (Gram-positive and Gram-negative) and a fungus using agar well diffusion.[36,37] Figure 5 shows the different zones of inhibition formed by synthesized platinum and palladium nanoparticles, antibiotics, algal extract, and salts of platinum and palladium against the test strains. The well filled with algal extract did not show any zone of inhibition but the nanoparticles synthesized from that algal culture show both antibacterial and antifungal activity with a zone of inhibition ranging from 7 to 16 mm (Table 1, Figure 6).[38] PtNps and PdNps at 400 µg/mL concentration showed the maximum zone of inhibition against the test strains.

Determination of minimum inhibitory concentration

The MIC[39] required to inhibit the growth of microbes is less in the case of platinum as compared with palladium (Figure 7). These synthesized nanoparticles show the least activity towards the fungus tested, *F. oxysporum*. The positive control drugs used

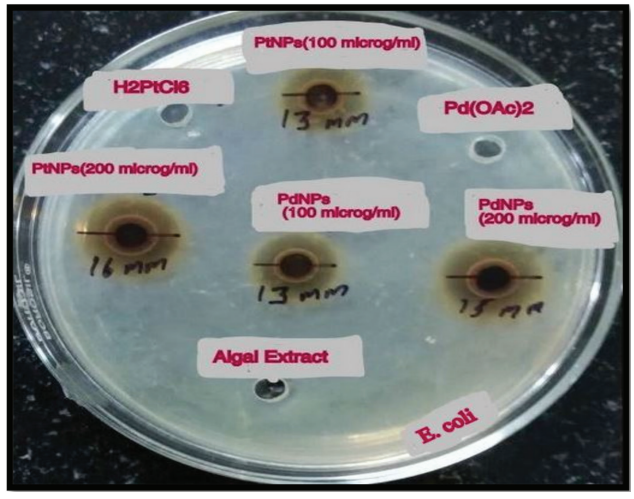

Figure 5. Antibacterial assay: zone of inhibition against *Escherichia coli*

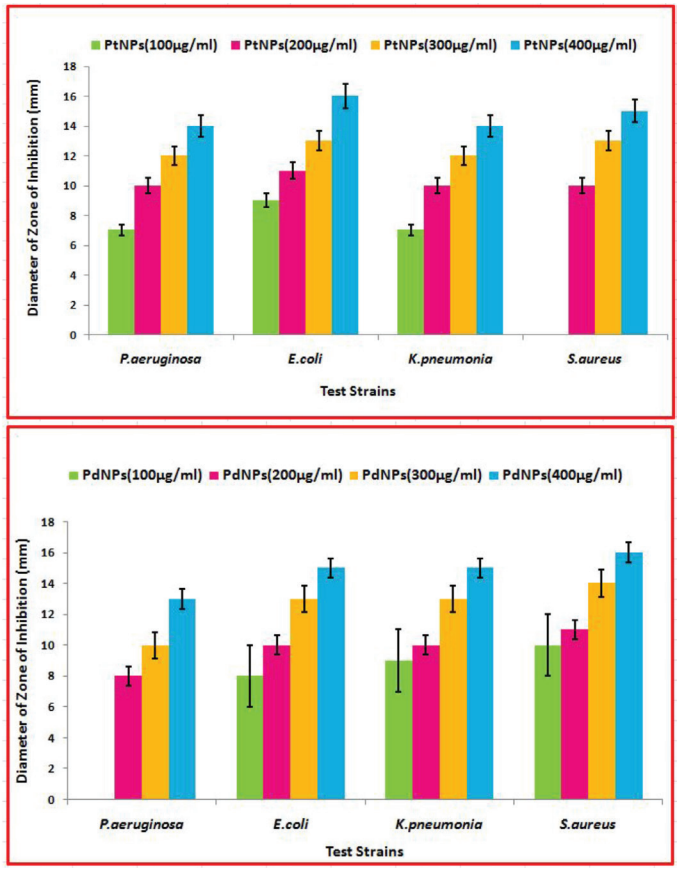

Figure 6. Comparative representation of zone of inhibition diameters formed against the test strains

against both gram positive and gram negative bacteria were chloramphenicol and ampicillin. Nystatin and griseofulvin were used as the positive control drugs for *F. oxysporum*. The antibiotic ampicillin does not show any activity against *P. aeruginosa* as compared to PtNps and PdNps, which show significant activity. The antimicrobial activity of nanoparticles was considered to be good if its MIC was less than 100 µg/mL, moderate if MIC was from 100 to 500 µg/mL, and poor over 500 µg/mL (Table 2).[40, 41, 4]

Antioxidant activity

The antioxidant potential of the green synthesized palladium and platinum nanoparticles was evaluated by quantifying the DPPH free radical scavenging activity (Figure 8, Table 3). In the presence of nanoparticles, the color of the DPPH solution gradually changed from purple to pale yellow with time. The percentage scavenging of DPPH increased linearly with an increase in nanoparticle concentration from 1 to 20 µg/mL and reached 82.43% within 30 min at 20 µg/mL in the case of palladium and 78.14% at 25 µg/mL in the case of platinum. However, the positive control ascorbic acid showed 94.0% scavenging activity at a concentration of 50 µg/mL. The negative control wells loaded with algal extract did not show any color change from purple.[41,42]

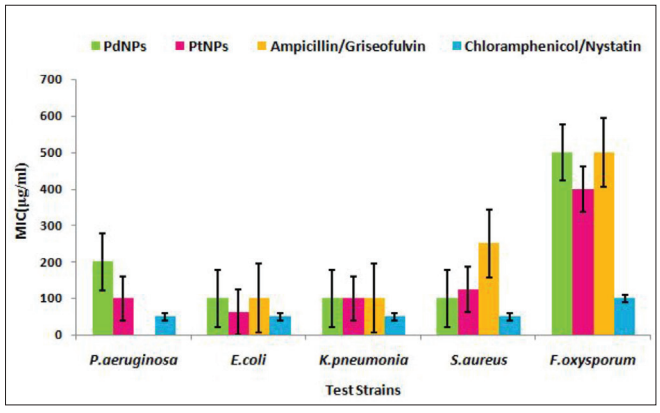

Figure 7. Representation of MIC value against the test strains
MIC: Minimum inhibitory concentration

CONCLUSION

In the present work, a successful, rapid combustion method is demonstrated for the synthesis of stabilized nanoscale palladium and platinum particles for the first time with the use

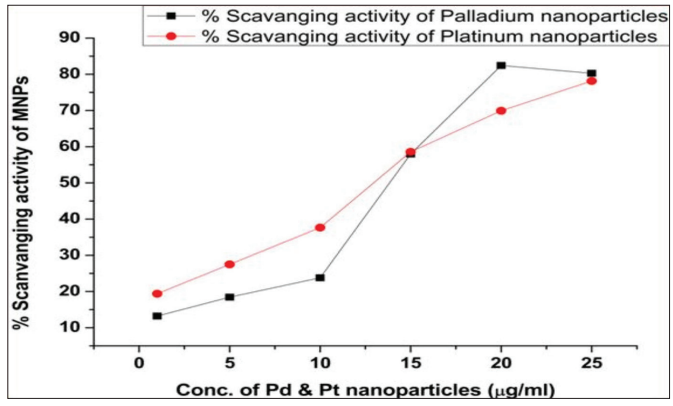

Figure 8. Graph representing % scavenging activity of nanoparticles

Table 1. Diameter of zone of inhibition observed against the different test strains

Microbial strain	Diameter of zone of inhibition (in mm)							
	Palladium nanoparticles concentration (µg/mL)				Platinum nanoparticles concentration (µg/mL)			
	100	200	300	400	100	200	300	400
Pseudomonas aeruginosa	-	8±1.56	10±1.4	13±1.23	7±1.86	10±0.5	12±1.2	14±1.16
Escherichia coli	8±0.6	10±1.5	13±1.8	15±1.66	9±1.26	11±1.4	13±1.2	16±1.96
Klebsiella pneumoniae	9±1.5	11±1.5	13±0.55	16±0.76	7±0.53	10±0.1	12±0.5	14±0.33
Staphylococcus aureus	10±0.1	11±1.5	14±1.56	16±0.86	-	10±0.7	13±0.3	15±0.2

Table 2. Minimum inhibitory concentration observed against the different test strains

Nanoparticles (500 µg/mL)	Minimum inhibitory concentration (µg/mL)				
	Gram negative bacterial strains		Gram positive bacterial strains		Fungal strain
	Pseudomonas aeruginosa	*Escherichia coli*	*Klebsiella pneumoniae*	*Staphylococcus aureus*	*Fusarium oxysporum*
Palladium	200	100	100	100	500
Platinum	100	62.5	100	125	400
Ampicillin	-	100	100	250	-
Chloramphenicol	50	50	50	50	-
Nystatin	-	-	-	-	100
Griseofulvin	-	-	-	-	500

Table 3. Comparison of DPPH scavenging activity of palladium and platinum nanoparticles

Concentration of palladium/platinum nanoparticles (µg/mL)	% Scavenging activity of palladium nanoparticles	% Scavenging activity of platinum nanoparticles
1	13.22	19.37
5	18.44	27.51
10	23.78	37.66
15	57.96	58.57
20	82.43	69.93
25	82.27	78.14

DPPH: 1,1-diphenyl-2-picrylhydrazyl

of extract of the green alga *B. braunii* as a reducing stabilizing and capping agent. The biogenically synthesized nanoparticles were characterized by different techniques including FTIR spectroscopy, scanning electron microscopy, and X-ray diffraction. The FTIR spectrum confirms the interaction of algal biomolecules and the formation of palladium and platinum nanoparticles. From the SEM images and XRD patterns, the prepared nanoparticles exhibited cubical, spherical, and truncated triangular shape with 4.89 nm and 86.96 nm palladium and platinum nanoparticles, respectively. The green synthesized nanoparticles exhibited antimicrobial activity against Gram positive and Gram negative bacterial strains, antifungal activity against a fungus, and antioxidant activity. This conversion of metal ions into metal nanoparticles will one day replace the other methods of synthesis of nanoparticles and could possibly be used for large-scale synthesis of technologically important applications.

ACKNOWLEDGEMENT

The authors are thankful to the North Cap University for providing facilities for the research work.

Conflicts of interest: No conflict of interest was declared by the authors. The authors alone are responsible for the content and writing of the paper.

REFERENCES

1. Sau TK, Murphy CJ. Room temperature, high-yield synthesis of multiple shapes of gold nanoparticles in aqueous solution. J Am Chem Soc. 2004;126:8648-8649.
2. Castro L, Blazquez ML, Munoz JA, Gonzalez F, Ballester A. Biological synthesis of metallic nanoparticles using algae. IET Nanobiotechnology. 2013;7:109-116.
3. Rai UN, Pal D, Saxena PN. Mineral nutrition of the green alga *Botryococcus braunii*. Kuetz New Botanist. 1987;14:1-7.
4. Narayanan BK, Sakthivel N. Green synthesis of metal nanoparticles by terrestrial and aquatic phototrophic and heterotrophic eukaryotes and biocompatible agents. Adv Colloid Interface Sci. 2011;169:59-79.
5. Azizi S, Ahmad MB, Namvar F, Mohamad R. Green biosynthesis and characterization of Zinc oxide nanoparticles using brown marine macroalga Sargassum muticum aqueous extract. Mater Lett. 2014;116:275-277.
6. Akhtar MS, Panwa J, Yun YS. Biogenic synthesis of metallic nanoparticles by plant extract. ACS Sustainable Chem Eng 2013;1:591-602.
7. Elango G, Roopan SM. Green synthesis, spectroscopic investigation and photocatalytic activity of lead nanoparticles. Spectrochim Acta A Mol Biomal Spectrosc. 2015;139:367-373.
8. Narayanan R, El-Sayed MA. Catalysis with transition metal nanoparticles in colloidal solution: nanoparticles shape dependence and stability. J Phy Chem B. 2005;109:12663-12676.
9. Thakkar KN, Mhatre SS, Pankh RY. Biological synthesis of metallic nanoparticles. Nanomedicine. 2010;6:257-262.
10. Nasrollahzadeh M, Sajadi SM, Maham M. Green synthesis of palladium nanoparticles using Hippophae rhamnoides Linn leaf extract and their catalytic activity for the Suzuki-Miyaura coupling in water. J Mol Catal A Chem. 2015;396: 297-303.
11. Ramkumar VS, Pugrzhendhi, A, Prakash S, Ahila NK, Vinoj G, Selvam S, Kumar G, Kannapiran E, Rajendran BR. Synthesis of platinum nanoparticles using seaweed Padina gymnospora and their catalytic activity at PVP/PtNps nano-composite towards biological applications. Biomed Pharmacother. 2017;92:479-490.
12. Siddiqi KS, Husen A. Green synthesis, characterization and uses of palladium/platinum nanoparticles. Nanoscale Res Lett. 2016;11:482.
13. Sa'nchez-Moreno C, Larrauri JA, Saura-Calixto F. Free radical scavenging capacity and inhibition of lipid oxidation of wines, grape juices and related polyphenolic constituents. Food Res Int. 1999;32:407-412.
14. Schwarz K, Bertelsen G, Nissen LR, Gardner PT, Heinonen MI, Hopia A, Huynh-Ba T, Lambelet P, McPhail D, Skibsted LH, Tijburg L. Investigation of plant extracts for the protection of processed foods against lipid oxidation. Comparison of antioxidant assays based on radical scavenging, lipid oxidation and analysis of the principal antioxidant compounds. Eur Food Res Technol. 2001;212:319-328.
15. Chu SP. The influence of the mineral composition of the medium on the growth of planktonic algae: Part I. Methods and Culture media. J Ecol. 1942;30:284-325.
16. Ramakrishana M, Babu DR, Gengan RM, Chandra S, Rao GN. Green synthesis of gold nanoparticles using marine algae and evaluation of their catalytic activity. J Nanostruct Chem. 2015;6:1-13.
17. Arsiya F, Sayadi MS, Sobhani S. Green synthesis of palladium nanoparticles using Chlorella vulgaris. Mater Lett. 2016;186:113-115.
18. Balouiri M, Sadiki M, Ibnsouda SK. Methods for *in vitro* evaluating antimicrobial activity: A review. J Pharm Anal. 2016;6:71-79.
19. Wiegand I, Hilpert K, Hancock RE. Agar and broth dilution methods to determine the minimal inhibitory concentration (MIC) of antimicrobial substances. Nature Protoc. 2008;3:163-175.
20. Blois MS. Antioxidant determinations by the use of a stable free radical. Nature. 1958;181:1199-1200.
21. Arya A, Gupta K, Chundawat TS, Vaya D. Biogenic Synthesis of Copper and Silver Nanoparticles using Green Alga Botryococcus braunii and its antimicrobial activity. Bioinorg Chem App. 2018:1-9.
22. Rajathi FAA, Nambaru VRMS. Phytofabrication of nanocrystalline platinum particles by leaves of Cerbera manghas and its antibacterial efficacy. Int J Pharma Bio Sci. 2014;5:619-628.

23. Kalaiselvi A, Roopan SM, Madhumitha G, Ramalingam C, Elango G. Synthesis and characterisation of Palladium nanoparticles using Catharanthusroseus leaf extract and its application in the photo-catalytic degradation. Spectrochimica Acta Part A: Moleculer and Biomoleculer Spectroscopy. 2015;135:116-119.

24. Aboelfetoh EF, El-Shenody RA, Ghobara MM. Eco-friendly synthesis of silver nanoparticles using green alga (Caulerpa serrulata): reaction optimization, catalytic and antibacterial activities. Environ Monit Assess. 2017;189:349.

25. Sharma B, Purkayastha DD, Hazra S, Gogoi L, Bhattacharjee CR, Ghosh NN, Rout J. Biosynthesis of gold nanoparticles using fresh water green alga Prasiola crispa. Mater Lett. 2013;116:94-97.

26. Shende S, Gade A, Rai M. Large Scale synthesis and antibacterial activity of fungal derived silver nanoparticles. Environ Chem Lett. 2016;15:427-434.

27. Elango G, Roopan SM, Al-Dhabi NA, Arasu MA, Damodharan KI, Elumalai K. Cocosnuciferacoir-mediated green synthesis of PdNPs and its investigation against larvae and agricultural pest. Artificial Cells Nanomed Biotechnol. 2017;45:1581-1587.

28. Govender Y, Riddin TL, Gericke M, Whiteley CG. On the enzymatic formation of platinum nanoparticles. J Nanoparticle Res. 2010;12:261-271.

29. Coccia F, Tonucci L, Bosco D, Bressan M, Alessandro DN. One pot synthesis of lignin stabilized platinum and palladium nanoparticles and their catalytic behaviour in oxidation and reduction reactions. Green Chemistry. 2012;14:1073-1078.

30. Raut RW, Haroon ASM, Malghe YS, Nikam BT, Kashid SB. Rapid biosynthesis of platinum and palladium metal nanoparticles using root extract of Asparagus racemosus linn. Adv Mater Lett. 2013;4:650-654.

31. Nematollahzadeh A, Abdekhodaie MJ, Shojaei A. Submicron nanoporous polyacrylamide beads with tunable size for verapamli imprinting. J Appl Polym Sci. 2012;125:189-199.

32. Azizi S, Shahri MM, Rahman HS, Rahim RA, Rasedee A, Mohamad R. Green synthesis Palladium nanoparticles mediated by white tea (Camellia sinesis) extract with antioxidants, antibacterial and antiproliferative activities towards the human leukaemia (MOLT-4) cell line. Int J Nanomed. 2017;12:8841-8853.

33. Ganaie SU, Abbasi T, Abbasi SA. Biomimetic synthesis of platinum nanoparticles utilizing a terrestrial weed antigononleptopus. Particul Sci Technnol. 2018;36:681-688.

34. Naveen BS, Padmesh TVN. Seaweed (Sargassum ilicifolium) assisted green synthesis of Palladium nanoparticles. Int J Sci Eng Res. 2014;5:229-231.

35. Hazarika M, Borah D, Bora P, Silva AR, Das P. Biogenic synthesis of palladium nanoparticles and their applications as catalyst and antimicrobial agent. PLOS ONE. 2017;12:1-19.

36. Obreja L, Daniela P, Neculai F, Viorel M. Platinum nanoparticles synthesis by sonoelectrochemical methods. Material Plastice. 2010;47:42-47.

37. Letaba GM, Lang CI. Synthesis of bimetallic platinum nanoparticles for biosensors. Sensors (Basel). 2013;13:10358-10369.

38. Magaldi S, Mata-Essayag S, Hartungde-Capriles C, Perez C, Colella MT, Olaizola C, Ontiveros Y. Well diffusion for antifungal susceptibility testing. Int J Infect Dis. 2004;8:39-45.

39. Valgas C, DeSouza SM, Smânia EFA, Smania Jr A. Screening methods to determine antibacterial activity of natural products. Braz J Microbiol. 2007;38:369-380.

40. Srinivasan S, Sarada DVL. Antifungal activity of phenyl derivative of pyranocoumarin from Psoralea corylifolia L. seeds by inhibition of acetylation activity of trichothecene 3-o-acetyltransferase (Tri101). J Biomed Biotechnol. 2012;2012:310850.

41. Sarkar M, Reneer DV, Carlyon JA. Sialyl-Lewis x-Independent Infection of Human Myeloid Cells by *Anaplasma phagocytophilum* Strains HZ and HGE1. Infect Immun. 2007;75:5720-5725.

42. Lee CJ, Chen LW, Chen LG, Chang TL, Huang CW, Huang MC, Wanga CC. Correlations of the components of tea tree oil with its antibacterial effects and skin irritation. J Food Drug Anal. 2013;21:169-176.

Turk J Pharm Sci 2020;17(3):307-318
DOI: 10.4274/tjps.galenos.2019.26096

ORIGINAL ARTICLE

Mapping the Impact of a Polar Aprotic Solvent on the Microstructure and Dynamic Phase Transition in Glycerol Monooleate/Oleic Acid Systems

Gliserol Monooleat/Oleik Asit Sistemlerinde Polar Aprotik Çözücünün Mikroyapı ve Dinamik Faz Geçişine Etkisinin Haritalanması

Marzuka Shoeb KAZI*, Mohammed Hassan DEHGHAN

Y.B. Chavan College of Pharmacy, Department of Pharmaceutics, Dr. Rafiq Zakaria Campus, Aurangabad, India

ABSTRACT

Objectives: The impact of incorporating a polar aprotic solvent, dimethyl sulfoxide (DMSO), in glycerol monooleate/oleic acid systems was evaluated briefly to map its influence on the gel microstructure and dynamic phase transition in controlling the performance of a polyene antifungal drug delivery system.

Materials and Methods: An *in situ* gelling fluid precursor system (IGFPS) exhibiting inverse lyotropic liquid crystalline phases was developed by simple solution add-mixture method. Polarized light microscopy, small angle X-ray scattering (SAXS), differential scanning calorimetry (DSC), and oscillatory rheological assessments were performed to ascertain microstructural modulations. The developed system was examined for minimum gelling volume, gelling time, swelling behavior, mucoadhesion, *in vitro* antifungal activity, and *in vitro* drug release.

Results: The SAXS study identifies the coexistence of Im3m cubic phase with HCP P63/mmc hexagonal structures. The SAXS and DSC data highlight DMSO's unique ability to work both as a kosmotropic or chaotropic solvent and to be a function of its concentration. The *in vitro* antifungal test results indicate the concentration of DMSO to be a controlling factor in drug release and diffusion. The *in vitro* drug release kinetic studies reveal that most of the gel samples follow the matrix model and anomalous type release as implied by Peppas model.

Conclusion: Finally, the antifungal IGFPS formulated was found to have the required low viscosity, responsive sol-gel phase transition, appreciative mechanical properties, and desirable antifungal effect with sustained drug release performance.

Key words: Dimethyl sulfoxide, glycerol monooleate, microstructure, oleic acid, small angle X-ray scattering

ÖZ

Amaç: Bir polien antifungal ilaç taşıyıcı sistem performansını kontrol etmek için polar aprotik çözücü olan dimetil sülfoksit'in (DMSO), gliserol monooleat/oleik asit sistemlerine dahil edilmesinin, jel mikroyapısı ve dinamik faz geçişi üzerindeki etkisi araştırılmıştır.

Gereç ve Yöntemler: İnvers liyotropik sıvı kristalin (LLC) fazları sergileyen in situ jelleşen öncü sıvı sistemi (IGFPS), basit çözelti ilave etme yöntemi ile geliştirilmiştir. Polarize ışık mikroskopisi (PLM), küçük açılı X-ışını saçılması (SAXS), diferansiyel tarama kalorimetrisi (DSC) ve reolojik osilatör ölçümleri mikroyapısal modifikasyonları belirlemek için yapılmıştır. Geliştirilen sistem, minimum jelleşme hacmi, jelleşme süresi, şişme davranışı, mukoyapışkanlık, *in vitro* antifungal aktivite ve *in vitro* ilaç salımı açısından incelenmiştir.

Bulgular: SAXS çalışması, Im3m kübik fazın HCP P63/mmc altıgen yapılarla bir arada varlığını tanımlamıştır. SAXS ve DSC verileri, DMSO'nun hem bir kozmotropik hem de kaotropik çözücü olarak görev yaptığını ve işlevini konsantrasyon bağımlığı olarak gerçekleştirdiğini gösterdiğinden DMSO'nun eşsiz yeteneğini vurgulamıştır. *İn vitro* antifungal test sonuçları, DMSO konsantrasyonunun ilaç salımı ve difüzyonunda kontrol edici bir faktör olduğunu göstermiştir. *İn vitro* ilaç salım kinetik çalışmaları, jel örneklerinin çoğunun matris modeli ve Peppas modelinin belirttiği gibi anormal tip salım kinetiğini takip ettiğini ortaya koymuştur.

Sonuç: Sonuç olarak, formüle edilen antifungal IGFPS'nin, gerekli düşük viskoziteye, duyarlı sol-jel faz geçişine, istenen mekanik özelliklere ve sürekli ilaç salım performansı ile arzu edilen antifungal etkiye sahip olduğu bulunmuştur.

Anahtar kelimeler: Dimetil sülfoksit, gliserol monooleat, mikroyapı, oleik asit, küçük açılı X-ışını saçılması

*Correspondence: **E-mail:** marzi345@gmail.com, **Phone:** +919975145944 **ORCID-ID:** orcid.org/0000-0002-6103-7806
Received: 04.06.2019, **Accepted:** 03.08.2019

INTRODUCTION

Dimethyl sulfoxide [(DMSO, $(CH_3)_2SO$)] is a short amphiphilic moiety, conventionally used as a cryoprotectant and solvent for lipophilic drugs, and it is the solvent of choice for the synthesis of sugar ester (used for ice cream production), cell fusogen, and chemical penetration enhancer to deliver active molecules through the skin and into the cell.[1,2] DMSO interacts with lipids to replace water in the inner region of lipid head groups, increasing the area of lipid and decreasing its thickness.[3] The hydrophilic group of DMSO interrelates with water and polar head groups of lipids, whereas the two hydrophobic methyl groups intermingle with the hydrophobic inner membrane region of lipids.[4] Due to its dual character, DMSO occupies the inner interface region and acts as a surfactant to stabilize the presence of water molecules. Lipids such as oleic acid (OA) and glycerol monooleate (GMO) have a polar head and a relatively short hydrophobic carbon chain. GMO is categorized as a GRAS approved nontoxic, biodegradable, and biocompatible material and is also cited in the Food and Drug Administration Inactive Ingredients Guide. GMO was introduced for the first time in 1930, for margarine production; since then it has been extensively used in the food industry as an emulsifier and stabilizer for foams in bread, cakes, margarine, ice cream, and chewing gum.[5] OA is a monounsaturated fatty acid (triglyceride) component of the human diet obtained from animal fats and vegetable oils.

The interaction of DMSO with OA and GMO results in modulation of the microstructure of the lyotropic liquid crystalline (LLC) system, which is formed due to transformation of the sol system to the gel phase upon contact with external stimuli like body fluids and excess water. The microstructure formed is primarily controlled by additives in the system and the nature of the drug, i.e. hydrophilic or lipophilic. The reversed hexagonal and bicontinuous cubic mesophases are spontaneously formed from the *in situ* gelling liquid crystal forming system with impetus to an external stimulus. The tortuous networks of aqueous nanochannels formed in these mesophases partake as gateways for the sustained release of drugs from the gelled liquid crystal structure. In the present investigation, an *in situ* gelling system was developed by adding a polyene antifungal agent, nystatin, widely used against susceptible cutaneous and mucocutaneous fungal infections caused by *Candida* species and exhibiting a broad spectrum of activity against other fungi such as *Aspergillus* and *Cryptococcus*. Interestingly, there are reports that this polyene moiety interacts with phospholipids and therefore liposomal formulations have been developed to reduce its toxic effects.[6]

In the present study, the impact of incorporating a polar aprotic solvent, DMSO, in a GMO/OA system was evaluated briefly to map its influence on the gel microstructure and dynamic phase transition in controlling the performance of a polyene antifungal drug delivery system.

MATERIALS AND METHODS

Materials

Nystatin was procured as a gift sample from Glenmark Pharmaceuticals, Mumbai. Cithrol GMO-HP-SO-LK was a gift sample obtained from Croda. OA, DMSO, methanol, dimethyl formamide, and chloroform were acquired from Loba Chemie, Mumbai. Dextrose, peptone, and agar were purchased from Fisher Scientific, India. *Aspergillus fumigatus* (NCIM 902) and *Candida albicans* (ATCC 18804) were procured from the National Chemical Laboratory, Pune. Cellulose acetate membrane pore size 0.45 µm was purchased from Millipore. Goat intestinal mucosa was obtained from a local slaughterhouse.

Formulation of in situ gelling fluid precursor systems (IGFPS)

The formulation of IGFPS is summarized in Table 1. To prepare it by simple add-mixture method, briefly nystatin (2.23% w/w) was dissolved in DMSO; the resulting solution was added to OA and vortex mixed (B-6R-47, Biocraft Scientific Systems) for 5 min to obtain a homogeneous solution. The resulting solution was then added to melted (40±2 °C) GMO and vortex mixed for an additional 15 min. The IGFPS were stored at room temperature until further characterization was performed.

Characterization

In situ gelling ability and gelation time

The minimum solvent (Vm) and minimum time (Tm) required for complete gelation of IGFPS was determined by magnetic stirring method.[7] First 1 g of the IGFPS was aliquoted into a 5 mL vial and then a magnetic bar (10 mm×6 mm) was added to the vial. The temperature was maintained at 37.0±0.5 °C and the speed of the magnetic bar was set at 30 rpm. Distilled water (10 µL) was added to the vial each minute, until the magnetic bar completely stopped moving due to gelation. For Tm the above procedure was used and an excess amount of distilled water was added to the vial; the time required for complete halt of magnetic bar was noted as Tm.

Table 1. Formulation of IGFPS

Formulation	Oleic acid:DMSO (%w/w)
F1	1:3
F2	1:5
F3	1:4
F4	3:4
F5	1:1
F6	3:5
F7	2:3
F8	2:5
F9	1:2

*GMO was added quantity sufficient to 100%w/w
GMO: Glycerol monooleate, IGFPS: *In situ* gelling fluid precursor systems, DMSO: Dimethyl sulfoxide

Drug content and pH value of IGFPS

For drug content determination, briefly 1 g of formed gel was dissolved in 100 mL of solvent system comprising methanol:dimethylformamide (DMF):water (55:15:30) and was evaluated at 306 nm using a Shimadzu ultraviolet (UV)-1600 spectrophotometer. The pH value of IGFPS was determined using a Systronics Digital pH meter 335.

Swelling studies

The water uptake of the systems was measured gravimetrically at fixed time intervals. Briefly 0.5 g of IGFPS was weighed on filter paper (40 mm in diameter) soaked in distilled water and positioned on top of a sponge (5 cm×5 cm×2 cm) previously soaked in the hydration medium and placed in a petri dish filled with distilled water to a height of 0.5 cm.[8] This investigational set-up was kept closed. The water uptake was determined as the increase in the weight of the sample over time normalized to the initial weight of the dry systems.[8] The data were subjected to mathematical models[9] using the following equations to affirm whether the kinetics of swelling was first order or second order.

$$\ln \frac{w_\infty}{w_{\infty-w}} = kt \quad 1 \qquad \frac{t}{w} = \frac{1}{kw_\infty^2} + \frac{t}{w_\infty} \quad 2$$

where W∞- maximum water uptake, W - water uptake at time t, (W∞-W) represents the unrealized water uptake, and k is the proportionality constant. For second order kinetics, the initial rate of swelling is the reciprocal of the y-intercept in the plot of t/W versus t. The reciprocal of the slope indicates W∞, which is the maximum or equilibrium water uptake. The units of W∞ are grams of buffer absorbed per gram of matrix (g/g), and the units of the initial swelling rate are grams of buffer absorbed per gram of dry matrix per hour (g/g h).[10,11]

Polarized light microscopy (PLM)

The hydrated gels were evaluated at 20±0.5 °C, 27±0.5 °C, and 37±0.5 °C using microscopy (Carl Zeiss Jena, Germany) images under 40× magnifications. The samples were inserted between two glass microscope slides and observed with cross polarizers to ascertain the type of lyotropic liquid crystal mesophase formed on the basis of characteristic textures.[12]

Mucoadhesion measurement by tensile strength method

A CT3 Texture Analyzer (Brookfield Engineering, UK) was used for the tensile strength measurements. Fresh goat intestinal mucosa was obtained from a local slaughterhouse. The dissected mucosal pieces were kept in saline solution in an ice bath until the tests were performed. The mucosa was fastened to a 10 mm analytical movable probe of the texture analyzer by a rubber ring and the formulation was located on the lower platform. The system was maintained at 37±1 °C by a thermostatic bath. The measurement was triggered to begin as the upper probe encountered a force of 3 mN upon contact with the sample (1 g). The probe was kept in contact with no force applied for 60 s, after which it was raised at a speed of 1 mm/s, and the force needed for detachment was estimated. The tensile work, which is proportional to the area under the force–time curve, was used to describe the mucoadhesive characteristics.

Rheological measurements

Rotational and oscillatory rheological tests were performed for formed gel samples using a Kinexus Rheometer (Malveran Instruments Ltd, UK). Rotational and oscillatory tests were performed at 37.0±0.1 °C. Rotational tests were used to determine the viscosity and the data were analyzed for type of flow pattern. Oscillatory tests were performed to define the elastic modulus, loss modulus, and complex viscosity. The shear rate during the rotational tests ranged from 2 to 100 s^{-1}. For oscillatory analysis, first stress sweep measurements (0.001-10%) were performed at a constant frequency of 1 Hz in order to determine the linear viscoelastic region. Afterwards, oscillatory shear measurements were carried out as a function of frequency (0.1-100 Hz) at a constant strain of 0.1%.

Small angle X-ray scattering (SAXS)

Scattering data were obtained by using a NANO-Viewer (Rigaku, Japan) with a 2D hybrid pixel array detector; Cu Kα was used as the radiation source (0.154 Å) from the micro-focus rotating anode X-ray generator operated at a power rating of 40 kV and 30 mA. Samples were subjected to X-ray exposure for 10 min with the sample to detector distance set at 800 mm. The measurements were performed at various temperatures, i.e. 20 °C, 27 °C, and 37 °C with a q range of 0.028 to 0.213 $Å^{-1}$.

Differential scanning calorimeter (DSC)

A DSC Q 20 (TA Instruments) was used for analyzing the prepared samples. Indium and zinc standards were used for calibration of the instrument. First 10±3 mg of hydrated sample was placed in aluminum crucibles separately. Then the crucibles were equilibrated at 25 °C and the samples were rapidly cooled in liquid nitrogen from 25 °C to -25 °C, at a rate of 10 °C min^{-1}. The samples were held at this temperature for 30 min and then were heated at a rate of 2 °C min^{-1} to 50 °C. An empty pan was used as reference. The fusion temperatures of the components and the total heat transferred in the thermal processes were determined.

In vitro antifungal activity

The *in vitro* antifungal activity of the formed gel was evaluated against *Aspergillus fumigatus* (NCIM 902) and *Candida albicans* (ATCC 18804). Briefly culture suspension of *Candida albicans* was prepared from fresh cultures (2 days old) grown on Sabouraud dextrose agar (SDA) slants, by dispersing one loopful of culture in 5 mL of sterile water and vortex mixing for 15 s to obtain a homogeneous suspension. The optical density of the resulting culture was determined by Elico spectro colorimeter CL 153 set at value 1 at 600 nm.[13] Inoculum suspensions of *Aspergillus fumigatus* were prepared from fresh, mature (3-5 day old) cultures grown on SDA slants. The colonies were covered with 5 mL of distilled sterile water. Tween 20 (1%) was added to facilitate the preparation of *Aspergillus* inocula.[14] The inocula were achieved by carefully rubbing the colonies with a sterile loop; the isolates were then shaken vigorously for 15 s with a vortex mixer and then transferred to a sterile tube.[14]

The optical density of the suspensions was measured by UV spectrophotometer (Shimadzu UV-1600) set as 0.13 at 530 nm.[14] Agar well diffusion was used to evaluate antifungal activity; 1 mL of microbial inoculum was seeded into SDA medium and poured into petri plates, a sterile cork borer of diameter 6 mm was punched aseptically to create a well, and a gel sample (0.1 g) was added to the well. The plates were incubated for 24 h at 27 °C (*Candida albicans*) and 48 h at 27 °C (*Aspergillus fumigatus*). The drug released from the prepared gel was compared with standard drug solution of nystatin prepared in DMF (1000 units/mL). The antimicrobial agent diffuses in the agar medium and inhibits the growth of the microbial strain tested.

In vitro drug release

In vitro drug release was evaluated by placing cellulose acetate membrane (0.45 µm) between the donor and the receptor chambers of a Franz diffusion cell. Briefly 1 g of prepared gel was placed on the membrane, the receptor compartment was filled with 50 mL of methanol:DMF:water (55:15:30) as the dissolution medium,[15] and at fixed time interval 1 mL of the sample was withdrawn and replaced by fresh solvent to maintain sink condition. The temperature was maintained at 37 °C by circulating water bath. UV spectrophotometric analyses of aliquots were performed at 306 nm to estimate drug release. The experimental data obtained from the drug release experiments were evaluated for drug release kinetics, and PCP-Disso-V 2.08 software was used to fit models to the release data. The models were assessed on the basis of correlation coefficient (R^2) to mark the best fit model.

Statistical analysis

The data were articulated as mean±SD. ANOVA followed by *post hoc* Tukey test (GraphPad Prism 8.0.1) was employed to statistically analyze the data at 95% confidence level.

RESULTS AND DISCUSSION

In situ gelling ability (Vm) and gelling time (Tm)

The additives added induce a change in the hydration state of the polar lipid head and affect the critical packing parameter (CPP) of the lipid.[16-19] The effect of solvent on the gelling property of IGFPS is given in Table 2. It is observed that increasing the concentrations of DMSO and OA had a significant effect on the minimum amount of distilled water required for *in situ* gelling. A large amount of distilled water was required for gelling in the case of IGFPS of F2, whereas the smallest amount of solvent was required in F5. A higher concentration of DMSO results in disruption of water channels.[20-22] In the case of F5 equal proportions of OA and DMSO cause the solvent to partition between both phases, i.e. the lipids and DMSO, thus making the polar heads of lipids easily available for hydration. Table 2 indicates the results obtained for Tm. It was found that there was a reverse relationship between the concentration of DMSO and the time required for gelling. The Tm was obtained in the following order for formulations containing higher DMSO content: F2>F3>F1>F8>F6, whereas an increase in OA concentration showed a reduction in gelation time F5<F4<F7<F9. Statistical analysis done using ANOVA followed by *post hoc* Tukey test for Tm reveal that comparing means of each group with the other showed a highly significant difference ($p<0.05$, <0.0001), whereas an insignificant difference was seen in the case of F4 vs F5 ($p>0.05$, 0.1043) and F6 vs F9 ($p>0.05$, 0.9762). In the case of Vm, an insignificant difference was seen for F7 vs F9 ($p>0.05$, 0.2233), F4 vs F7 ($p>0.05$, 0.6063), F4 vs F9 ($p>0.05$, 0.9970), F3 vs F8 ($p>0.05$, 0.9717), and F1 vs F6 ($p>0.05$, 0.999), while the other groups showed a significant difference ($p<0.05$, <0.0001).

pH of the sol and drug content

pH values of the sol and drug content are presented in Table 2. Almost all formulations showed a drug content in the range 99% to 100%, while the pH of the sol for all formulations ranged from 5.5±0.11 to 7±0.34.

Swelling studies

The concentration of DMSO in IGFPS played an important role in modulating the microstructure of the formed gel and had a marked effect on rate of swelling. Figures 1a-1c highlight the swelling behavior: it was monitored for 8 h. IGFPS formulations

Table 2. Minimum volume of solvent for gelation, gelation time and pH

Formulation	Vm (µL)	Water (%w/w)	Tm (s)	pH	Drug content (%)
F1	120±2.51	10.86±0.75	145±5	6.2±0.21	98.72±0.05
F2	180±1.81	15.51±1.15	180±2.88	7±0.34	99.10±0.01
F3	150±2.88	13.15±0.95	165±3	6.6±0.12	98.55±0.02
F4	90±2.51	8.33±0.5	75±5	6.3±0.15	99.05±0.07
F5	70±2	6.66±0.4	60±4	5.5±0.11	98.82±0.03
F6	120±4.04	10.9±0.8	105±2.88	6.7±0.09	99.32±0.01
F7	90±5.77	8.4±0.6	90±5	5.8±0.17	99.5±0.015
F8	150±5	13.15±1.02	120±5	6.8±0.12	98.67±0.04
F9	100±5.17	9.25±0.75	100±1.88	6.4±0.13	99.18±0.025

(Mean ± standard deviation, n=3), Vm: Minimum solvent, Tm: Minimum time

with higher concentration of DMSO had higher rates of swelling, whereas formulations with higher concentration of OA had lower rates of swelling. It was markedly observed that formulations F7 and F5 in the initial hour showed faster rates of swelling (Figure 1b), but the same declined later and at the end of 8 h the maximum swelling observed was 24% and 22.75%, respectively, and it was found to be dependent on water uptake.[10] The rapid swelling is consistent with other studies signifying that formation of a viscous cubic or inverted hexagonal phase (HCP) is a fast process.[23-25] IGFPS F2 exhibited the highest rate of swelling, i.e. 47% at 8 h. Herein the concentration of DMSO, a polar additive, was higher, which preferentially led to the formation of a lamellar phase; thus DMSO had an opposite effect, as compared to OA, which could also be a reason for the higher rate of swelling. Moreover, the interaction of GMO with OA and subsequent hydration with water results in reversed hexagonal phases, whereas the interaction of DMSO with a high concentration of hydrated GMO results in predominant cubic phase existence.[26,27] The results for minimum gelation volume are also along the same lines and demonstrate that concentration of DMSO has a significant effect on gelling as seen for swelling ability. The results of the statistical analysis show that an insignificant difference was noted ($p>0.05$) on comparing the mean of each group with another; however, a significant difference was seen ($p<0.05$, <0.01) for F2 vs F4, F2 vs F5, F2 vs F7, and F2 vs F9. Figure 1c indicates that all formulations followed second order swelling kinetics, which is in agreement with earlier reported studies.[11,25,26]

Polarized light microscopy

IGFPS undergo dynamic structural transition *in situ* to high-viscous gel on exposure to excess water. This change from a less viscous system into a lamellar, bicontinuous cubic structure or inverted HCP can be elucidated by the CPP.[28,29] Figure 2 indicates PLM images at 20 °C; all gel formulations except F2 exhibited a dark background with no birefringence characteristic of isotropic liquid crystalline

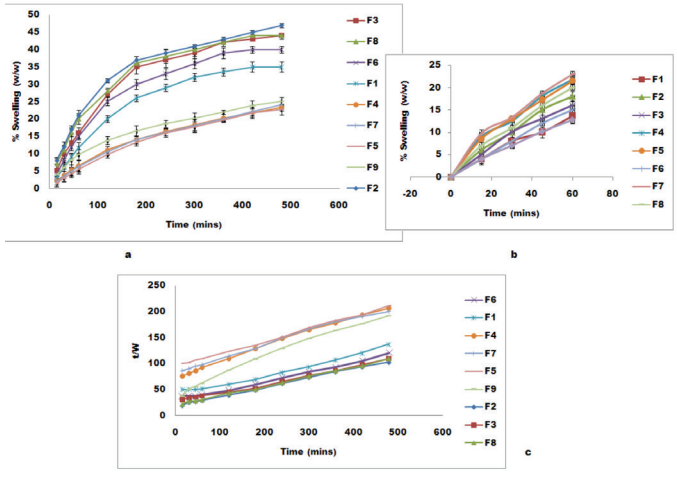

Figure 1. (a) Plots of the percentage increase in the weight as a function of time when placed in excess of water, (b) plots of percentage increase in weight in the initial hour when placed in excess of water, (c) plots of swelling kinetics of different formulation according to second order kinetics

mesophase structure and very possibly a mesomorphic form of bicontinuous cubic structure, whereas F2 gels cast a two phase region of lamellar reflects presenting partial textures of birefringence pattern typical of a Maltese cross and black background of a cubic phase. PLM images obtained at 25 °C and 37 °C (Figure 2) exhibit typical dark backgrounds for F1 and F6 highlighting a cubic phase, whereas F2 typically shows only a Maltese cross pattern, thus indicating complete phase transformation to a lamellar structure. For the rest of the gel formulations, the coexistence of a two phase region with the formation of anisotropic structures with specific fan-like texture was distinctive of a reverse hexagonal structure on an isotropic black background featuring a cubic phase.

Mucoadhesion measurement by tensile strength method

The mucoadhesive properties of LLC systems are seen to be dependent on the dehydration of the mucosa and *in situ* absorption of water. Intestinal mucosa was selected as a model tissue to understand the influence of formulation additives and mesophase formation on mucodhesion. Table 3 highlights the results for mechanical parameters and bioadhesive force of the gel. The findings indicate that formulation F7 had the highest hardness (1274±60 mN), compressibility (1.612±0.072 mJ), adhesiveness (3.143±0.12 mJ), cohesiveness (1.961±0.053), and bioadhesion force (1010.08±50 mN). On comparing the mean values between formulation F5, F7, and F4 a significant difference ($p<0.05$) was noted for the mentioned parameters. The findings indicate that increasing concentration of OA imparted a better adhesiveness and gel strength for F7, whereas the adhesive force of the gels decreased as the OA content increased as seen for formulations F4 and F5. As the compactness of the microstructure increases with an increase in OA concentration, the lattice parameter value decreases with narrowing of the water channels, leading to a decline

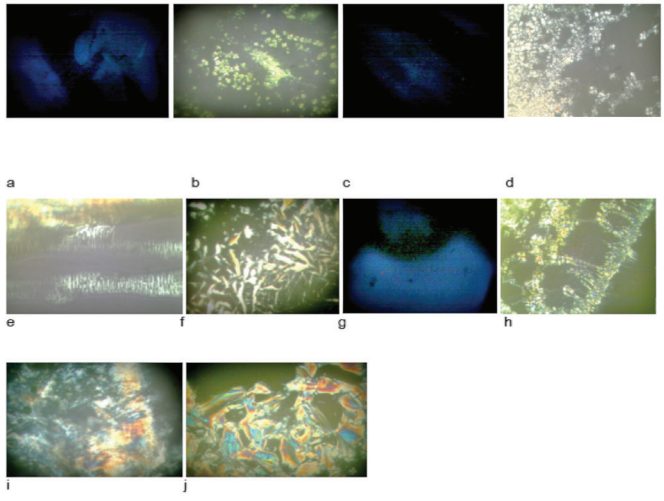

Figure 2. (a) F1, F6, F3 cubic phase at 20 °C and 27 °C, (b) F2 cubic and lamellar phase at 20 °C, (c) F4, F5, F7, F8, F9 cubic phase at 20 °C, (d) F2 lamellar phase 27 °C, (e) F3, F8 cubic and hexagonal phase at 27 °C, (f) F4, F5, F7, F9 cubic and hexagonal phase at 27 °C, (g) F1, F6 cubic phase at 37 °C, (h) F2 lamellar phase at 37 °C, (i) F3, F8 cubic and hexagonal phase at 37 °C, (j) F4, F5, F7, F9 cubic and hexagonal phase at 37 °C

Table 3. Mechanical properties and bioadhesive force of preformed gel formulations

Formulation	Mechanical parameters (n=3)				
	Hardness (mN)	Compressibility (mJ)	Adhesiveness (mJ)	Cohesiveness (dimensionless)	Work of bioadhesion (mN)
F1	480±40	0.533±0.025	1.111±0.018	1.495±0.030	441.29±20
F2	313.8±30	0.405±0.020	0.634±0.012	1.175±0.025	254.97±15
F3	333.8±20	0.486±0.015	0.678±0.015	1.294±0.020	313.81±12
F4	1002.08±50	1.452±0.022	2.943±0.075	1.816±0.021	935.49±30
F5	657.04±25	1.256±0.025	2.413±0.022	1.682±0.025	539.36±25
F6	363.84±15	0.824±0.015	1.323±0.017	1.492±0.028	342.65±10
F7	1245.44±60	1.712±0.072	3.143±0.12	1.961±0.053	1010.08±50
F8	345.199±18	0.674±0.013	0.956±0.005	1.323±0.025	304.006±14
F9	382.039±16	1.034±0.012	1.338±0.011	1.582±0.021	383.61±20

(Mean ± standard deviation, n=3)

in adhesiveness and gel strength. Our results corroborate the reported findings.[30] For formulation F2 lower values of hardness (313.8±30 mN), compressibility (0.445±0.020 mJ), adhesiveness (0.634±0.012 mJ), cohesiveness (1.175±0.025), and bioadhesion force (254.97±15 mN) were obtained. The results for F2 showed a significant difference ($p<0.05$) when compared to the means of F7, poor mechanical parameters were obtained due to predominant lamellar microstructuring of the gel due to high content of DMSO, and as reported lamellar phases have poor adhesion in comparison to hexagonal and cubic structures.[31]

Rheological measurements

Tables 4 and 5 indicate the results for the rotational and oscillatory tests, respectively. The value $n<1$ proves the system to be non-Newtonian, typically to be pseudoplastic; the oscillatory parameters complex modulus, elastic modulus, viscous modulus, and phase angle (tan δ) reported are calculated at a frequency of 1 Hz. As can be seen, the formulations where DMSO concentration was high showed lower values of consistency index, whereas with an increase in concentration of OA a subsequent rise in consistency index was noted. The general performance of G' and G" as a function of frequency at constant strain 0.1% by the gel sample is illustrated in Figure 3. F1, F3, F4, F6, F7, and F9 typically exhibited frequency dependent moduli curves akin to a cubic mesophasic structure. Figure 4 depicts G" to be predominant at lower frequencies (<0.1 Hz not used), while G' is dominant at higher frequencies since no cross over was seen at the frequencies used in the present study. The composition of the sample plays a key role in defining the frequency at which the crossover (G'>G") occurs. As the value of G' levels out after an initial increase, G" is constantly reduced with increasing frequencies. All formulations indicated G' to be higher than one order of magnitude over G". The change from a primarily liquid-like behavior to a solid with increasing frequency is supplementary reflected by tan δ values ≥1 at low frequency, followed by a swift decline at the crossover, and finally reaching out at tan δ values ≤0. The curve for F5 showed some atypical behavior; the tan δ values decreased with an increase in frequency, but at higher frequency the value was

Table 4. Rheological parameters of IGFPS sol and preformed gel

Formulation	Viscosity of sol (Pa.s)	n	k (Pa.s)
F1	0.17±0.001	0.0925±0.01	13.5±0.14
F2	0.103±0.0011	0.08612±0.02	10.5±0.21
F3	0.15±0.002	0.09147±0.03	13.1±0.25
F4	0.449±0.015	0.1467±0.005	450.87±1.57
F5	0.555±0.018	0.1598±0.001	571.89±1.25
F6	0.1928±0.0012	0.1102±0.032	50.5±0.1
F7	0.3899±0.002	0.1246±0.004	341.87±1.11
F8	0.1684±0.0013	0.09695±0.01	30.2±0.5
F9	0.3599±0.001	0.099±0.012	138.18±1.02

(Mean ± standard deviation, n=3), IGFPS: *In situ* gelling fluid precursor systems

Table 5. Oscillatory test parameters of preformed gels at a frequency of 1 Hz

Formulation	Tan δ	Complex modulus (Pa) G*	Elastic modulus (Pa) G'	Viscous modulus (Pa) G"
F1	14.69	5.76×10^{4}	6.55×10^{4}	1.71×10^{3}
F2	9.13	1.76×10^{4}	2.95×10^{4}	4.8×10^{3}
F3	11.36	3.12×10^{4}	3.06×10^{4}	6.13×10^{3}
F4	19.64	7.68×10^{4}	7.23×10^{4}	2.58×10^{4}
F5	13.91	1.35×10^{5}	1.31×10^{5}	3.8×10^{4}
F6	16.91	1.10×10^{5}	9.71×10^{4}	2.95×10^{4}
F7	17.2	8.3×10^{4}	7.96×10^{4}	2.47×10^{4}
F8	15.84	5.22×10^{4}	5.02×10^{4}	1.43×10^{4}
F9	15.9	7.32×10^{4}	7.04×10^{4}	2.00×10^{4}

(Mean, n=3)

>0; the same has been reported elsewhere.[32] It could be due to the high provenance of the HCP P63/mmc structure. G" and G' were found to increase at higher frequency and so it can be presumed that the crossover might occur at higher frequency. The sample characterized as F2 also showed a markedly different frequency dependent moduli curve quite similar to that seen for cubic to lamellar structures transformation; herein at higher frequency G" sharply shoots up and again the crossover occurs at higher frequency, thus exhibiting a viscous property at higher frequency value, although the tan δ values were ≤0.

Table 5 highlights the least complex modulus for F2, whereas F5 exhibited the highest value for complex modulus. Statistical evaluation of the oscillatory test parameters obtained at a frequency of 1 Hz point out no significant differences (p>0.05) for F4 vs F7, F4 vs F9, and F7 vs F9, whereas on comparing with F5 all formulations displayed a significant difference (p<0.05, <0.001).

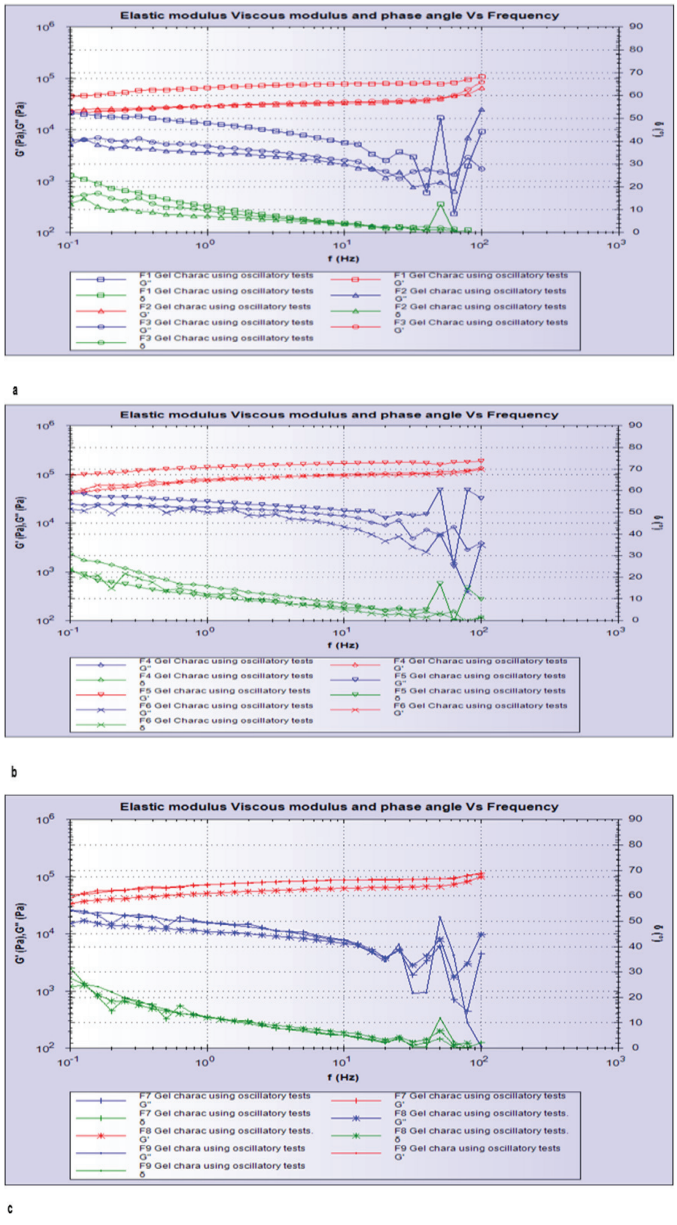

Figure 3. (a) Elastic modulus, viscous modulus and phase angle vs frequency for F1, F2, F3, (b) elastic modulus, viscous modulus and phase angle vs frequency for F4, F5, F6, (c) elastic modulus, viscous modulus and phase angle vs frequency for F7, F8, F9

Small angle X-ray scattering measurements

The liquid crystalline gel microstructure although analyzed by PLM did not show the type of mesomorphic cubic and hexagonal structure formed. Hence, SAXS analysis of the samples becomes essential at different temperatures to affirm the type of mesomorphic structure formed on the basis of Miller indices and change in lattice parameter values. We report intriguing polycontinuous interfaces of HCP P63/mmc[33,34] coexisting with Im3m at 25 °C and 37 °C. Previous studies have reported the coexistence of HCP P63/mmc with Fm3m.[35] The coexistence is a function of the concentration of additive and drug moiety, based on negative interfacial curvature. Studies also point to rigid and closely packed mixed films of phospholipid with nystatin.[36] It has been previously reported that DMSO expands the Im3m/Pn3m cubic phase coexistence region in the phase diagram and increases the lattice constant of the Pn3m monoolein cubic phase.[26] Our results were in contrast to the obtained finding; the presence of OA and nystatin could be the reason for this, although an increase in lattice constant value is seen for Im3m cubic phase with an increase in DMSO concentration. SAXS analysis was performed on all the gel formulations and diffractograms were taken at various temperatures, i.e. 20 °C, 25 °C, and 37 °C, to ascertain the effect of temperature on phase transformation and change in lattice parameter. Figure 4 indicates the SAXS diffractograms for all formulations at 20 °C; it was seen that all gel samples except for F2 exhibited Im3m (√2:√4:√6:√8:√10:√12:√14), a primitive type of cubic phase structure characterized by three interpenetrating continuous networks, whereas for F2 Im3m phase coexisted with lamellar phase lamellar (Lα) (√1:√4:√9:√16). On cooling self-assembled lipid structures at lower temperature, reduction of bilayer curvature occurs, which causes an increase in lattice parameter.[37,38] The SAXS diffractogram at 25 °C is shown in Figure 5, which indicates that they are sensitive to change in temperature; F2 was seen to stand apart from the rest with distinctive lamellar peak ratios; and F1 and F6 demonstrate the presence of only Im3m phase, whereas the others indicate coexistence of Im3m with P63/mmc (√4:√16:√1:√2:√5). Complete phase transformation for F2 is seen at 25 °C, as the bilayers lack excess area in the form of thermal undulations and less lateral tension in the bilayers leads to complete transformation to lamellar phase. The SAXS diffractogram at 37 °C indicates a decline in lattice parameter due to shrinking of the water channels with retention in the mesophasic structure (Table 6). The findings relate to DMSO's unique ability to act both as a kosmotrope (water-structure maker) and chaotrope (water structure breaker) based on its concentration. Finally, the obtained PLM images for all gel samples at respective temperature are in good agreement with the SAXS diffractograms.

Differential scanning calorimeter

DSC studies are used in surfactant based microstructures to identify different types and states of water.[39,40] The phase structure in a surfactant system and interaction among polar moieties and water molecule can be identified briefly through understanding the state of water in the microstructure by subjecting samples to subzero temperature DSC scanning.

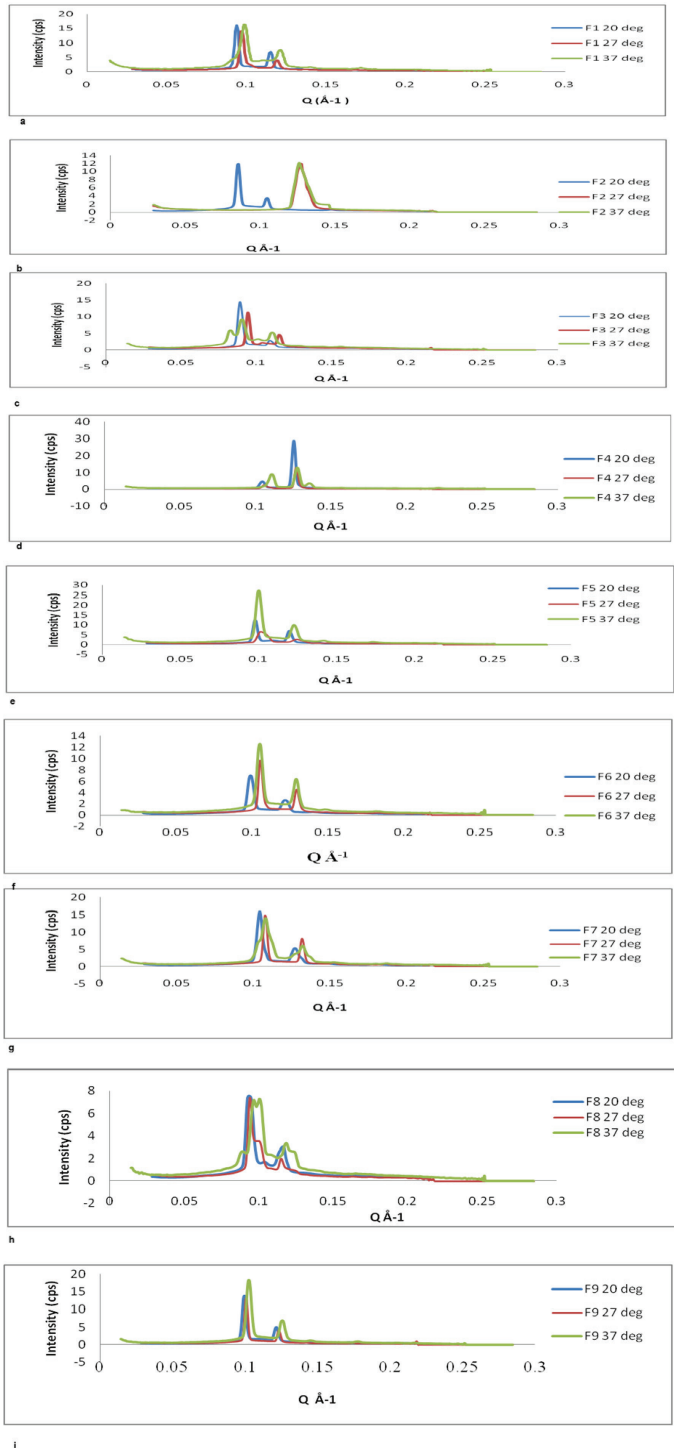

Figure 4. SAXS profile of preformed gel samples at 20 °C, 27 °C, and 37 °C (a) F1, (b) F2, (c) F3, (d) F4, (e) F5, (f) F6, (g) F7, (h) F8, (i) F9

SAXS: Small angle X-ray scattering

Table 7 and Figure 5 depict a sharp depression in the freezing point of free water characterized by an exothermic peak corresponding to crystallization of ice and two endothermic peaks. The first endothermic peak corresponds to melting for GMO/OA/DMSO interactions, whereas the second peak at low temperature indicates melting of interfacial water/bounded water. The interfacial water corresponds to the water entrapped in the highly ordered mesophasic structures. An endothermic peak for free water was not seen for any formulation but one was noted and is ascribed to crystallization of the ice formation in DMSO/water solvent mixture out of the inter-membrane space in the bulk solvent. Minimal changes in endothermic peak temperature were seen for interfacial water in gel samples. The data indicate that the exothermic peak temperature was dependent on DMSO concentration in the gel system and thus F2 indicated high depression in the freezing temperature for crystallization of ice in the binary mixture of DMSO and water. It is reported that at low concentration DMSO is strongly bonded to two water molecules and thus rigidifies the water structure, whereas at higher concentration it breaks the water structure and this is strongly evident by a decrease in the coordination number of water, which leads to a more distorted tetrahedral structure.[39,40] Exothermic peak temperatures obtained for formulations F4, F5, and F7 are in corroboration with the above statement. In agreement with the SAXS data, the DSC results also show DMSO's ability to work as either a kosmotropic or chaotropic solvent depending on its concentration. At low concentration it works as a water structure maker, whereas at high concentration it breaks the water structure and this is explained by a change in the exothermic peak temperature of free water in various gel formulations. The results obtained for DSC studies are in line with the minimum volume of solvent required for gelation.

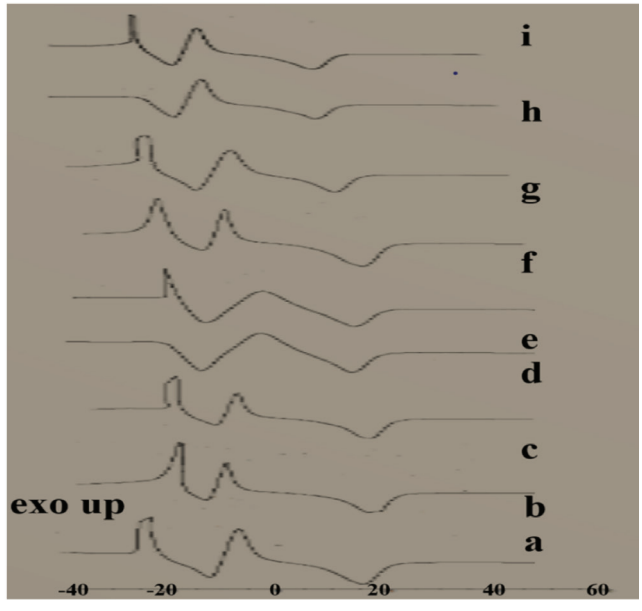

Figure 5. DSC thermograms of preformed gel samples (a) F1, (b) F2, (c) F3, (d) F4, (e) F5, (f) F6, (g) F7, (h) F8, (i) F9

DSC: Differential scanning calorimeter

Table 6. Lattice parameter, microstructure and lattice ratio of preformed gel samples at 20 ˚C, 27 ˚C, and 37 ˚C

Temp.	20 ˚C			27 ˚C			37 ˚C		
Gel	α (Å)	Lattice ratio	Structure	α (Å)	Lattice ratio	Structure	α (Å)	Lattice ratio	Structure
F1	94.28±0.611	-	Im3m, Q^{229}	91.32±0.39	-	Im3m, Q^{229}	91.32±0.85	-	Im3m Q^{229}
F2	157.85±0.086 104.53	1.509	Lamellae, Lα Im3m, Q^{229}	150.43±0.825	-	Lamellae Lα	144.43±0.83	-	Lamellae Lα
F3	99.54±0.889	-	Im3m, Q^{229}	98.19±0.687 84.3±0.513	1.164	Im3m, Q^{229} HCP (P63/mmc)	94.18±0.57 81.64±0.826	1.15	Im3m, Q^{229} HCP (P63/mmc)
F4	84.99±1.15	-	Im3m, Q^{229}	83.33±0.577 64.75±0.507	1.28	Im3m, Q^{229} HCP (P63/mmc)	80.274±0.72 64.33±0.69	1.24	Im3m, Q^{229} HCP (P63/mmc)
F5	89.03±1	-	Im3m, Q^{229}	88.86±1.037 67.35±0.7	1.319	Im3m Q^{229} HCP (P63/mmc)	80.52±1.26 62.13±0.618	1.295	Im3m, Q^{229} HCP (P63/mmc)
F6	88.06±0.970	-	Im3m, Q^{229}	84±0.577	-	Im3m, Q^{229}	84.6±0.923	-	Im3m, Q^{229}
F7	84.9±0.802	-	Im3m, Q^{229}	82.57±0.906 66.02±0.59	1.25	Im3m, Q^{229} HCP (P63/mmc)	79.11±1.06 64.14±0.621	1.23	Im3m, Q^{299} HCP (P63/mmc)
F8	93.23±0.577	-	Im3m, Q^{229}	92.67±0.964 82.07±0.558	1.12	Im3m, Q^{229} HCP (P63/mmc)	89.4±0.635 80.6±0.808	1.109	Im3m, Q^{229} HCP (P63/mmc)
F9	88.21±0.512	-	Im3m, Q^{229}	87±0.577 70.16±0.628	1.24	Im3m, Q^{229} HCP (P63/mmc)	83±0.57 68.57±0.794	1.211	Im3m, Q^{229} HCP (P63/mmc)

(Mean ± standard deviation, n=3), HCP: Hexagonal phase, Lα: Lamellar, Temp: Temperature

Table 7. Endothermic and exothermic events their peak temperature and enthalpy of preformed gel samples

Formulation	Endothermic peak temperature (˚C)		Enthalpy (W/g) for endothermic peaks		Exothermic peak temperature (˚C)	Enthalpy (W/g) for exothermic peak
	Interfacial water	Nonwater melting events	Interfacial water	Nonwater melting events	Free water	Free water
F1	-12.40	15.68	-0.9272	-1.16	-6.95	0.8507
F2	-16.55	12.83	-0.7723	-1.36	-12.88	0.9938
F3	-15.37	14.73	-0.7966	-1.46	-10.86	0.8696
F4	-15.48	11.65	-1.042	-1.103	-5.12	0.2856
F5	-16.08	11.41	-0.9168	-1.052	-5.05	0.2587
F6	-15.84	15.68	-0.6651	-1.276	-11.09	0.9765
F7	-13.94	12.83	-1.253	-1.327	-6.35	0.8252
F8	-15.72	11.65	-1.049	-1.14	-10.16	0.9126
F9	-15.25	13.19	-1.025	-1.231	-9.856	0.9838

In vitro drug release rate

The release profiles of a water-insoluble drug, nystatin, from preformed mesophasic gel formulations were studied to understand the effect of various factors such as addition of components to liquid crystalline phases, lattice parameter, and the rate of swelling.[24] The results obtained corroborate with such findings as depicted in Figure 6. F2 exhibited the maximum rate of swelling, showing rapid release of drug, i.e. 94% at 8 h. Higher concentrations of DMSO in F2 work as a cosolvent in solubilization of nystatin and the head groups are better hydrated, thereby forming larger water channels; this is ascertained by the higher lattice parameter value of 144.43. The

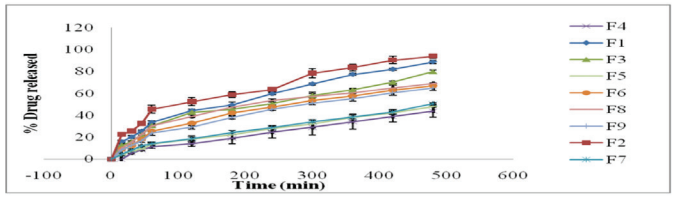

Figure 6. % Drug released vs time profile of gelled samples

assessment for F5 indicates a lower rate of swelling and thus a lower drug release of 48% at the end of 8 h. In agreement with previous findings,[41,42] the following reason may be alluded to in order to understand the observed behavior: nystatin, although

Table 8. Drug release kinetics of the gelled samples

Formulation	R^2 value					Best fit model	Parameters for Korsemeyer Peppas equation	
	Zero order	First order	Matrix	Peppas	Hixson Crowell		k	n
F1	0.9295	0.5151	0.9929	0.9898	0.9585	Matrix	3.0918	0.52103
F2	0.9031	0.4295	0.9871	0.9174	0.9761	Matrix	6.4823	0.4572
F3	0.9445	0.5039	0.9984	0.9975	0.9797	Martix	3.8208	0.5069
F4	0.9802	0.6651	0.9784	0.9971	0.9873	Peppas	1.1058	0.6255
F5	0.9798	0.6971	0.9852	0.9928	0.9891	Peppas	0.6921	0.6691
F6	0.9327	0.5629	0.9933	0.9912	0.9444	Matrix	2.7079	0.5063
F7	0.9783	0.6681	0.9791	0.9951	0.9862	Peppas	1.1009	0.6391
F8	0.8666	0.5029	0.9781	0.9746	0.9333	Matrix	3.2506	0.4752
F9	0.9265	0.5776	0.9965	0.9929	0.9712	Matrix	1.8137	0.5830

solubilized, is localized at the lipid/water interface, and the partitioning into the continuous hydrophobic phase (formed by GMO and OA) and aqueous channels becomes the rate limiting step for drug release. In addition, investigating SAXS analyses for F5 confirms a bicontinuous cubic phase (Im3m) with an interstice of inverted HCP (P63/mmc) structure. For F5 the lattice parameter ratio of Im3m/HCP (P63/mmc) at 37 °C also governed the drug release pattern. F5 exhibited a ratio of 1.295, whereas F4 and F7 displayed a ratio of 1.24 and 1.23, respectively. Thus, it can be concluded that an inverse relationship exists between the lattice parameter ratio and drug release; as the ratio increases the drug release decreases. The statistical evaluation revealed an insignificant difference among F4, F5, and F7 ($p>0.05$, >0.999), whereas a significant difference was noted on comparing means of F4, F5, and F7 against means of F2 ($p<0.05$, <0.03). This clarifies the effect of DMSO as a solubilizing cosolvent at high concentration and its role in modulating microstructure, thus controlling the release of drug.

The drug release data were subjected to kinetic modeling and the results are presented in Table 8. It is revealed that all formulations showed a matrix type of release pattern except for F4, F5, and F7, which indicated the Peppas model of release pattern. This identifies that LLC phases do not follow simple diffusion or erosion, and a thus anomalous ($0.45<n<0.89$) mechanism is involved.

In vitro antifungal activity

The *in vitro* antifungal activity of the formulated IFGPS was evaluated to ascertain its efficacy against *Aspergillus fumigatus* and *Candida albicans*. *In vitro* antifungal activity was also tested to substantiate the *in vitro* drug releasing ability of gel formulations. Figure 7 shows the zone of inhibition (mm) for IFGPS and standard nystatin drug solution. Concentration of DMSO played a crucial role in controlling *in vitro* antifungal activity; IFGPS F2 exhibited a zone of inhibition of 18 mm and 17 mm against *Candida albicans* and *Aspergillus fumigatus*, respectively. The standard drug solution in DMSO was used

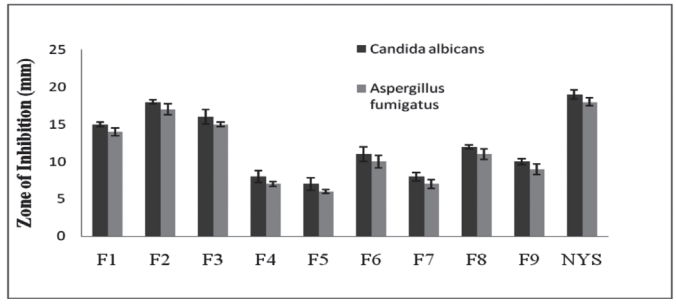

Figure 7. Zone of inhibition of gel samples obtained against Aspergillus fumigatus and Candida albicans

as a control to compare against the formulated IFGPS. In comparison to the standard drug solution, formulation F2 showed no significant difference ($p>0.05$, 0.3546), whereas for all the other IFGPS a significant difference ($p<0.0001$) was seen. OA has a mitigating role in the release of nystatin. An increase in its concentration led to a decrease in the zone of inhibition and this could be due to higher partitioning of the drug into the oil phase and being retained either at the oil/water interface or being bonded to the lipophilic groups of GMO or OA, thus being unable to be released from the matrix. On comparing formulations F4, F5, and F7 against the mean values of F2 a significant difference ($p<0.0001$) was noted, whereas on comparing the mean of F4, F5, and F7 amongst each other no significant difference ($p>0.05$, 0.1229, >0.99) was obtained. The results are in agreement with the data obtained for *in vitro* drug release. Moreover, the matrices of formulation F5, F4, and F7 did reveal an increase in the zone of inhibition on examination after 48 h in a range of 2±0.08 mm, and thus are shown to be sustained release matrices.

CONCLUSION

The results of the present work revealed that IGFPS containing GMO/OA/DMSO could be used for sustaining the release of a polyene antifungal agent, nystatin. The impact of incorporating a polar aprotic solvent had a divergent effect on modulation

of the gel microstructure, which ultimately improved the performance magnitude of the delivery system. The IGFPS formed various mesophasic structures like Lα and bicontinuous cubic Im3m, and coexistence of Im3m with hexagonal HCP P63/mmc was affirmed by SAXS and polarized optical microscopy. DSC and SAXS studies highlight DMSO's ability to work either as a kosmotropic or chaotropic solvent, being a function of its concentration. Rheological and oscillatory assessments confirmed all samples show shear thinning behavior, and the gels show frequency dependent rheograms of entirely elastic nature G'>G". Texture analysis results underline the presence of requisite mechanical and mucoadhesive properties.

Finally, an *in vitro* antifungal activity and an *in vitro* drug release kinetic study proved that in F7 IGFPS containing nystatin has the suitable controlled release property required for an effective mucoadhesive sustain release delivery system. *In vivo* and stability studies are essential to substantiate the obtained findings, and the model needs to be studied for specific route of administration.

ACKNOWLEDGEMENTS

The authors are thankful to Glenmark Pharmaceuticals, India, for providing nystatin as gift sample, and Croda, India for giving Cithrol GMO HP-SO-(LK). We are highly obliged to Malveran, India, for offering technical support for the oscillatory analysis.

Conflicts of interest: No conflict of interest was declared by the authors. The authors alone are responsible for the content and writing of the paper.

REFERENCES

1. Kligman AM. Topical pharmacology and toxicology of dimethyl sulfoxide. JAMA. 1965;193:796-804.
2. Vignes R. Dimethyl sulfoxide (DMSO), A "new" clean, unique, superior solvent. Annual Meeting. Washington, DC.; 2000.
3. Yu ZW, Quinn PJ. The effect of dimethyl sulphoxide on the structure and phase behaviour of palmitoleoylphosphatidylethanolamine. Biochim Biophys Acta. 2000;1509:440-450.
4. de Menorval MA, Mir LM, Fernandez ML, Reigada R. Effects of dimethyl sulfoxide in cholesterol-containing lipid membranes: a comparative study of experiments in silico and with cells. PloS One. 2012;7:e41733.
5. Milak S, Zimmer A. Glycerol monooleate liquid crystalline phases used in drug delivery systems. Int J Pharm. 2015;478:569-587.
6. Ng AW, Wasan KM, Lopez-Berestein G. Development of liposomal polyene antibiotics: an historical perspective. J Pharm Sci. 2003;6:67-83.
7. Chen Y, Liang X, Ma P, Tao Y, Wu X, Wu X, Chu X, Gui S. Phytantriol-based in situ liquid crystals with long-term release for intra-articular administration. AAPS PharmSciTech. 2015;16:846-854.
8. Dehghan MHG, Marzuka M. Lyophilized Chitosan/xanthan Polyelectrolyte Complex Based Mucoadhesive Inserts for Nasal Delivery of Promethazine Hydrochloride. Iran J Pharm Res. 2014;13:769-784.
9. Schott H. Kinetics of swelling of polymers and their gels. J Pharm Sci. 1992;81:467-470.
10. Souza C, Watanabe E, Borgheti-Cardoso LN, De Abreu Fantini MC, Lara MG. Mucoadhesive system formed by liquid crystals for buccal administration of poly(hexamethylene biguanide) hydrochloride. J Pharm Sci. 2014;103:3914-3923.
11. Lee J, Choi SU, Yoon MK, Choi YW. Kinetic characterization of swelling of liquid crystalline phases of glyceryl monooleate. Arc Pharm Res. 2003;26:880-885.
12. Rosevear FB. The microscopy of the liquid crystalline neat and middle phases of soaps and synthetic detergents. J Am Oil Chem Soc. 1954;31:628-639.
13. Mitchell BM, Wu TG, Jackson BE, Wilhelmus KR. Candida albicans strain-dependent virulence and Rim13p-mediated filamentation in experimental keratomycosis. Invest Ophthalmol Visl Sci. 2007;48:774-780.
14. Petrikkou E, Rodriguez-Tudela JL, Cuenca-Estrella M, Gomez A, Molleja A, Mellado E. Inoculum standardization for antifungal susceptibility testing of filamentous fungi pathogenic for humans. J Clin Microbiol. 2001;39:1345-1347.
15. Fernandez-Campos F, Naveros BC, Lopez Serrano O, Alonso Merino C, Campmany ACC. Evaluation of novel nystatin nanoemulsion for skin candidosis infections. Mycoses. 2013;56:70-81.
16. Fong WK, Hanley T, Boyd BJ. Stimuli responsive liquid crystals provide 'on-demand' drug delivery in vitro and in vivo. J Control Release. 2009;135:218-226.
17. Kwon TK, Kim JC. Monoolein cubic phase containing acidic proteinoid: pH-dependent release. Drug Dev Ind Pharm. 2011;37:56-61.
18. Negrini R, Mezzenga R. pH-responsive lyotropic liquid crystals for controlled drug delivery. Langmuir. 2011;27:5296-5303.
19. de Campo L, Yaghmur A, Sagalowicz L, Leser ME, Watzke H, Glatter O. Reversible phase transitions in emulsified nanostructured lipid systems. Langmuir. 2004;20:5254-5261.
20. Cowie JMG, Toporowski PM. Association in the binary liquid system dimethyl sulphoxide-water. Can J Chem. 1961;39:2240-2243.
21. Ur-Rehman T, Tavelin S, Gröbner G. Effect of DMSO on micellization, gelation and drug release profile of Poloxamer 407. Int J Pharm. 2010;394:92-98.
22. Watase MNK. Effects of pH and DMSO content on the thermal and rheological properties of high methoxyl pectin-water gels. Carbohydrate Polymers. 1993;20:175-181.
23. Lara MG, Bentley MVLB, Collett JH. *In vitro* drug release mechanism and drug loading studies of cubic phase gels. Int J Pharm. 2005;293:241-250.
24. Rizwan SB, Hanley T, Boyd BJ, Rades T, Hook S. Liquid crystalline systems of phytantriol and glyceryl monooleate containing a hydrophilic protein: Characterisation, swelling and release kinetics. J Pharm Sci. 2009;98:4191-4204.
25. Chang CM, Bodmeier R. Swelling of and drug release from monoglyceride-based drug delivery systems. J Pharm Sci. 1997;86:747-752.
26. Abe S, Takahashi H. A comparative study of the effects of dimethylsulfoxide and glycerol on the bicontinuous cubic structure of hydrated monoolein and its phase behavior. Chem Phys Lipids. 2007;147:59-68.
27. Conn CE, Ces O, Mulet X, Finet S, Winter R, Seddon JM, Templer RH. Dynamics of structural transformations between lamellar

and inverse bicontinuous cubic lyotropic phases. Phys Rev Lett. 2006;96:108102.

28. Mulet X, Boyd BJ, Drummond CJ. Advances in drug delivery and medical imaging using colloidal lyotropic liquid crystalline dispersions. J Colloid Interface Sci. 2013;393:1-20.
29. Hartnett TE, Ladewig K, O'Connor AJ, Hartley PG, McLean KM. Size and Phase Control of Cubic Lyotropic Liquid Crystal Nanoparticles. J Phys Chem B. 2014;118:7430-7439.
30. Oyafuso MH, Carvalho FC, Takeshita TM, De Souza ALR, Araujo DR, Merino V, Gremiao MPD, Chorilli M. Development and In Vitro Evaluation of Lyotropic Liquid Crystals for the Controlled Release of Dexamethasone. Polymers (Basel). 2017;9:330.
31. Evenbratt H, Ström A. Phase behavior, rheology, and release from liquid crystalline phases containing combinations of glycerol monooleate, glyceryl monooleyl ether, propylene glycol, and water. RSC Advances. 2017;7:32966-32973.
32. Schröder-Turk GE, Varslot T, de Campo L, Kapfer SC, Mickel W. A Bicontinuous Mesophase Geometry with Hexagonal Symmetry. Langmuir. 2011;27:10475-10483.
33. Shearman GC, Tyler AI, Brooks NJ, Templer RH, Ces O, Law RV, Seddon JM. A 3-D hexagonal inverse micellar lyotropic phase. J Am Chem Soc. 2009;131:1678-1679.
34. Soni SS, Brotons G, Bellour M, Narayanan T, Gibaud A. Quantitative SAXS analysis of the P123/water/ethanol ternary phase diagram. J Phys Chem B. 2006;110:15157-15165.
35. Chen Z, Jiang Y, Dunphy DR, Adams DP, Hodges C, Liu N, Zhang N, Xomeritakis G, Jin X, Aluru NR, Gaik SJ, Hilhouse HW, Brinker CJ. DNA translocation through an array of kinked nanopores. Nat Mater. 2010;9:667-675.
36. Hac-Wydro K, Dynarowicz-Latka P. Interaction between nystatin and natural membrane lipids in Langmuir monolayers--the role of a phospholipid in the mechanism of polyenes mode of action. Biophys Chem. 2006;123:154-161.
37. Borné J, Nylander T, Khan A. Phase Behavior and Aggregate Formation for the Aqueous Monoolein System Mixed with Sodium Oleate and Oleic Acid. ACS Publications Most Trusted Most Cited Most Read. 2001;17:7742-7751.
38. Gurfinkel J, Aserin A, Garti N. Interactions of surfactants in nonionic/anionic reverse hexagonal mesophases and solubilization of α-chymotrypsinogen A. Colloids and Surfaces A Physicochemical and Engineering Aspects. 2011;392:322-328.
39. Shashkov SN, Kiselev MA, Tioutiounnikov SN, Kiselev AM, Lesieur P. The study of DMSO/water and DPPC/DMSO/water system by means of the X-Ray, neutron small-angle scattering, calorimetry and IR spectroscopy. Physica B: Condensed Matter. 1999;271:184-191.
40. Yaghmur A, Weng LS. In situ forming drug delivery systems based on lyotropic liquid crystalline phases : structural characterization and release properties. J Drug Deliv Sci Technol. 2013;23:325-332.
41. Mei L, Huang X, Xie Y, Chen J, Huang Y, Wang B, Wang H, Pan X, Wu C. An injectable in situ gel with cubic and hexagonal nanostructures for local treatment of chronic periodontitis. Drug Deliv. 2017;24:1148-1158.
42. Patil SS, Venugopal E, Bhat S, Mahadik KR, Paradkar AR. Exploring Microstructural Changes in Structural Analogues of Ibuprofen-Hosted In Situ Gelling System and Its Influence on Pharmaceutical Performance. AAPS PharmSci Tech. 2015;16:1153-1159.

Turk J Pharm Sci 2020;17(3):319-328
DOI: 10.4274/tjps.galenos.2019.47135

ORIGINAL ARTICLE

Phytochemical Screening and Establishment of the Antidiabetic Potential of Aqueous Leaf Extract of the Endangered Plant *Decalepis nervosa* in Rats with Alloxan-induced Diabetes

Alloksan ile İndüklenen Sıçan Diyabet Modelinde Soyu Tükenmekte Olan *Decalepis nervosa* Bitkisinin Sulu Yaprak Ekstraktının Antidiyabetik Potansiyelinin Araştırılması ve Fitokimyasal Taraması

Kuntal DAS*, Saifulla KHAN M, James SOUNDER, Usha MOHAN, Venkatesh PRASAD S

Krupanidhi College of Pharmacy Department of Pharmacognosy and Phytochemistry, Bangalore, India

ABSTRACT

Objectives: To evaluate the presence of phytochemicals in and the antidiabetic activity of aqueous extract of *Decalepis nervosa* (AEDN) leaf.

Materials and Methods: Either sex rats were grouped into 5 classes. Alloxan monohydrate and glibenclamide were used as diabetes induction drug and standard drug, respectively. Aqueous extract of the endangered medicinal plant DN was used in two different doses. Diabetes was induced with alloxan monohydrate at 150 mg/kg b.w. The AEDN was standardized with pharmacognostic and phytochemical screening and a chemical test confirmed the presence of phytoconstituents like glycoside, alkaloid, phenols, and flavonoids. Acute toxicity was evaluated for dose selection in an antidiabetic study.

Results: Glibenclamide (5 mg/kg b.w.) and AEDN (200 and 400 mg) were given to all rats with induced diabetes. The reduced blood glucose level may be correlated with the presence of plant secondary metabolites (phenolic compounds), which was identified by thin layer chromatography and confirmed by high performance liquid chromatography studies. The decreased levels of serum total cholesterol, triglyceride, and liver enzyme activity showed the dose dependency of AEDN extract. An oral glucose tolerance test was performed after administration of 200 and 400 mg of AEDN and 5 mg of glibenclamide to different groups, which showed significantly lower oral glucose load during blood sample collection. Animal body weight and dose of AEDN extract had a significant effect on the glucose level in blood ($p<0.01$).

Conclusion: The first report on the phytochemicals and therapeutic activity of AEDN leaf showed potential antidiabetic activity by increased insulin secretion via enhanced peripheral glucose utilization mechanism.

Key words: Alloxan, biochemical estimation, correlation, *Decalepis nervosa*, phytochemicals

ÖZ

Amaç: Decalepis nervoza (AEDN) yaprağının sulu ekstraktında fitokimyasalların varlığını göstermek ve antidiyabetik aktivitesini değerlendirmektir.

Gereç ve Yöntemler: Her iki cinsiyette sıçan içeren 5 grup oluşturuldu. Alloksan monohidrat ve glibenklamid, sırasıyla diyabet indüksiyon ilacı ve standart ilaç olarak kullanıldı. Soyu tükenmekte olan tıbbi bitki *Decalepis nervoza*'nın sulu ekstresi iki farklı dozda kullanılmıştır. Diyabet 150 mg/kg alloksan monohidrat ile indüklendi. AEDN, farmakolojik teşhis ve fitokimyasal tarama ile standartlaştırıldı ve kimyasal test, glikozit, alkaloid, fenoller ve flavonoidler gibi fito-bileşenlerin varlığını doğruladı. Antidiyabetik çalışmada doz seçimi için akut toksisite değerlendirildi.

Bulgular: Diyabetli tüm sıçanlara glibenklamid (5 mg/kg) ve AEDN (200 ve 400 mg) verildi. Düşük kan şekeri seviyesi, ince tabaka kromatografisi ile tespit edilen ve yüksek performanslı sıvı kromatografisi çalışmaları ile teyit edilen bitki sekonder metabolitlerinin (fenolik bileşikler) varlığı ile ilişkilendirilebilir. Serum toplam kolesterol, trigliserit ve karaciğer enzim aktivitesindeki azalma, AEDN ekstresinin doz bağımlı olarak etki ettiğini gösterdi. 200 ve 400 mg AEDN ve 5 mg glibenklamidin farklı gruplara uygulanmasından sonra bir oral glukoz tolerans testi yapılmıştır; kan örneği

*Correspondence: E-mail: drkkdsd@gmail.com, Phone: 09632542846 ORCID-ID: orcid.org/000-0001-6118-5270
Received: 12.04.2019, Accepted: 20.07.2019

alınması sırasında oral glukoz yükünün önemli ölçüde düşük olduğu saptanmıştır. Hayvanların vücut ağırlığının ve AEDN ekstresi dozunun, kandaki glukoz seviyesi üzerinde önemli bir etkiye sahip ($p<0,01$) olduğu bulunmuştur.

Sonuç: AEDN yaprağının fitokimyasalları ve terapötik aktivitesini konu alan ilk çalışmadır. Ekstraktın, artmış periferik glukoz kullanım mekanizması yoluyla insülin sekresyonunu arttırarak potansiyel antidiyabetik aktivite gösterdiği bulunmuştur.

Anahtar kelimeler: Alloksan, biyokimyasal tahmin, korelasyon, *Decalepis nervoza*, fitokimyasallar

INTRODUCTION

Among the serious metabolic disorders, diabetes mellitus is a most critical disorder throughout the world, with India listed in the top three countries. It is life threatening and responsible for many complications (such as retinopathy, neuropathy, and angiopathy) affecting various organs in the body, especially the eyes, followed by dysfunction and failure of various functional organs. Ample numbers of medicines are available in the world pharmaceutical market, but the related complications are increasing day by day. Hence traditional natural healing is an alternate method for its treatment. Herbal plants are known as a source of natural medicines. A literature survey revealed that a vast number of plants are used for their hypoglycemic activities with very few or no side effects.[1] Hence searching for phytoconstituents in novel antidiabetic plants without side effects is the main focus.

Of late, *Decalepis nervosa* (DN) (Wight and Arn.) Venter has become an endangered species of the genus *Decalepis* and family Apocynaceae. DN is a medicinal plant, distributed throughout the Western Ghats and the Nilgiris, occupying the western corner of Tamil Nadu, which borders Karnataka and Kerala states. The plant is a woody climbing shrub; its stem is purplish and pubescent and the leaves contain milky latex. Simple leaves are oppositely arranged. Its leaves are elliptical and acute.[2] There are many reports available on other species for their phytochemicals as well as medicinal activities but no such research evidence is available on DN leaves.[3] It is worthwhile to quantitatively determine the phytoconstituents like flavonoids and total phenolics present in the leaf, which is important for correlation with the present study. Therefore, the present study involved phytochemical screening in relation to the antidiabetic potential of aqueous leaf extract of DN and this is the first report on this plant for any therapeutic application with possible mechanism of action.

MATERIALS AND METHODS

Plant material and extract preparation

DN leaves were collected from the forest area of Coimbatore, Tamil Nadu (Western Ghat Region) and authenticated by the botanist Prof. P.E. Rajashekaran, Principal Scientist, Department of Biotechnology, IIHR, Hessaraghatta, Bangalore (Figure 1). A voucher herbarium specimen, number DN-317/KCP/2018, was preserved in the Pharmacognosy Department of Krupanidhi College of Pharmacy, Bangalore. The leaves were shade dried and coarsely powdered by grinder and stored in an airtight container at room temperature.

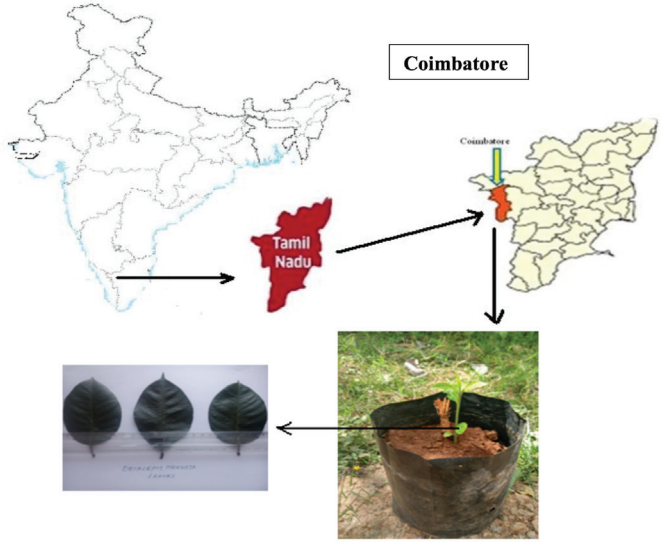

Figure 1. Collection of plant sample (DN leaves)
DN: *Decalepis nervosa*

DN powered leaf (500 g) was used for extraction by distilled water using reflux method for 6 h. Then the extract was filtered and concentrated using a rotary flash evaporator at 45 °C. The percentage yield was reported. The extract was preserved in a refrigerator at 4 °C in a glass bottle until further use.

Phytochemical analysis

A preliminary chemical test was performed for the leaf extract by various chemical tests as reported by Trease and Evans.[4] Furthermore, thin layer chromatography (TLC) of the extract was carried out with a standard phenolic compound (gallic acid) and flavonoids (epicatechin, catechin, and rutin).

Estimation of total flavonoids

Total flavonoid content was estimated by comparing with standard rutin (25, 50, 150, 300 and 600 µg/mL) with added aluminum trichloride. Next 125 µL of extract solution was added with 75 µL of 5% $NaNO_2$ solution. The mixture was left to stand for 10 min and thereafter 10% aluminum trichloride (150 µL) was added followed by incubation for 5 min. After that 750 µL of 1 M NaOH was added and the final volume of the solution was adjusted with distilled water up to 2500 µL. A pink color appeared after 15 min of incubation and then the absorbance was measured (at 510 nm) for the solution. From the standard curve of rutin, the total flavonoid content was measured and expressed as mg E catechin/g dry matter.[5]

Estimation of total phenolics

Total phenolics in aqueous extract of DN (AEDN) were determined by spectrophotometry using the Folin-Ciocalteu assay. First, 1 mL of AEDN was mixed in distilled water (9 mL) and then 1 mL of Folin-Ciocalteu reagent was added to the solution. After 10 min, 7% sodium carbonate solution (10 mL) was added and the final volume was made up to 25 mL. Standard solutions of gallic acid were prepared at various concentrations (20, 40, 60, 80, and 100 µg/mL). The mixed solution was kept for 2 h at 25±2 °C and then absorbance was recorded (at 550 nm) for both test and standard solutions. A blank sample was prepared for reading corrections. The phenolics content was estimated and expressed as mg of gallic acid equivalent of extract.[6]

Acute oral toxicity studies

As per the Organisation for Economic Co-operation and Development (OECD) guideline (guideline no. 423), the acute oral toxicity studies of AEDN were carried out in July 2018 after approval was received from the CPCSEA meeting held in Krupanidhi College of Pharmacy, Bangalore.[7] A minimum number of animals (n=3) were kept fasting overnight with only drinking water and the next day administration of the AEDN was carried out in the test animals. The AEDN dose was administered and the animals were kept overnight under observation followed by observation for up to 7 days for any changes in general behavior and other physical activities. After 24 h, no animal deaths were observed, which indicates safe action of the aqueous extract.

Experimental animals and their grouping

Adult albino Wistar rats (150-200 g) of either sex were procured from Adithi Biosys, Tumkur, and maintained in the animal house of Krupanidhi College of Pharmacy. The animals were well acclimatized under controlled temperature (22±5 °C) and humidity (55±5%). Twelve-hour light and dark cycles were maintained and, as a basal diet, standard pellets obtained from Sri Manjunatha Rice Mill, Ganagular Panchayathi, Hosakote Taluk, were used during the experimental period and all the animals were given normal food and drinking water *ad libitum*. All experiments were conducted as per the ethical norms approved by the CPCSEA and ethical clearance was granted by institutional ethical committee on 14 February 2018 at Krupanidhi College of Pharmacy, Bangalore (IAEC reg. no: KCP/PCOL/15/2018). Drugs like alloxan monohydrate, used for inducing diabetes, and glibenclamide as standard drug, glucose, Accu-chekÆ Active Glucometer, to check glucose level, and blood glucose strips were used.

The study was conducted on 40 Wistar albino rats randomly allocated to each of the five groups (8×5=40). The groups were treated as follows:

Group I: Normal rats, no treatment, only water and food.

Group II: Diabetic rats treated with alloxan (150 mg/kg b.w.) by i.p. injection.

Group III: Induced diabetic rats with orally given DN aqueous leaf extract (200 mg/kg b.w.) once daily for 28 days (Induced diabetic+DN 200 mg/kg).

Group IV: Induced diabetic rats with orally given DN aqueous leaf extract (400 mg/kg b.w.) once daily for 28 days (Induced diabetic+DN 400 mg/kg).

Group V: Induced diabetic rats with standard glibenclamide at 5 mg/kg b.w. once daily for 28 days (oral).

After experimentation, the rats were sacrificed by cervical decapitation and blood was collected with ethylenediaminetetraacetic acid (EDTA) as anticoagulant and plasma was separated by centrifuging the blood at 3000 rpm for 20 min. The serum was separated from the blood without EDTA and centrifuged at 6000 rpm for 10 min.

Induction of diabetes

The animals were acclimatized for 1-2 weeks and then a freshly prepared solution of alloxan monohydrate (dissolved in 0.9% normal saline solution) at a dose of 150 mg/kg body weight was injected i.p. into the experimental rats. Hyperglycemic rats were determined after treating with alloxan by tail vein blood glucose level with the help of a glucometer. A concentration of glucose level >250 mg/dL was considered to indicate hyperglycemia in the experiment.[8]

Oral glucose tolerance test (OGTT)

Fasted rats were separated into four groups, each with eight animals. Group I: treated as control, group II: treated with standard drug, groups III and IV: different extracts. All rats were orally treated with glucose (2 g/kg) after 30 min of extract administration. The blood samples were collected from the rat tail vein just before glucose administration (0 min) and after glucose administration (every after half an hour, i.e. at 30, 60, and 90 min).[9] A glucometer was used to measure blood glucose levels in the animals.

Body weight measurement

During the course of the study period, body weight was recorded five times, i.e. before alloxan (initial values), day 0, and days 7, 14, 21, and 28 of the total treatment period. A digital weighing balance was used and initial body weight and final body weight were recorded.[10]

Estimation of blood glucose level[11]

Blood samples were collected at weekly intervals up to the end of the study (i.e. 4 weeks). Blood glucose was estimated by one touch electronic glucometer using blood glucose strips. On day 28, blood was collected from the retro-orbital plexus (carbon dioxide gas used for anesthesia) from overnight fasted rats and blood sugar (fasted) was estimated. Separated serum was analyzed for serum cholesterol and serum triglycerides by enzymatic DHBS colorimetric method, and serum High-density lipoprotein (HDL), serum low-density lipoprotein (LDL), serum creatinine, and serum urea as well as the activities of alkaline phosphatase (ALP), aspartate, and alanine transaminases (AST and ALT) were determined using Randox Assay kits.

Statistical analysis

The results were analyzed by comparing values for the control and the different treated groups and expressed as mean ± standard error of the mean. One-way analysis of variance followed by Dunnet's t-test for multiple comparisons was applied. Values of $p<0.05$ were considered significant. Further blood glucose was tested based on the dose and body weight of animals using a 2×2 full factorial design with replicates (Table 1). Eight experiments were constructed, varying the dose and body weight using the software JMP version 11. Using this design the magnitude of the effect of each parameter on the resulting response of blood glucose was calculated. Each parameter was tested at 2 levels, i.e. dose (low, 200 mg and high, 400 mg) and body weight (low, 150±5 g and high 190±5 g).

RESULTS AND DISCUSSION

Primary phytochemical evaluation

Extraction of DN plant was carried out and the percentage yield was calculated as 5.28% (26.4 g w/w). Chemical tests of an aqueous extract of a new plant like DN were carried out and revealed the presence of phytoconstituents like alkaloids, flavonoids, glycoside, and phenols, which play an important role in controlling diabetes. Furthermore, TLC of extract in chloroform, methanol, and water as mobile phase (6:3:1) showed the presence of phenolics (gallic acid) and flavonoid (rutin) in the extract (Figure 2), which was further confirmed with the high performance liquid chromatography (HPLC) study. HPLC data showed retention time (R_t) of standard rutin and standard gallic acid at 7.58 min and 3.10 min, respectively, at 203 nm with the mobile phase methanol:water (60:40) (Figures 3a and 3b). The same conditions were used for the AEDN extract and showed the presence of these two compounds (rutin and gallic acid) in the extract with R_t of 7.58 min and 3.10 min, respectively (Figure

Table 1. 2x2 full factorial model

Runs	Pattern	Dose in mg	Body weight in g
1	+2	400	High
2	-1	200	Low
3	+2	400	High
4	+1	400	Low
5	-2	200	High
6	-2	200	High
7	-1	200	Low
8	+1	400	Low

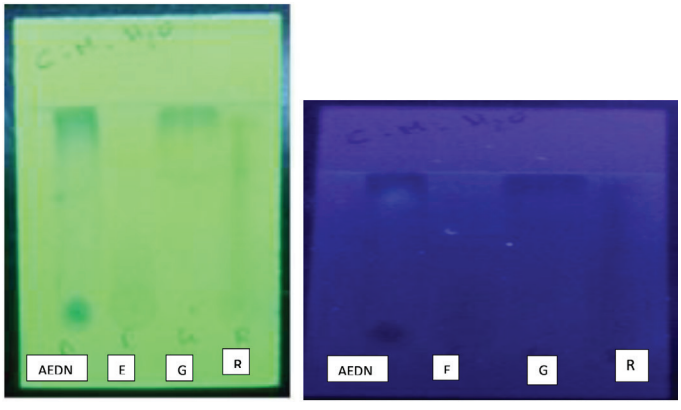

Figure 2. TLC of DN extract with standard drugs for identification of compound

TLC: Thin layer chromatography, DN: *Decalepis nervosa*, AEDN: Aqueous extract of *Decalepis nervosa*, E: Ellagic acid, G: Gallic, R: Rutin

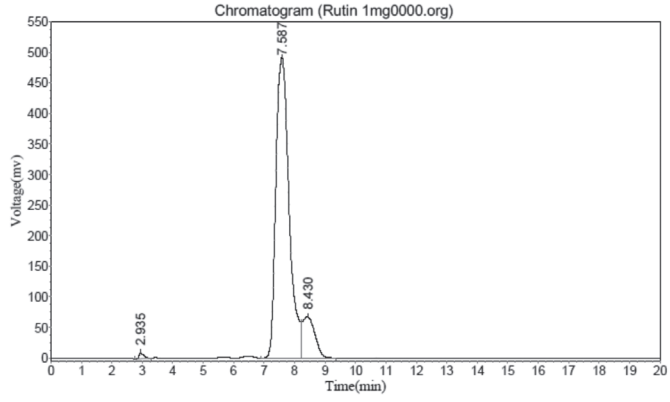

Figure 3a. HPLC of standard rutin (97% purity)

HPLC: High performance liquid chromatography

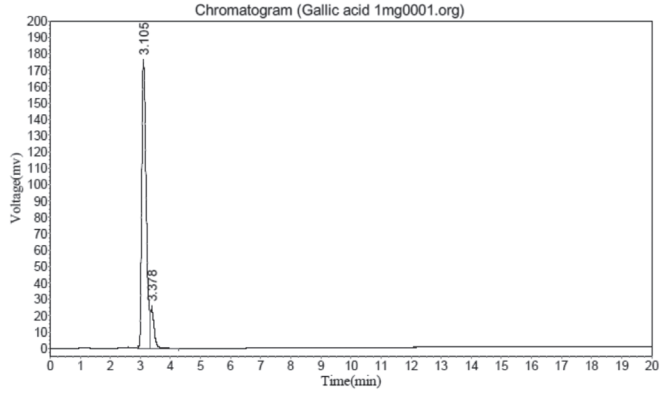

Figure 3b. HPLC of standard gallic acid (98% purity)

HPLC: High performance liquid chromatography

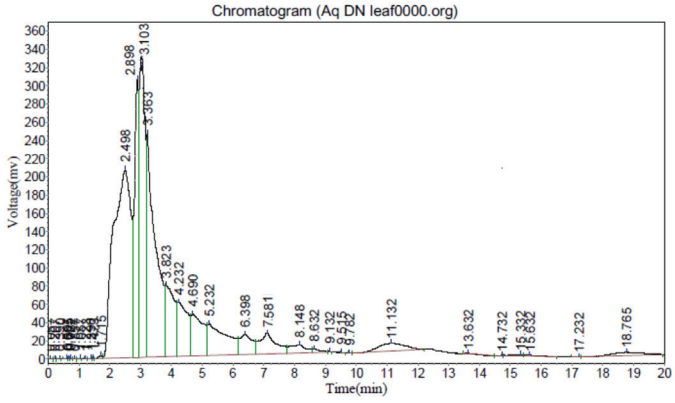

Figure 3c. HPLC of DN aqueous leaf extract

HPLC: High performance liquid chromatography

3c). Furthermore, the amounts were estimated by comparing with standards and it was found that higher amounts of gallic acid were present (2.32 µg) in the leaf than rutin (0.054 µg). Hence the two compounds gallic acid and rutin were identified in DN extract for the first time in the present investigation.

Phytochemical evaluation with respect to chemical tests is required to identify preliminary phytoconstituents present in herbal extracts. Plant phytoconstituents are essential for therapeutic efficacy. Hence, the chemical test indicates the possible mechanism for the particular disease treatment as well as the discovery of novel drugs from the isolated constituent. Mechanisms of action of phytoconstituents involve regulating glycemic metabolism or decreasing cholesterol levels or increasing secretion of insulin or by improving microcirculation. The present investigation was carried out for qualitative identification of the phytoconstituents present in the aqueous extract of DN, an endangered plant species. Aqueous extract was selected because most of the important phytoconstituents related to antidiabetic activity are soluble in aqueous solvent. Furthermore, aqueous solvent is more cost effective and easily available than other solvents, and in future for preparation of herbal formulations aqueous extract of plant samples is widely acceptable.

Estimation of total flavonoids and total phenolics

The catechin solution of concentration (25-600 ppm) conformed to Beer's law at 510 nm with a regression coefficient (R^2) of 0.997. The plot has a slope of 0.000 and an intercept of 0.031. The equation of the standard curve is y=0.000x+0.031 (Figure 4; Table 2) and the amount found was 2.52 mg.

The total phenolics in AEDN were determined using standard gallic acid. The gallic acid solution of concentration (20-100 ppm) conformed to Beer's law at 550 nm with a R^2 of 0.997. The plot has a slope (m) of 0.012 and an intercept of 0.025. The equation of the standard curve is y=0.012x+0.025 (Figure 5; Table 2) and the amount found was 5.81 mg.

Table 2. Total flavonoids and total phenolics content in aqueous extract of DN

Extract	Part used	Total flavonoids (mg/g)	Total phenolics (mg/g)
Aqueous extract of DN	Leaves	0.52±0.18	0.58±0.02

DN: *Decalepis nervosa*

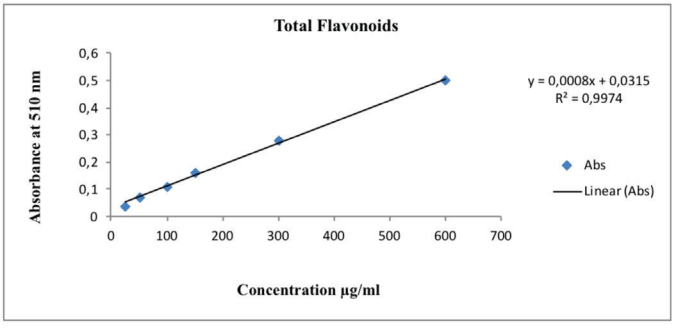

Figure 4. Estimation of total flavonoids with respect to standard catechin

Table 2 indicates the amounts of flavonoids and phenolics are present in quite high amounts. It was evident that higher concentrations of phenolics as well as flavonoids are highly soluble in polar solvents like water.[12] They mainly act as antioxidants and play a vital role in antidiabetic activity due to the presence of hydroxyl groups, some double bonds, and ketonic functional groups in their structures.[13,14] Therefore, it was essential to determine the total contents of flavonoids and phenolics in AEDN leaf.

Acute oral toxicity study of Decalepis nervosa leaf extract

The nontoxic nature of the AEDN is revealed by acute oral toxicity. There were no lethality or toxic reactions found until a dose of 5000 mg/kg as per the OECD guideline up to the end of the study period. All the animals were alive, healthy, and active during the observation period, which indicates the selected plant extract is safe for the present experiment and two suitable doses were selected, i.e. 200 mg/kg b.w. and 400 mg/kg b.w.

An acute toxicity study of AEDN leaf was carried out to determine the lethal dose (LD_{50}). The study confirmed LD_{50} when two selected doses resulted in mortality higher than 0% and lower than 100%. Previous reports have described safety dose determination and so the present study was performed for new endangered plant species and the selected doses were safe for further investigation.[15,16]

Oral glucose tolerance test

The effects of AEDN on the OGTT in normal rats were estimated. After 30 min of glucose administration a rapid increase in blood glucose occurred in the fasting animals and then decreased subsequently during the time intervals. The standard glibenclamide administered group (5 mg/kg) had reduced hyperglycemia (glucose induced) significantly at 30 min, 60 min, and 90 min (103.32±0.10, 102.11±0.01, and 84.60±0.11, respectively) as compared to the normal control group at the same time intervals. Maximum glucose tolerance in AEDN was observed as 92.22±0.03 and the minimum was observed as 87.22±0.11 in 90 min as compared with group I (Table 3) ($p<0.01$).

The OGTT was carried out to measure the ability to use a type of sugar by the body. The results revealed a dose-dependent reduction in glucose when treated with DN extract orally due to the identified flavonoids and phenolics in AEDN leaf.[17]

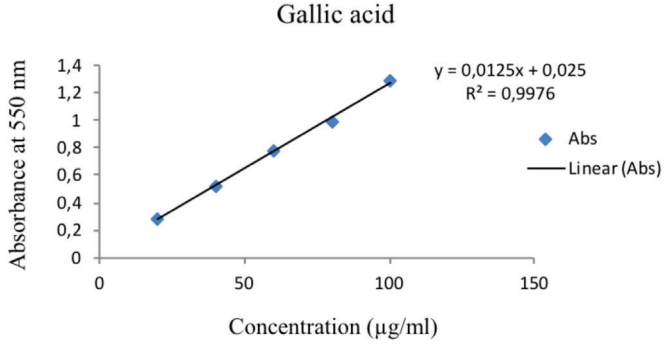

Figure 5. Total phenolic content with respect to standard gallic acid

Body weight determination

The body weights of all rats were calculated before alloxan induction, day 0, and days 7, 14, 21, and 28 and the results are given in Table 4. In group II body weight initially increased followed by a significant reduction on days 21 (156.19 g) and 28 (150.11 g) compared to the initial day (174.10 g). Groups IV and V also showed a significant reduction ($p<0.01$) in body weight compared to the normal group on day 28 (Table 4) in a dose-dependent manner.

In the present study, the standard drug (alloxan) caused a marked reduction in body weight, whereas AEDN increased body weight significantly. This may have been due to excessive fat utilized from fatty tissue for energy production in the body. The result is similar to that of earlier reports[18] where dose-dependent gain in body weight was seen with plant extract treatment. Alloxan is reported to cause a significant reduction in insulin release by damaging the beta cells (of islets of Langerhans) and induces hyperglycemia in animals,[19] which results in a decrease in body weight possibly due to catabolism of fats and proteins or by dehydration.

Estimation of blood glucose level and serum analysis

Blood glucose was estimated at 1, 7, 14, 21, and 28 days. The glibenclamide and DN aqueous extract treated groups (200, 400 mg/kg), showed a significant reduction ($p<0.05$) from day 7 to 28. Alloxan induced DN aqueous extract @ 400 mg showed a significant reduction in blood glucose level ($p<0.05$) (Figure 6).

Animals with diabetes induced with alloxan 150 mg/kg b.w. (i.p.) had elevated blood glucose on day 1 and after 28 days it was reduced a little but was higher than that in the normal group. Alloxan was used to induce diabetes without production of insulin. The result showed a dose-dependent decrease in fasting blood glucose in diabetic rats treated with different doses of the DN extract. This dose-dependent effect compares well with glibenclamide and especially at the dose of 400 mg/kg body weight the extract produced a more significant reduction in blood glucose level than 5 mg/kg glibenclamide on day 28, which may have been due to improved control mechanisms of glycemic as well as insulin secretions from the pancreatic cells of diabetic rats.[20] Furthermore, oxygen free radicals are involved in the diabetogenic action of alloxan and DN plant extract containing flavonoids and phenolics that are shown to be effective in diabetes due their antioxidant property.[21,22] Thereafter flavonoids are reported to suppress glucose level and also found to be a strong inhibitor of α-glucosidase (mainly luteolin).[23] DN leaf extracts also showed the presence of phenolics in higher content and that is the reason for the decrease in blood glucose level. Identified compounds such as gallic acid, which is a phenolic compound, enhanced insulin secretion and thereafter release from the beta cells[24] in the present study. On the other hand, rutin, which was identified in DN extract as a flavonoid, was also boosted in reduction of blood glucose in the present study. It acts by increasing the peripheral utilization of

Table 3. Effects of aqueous extract of DN on glucose tolerance test

Groups	Dose (mg)	Dose after 30 min (2 g/kg)	0 min	30 min	60 min	90 min
Normal	Vehicle	Glucose	87.02±0.23	197.12±0.14	189.36±0.11	186.02±0.02
Diabetic induced + standard drug glibenclamide	5	Glucose	83.07±0.11	103.32±0.10*	102.11±0.01*	84.60±0.11*
Diabetic induced + DN aqueous leaf extract	200	Glucose	82.86±0.20	106.11±0.23*	99.40±0.20*	92.22±0.03*
Diabetic induced + DN aqueous leaf extract	400	Glucose	83.09±0.03	102.22±0.20*	97.02±0.11*	87.22±0.11

The results represent mean ± SE (n=8). Data were analyzed by one-way ANOVA, followed by Dunnett comparison test against untreated animals. Values were considered significant where, *$p<0.01$: Medium significant, SE: Standard error, DN: *Decalepis nervosa*

Table 4. The effect of 4 week treatment with aqueous extract of DN on body weight (g) after alloxan (150 mg/kg i.p.) induced diabetes in rats

Group	Dose (mg)	Day 0 (g)	Day 7 (g)	Day 14 (g)	Day 21 (g)	Day 28 (g)
Normal control (group-I)	Vehicle	163.21±0.01	163.28±0.22	165.18±0.10	168.33±0.01*	169.21±0.01**
Diabetic control (group-II)	150	174.10±0.11	172.20±0.04	164.57±0.22	156.19±0.12*	150.11±0.23**
Diabetic induced + standard drug glibenclamide (group-III)	5	168.27±0.22	165.10±0.20	165.27±0.11	166.04±0.24*	167.11±0.03**
Diabetic induced + DN aqueous leaf extract (group-IV)	200	184.22±0.21	174.01±0.24	166.30±0.04	158.22±0.23*	151.06±0.12**
Diabetic induced + DN aqueous leaf extract (group-V)	400	182.24±0.31	176.20±0.20	169.11±0.01	164.34±0.21*	156.48±0.22**

The results represent mean ± SE (n=8). Data were analyzed by one-way ANOVA, followed by Dunnett comparison test against untreated animals. Values were considered significant where, *$p<0.05$: Low significant, **$p<0.01$: Medium significant, SE: Standard error, DN: *Decalepis nervosa*

glucose, inhibiting glucose transport from the intestine, which directly causes a significant reduction in blood glucose in both normal and diabetic rats. Glibenclamide (standard) was used in the present investigation because it caused voltage-dependent calcium channel depolarization of the cell membrane and hence increased the intracellular calcium of beta cells, subsequently stimulating insulin secretion to treat diabetes.[25]

Serum lipid analysis

On day 28, alloxan-treated animals had increased serum glucose, cholesterol, serum triglycerides, LDL, creatinine, and urea and decreased HDL level, but glibenclamide (5 mg/kg) and DN aqueous extract in the two different doses reversed these alloxan-induced changes. Both the extracts showed significant elevation ($p<0.05$) in serum HDL level compared to diabetic control rats after 28 days of treatment in a dose-dependent manner (Table 5).

In the present study, HDL-cholesterol had slightly lower values with a significant ($p<0.05$) increase in the level of LDL-cholesterol in the diabetic control group as compared to the other

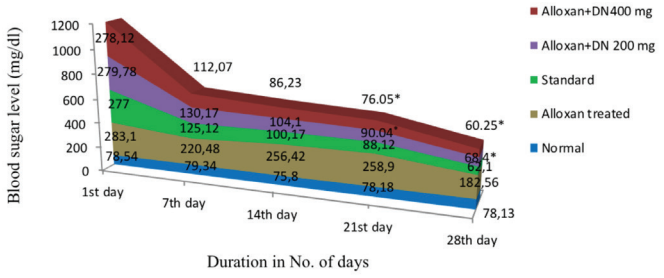

Figure 6. The effect of 4 week treatment with aqueous extract of DN on blood glucose level after alloxan induced diabetes in rats

Values are expressed as mean ± SE (n=3). *p<0.05, **p<0.01, ***p<0.001 when compared with normal group (ANOVA followed by Dunnet's test)
DN: Decalepis nervosa

treatment groups. Thereafter, mean values of HDL-cholesterol were significantly ($p<0.05$) increased, while mean values of LDL-cholesterol were significantly ($p<0.05$) decreased in both glibenclamide and in DN extract treated groups, which showed their potential to have a hypolipidemic action, consistent with earlier literature[26] showing the same results. Diabetes results from carbohydrate, protein, and lipid metabolism. Diabetes mellitus results in hyperlipidemia due to abnormalities in lipid metabolism, which in turn leads to atherosclerosis, myocardial infarction, etc.[27] Increased HDL level plays a significant role in the human body and is known as "beneficial cholesterol" because its increased level is associated with a decreased risk of myocardial infarction by removal of cholesterol from other tissues to the liver. It fosters the removal of cholesterol from peripheral tissue to the liver for catabolism and excretion and competes with LDL receptor sites on arterial smooth muscle cells that partially inhibit LDL uptake and degradation. Furthermore, HDL plays a role in lipid metabolism, complement regulation, immune response, and bringing excess cholesterol to the liver, helping to convert it into bile acids, and finally it is excreted into the small intestine.[26] An aqueous extract of DN leaves plays a significant role in decreased levels of serum cholesterol, serum glucose, serum triglycerides, LDL, creatinine, and urea and increased level of HDL, and this indicates DN leaves are a good source of antidiabetic drug by reducing the risk of developing heart disease. This may be due to the presence of polyphenolic compounds, especially flavonoids in the leaves, which are incorporated into lipoprotein within the liver or intestine and transported within the lipoprotein particles. Mainly flavonoid consumption is inversely associated with mortality from coronary heart disease and hence flavonoids and phenolics may be located for protection of LDL from oxidation. The same result was revealed earlier.[28]

Table 5. Effect of various groups of DN aqueous extract on serum profile in alloxan (150 mg/kg, i.p.) induced diabetic rats after 28 days of treatment (fasting condition)

Parameters	Group				
	Normal control (group-I)	Diabetic control (group-II)	Diabetic induced + glibenclamide (group-III)	Diabetic induced + DN aqueous leaf extract (200 mg) (group-IV)	Diabetic induced + DN aqueous leaf extract (400 mg) (group-V)
Serum glucose (mg/dL)	82.83±0.13	282.40±0.23**	145.50±0.12*2*	151.33±0.12*	147.66±0.24*
Total cholesterol (mg/dL)	74.66±0.20	170.33±0.10**	98.20±0.02*	106.50±0.10*	100.83±0.13*
Serum triglycerides (mg/dL)	56.83±0.11	154.00±0.04**	93.66±0.31*	98.00±0.02*	95.10±0.11*
Serum HDL (mg/dL)	48.83±0.03	36.16±0.14**	46.86±0.10*	64.33±0.11*	76.50±0.40*
serum LDL (mg/dL)	49.05±0.24	132.74±0.20**	51.06±0.16*	54.78±0.32*	46.90±0.41*
serum creatinine (mg/dL)	45.56±0.21	138.16±0.10**	61.80±0.21*	65.60±0.34*	63.07±0.03*
Serum urea (mg/dL)	48.23±0.22	141.14±0.11**	57.12±0.32*	64.12±0.14*	62.03±0.04*

The results represent mean ± SE (n=8). Data were analyzed by one-way ANOVA, followed by Dunnett comparison test against untreated animals. Values were considered significant where, *p<0.05: Low significant, **p<0.01: Medium significant
HDL: High-density lipoprotein, DE: *Decalepis nervosa*, SE: Standard error

Serum enzyme level

Activities of serum enzymes such as ALP, AST and ALT were determined. The activity of enzymes is increased much higher (alloxan induced rats) than normal, which gave significant ($p<0.001$) results in 28 days. Furthermore, diabetic animals treated with the standard drug showed a significant decrease in enzyme activity compared to the animals given only alloxan. With DN aqueous extract it also decreased significantly and the values are close to those of the animals given glibenclamide standard drug ($p<0.01$) and the decreased levels are dose dependent over 28 days (Figure 7).

In the current study, there was a significant rise in the AST, ALT, and ALP activities in the diabetic control group compared to the normal control group and thereafter the standard drug decreased the values, but they were higher than those in the normal control group, possibly due to cell membrane damage of hepatocytes or due to increased cell membrane permeability. Similar research was also reported previously.[29] AST and ALT are mainly used as biomarkers to determine liver toxicity. Increased levels of AST, ALT, and ALP in diabetic rats indicate excessive accumulation of glutamate and alanine in the serum of diabetic animals from protein stores. The elevated activities of the serum aminotransferases in the liver indicate cardiovascular disease as well as diabetes among people. The activities of ALT, AST, and ALP in serum are increased due to the leakage of these enzymes (in the liver cytosol)[30] and as a result diabetes may induce hepatic dysfunction. When DN aqueous extract was administered orally to diabetic animals, it resulted in a significant reduction in serum enzymes such as AST, ALT, and ALP compared to those given just alloxan.

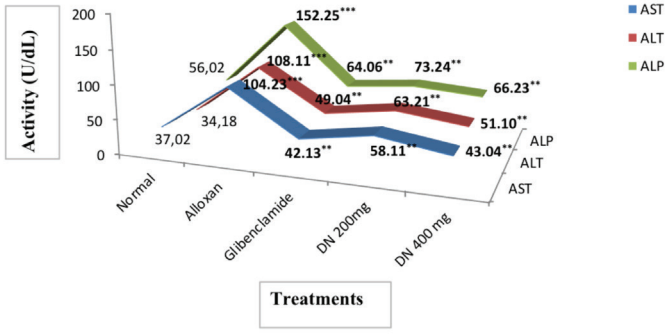

Figure 7. Activity of serum enzymes Values are expressed as mean ± SE (n=8). *p<0.05, **p<0.01, ***p<0.001 (ANOVA followed by Dunnet's test). Diabetic control was compared with normal control ($p<0.001$) and extract treated groups were compared with the diabetic control ($p<0.01$)
ALP: Alkaline phosphatase, ALT: Alanine aminotransferase, AST: Aspartate aminotransferase

Table 6. Analysis of variance

Source	DF	Sum of squares	Mean square	F ratio
Model	3	86.752150	28.9174	42.2121
Error	4	2.740200	0.6851	**Prob > F**
C. total	7	89.492350		0.0017*

DF: Degrees of freedom, C. total: Number of columns, Prob > F: The p value for the whole model test, *p<0.05: Significant

This indicates the extract has liver protection activity due to the presence of flavonoids as the result is correlated with an earlier study.[31] Results obtained from the present investigation are clearly in agreement with previous reports related to the hepatoprotective activity of menthi, guduchi, and gymnema herbal extracts reducing the elevated levels of ALT, AST, and ALP, respectively, in diabetes.[32,33]

Effect of different doses of AEDN and body weight of animals on blood glucose level

The full factorial design was evaluated at a significance level of $p<0.05$. The variance analysis of the whole experiment showed a p value of 0.0017 (Table 6).

Analysis of response to blood glucose showed the actual level by predicting plot with an root mean square error of 1.028 (Figure 8).

The leverage plot showed (Figures 9-11) the significant effect of dose and body weight of animals and its confounding effects with blood glucose level. The data are shown in Table 7. The response surface graph as shown in Figure 12 explored the relationship between body weight and dose on blood glucose.

Finally, 2×2 full factorial statistical design studies confirmed the significant effect of body weight and dose on blood glucose reduction. This result confirmed that present endangered

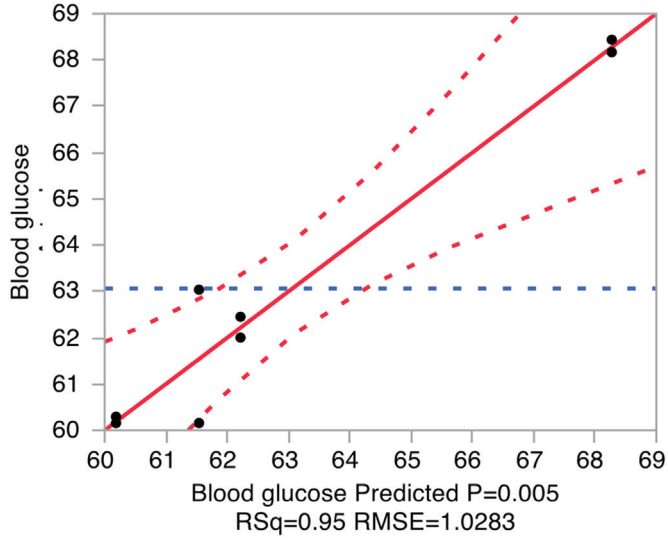

Figure 8. Actual by predicted plot

Table 7. Effect of dose and body weight and its confounding effects with blood glucose level

Term	Estimate	Standard error	t ratio	Prob > |t|
Intercept	63.065	0.363555	173.47	<0.0001*
Dose (200, 400)	-1.8575	0.363555	-5.11	0.0069*
Body weight (low)	2.185	0.363555	6.01	0.0039*
Dose x body weight (low)	-1.1675	0.363555	-3.21	0.0325*

Prob > |t|: Differentiation between p values of two trial test, *p<0.05: Significant

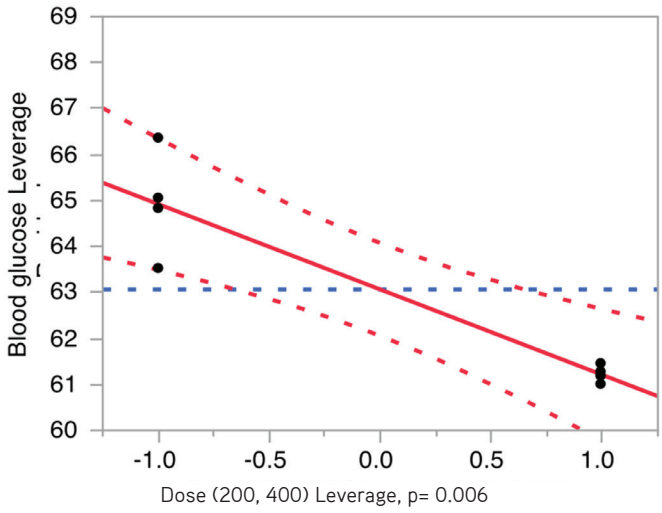

Figure 9. Leverage plot: dose vs blood glucose blood glucose

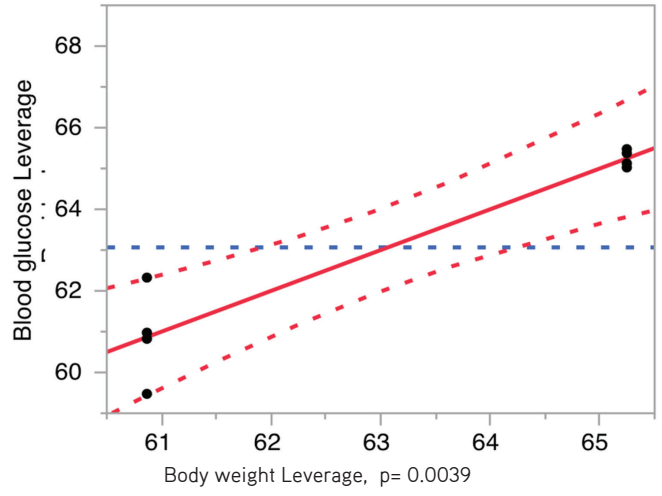

Figure 10. Leverage plot: body weight vs

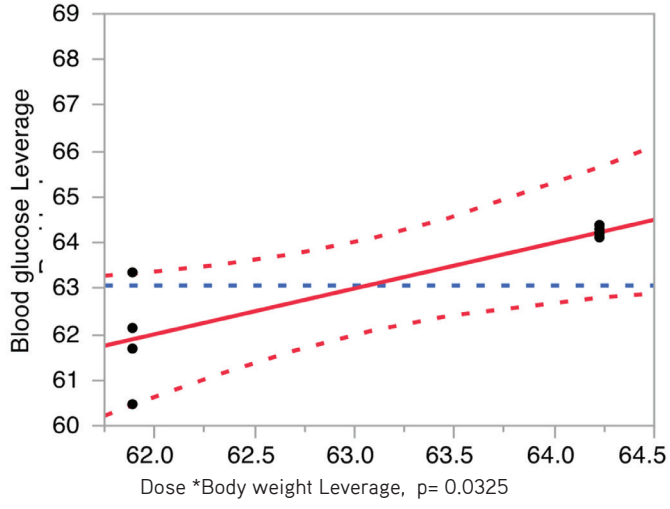

Figure 11. Leverage plot: dose and body weight together vs blood glucose level

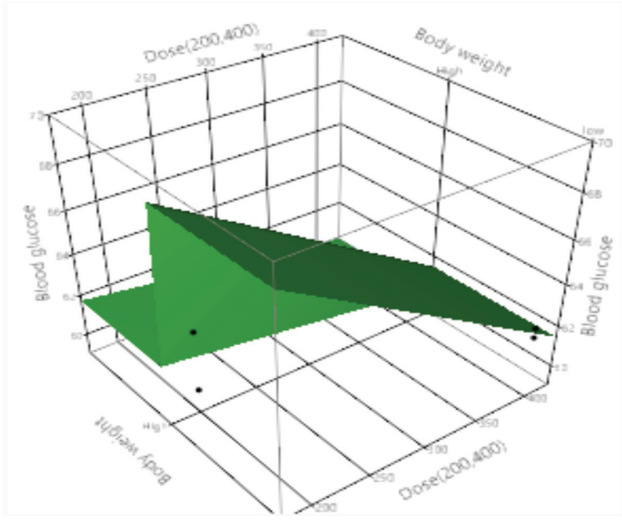

Figure 12. The relationship between body weight and dose on blood glucose

DN species have essential phytoconstituents especially polyphenolic compounds (rutin and gallic acid) that resulted in potential antidiabetic activity.

CONCLUSION

The present study concludes that various plant constituents, i.e. flavonoids, phenolics, glycosides, and alkaloids, are present in endangered AEDN leaf. TLC and HPLC confirmed rutin and gallic acid in an extract, which may trigger insulin secretion, and demonstrated significant lowering of blood glucose level, serum sugar level, and biochemical parameters, and statistical improvement in the body weight of animals in a dose-dependent manner by enhanced peripheral glucose utilization by direct stimulation of glucose uptake and reduced blood glucose level. The acute oral toxicity study revealed the safe use of all these chemical compounds that are present in DN extract. Hence, it is clear that these compounds could have hypoglycemic effects in diabetic people. Furthermore, for the first time 2×2 factorial design studies were carried out and showed a significant correlation of dose of DN extract and body weight of animals in lowering of blood glucose level. Therefore, it is ascertained that AEDN leaf has antidiabetic activity. Further research is under way for isolation of active constituents for the discovery of new drugs from DN.

Conflicts of interest: No conflict of interest was declared by the authors. The authors alone are responsible for the content and writing of this article.

REFERENCES

1. Upendra Rao M, Sreenivasulu M, Chengaiah B, Jaganmohan Reddy K, Madhusudhana Chetty C. Herbal medicines for diabetes mellitus: a review. Int J Pharm Tech Res. 2010;2:1883-1892.
2. Solomon Raju AJ, Venkata Ramana K. Lonta GM. Traditional preparation of a health drink Nannari Sharbat from the root extract of *Decalepis hamiltonii* Wight & Arn. Ind J Nat Prod Resources. 2011;2:121-124.

3. Sharma S, Shahzad A. An Overview on Decalepis: A Genus of Woody Medicinal Climbers. J Plant Sci Res. 2014;1:104.
4. Trease G, Evans SM. Pharmacognosy. 15th ed. London: Bailer Tindal; 2002:23-67.
5. Struchkov P, Beleborodov V, Kolkhir V, Voskoboynikova I, Sawateev A. Comparison of spectrophotometric methods of total flavonoid assay based on complex formation with aluminium chloride as applied to multicomponent herbal drug angionom. J Pharm Negative Results. 2018;9:1-7.
6. Sembiring EN, Elya B, Sauriasari R. Phytochemical Screening, Total Flavonoid and Total Phenolic Content, and Antioxidant Activity of Different Parts of *Caesalpinia bonduc* (L.) Roxb. Pharmacog J. 2018;10:123-127.
7. Unuofin JO, Otunola GA, Afolavan AJ. Evaluation of acute and subacute toxicity of whole-plant aqueous extract of *Vernonia mespilifolia* Less. in Wistar rats. J Integr Med. 2018;16:335-341.
8. Kotadiya C, Patel UD, Patel HB, Modi C, Fefar D. Evaluation of effects of *Opuntia elatior* Mill. fruit juice and quercetin on biochemical parameters and histopathological changes in diabetic rats. Ind J Trad Know. 2018;17:576-583.
9. Kalarani DH, Dinakar A, Senthilkumar N. Antidiabetic activity of ethanolic extracts of *Alangium salvifolium* and *Pavonia zeylanica* in streptozotocin induced diabetic rats. Int J Pharm Pharmaceuti Sci. 2012;4:337-339.
10. Ahmet O, Luka CD, Tijjani H, Obidola SM, Joel EB. Anti-diabetic activity of aqueous extract of *Curcuma longa* (Linn) rhizome in normal and alloxan-induced diabetic rats. Researcher. 2014;6:58-65.
11. Singh A, Srivastav R, Pandey AK. Effect of the seeds of *Terminalia chebula* on blood serum, lipid profile and urine parameters in STZ induced Diabetic rats. J Pharmacog Phytochem. 2018;7:1-5.
12. Dehpeur MA, Ebrahimzadeh MA, Fazel NS, Mohammad NS. Antioxidant activity of the methanol extract of *Ferula assafoetida* and its essential oil composition. Grasas Y Aceites. 2009;60:405-412.
13. Sarian MN, Ahmed QU, Mat So'ad SZ, Alhassan AM, Murugesu S, Perumal V, Mohamad SNA S, Khatib A, Latip J. Antioxidant and Antidiabetic Effects of Flavonoids: A Structure-Activity Relationship Based Study. Bio Med Res Int. 2017;2017:8386065.
14. Karima O, Righi S, Belhocin A, Mekness A, Meddah B, Tirtouil A. Phytochemical Study and Antioxidant Activity of Some Anti-Diabetic Plants in the Wilaya of Mascara. J Antimicrob Agents. 2018;4:1-5.
15. Ecobichon DJ. The basis of toxicology testing. New York; CRC press;1997:43-86.
16. Saeed F, Ahmad M. Anti-diabetic and acute toxicity studies of *Annona squamosa* L. ethanolic leaves extract. Int J Phytomedicine. 2017;9:642-647.
17. Sornalakshmi V, Tresina Soris P, Paulpriya K, Packia Lincy M, Mohan VR. Oral Glucose Tolerance Test (OGTT) in Normal Control and Glucose Induced Hyperglycemic Rats with *Hedyotis leschenaultiana* DC. Int J Toxicol Pharmacol Res. 2016;8:59-62.
18. Tomar RS, Sisodia SS. Antidiabetic activity of *Annona squamosa* Linn. in alloxan-induced diabetic rats. Int J Green Pharm. 2014:237-241.
19. Balamurugan K, Nishanthini A, Mohan VR. Antidiabetic and antihyperlipidaemic activity of ethanol extract of *Melastoma malabathricum* Linn. leaf in alloxan induced diabetic rats. Asian Pac J Trop Biomed. 2014;4(Suppl 1):442-448.
20. Jansen J, Lai YC. Regulation of muscle glycogen synthase phosphorylation and kinetic properties by insulin, exercise, adrenaline and role in insulin resistance. Arch Physiol Biochem. 2009;115:13-21.
21. Jafri MA, Aslam M, Javed K, Sing S. Effect of *Punica granatum* Linn. (flowers) on blood glucose level in normal and alloxan-induced diabetic rats. J Ethnopharmacol. 2000;70:309-314.
22. Syed MA, Vrushabendra SB, Gopkumar P, Dhanapal R, Chandrashekara VM. Anti-diabetic activity of Terminalia catappa Linn. leaf extracts in alloxan-induced diabetic rats. Int J Pharm Technol. 2005;4:36-39.
23. Kim JS, Kwon CS, Son KH. Inhibition of alpha-glucosidase and amylase by luteolin, a flavonoid. Biosci Biotechnol Biochem. 2000;64:2458-2461.
24. Sameermahmood Z, Raji L, Saravanan T, Vaidya A, Mohan V, Balasubramanyam M. Gallic acid protects RINm5F β-cells from glucolipotoxicity by its antiapoptotic and insulin-secretagogue actions. Phytother Res. 2010;24(Supll 1):83-94.
25. Serrano-Martín X, Payares G, Mendoza-León A. Glibenclamide, a blockerof K+(ATP) channels, shows antileishmanial activity in experimental murine cutaneous leishmaniasis. Antimicrob Agents Chemother. 2006;50: 4214-4216.
26. Ortega FJ, Gimeno-Bayon J, Espinosa-Parrilla JF, Carrasco JL, Batlle M, Pugliese M, Mahy N, Rodriguez MJ. ATP-dependent potassium channel blockade strengthens microglial neuroprotection after hypoxia-ischemia in rats. Exp Neurol. 2012;235:282-296.
27. Yadav AV, Undale VR, Bhosle AV. Antidiabetic activity of Plumeria rubra L. in normal and alloxan induced diabetic mice. Int J Basic Clinic Pharmacol. 2016;5:884-889.
28. Safdar M, Khan A, Khan Khattak MMA, Siddique M. Effect of various doses of cinnamon on blood glucose in diabetic individuals. Pak J Nutri. 2003;2:313-319.
29. Nwufo C, Ene AC, Emejulu AA, Obasi UK, Ene CU. Antidiabetic properties of ethanolic root extract of *Mucuna pruriens* on alloxan induced diabetic rats. Int J Res Pharm Biosciences. 2017;4:17-29.
30. Rahman MF, Siddiqui MK, Jamil K. Effects of vepacide (*Azadirachta indica*) on aspartate and alanine aminotransferase profiles in a subchronic study with rats. *Hum Exp Toxicol. 2001;*20:243-249.
31. Stanely P, Prince M, Menon VP. Hypoglycaemic and other related actions of *Tinospora cordifolia* roots in alloxan induced diabetic rats. J Ethnopharmacol. 2000;70:9-15.
32. Renuka C, Ramesh N, Saravanan K. Evaluation of the antidiabetic effect of *Trigonella foenum-graecum* seed powder on alloxan induced diabetic albino rats. Int J pharm Tech Res. 2009;1:1580-1584.
33. El Shafey AAM, El-Ezabi MM, Seliem MME, Ouda HHM, Ibrahim DS. Effect of Gymnema sylvestre R. Br.leaves extract on certain physiological parameters of diabetic rats. J King Saud Univer Sci. 2013;25:135-141.

Turk J Pharm Sci 2020;17(3):329-336
DOI: 10.4274/tjps.galenos.2018.60566

ORIGINAL ARTICLE

Anti-inflammatory and Analgesic Effects of *Limnophila repens* (Benth.)

Limnophila repens (Benth.) Anti-enflamatuvar ve Analjezik Etkileri

Venkateswarlu GUNJI[1]*, Ganapaty SERU[2]

[1]A.M. Reddy Memorial College of Pharmacy, Department of Pharmacognosy and Phytochemistry, Andhra Pradesh, India
[2]GITAM Institute of Pharmacy, Department of Pharmacognosy and Phytochemistry, Andhra Pradesh, India

ABSTRACT

Objectives: The analgesic and anti-inflammatory effects of methanolic extract of *Limnophila repens* (MELR) were assessed at 200 and 400 mg/kg.

Materials and Methods: In carrageenan-mediated paw edema, the anti-inflammatory effect of MELR was investigated and analgesic activity was assessed by central and peripheral models

Results: MELR had strong analgesic and anti-inflammatory effects at different dosages (200 and 400 mg/kg). The study results confirmed the use of *Limnophila* as both an analgesic and anti-inflammatory. The strong anti-inflammatory and analgesic effects can be caused by anabolic steroids, i.e. β-sitosterol and stigmasterol; and flavonoids, i.e. quercetin and glycosides, in the extraction of some kind of inflamed arbitrators.

Conclusion: Based on the study, we can conclude that *Limnophila repens* had analgesic and anti-inflammatory activity. In addition to organic studies, however, additional phytochemicals are required to evaluate the extra energetic chemicals responsible for the antinociceptive and anti-inflammatory effects.

Key words: *Limnophila repens*, carrageenan, phytochemical screening, β-sitosterol

ÖZ

Amaç: *Limnophila repens* (MELR) metanol ekstresinin analjezik ve anti-enflamatuvar etkileri 200 ve 400 mg/kg dozda değerlendirildi.

Gereç ve Yöntemler: Karagenin ile indüklenen pence ödeminde MELR'nin anti-enflamatuvar etkisi araştırıldı ve analjezik aktivite merkezi ve periferik modellerle değerlendirildi.

Bulgular: MELR, farklı dozlarda (200 ve 400 mg/kg) güçlü analjezik ve anti-enflamatuvar etki göstermiştir. Çalışma sonuçları, *Limnophila*'nın hem analjezik hem de anti-enflamatuvar olarak kullanımını doğrulamıştır. Güçlü anti-enflamatuvar ve analjezik etkilerden anabolik steroidlerin (β-sitosterol ve stigmasterol gibi); flavonoidlerin (kuersetin ve glikozitler gibi) sorumlu olabileceği değerlendirilmiştir.

Sonuç: Çalışmaya dayanarak *Limnophila repens*'in analjezik ve anti-enflamatuvar aktiviteye sahip olduğu sonucuna varabiliriz. Bununla birlikte, organik çalışmalara ek olarak, antinosiseptif ve anti-enflamatuvar etkilerden sorumlu ekstra enerjik kimyasalları değerlendirmek için ek fitokimyasallar gereklidir.

Anahtar kelimeler: *Limnophila repens*, karagenin, fitokimyasal tarama, β-sitosterol

***Correspondence: E-mail:** gvr9885@gmail.com, **Phone:** 9000079873 **ORCID-ID:** orcid.org/0000-0001-7076-5090
Received: 04.09.2018, **Accepted:** 01.11.2018

INTRODUCTION

Herbal treatments, particularly therapeutic plants, were our ancestors' primary or only source of healthcare. Despite the rise of the healthcare industry, therapeutic plants and medicines that can be developed from them have never been totally discarded and people still resort to traditional medicine.[1] Basically, the use of natural flora in the treatment of illnesses and pain management is a key remedy.[2]

Limnophila is used to treat heart attacks, elephantiasis, diarrhea, dyspepsia, high temperature, dysentery, acid indigestion, dysmenorrhea, and stomach pain.[3-5]

Phytochemical examination of *Limnophila* shows a number of primary and secondary phytoconstituents.[6] This variety of substances justifies the traditional use of *L. repens*.

Limnophila is already very prevalent and frequently used in herbal remedies as an antimycobacterial, antioxidant, antineoplastic, and antimicrobial,[7-11] but no natural research studies have been performed on this herb. Subsequently, the present experiment was performed to determine the anti-inflammatory and antinociceptive activities of *L. repens*.

MATERIALS AND METHODS

Plant selection and authentication

During September 2017, *L. repens* was collected at Tirupati. Dr. K. Madhava Chetty identified and tested the examined herb. GITAM Institute of Pharmacy, Visakhapatnam, deposited an herb specimen with the voucher number 1568.

Preparation of extract

The powder (1 kg) was obtained by petroleum ether method suggested for removing both fatty and waxy materials. The methanol extract was initially extracted in alcoholic water through a splitting-up channel and then sequentially segmented together with petrol ether, chloroform, ethyl acetate, and n-butanol to obtain portions of these solvents. These extracts had been subjected to preparatory phytochemical evaluation and had, in addition, been kept in the fridge at 4°C for potential further use.[12]

Phytochemical screening

Various extracts of *L. repens* were subjected to qualitative chemical assessment using uniform criteria.[13-16]

Separation of phytoconstituents

Column chromatography on silica gel (60-120 mesh) using n-hexane, ethyl acetate, and 100% methanol afforded an 18 g petroleum ether portion. The fractions on the thin-layer chromatography (TLC) plate were pooled and crystallized, and named *Limnophila repens* (LR-1) and LR-2.[17] A silica gel column eluted from the chloroform-methanol phase gradient (from 100:0 to 4:1) chromatographed the ethyl acetate section and put eight sections on their TLC. In the Sephadex LH-20, chloroform methanol (1:10) was chromatographed with methanol to provide LR-3.[18]

Animals

All the experimental animals used for this research were acquired from Nicholas Piramal India Limited, Mumbai. They were subsequently put in the Animal House of A.M. Reddy Memorial College of Pharmacy with IAEC Approval no. AMRMCP/05/IAEC/18-19/PHD. While in the Animal House they were allowed to consume water and eat. The animal usage complied with OECD-423 guidelines.[19]

Acute toxicity study

Test methanolic extract of *Limnophila repens* (MELR) toxicity in an acute toxicity study was based on OECD 423 recommendations for 2000 mg/kg dose. The test animals were regularly checked at 1 h, then 4 h, and finally every 24 h for 14 days for body signs and symptoms of poisoning, consisting of squirming, gulping, or pulsation as well as decreased respiratory system rate or even impermanence. No fatality was observed in this study.[20]

Grouping of animals and selection of dose

Furthermore, male rodents were randomly divided into four groups (control, regular, and pair of examination groups) composed of 5 animals each for analgesic and anti-inflammatory study. The first group was initially designated as the control, with 10 mL/kg distilled water. Group II specified as reference group was given the standard drug tramadol 10 mg/kg p.o. Groups III and IV received MELR (200 mg/kg and 400 mg/kg, respectively) in distilled water.

Pharmacological activity

Antinociceptive activity

The peripheral study behavior of MELR was evaluated using acetate-induced acid while the central analgesic function was investigated using the hot plate and tail-flick techniques.

Hot plate technique

Each rodent was individually placed independently on the hot plate at 55±2 °C. The response time was videotaped for each mouse at 30 min, 60 min, and 90 min, monitoring medicine or vehicle administration along with 15 s cut-off to avoid injury. Increased response time and extracts were matched to the control group.[21,22]

Percentage of analgesic activity was calculated by using the formula

$$\% \text{ Analgesic activity} = \frac{(Ta-Tb) \times 100}{Tb}$$

Ta: Average reaction time after extract; Tb: Average initial reaction time

Tail immersion test

The lower part of the rodent tail was immersed in warm water, around 55 °C, which caused a painful reaction. The time, in seconds, for tail withdrawal from the water was recorded as the response period, having a cut-off time for immersion set at 15 s. The latent period of the tail immersion response was determined at 0, 30, 60, 90, 120 and 180 min after the oral administration of standard and MELR. In addition, the percentage of inhibition was calculated using the formula[23]

$$\text{Inhibition} = \frac{\text{Ln-Lo}}{15 \text{ s-Lo}} \times 100 ,$$

where Lo: Latent time before drug administration in seconds, Ln: Latent time after drug administration in seconds (n=30 to 180 min).

Writhing test

The mice (n=5) were grouped into MELR teams; in addition, two more teams (n=5) were used for control and standard testing. They were divided into four teams, w here groups III and IV were given MELR at a dose of 100 and 200 mg/kg b.wt. explicitly (by i.p.), while group II was administered along with the normal aspirin 100 mg/kg drug, p.o. 1 h before acetic acid induction. The group's percentage restraint was calculated by[24,25]

$$\% \text{ Inhibition} = \frac{\text{Mean no. of writhes (control) - Mean no. of writhes (Treated)}}{\text{Mean no. of writhes control}} \times 100$$

Anti-inflammatory activity

Carrageen-induced paw edema

The rat paw edema procedure caused abrupt inflammation in the rodents by administration of 00.1 mL of prepared carrageenan fluid (1% w/v) to the subplantar area. For each sample the rodents were categorized into four sections (n=5) and control and norm groups (n=5). The control group was given vehicle; the standard group received diclofenac 10 mg/kg p.o and the groups assigned for extracts received 200 and 400 mg/kg p.o. before 60 min of carrageenan injection. Upon carrageenan infusion, paw volume was assessed with an electronic plethysmometer at 1, 2, and 3 h. % Inhibition was calculated using the formula[26]

$$\% \text{ Inhibition} = T_o - T_t / T_o \times 100,$$

where T_o: Paw thickness of rats given test extract at the same time; T_t: Paw thickness of control rats.

Statistical analysis

The data are expressed as mean ± standard error of the mean (SEM). ANOVA software (GraphPad Prism 5) was used to perform the statistical analysis. The level of statistical significance was $p<0.05$.

RESULTS

Phytochemical screening

The results of the phytochemical analysis of different extracts are shown in Table 1.

Characterization of LR-1

White powder, $C_{29}H_{48}O$, MW 412.69. ultraviolet - max ($CHCl_3$) nm: 257; IR (KBr) IR (KBr) total cm^{-1}: 3418 (-OH stretch), 2934 (C-H stretch in CH_2 and CH_3), 2866 (=C-H stretch), 2339, 1602 (C=C asymmetric stretch), 1566, 1461 (C-H deformation in gem dimethyl), 1409, 1383, 1251, 1191, 1154, 1109, 1089, 1053 (cycloalkane), 1020, 791; (MS-ES-APCI, m/z): 409.2, 395.3, 335. The above spectral data (mass, NMR) showed the molecular formula $C_{29}H_{48}O$, similar to stigmasterol (Figure 1).

LR-02

White powder, $C_{29}H_{50}O$, MW 414.70; IR (KBr) max cm^{-1}: 3424 (-OH stretch), 2959 (-CH, CH_2, and $-CH_3$), 2936, 2867 (=C-H), 1602, 1565, 1465 (C-H deformation in gem dimethyl), 1382, 1332, 1242, 1191, 1154, 1051 (cycloalkane), 779 cm^{-1}; ^{1}H NMR data (400 MHz, $CDCl_3$). The above spectral data (mass, NMR) showed the molecular formula $C_{29}H_{50}O$, similar to β-sitosterol (Figure 2).

LR-03

Yellow powder, $C_{15}H_{10}O_7$, MW 302.23; IR (KBr) max cm^{-1}: 3413 (-OH bending), 2340, 1607, 1565, 1523, 1462, 1408, 1383, 1320, 1263 (C-O stretch), 1199, 1168, 1131, 1014, 959, 782 (=C-H bending); ^{1}H NMR data (400 MHz, $CDCl_3$) 9.57 (1H, s), 9.29-9.33 (2H, d), 7.68-7.69 (1H, d), 7.53-7.69 (1H, m), 6.88-6.90 (1H, d), 6.41 (1H, d), 6.19 (1H, d); ^{13}C NMR data (400 MHz, $CDCl_3$) and others: 175.81 (C-4), 163.85 (C-7), 160.70 (C-5), 156.17 (C-9), 147.67 (C-2), 146.81 (C-31), 145.03 (C-3), 135.68 (C-61), 121.96. The above spectral data (mass, NMR) showed the molecular formula $C_{15}H_{10}O_7$, similar to quercetin (Figure 3).

Acute toxicity studies

An oral MELR dosage of 2000 mg/kg caused no immediate toxic symptoms. Furthermore, no rodents died during 24 h surveillance. The extracts have been considered to be safe at the highest allowable dose of 2000 mg/kg; the highest possible dosage was generally chosen for analgesic and anti-inflammatory activities, i.e. 200 and 400 mg/kg, 1/5th and 10-fold drops.

Analgesic activity

Hot plate tests

The mean ± SEM showed that the MELR (200 and 400 mg/kg) caused an improvement in basal reaction time from 9.62±0.22 and 9.49±0.22 at 0 min to 12.95±0.62 and 14.95±0.85 at 90 min, respectively (Figure 4, Table 2).

Tail immersion test

The tail immersion approach showed a marked increase of 6.39±0.15 in MELR (200 mg/kg) and 7.75±0.31 in MELR (400 mg/kg) at 180 min (Figure 5). The inhibition was the strongest at 400 mg/kg dose at 180 min, lower than normal (Table 3).

Writhing test

Table 4 revealed *Limnophila*'s peripheral pharmacological behavior on visceral squirming in mice. The control group displayed maximal writhing (26±2.12), while MELR had a strong antinociceptive effect against acetic acid-induced writhing at doses of 200 and 400 mg/kg, inhibiting pain 33.07% and 49.23% relative to the control (Figure 6). At 10 mg/kg, diclofenac caused 68.46% ($p<0.001$) writhing reaction inhibition.

Carrageenan-induced paw edema

Table 5 demonstrates MELR's effect on the paw edema model relative to carrageenan treatment at different stages. A dosage of 200 mg/kg MELR was given. MELR administered at a dose of 200 mg/kg p.o. prevented carrageenan-induced paw edema with a percentage inhibition of 19.44%, 26.61%, 33.41%, and 41.73% at 1, 2, 3, and 4 h, respectively, and 31.94%, 40.32%,

Table 1. Phytochemical analysis of various extracts of *Limnophila repens*

Phytoconstituents	Method	Pet. ether extract	Chloroform extract	Ethyl acetate extract	Methanolic extract	n-Butanol extract	Aqueous extract
Flavonoids	Shinoda test	-	-	+	+	-	+
	Zn + HCl test	-	-	+	+	-	+
	Lead acetate test	-	-	+	+	-	+
Volatile oil	Stain test	+	-	-	+	-	+
Alkaloids	Wagner test	-	+	-	+	-	+
	Hager's test	-	+	-	+	-	+
Tannins and phenols	$FeCl_3$ test	-	-	+	+	+	+
	Potassium dichromate test	-	-	+	+	+	+
Saponins	Foam test	-	-	-	-	-	-
Phytosterols	Libermann's test	+	+	-	+	-	-
Carbohydrates	Molish test	-	-	-	+	-	+
Acid compounds	Litmus test	-	-	-	-	-	-
Glycoside	Borntragers test	-	-	-	+	-	+
Amino acids	Ninhydrin test	-	-	-	+	-	+
Proteins	Biuret test	-	-	-	+	-	+
Fixed oils and fats	Spot test	+	-	-	-	-	-

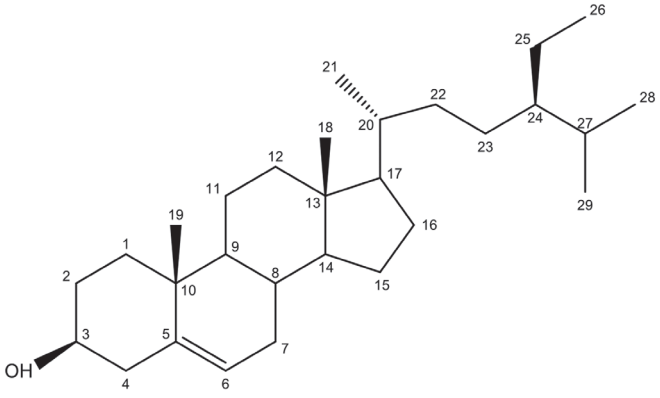

Figure 1. Structure of LR-01 (stigmasterol)
LR: Limnophila repens

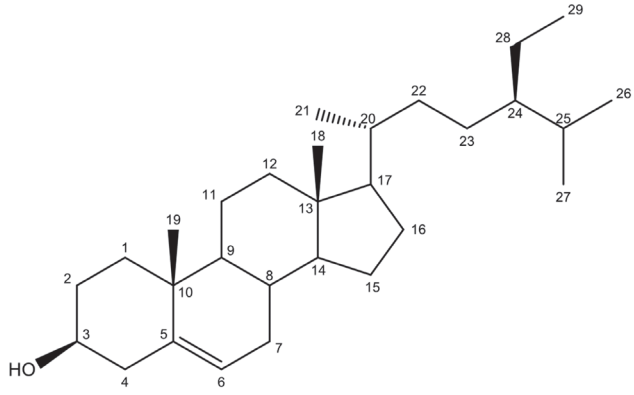

Figure 2. Structure of LR-02 (β-sitosterol)
LR: Limnophila repens

50.25%, and 61.44% at a dose of 400 mg/kg p.o. at 1, 2, 3, and 4 h, respectively. Diclofenac sodium at a dose of 10 mg/kg p.o. prevented carrageenan-induced paw edema with a percentage inhibition of 52.08%, 60.48%, 70.46%, and 73.91% at 1, 2, 3, and 4 h, respectively (Figure 7).

DISCUSSION

Preliminary phytochemical analysis of *L. repens* revealed many compounds including flavonoids, volatile oils, alkaloids, tannins, phytosterols, sugars, glycosides, proteins, and fixed oils.

It is well known that inflammation and pain are the most common diseases in human and animals, and the current treatment is to use steroidal and nonsteroidal anti-inflammatory drugs, which have several side effects.[27,28] *L. repens* has a long history of being used for various diseases and is a well-known Indian medicine, but its analgesic and anti-inflammatory features have never been reported. We have shown important antinociceptive and anti-inflammatory behavior of *L. repens* in various animal models. The hot-plate test exemplifies centrally moderated antinociceptive responses, which typically work on modifications over a spinal-cord degree. MELR's major discomfort-endurance implies core involvement. Some complex therapies like opiate, dopaminergic, noradrenergic, and serotonergic units usually centrally treat pain. The analgesic result due to the extract may be through major operations consisting of these types of receptors or even through specific procedures associated with prostaglandin inhibition, leukotrienes, and numerous other endogenous chemicals that may lead to swelling and discomfort.[29]

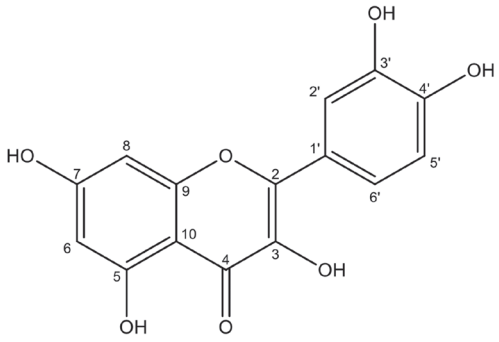

Figure 3. Structure of LR-03 (quercetin)
LR: Limnophila repens

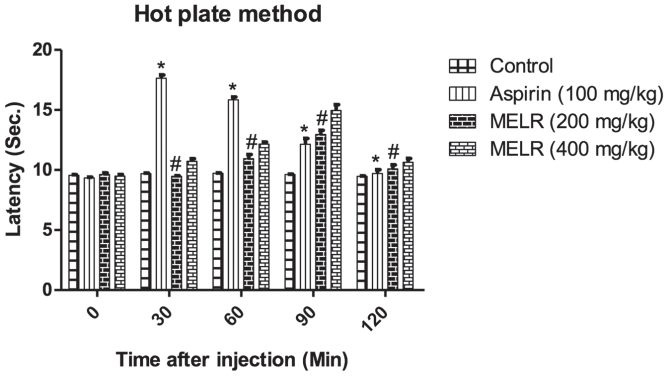

Figure 4. Effect of MELR on hot-plate method. All the values are expressed as mean ± SEM, n=5 rat in each group, by one-way ANOVA followed by Tukey's multiple comparison test *p<0.05 significant compared to control and #p<0.05 significant compared to standard
MELR: Methanolic extract of *Limnophila repens*, SEM: Standard error of the mean

The abdominal constriction response evoked by acetic acid is a sensitive process to assess peripherally acting analgesics. Acetic acid usually induces pain by releasing endogenous components such as bradykinins, histamine, serotonin, and prostaglandins, which trigger nerve endings. Peritoneal receptors are implied to communicate with stomach constraints. The strategy also requires elevated rates of prostaglandin E2 (PGE2) and PGF2 in peritoneal and lipoxygenase materials.[30] The major reduction in MELR-induced acetic acid writhes indicates that the analgesic activity may be moderated peripherally along with restriction of development and discharge of prostaglandins alongside endogenous drugs.

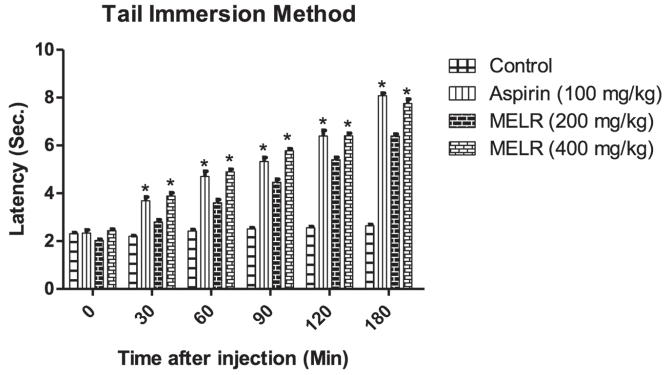

Figure 5. Protective effect of MELR on tail withdrawal reflexes induced by tail immersion method in rats. All the values are expressed as mean ± SEM, n=5 rats in each group, by one-way ANOVA followed by Tukey's multiple comparison test. Results are presented as mean ± SEM, (n=5), *p<0.05 versus control
MELR: Methanolic extract of *Limnophila repens*, SEM: Standard error of the mean

Table 2. Effect of MELR on hot-plate method

Treatment	Reaction time (s)				
	Time after treatment (min)				
	0	30	60	90	120
Control	9.55±0.94	9.68±0.97	9.72±0.6	9.62±0.68	9.48±0.62
Aspirin (100 mg/kg)	9.34±011	17.64±0.46*	15.84±0.39*	12.13±0.84*	9.71±0.54*
MELR (200 mg/kg)	9.62±0.22	9.46±0.1#	10.95±0.58#	12.95±0.62#	10.09±0.56#
MELR (400 mg/kg)	9.49±0.22	10.72±0.38	12.15±0.31	14.95±0.85	10.64±0.54

All the values are expressed as mean ± SEM, n=5 rats in each group, by one-way ANOVA followed by Tukey's multiple comparison test. *p<0.05 significant compared to control and #: p<0.05 significant compared to standard, MELR: Methanolic extract of *Limnophila repens*, SEM: Standard error of the mean

Table 3. Protective effect of MELR on tail withdrawal reflexes induced by tail immersion method in rats

Treatment	Reaction time (s)					
	Time after treatment (min)					
	0	30	60	90	120	180
Control	2.31±0.06	2.2 ±0.04	2.42±0.11	2.51±0.08	2.56±0.08	2.64±0.09
Aspirin (200 mg/kg)	2.34±0.23	3.68±0.28	4.7±0.36	5.33±0.28	6.39±0.39	8.08±0.17
MELR (200 mg/kg)	2.03±0.07	2.8±0.15	3.6±0.22	4.46±0.22	5.4±0.16	6.39±0.15
MELR (400 mg/kg)	2.44±0.11	3.89±0.23	4.89±0.18	5.78±0.14	6.4±0.18	7.75±0.31

All the values are expressed as mean ± SEM, n=5 rats in each group, by one-way ANOVA followed by Tukey's multiple comparison test. Results are presented as mean ± SEM, (n=5), *p<0.05 versus control, MELR: Methanolic extract of *Limnophila repens*, SEM: Standard error of the mean

As an animal model for extreme swelling, carrageen-induced edema remains largely unused and is actually considered

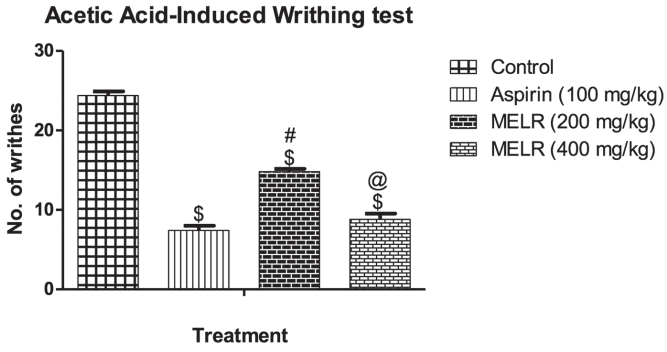

Figure 6. Effect of MELR on acetic acid-induced writhing behavior in mice
$p<0.001 versus control, #p<0.001 versus aspirin, and @p<0.001 versus MELR (200 mg/kg),
MELR: Methanolic extract of *Limnophila repens*

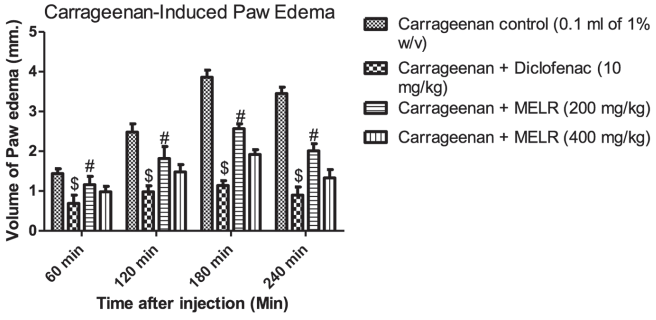

Figure 7. Effect of MELR on carrageenan-induced paw edema method. Results are presented as mean ± SEM, (n=5), $p<0.001 versus control; #p<0.001 versus diclofenac (10 mg/kg)
MELR: Methanolic extract of Limnophila repens, SEM: Standard error of the mean

biphasic. The initial stage (1-2 h) is largely solved in cell-ruined environments by histamine, serotonin, and increased prostaglandin formation. The latter stage (3 h) is liable to release prostaglandin and regulated by tissue macrophages,[31,32] bradykinin, and leukotrienes. In MELR's late-stage, substantial suppressive activity ($p<0.05$) indicates its powerful anti-inflammatory effect. It is comparable to diclofenac, which prevented edema at 10 mg/kg by 61.44%, a statistically significant finding ($p<0.05$). Ueno et al.[33] reported that rodent paw carrageen therapy results in bradykinin production that eventually leads to prostaglandin biosynthesis, as well as many other autacoids that accumulate inflammatory exudates.[34] PGE2 is a dominant vasodilator with many endogenous vasodilators, notably histamine and bradykinin, in severe inflammatory environments. Extract action mode is firmly recommended to suppress prostaglandin synthesis. Tests revealed that MELR has essential anti-inflammatory properties at various stages. Carrageenan-induced inflammation is an essential way to determine anti-inflammatory function. Edema formation in the rat paw following carrageen injection stems from histamine, serotonin, and prostaglandin release and associated substances. MELR has good anti-inflammatory behavior.[35-37] Due to anabolic steroids, i.e. β-sitosterol and stigmasterol,[38] flavonoids such as quercetin,[39] and glycosides present in the extract, this significant anti-inflammatory and analgesic impact results from the inhibition of any inflammatory mediators. The latest results indicate *Limnophila*'s efficacy in treating acute inflammation. The result also confirms the folklore information on the anti-inflammatory and analgesic property of the *L. repens* extract. Yet, additional phytochemical along with pharmacological

Table 4. Effect of MELR on acetic acid-induced writhing behavior in mice

Treatment	Writhing count					Writhings (mean ± SEM)	% of writhing	% of inhibition
	M-1	M-2	M-3	M-4	M-5			
Control	28	26	25	23	28	26±2.12	100	0
Diclofenac sodium (5 mg/kg)	7	9	11	6	8	8.2±1.92	31.54	68.46
MELR (200 mg/kg)	16	20	12	18	21	17.4±3.57	66.93	33.07
MELR (400 mg/kg)	12	15	8	16	15	13.2±3.27	50.77	49.23

M-1: Mouse 1, M-2: Mouse 2, M-3: Mouse 3, M-4: Mouse 4, M-5: Mouse 5, MELR: Methanolic extract of *Limnophila repens*, SEM: Standard error of the mean

Table 5. Effect of MELR on carrageenan-induced paw edema method

Group	Change in paw thickness (mm) ± SD				% Inhibition at hours			
	1 h	2 h	3 h	4 h	1 h	2 h	3 h	4 h
Carrageenan (1% w/v of 0.1 mL)	1.44±0.12	2.48±0.21	3.86±0.18	3.45±0.16	-	-	-	-
Carrageenan + diclofenac (10 mg/kg)	0.69±0.21$	0.98±0.15$	1.14±0.12$	0.9±0.2$	52.08	60.48	70.46	73.91
Carrageenan + MELR (200 mg/kg)	1.16±0.21#	1.82±0.3#	2.57±0.12#	2.01±0.18#	19.44	26.61	33.41	41.73
Carrageenan + MELR (400 mg/kg)	0.98±0.14	1.48±0.18	1.92±0.12	1.33±0.21	31.94	40.32	50.25	61.44

Results are presented as mean ± SEM, (n=5), $: p<0.001 versus control, #p<0.001 versus diclofenac (10 mg/kg), MELR: Methanolic extract of *Limnophila repens*, SD: Standard deviation, SEM: Standard error of the mean

activity are needed to figure out the various other chemical components responsible for the anti-nociceptive and also anti-inflammatory effects.

Conflict of Interest: No conflict of interest was declared by the authors.

REFERENCES

1. Metrouh-Amir H, Amir N. Evaluation *in vivo* of anti-inflammatory and analgesic properties of Matricaria pubescens alkaloids. South African Journal of Botany. 2018;116:168-174.
2. Husseini Y, Sahraei H, Meftahi GH, Dargahian M, Mohammadi A, Hatef B, Zardoozc H, Ranjbarana M, Hosseinia SB, Alibeigb H, Behzadniaa M, Majdb A, Baharic Z, Ghoshoonia H, Jalilid C, Golmanesha L. Analgesic and anti-inflammatory activities of the hydro-alcoholic extract of Lavandula officinalis in mice: possible involvement of the cyclooxygenase type 1 and 2 enzymes. Rev Bras Farmacogn. 2016;26:102-108.
3. Les DH. Aquatic dicotyledons of North America: ecology, life history, and systematics: CRC Press; 2017.
4. Hsu H, Chen Y, Sheu S, Hsu C, Chen C, Chang H. Oriental materia medica: a concise guide. Keats Publishing; Inc; 1996.
5. Pullaiah T. Encyclopaedia of world medicinal plants: Daya Books; 2006.
6. Brahmachari G. Limnophila (Scrophulariaceae): Chemical and Pharmaceutical Aspects-An Update. The Open Natural Products Journal. 2014;7:1-14.
7. Do QD, Angkawijaya AE, Tran-Nguyen PL, Huynh LH, Soetaredjo FE, Ismadji S, Ju YK. Effect of extraction solvent on total phenol content, total flavonoid content, and antioxidant activity of Limnophila aromatica. J Food Drug Anal. 2014;22:296-302.
8. Kukongviriyapan U, Luangaram S, Leekhaosoong K, Kukongviriyapan V, Preeprame S. Antioxidant and vascular protective activities of Cratoxylum formosum, Syzygium gratum and Limnophila aromatica. Biol Pharm Bull. 2007;30:661-666.
9. Rao JV, Aithal KS, Srinivasan KK. Antimicrobial activity of the essential oil of Limnophila gratissima. Fitoterapia. 1989;60:376-377.
10. Nanasombat S, Teckchuen N. Antimicrobial, antioxidant and anticancer activities of Thai local vegetables. J Med Plants Res. 2009;3:443-449.
11. Suksamrarn A, Poomsing P, Aroonrerk N, Punjanon T, Suksamrarn S, Kongkun S. Antimycobacterial and antioxidant flavones from Limnophila geoffrayi. Arch Pharm Res. 2003;26:816-820.
12. Ahmed D, Saeed R, Shakeel N, Fatima K, Arshad A. Antimicrobial activities of methanolic extract of Carissa opaca roots and its fractions and compounds isolated from the most active ethyl acetate fraction. Asian Pac J Trop Biomed. 2015;5:541-545.
13. Khandelwal KR. Practical pharmacognosy: techniques and experiments. Maharashtra; Niral Prakashan; 2008.
14. Kokate C. Practical pharmacognosy. Vallabh Prakashan, New Delhi; 1994;1:15-30.
15. Wallis TE. Practical pharmacognosy. 1925.
16. Yarnalkar S. Practical pharmacognosy. Pune; Nirali Prakashan; 1991:38.
17. Habib MR, Nikkon F, Rahman M, Haque ME, Karim MR. Isolation of stigmasterol and ß-sitosterol from methanolic extract of root. Pak J Biol Sci. 2007;10:4174-4176.
18. Wan C, Yu Y, Zhou S, Tian S, Cao S. Isolation and identification of phenolic compounds from Gynura divaricata leaves. Pharmacogn Mag. 2011;7:101-108.
19. Oecd. OECD Guidelines for the Testing of Chemicals: Organization for Economic; 1994.
20. Kiran PM, Raju AV, Rao BG. Investigation of hepatoprotective activity of Cyathea gigantea (Wall. ex. Hook.) leaves against paracetamol-induced hepatotoxicity in rats. Asian Pac J Trop Biomed. 2012;2:352-356.
21. Vogel HG. Drug discovery and evaluation: pharmacological assays: Springer Science & Business Media; 2002.
22. Kumar Paliwal S, Sati B, Faujdar S, Sharma S. Studies on analgesic, anti-inflammatory activities of stem and roots of Inula cuspidata C.B Clarke. J Tradit Complement Med. 2017;7:532-537.
23. Wang YX, Gao D, Pettus M, Phillips C, Bowersox SS. Interactions of intrathecally administered ziconotide, a selective blocker of neuronal N-type voltage-sensitive calcium channels, with morphine on nociception in rats. Pain. 2000;84:271-281.
24. Xu Q, Wang Y, Guo S, Shen Z, Wang Y, Yang L. Anti-inflammatory and analgesic activity of aqueous extract of Flos populi. J Ethnopharmacol. 2014;152:540-545.
25. Arumugam P, Murugan M, Thangaraj N. Evaluation of anti-inflammatory and analgesic effects of aqueous extract obtained from root powder of Inula racemosa Hook. f. J Med Plants Res. 2012;6:2801-2806.
26. Badole SL, Zanwar AA, Ghule AE, Ghosh P, Bodhankar SL. Analgesic and anti-inflammatory activity of alcoholic extract of stem bark of Pongamia pinnata (L.) Pierre. Biomedicine & Aging Pathology. 2012;2:19-23.
27. Collier HO, Dinneen LC, Johnson CA, Schneider C. The abdominal constriction response and its suppression by analgesic drugs in the mouse. Br J Pharmacol Chemother. 1968;32:295-310.
28. Deraedt R, Jouquey S, Delevallée F, Flahaut M. Release of prostaglandins E and F in an algogenic reaction and its Inhibition. Eur J Pharmacol. 1980;61:17-24.
29. Millan MJ. Descending control of pain. Prog Neurobiol. 2002;66:355-474.
30. Farouk L, Laroubi A, Aboufatima R, Benharref A, Chait A. Evaluation of the analgesic effect of alkaloid extract of Peganum harmala L.: possible mechanisms involved. J Ethnopharmacol. 2008;115:449-454.
31. Chavan MJ, Wakte PS, Shinde DB. Analgesic and anti-inflammatory activities of 18-acetoxy-ent-kaur-16-ene from Annona squamosa L. bark. Inflammopharmacology. 2011;19:111-115.
32. Oliveira de Melo J, Truiti MdCT, Muscara MN, Bolonheis SM, Dantas JA, Caparroz-Assef SM, Cuman RKN, Bersani-Amado CA. Anti-inflammatory activity of crude extract and fractions of Nectandra falcifolia leaves. Biol Pharm Bull. 2006;29:2241-2245.
33. Ueno A, Naraba H, Ikeda Y, Ushikubi F, Murata T, Narumiya S, Oh-İshi SN. Intrinsic prostacyclin contributes to exudation induced by bradykinin or carrageenin: a study on the paw edema induced in IP-receptor-deficient mice. Life Sci. 2000;66:155-160.
34. Simplice FH, Arm AB, Roger P, Emmanuel AA, Pierre K, Veronica N. Effects of Hibiscus asper leaves extracts on carrageenan induced oedema and complete Freunds adjuvant-induced arthritis in rats. Journal of Cell and Animal Biology. 2011;5:66-68.
35. Georgewill O, Georgewill U, Nwankwoala R. Anti-inflammatory effects of Morninga oleifera lam extract in rats. Asian Pac J Trop Med. 2010;3:133-135.

36. Winter CA, Risley EA, Nuss GW. Carrageenin-Induced Edema in Hind Paw of the Rat as an Assay for Anti-inflammatory Drugs. Proc Soc Exp Biol Med. 1962;111:544-547.

37. Georgewill OA, Georgewill UO. Evaluation of the anti-inflammatory activity of extract of Vernonia amygdalina. Asian Pac J Trop Med. 2010;3:150-151.

38. Saeidnia S, Manayi A, Gohari AR, Abdollahi M. The story of beta-sitosterol-a review. European J Med Plants. 2014;4:590.

39. Li Y, Yao J, Han C, Yang J, Chaudhry MT, Wang S, Liu H, Yin Y. Quercetin, Inflammation and Immunity. Nutrients. 2016;8:167.

Turk J Pharm Sci 2020;17(3):337-342
DOI: 10.4274/tjps.galenos.2019.57983

ORIGINAL ARTICLE

Global DNA Hypomethylation and *Rassf1a* and *c-myc* Promoter Hypermethylation in Rat Kidney Cells after Bisphenol A Exposure

Bisfenol A Maruziyeti Sonrası Sıçan Böbrek Hücrelerinde Global DNA Hipometilasyonu ve *Rassf1a* ile *c-myc* Promotör Hipermetilasyonu

Pınar TUZCUOĞLU, Sibel ÖZDEN*

İstanbul University Faculty of Pharmacy, Department of Pharmaceutical Toxicology, İstanbul, Turkey

ABSTRACT

Objectives: Bisphenol A (BPA) is a synthetic monomer used in the production of polycarbonate and an environmental contaminant with endocrine disrupting properties. BPA release from plastic carriers is thought to cause high amounts of exposure, which result in high risk to human and environment health.

Materials and Methods: The study examined the possible changes in global DNA methylation, CpG promoter DNA methylation, and gene expressions of *Rassf1a* and *c-myc* after BPA exposure in rat kidney epithelial cells (NRK-52E).

Results: The IC_{50} values of BPA in NRK-52E cells were 133.42 and 101.74 μM in the 3-(4,5-dimethylthiazol-2-yl)-2,5-diphenyltetrazolium bromide (MTT) and neutral red uptake tests, respectively. The cells were treated with BPA at 1 nM, 10 nM, 100 nM, 1 μM, and 10 μM concentrations for 24 h and at 100 nM concentration for 24, 48, 72, 96 h, and 6 days. Decreased global 5-methylcytosine levels were observed after 48, 72, 96 h, and 6 days at the concentration of 100 nM BPA. Changes in CpG promoter DNA methylation were detected in the genes of *Rassf1a* and *c-myc* in BPA-treated NRK-52E cells. Expression levels of *Rassf1a* and *c-myc* changed in response to BPA at the high concentrations after 24 h treatment, whereas 100 nM exposure to BPA altered gene expression after 48, 72, and 96 h.

Conclusion: These results indicate that changes in global and gene-specific DNA methylation may play an important role in the mechanism of BPA toxicity in kidney cells.

Key words: Bisphenol A, DNA methylation, *Rassf1a*, *c-myc*, NRK-52E cells

ÖZ

Amaç: Bisfenol A (BPA), polikarbonat üretiminde kullanılan sentetik bir monomerdir ve çevresel bir kontaminant olup endokrin bozucu özelliklere sahiptir. BPA'nın plastik taşıyıcılardan salınması yüksek oranda maruziyete sebep olabilir, bu durum insan ve çevre sağlığı üzerinde yüksek oranda riske sebep olabilir.

Gereç ve Yöntemler: Bu çalışmada, BPA'nın sıçan böbrek epitel hücrelerinde (NRK-52E) global DNA metilasyonu, *Rassf1a* ve *c-myc* genlerinin CpG promotör bölge DNA metilasyonu ve gen ekspresyonu üzerinde oluşturabileceği değişikliklerin araştırıldı.

Bulgular: BPA'nın IC_{50} değeri NRK-52E hücrelerinde 3-(4,5-dimethylthiazol-2-yl)-2,5-difenil tetrazolium bromid ve nötral kırmızı alım testi ile sırasıyla 105 μM ve 88 μM olarak bulundu. Hücreler 1 nM, 10 nM, 100 nM, 1 μM ve 10 μM konsantrasyonlarda BPA'ya 24 saat boyunca ve 100 nM konsantrasyonda BPA'ya 24, 48, 72, 96 saat ve 6 gün boyunca maruz bırakıldı. 48, 72, 96 saat ve 6 gün sonra 100 nM BPA konsantrasyonunda global 5-metilsitozin seviyelerinde azalma gözlendi. BPA'ya maruz bırakılmış NRK-52E hücrelerinde *Rassf1a* ve *c-myc* genlerinin CpG promotör bölgelerinde metilasyonda değişiklikler tespit edildi. *Rassf1a* ve *c-myc* genlerinin ekspresyon seviyeleri yüksek konsantrasyonlarda 24 saat BPA maruziyet ile ve 100 nM konsantrasyonda 48, 72 ve 96 saat BPA maruziyetleri ile değişiklik gösterdi.

Sonuç: Bu sonuçlar, böbrek hücrelerinde global ve gene özgü DNA metilasyonundaki değişikliklerin BPA'nın toksisite mekanizmasında önemli bir rol oynayabileceğini göstermektedir.

Anahtar kelimeler: Bisfenol A, DNA metilasyonu, *Rassf1a*, *c-myc*, NRK-52E hücreleri

*Correspondence: E-mail: stopuz@istanbul.edu.tr, Phone: +90 212 440 00 00 ORCID-ID: orcid.org/0000-0002-1662-2504
Received: 09.01.2019, Accepted: 21.02.2019

INTRODUCTION

Bisphenol A [(BPA); 4,4'-dihydroxy-2,2-diphenyl propane] is an organic compound used in the production of polycarbonate. BPA is found in the composition of many products such as medical supplies, the inner coating of food and beverage packaging, the coating of electrical materials, and protective clothing.[1] It was determined that BPA can pass into food and beverages from many materials in very small amounts. Even in normal conditions, BPA is indicated to be released from plastic carriers. Various studies have shown that BPA affects enzyme activities, metabolism, and gene activity in hormone receptors in target tissues, and deteriorates the endocrine system due to estrogenic and androgenic effects.[2] It was underlined that BPA may play a role in the etiology of many diseases such as diabetes, obesity, reproductive disorders, cardiovascular disorders, congenital anomalies, renal disorders, and breast cancer.[3]

Many studies have been performed to evaluate the toxicity mechanisms of BPA, especially epigenetic mechanisms in various systems.[3,4] Therefore, epigenetic events such as DNA methylation may play an important role in the toxicity of BPA as an endocrine disrupting chemical.[2,3,5,6] In the present study, we aimed to examine the effects of BPA on global and gene specific DNA methylation as epigenetic mechanisms in BPA toxicity in rat kidney epithelial cells (NRK-52E) cells. The results obtained are expected to contribute to a better understanding of the key molecular mechanisms of BPA toxicity.

MATERIALS AND METHODS

Chemicals

Stock solution (100 mmol/L) of BPA (99% purity, Sigma-Aldrich, St Louis, MO, USA) was prepared by dissolving it in dimethyl sulfoxide [(DMSO), Wisent Bioproducts, Saint-Jean-Baptiste, QC, Canada] and kept at -20 °C. Cell culture supplements were obtained from Wisent Bioproducts (Saint-Jean-Baptiste, QC, Canada) and sterile plastic materials were obtained from Greiner (Frickenhausen, Germany).

Cell culture and Bisphenol A treatment

The rat kidney proximal tubular epithelial cell line (NRK-52E) was used from the American type culture collection and cultured in Dulbecco's Modified Eagle's Medium/Ham's Nutrient Mixture F-12, supplemented with 10% fetal bovine serum and penicillin-streptomycin (100 U-100 µg/mL) under standard cell culture conditions (37 °C, humidified atmosphere with 5% CO_2). Subculturing was performed every 2-3 days (70-80% confluence) using trypsinization. Cells were counted by a LUNA automated cell counter (Logos Biosystems, Annandale, VA, USA).

For the cytotoxicity assays, cells ($1x10^4$ in 200 µL of medium in a 96 well plate) were exposed to BPA in the concentrations range of 31.25-1000 µM and DMSO (1%) as solvent control for 24 h.

For the DNA methylation and gene expression analysis, cells ($1.5x10^6$ in 10 mL of medium in a 25-cm^2 culture flask) were exposed to BPA at the concentrations of 1 nM, 10 nM, 100 nM, 1 µM, and 10 µM and DMSO (1%) as solvent control for 24 h, and BPA at the concentration of 100 nM and DMSO (1%) as control for 48 h, 72 h, 96 h, and 6 days. For all concentrations, it was tested in triplicate. Treated cells were performed for DNA isolation by High Pure PCR Template Preparation Kit (Roche Applied Science, Mannheim, Germany), and for total RNA isolation by High Pure RNA Isolation Kit (Roche Applied Science, Mannheim, Germany) according to the procedure provided by the manufacturer.

Cytotoxicity

After 24 h of BPA treatment, cytotoxicity tests were performed using 3-(4,5-dimethylthiazol-2-yl)-2,5-diphenyltetrazolium bromide (MTT) and neutral red uptake (NRU) tests. Briefly, in the MTT test, 20 µL of MTT solution was added to each well followed by gentle mixing, and then the plate was incubated for 3 h at 37 °C, 5% CO_2. After the incubation, 100 µL of DMSO (100%) was added to each well followed by gentle mixing again. The resulting purple solution was spectrophotometrically measured at 560 nm with a reference wavelength of 670 nm using a microplate spectrophotometer system (Biotek-Epoch, Winooski, VT, USA). In the NRU test, in a 96 well plate cells were washed with 150 µL of Phosphate buffered saline (PBS) solution and 100 µL of neutral red vital dye was added to the cells; then the plate was incubated for 3 h at 37 °C, 5% CO_2. The cells were washed with PBS and then 100 µL of neutral red vital dye dissolution was added to each well followed by gentle mixing. Then the optical density of the plate was read at 540 nm using a microplate spectrophotometer system (Biotek-Epoch, Winooski, VT, USA). The cytotoxicity results were expressed as 50% of inhibitory concentration (IC_{50}) of the BPA that caused 50% inhibition of the enzyme activity in the cells. Based on our cytotoxicity results and previous studies in various cells,[7-12] in the present study we chose BPA concentrations of 1 nM, 10 nM, 100 nM, 1 µM, and 10 µM for 24 h treatment and a concentration of 100 nM for 24, 48, 72, 96 h, and 6 day treatments for the analysis of DNA methylation and gene expression.

Global DNA methylation

Levels of global 5-methylcytosine (5-mC) were determined by using a 5-mC DNA ELISA kit (Zymo Research, Irvine, CA, USA) according to the instructions provided by the manufacturer. For this, 100 ng of each DNA was denatured at 98 °C for 5 min in a thermal cycler. The denatured DNA was added to the wells and incubated at 37 °C for 1 h. Then samples were incubated with antibody mix consisting of anti-5-mC and secondary antibody. After the washing steps, HRP developer was added to each well and absorbance was measured at 405 nm using a microplate spectrophotometer system (Biotek-Epoch, Winooski, VT, USA). The methylation ratio of DNA samples was calculated as a percentage using calibration standard curves by preparing mixtures of negative control (100 ng/µL) and positive control (100 ng/µL) standards.

Gene-specific DNA methylation

Determination of DNA methylation on CpG islands in promoter regions of *Rassf1a* and *c-myc* genes was performed using

methylation specific (MSP) PCR. In our previous study we described the study protocol in detail.[13] In MSP, genomic DNA is modified by treatment with sodium bisulfite, which converts all methylated cytosines to uracil and then to thymidine during the subsequent PCR step.[14,15] Bisulfite DNA modification was performed by using an EZ DNA Methylation-Gold Kit (Zymo Research, Irvine, CA, USA) according to the manual's instructions. Methylated and unmethylated primer pairs were used to amplify each region of interest. The primer sequences are listed in Table 1.[16,17] After the PCR reaction, MSP products were analyzed by agarose gel electrophoresis, stained with ethidium bromide, and visualized under ultraviolet light (Quantum ST4-Vilber Lourmat, Torcy, France).

Gene expression

First-strand cDNA synthesis was performed using 1000 ng of total RNA by using a Transcriptor First Strand cDNA Synthesis kit (Roche Applied Science, Mannheim, Germany) with a mixture of anchored-oligo (dT) and random hexamer primers according to the manual's instructions. Expression analysis of *Rassf1a* and *c-myc* genes was performed by using real-time quantitative PCR employing Light Cycler 480 Probes Master with Real Time ready Custom Single Assays (Universal ProbeLibrary Probes, Roche Applied Science, Mannheim, Germany) containing target specific primers for *Rassf1a* and *c-myc* according to our previous study.[9] Cycle threshold (Ct) values of *Rassf1a* and *c-myc* and the reference gene (β-*actin*) were determined and evaluation of the relative expression was performed by comparative Ct method.

Statistical analysis

Global methylation levels and cytotoxicity results were represented as mean ± standard deviation. Statistical analysis was performed by ANOVA (Tukey's multiple comparison procedure) using SPSS version 21.0 for Windows (IBM Analytics, New York, NY, USA). P values <0.05 and <0.001 were considered statistically significant.

RESULTS AND DISCUSSION

BPA has been frequently exposed in daily life and has been shown to be harmful in living organisms due to its endocrine disrupting properties.[2,18-20] Various studies have revealed that BPA affects enzyme activity and metabolism in various tissues, causing change in the number of hormone receptors and hormone receptor gene activity in target tissues, and deteriorates the endocrine system.[2] It has been revealed that BPA might induce cancer development and various studies have explained its relations with several cancer types.[21] BPA can induce epigenetic changes in early life in humans and may affect several cell signaling pathways via epigenetic mechanisms.[22] It has been reported in recent studies that epigenetic alterations could be useful biomarkers for the toxicity evaluation of endocrine disrupting chemicals.[6-9,23-25] Therefore, in the present study, we aimed to investigate the effects of dose-dependent BPA exposure for 24 h and time-dependent 100 nM concentration of BPA exposure on the alteration of global and gene specific DNA methylation and gene expression in NRK-52E cells. We chose NRK-52E cells with the characteristic properties of proximal tubule epithelial cells targeted by nephrotoxic agents to show the epigenetic effects of BPA in kidney cells.

Cell viability was determined by MTT and NRU assays in the BPA treated NRK-52E cells. The relationship between the exposure concentrations of BPA treated NRK-52E cells and % reduction in cell viability is shown in Figure 1. IC_{50} values of BPA were determined as 105 μM and 88 μM in NRK-52E cells by the MTT and NRU tests, respectively. Decreased global DNA methylation at a concentration of 100 nM BPA was observed in the range of 19.76%-25.30% after 48, 72, 96 h, and 6 days (Figure 2). However, there was no change in the global DNA methylation at the concentrations of 1 nM-10 μM BPA for 24 h exposure (data not shown). Accordingly, in our previous studies, global levels of 5-mC% decreased after 1 and 10 μM BPA treatment for 96 h in HepG2 cells[8] and 0.1 and 1 μM BPA treatments for 48 and 96 h in MCF-7 cells.[7] Conversely, in another previous study, we observed no global methylation changes after 48 h exposure

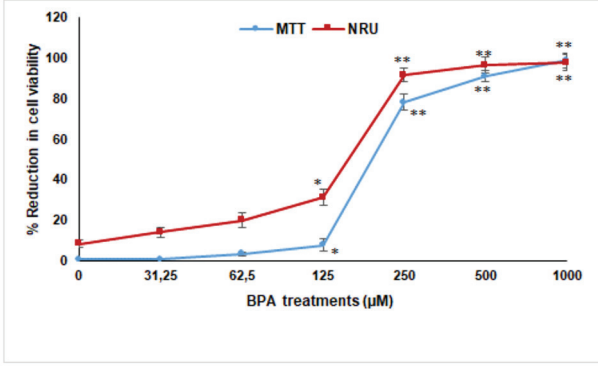

Figure 1. Effects of BPA (0-1000 μM) on cytotoxicity by MTT and NR in NRK-52E cells after 24 h exposure. Data are presented as mean ± SD. Statistical analysis was performed by ANOVA + dunnett post hoc test. Statistically significant changes are indicated by *p<0.05 and **p<0.001

BPA: Bisphenol A, MTT: 3-(4,5-dimethylthiazol-2-yl)-2,5-diphenyltetrazolium bromide, SD: Standard deviation, NRU: Neutral red uptake

Table 1. Primer sets for MSP analysis

Primer set	Forward primer 5' ® 3'	Reverse primer 3' ® 5'	Annealing temp (°C)	Reference
c-myc - M	ttt gtt ttt tcg att tta gag aga c	tta tcc tac gta tat taa tca ccg c	55	13,16
c-myc - U	tgt ttt ttt gat ttt aga gag atg a	ctt atc cta cat ata tta atc acc aca	55	
Rassf1a - M	ttt ttt tcg gtt ttt ttt cgt c	caa cta ata aat tcg taa cga acg taa caa cta	64	17
Rassf1a - U	tgt ttt ttt tgg ttt ttt ttt gtt	ata aat tca taa caa aca	59	

MSP: Methylation specific, M: Methylated, U: Unmethylated

to BPA, whereas significant increases were seen in the global level of 5-mC% (1.3 fold) after 10 µM of BPA for 96 h exposure in neuroblastoma (SHSY-5Y) cells.[9] According to the results of the present study, BPA decreased global DNA methylation in rat liver,[26] human fetal liver samples,[27] and porcine oocyte culture at 250 µM concentration.[28]

Rassf1 is a tumor suppressor gene that has a significant role in cancer and it is thought that its regulation was associated with CpG island promoter DNA methylation. *c-myc*, a proto-oncogene, codes a transcription factor and controls cell proliferation. It has been shown that increases in the expression of the *c-myc* gene were associated with hypomethylation, which could be related to cell proliferation in liver and renal cancers.[29-31] A representative profile of MSP for the *c-myc* gene in BPA treated NRK-52E cells is shown in Figure 3. Increases in promoter methylation were detected in *Rassf1* and *c-myc* genes at the

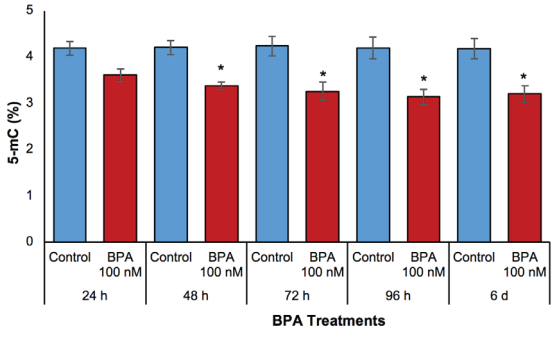

Figure 2. Effects of BPA (100 nM) in the levels of 5-mC% in NRK-52E cells after 24, 48, 72, 96 h, and 6 days exposure. Data are presented as mean ± SD. Genomic DNA was extracted, then 5-mC% levels were detected using the ELISA kit. Statistical analysis was performed by ANOVA + dunnett post hoc test. Statistically significant changes are indicated by *p<0.05

BPA: Bisphenol A, SD: Standard deviation

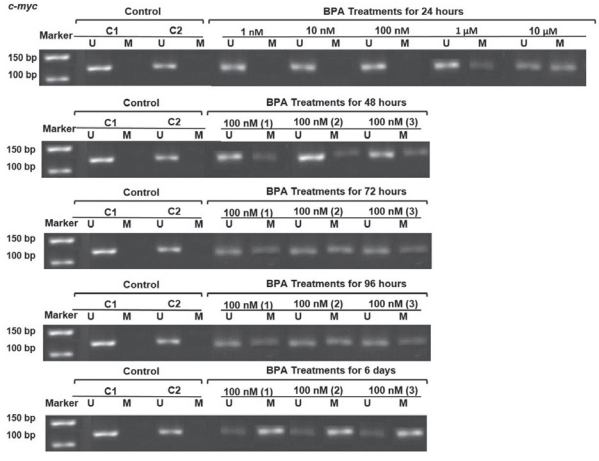

Figure 3. Effects of BPA on methylation status of *c-myc* in NRK-52E cells. A representative sample of NRK-52E cells treated with BPA at the concentrations of 1 nM, 10 nM, 100 nM, 1 µM, and 10 µM for 24 h and concentration of 100 nM for 24, 48, 72, 96 h, and 6 days is shown. Methylation was determined by bisulfite modification of the genomic DNA and MSP using primers for the U or M promoter sequence. C1 and C2=DMSO (1%) as control instead of BPA treatment

U: Unmethylated, M: Methylated, BPA: Bisphenol A, MSP: Methylation specific, DMSO: Dimethyl sulfoxide, C1: Contol 1, C2: Control 2

BPA concentrations of 1 and 10 µM in NRK-52E cells over 24 h while no methylation was detected in control samples by using MSP following bisulfide conversion. In addition, BPA caused increases in promoter methylation of *Rassf1* and *c-myc* genes at the concentration of 100 nM in a time-dependent manner (48 h, 72 h, 96 h, and 6 days) in NRK-52E cells. Expression levels of *Rassf1a* and *c-myc* genes are shown in Figures 4 and 5. In response to BPA, expression of *Rassf1a* and *c-myc* was decreased at 1 µM for 24 h (26.66% and 37.3%, respectively) and 10 µM for 24 h (25.11% and 22.24%, respectively). Moreover, 100 nM exposure of BPA caused decreases in expression of the *Rassf1a* and *c-myc* genes after 48, 72, and 96 h BPA treatment with regard to control samples, and there was a nonsignificant increase for 6-day BPA treatment (Figure 5). According to the results, the decrease in gene expression of *Rassf1a* and *c-myc* was correlated with DNA methylation results, which showed an increase in CpG promoter methylation of the genes. In our previous study in HepG2 cells, no change as observed in promoter methylation or gene expression of the *Rassf1a* gene after BPA exposure.[8]

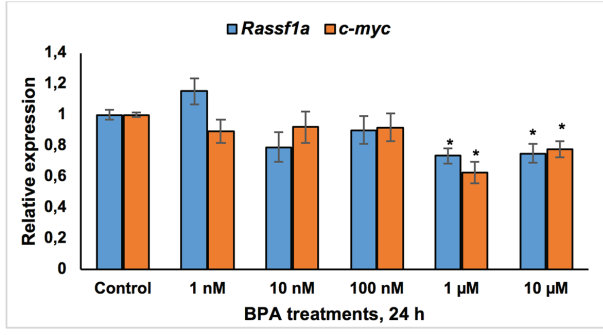

4. Effects of BPA (1 nM, 10 nM, 100 nM, 1 µM, and 10 µM) on expression of *Rassf1a* and *c-myc* genes by real-time PCR in NRK-52E cells after 24 h exposure. PCR reaction was done as described in the Materials and methods section. The real-time PCR results were standardized against β-actin and the relative ratios were calculated

*p<0.05, BPA: Bisphenol A

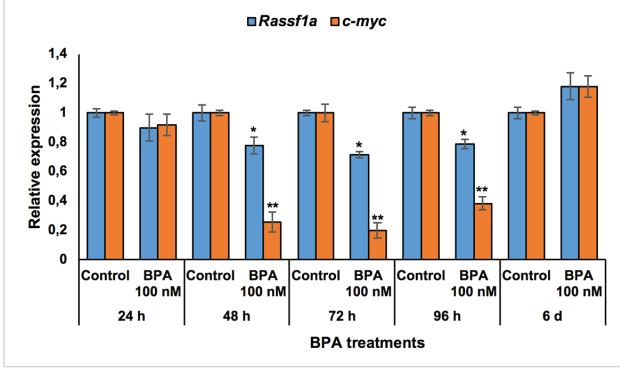

Figure 5. Effects of BPA (100 nM) on expression of Rassf1a and c-myc genes by real-time PCR in NRK-52E cells after 24, 48, 72, 96 h, and 6 days exposure. PCR reaction was done as described in the Materials and methods section. The real-time PCR results were standardized against β-actin, and the relative ratios were calculated

*p<0.05, **p<0.001, BPA: Bisphenol A

CONCLUSION

Based on the findings of the present study, BPA caused alterations in expression and methylation in the promoter region of the *Rassf1a* and *c-myc* genes associated with cancer related pathways in NRK-52E cells after 24-96 h exposure periods. It has been suggested that alterations in DNA methylation in the *Rassf1a* and *c-myc* genes might be key regulators in the toxicity mechanisms of BPA. Further studies on the expression of chromatin modifying enzymes, DNA methylation, and global and gene-specific histone modifications after BPA exposure in cell cultures are needed to better understand alterations in epigenetic mechanisms in BPA-induced toxicity.

ACKNOWLEDGEMENTS

This study was supported partly by Scientific Research Projects Coordination Unit of İstanbul University (Project number: 40333).

Conflicts of interest: No conflict of interest was declared by the authors. The authors alone are responsible for the content and writing of this article.

REFERENCES

1. Olea N, Pulgar R, Perez P, Olea-Serrano F, Rivas A, Novillo-Fertrell A, Pedraza V, Soto AM, Sonnenschein C. Estrogenicity of resin-based composites and sealants used in dentistry. Environ. Health Perspect. 1996;104:298-305.
2. EFSA (European Food Safety Authority). Scientific opinion of the panel on food additives, flavourings, processing aids and materials in contact with food (AFC) on a request from the commission on the toxicokinetics of bisphenol A. The EFSA Journal. 2008;759:1-10.
3. Rezg R, El-Fazaa S, Gharbi N, Mornagui B. Bisphenol A and human chronic diseases: current evidences, possible mechanisms, and future perspectives. Environ Int. 2014;64:83-90.
4. Kundakovic M, Champagne F.A. Epigenetic perspective on the developmental effects of bisphenol A. Brain, Behavior, and Immunity. 2011;25:1084-1093.
5. Fleisch AF, Wright R, Baccarelli A. Environmental epigenetics: a role in endocrine disease? J Mol Endocrinolog. 2012;12-0066.
6. Greally JM, Jacobs MN. *In vitro* and *in vivo* testing methods of epigenomic endpoints for evaluating endocrine disruptors. ALTEX. 2013;30:445-471.
7. Senyildiz M, Özden S. Alteration in global DNA methylation after bisphenol A exposure in MCF-7 cells. J Fac Pharm Istanbul. 2015;45:153-164.
8. Senyildiz M, Karaman EF, Baş SS, Pirinççi PA, Özden S. Alteration on global and gene-spesific DNA methylation and global histone modifications in HepG2 cells in response to BPA. J Fac Pharm Istanbul. 2016;46:97-114.
9. Senyildiz M, Karaman EF, Sancar Baş S, Arda Pirincci P, Ozden S. Effects of BPA on global DNA methylation and global histone 3 lysine modifications in SH-SY5Y cells: an epigenetic mechanism linking the regulation of chromatin modifiying genes. Toxicology in Vitro. 2017;44:313-321.
10. Nakagawa Y, Tayama S. Metabolism and cytotoxicity of bisphenol A and other bisphenols in isolated rat hepatocytes. Arch Toxicol. 2000;74:99-105.
11. Terasaka H, Kadoma Y, Sakagami H, Fujisawa S. Cytotoxicity and apoptosis inducing activity of bisphenol A and hydroquinone in HL-60 cells. Anticancer Res. 2005;25:2241-2247.
12. Aghajanpour-Mir SM, Zabihi E, Keyhani E, Akhavan-Niaki H, Bagherizadeh I, Biglari S, Behjati F. The genotoxic and cytotoxic effects of bisphenol-A (BPA) in MCF-7 cell line and amniocytes. Int J Mol Cell Med. 2016;5:19-29.
13. Demirel G, Alpertunga B, Ozden S. Role of fumonisin B1 on DNA methylation changes in rat kidney and liver cells. Pharm Biol. 2015;53:1302-1310.
14. Frommer M, McDonald LE, Millar DS, Collis CM, Watt F, Grigg GW, Molloy PL, Paul CL. A genomic sequencing protocol that yields a positive display of 5-methylcytosine residues in individual DNA strands. Proc Natl Acad Sci USA. 1992;89:1827-1831.
15. Herman JG, Graff JR, Myöhänen S, Nelkin BD, Baylin SB. Methylation-specific PCR: a novel PCR assay for methylation status of CpG islands. Proc Natl Acad Sci USA. 1996;93:9821-9826.
16. Li LC, Dahiya R. MethPrimer: Designing primers for methylation PCRs. Bioinformatics. 2002;18:1427-1431.
17. Niwa T, Yamashita S, Tsukamoto T, Kuramoto T, Nomoto T, Wakazono K, Fujita H, Matsushima T, Tatematsu M, Sugimura T, Ushijima T. Whole-genome analyses of loss of heterozygosity and methylation analysis of four tumor-suppressor genes in N-methyl-N0-nitro-N-nitrosoguanidine-induced rat stomach carcinomas. Cancer Sci. 2015;96:409-413.
18. LeBaron MJ, Rasoulpour RJ, Klapacz J, Ellis-Hutchings RG, Hollnagel HM, Gollapudi BB. Epigenetics and chemical safety assessment. Mutat Res. 2010;705:83-95.
19. Wolstenholme JT, Rissman EF, Connelly JJ. The role of Bisphenol A in shaping the brain, epigenome and behavior. Horm Behav. 2011;59:296-305.
20. Rochester JR. Bisphenol A and human health: a review of the literature. Reprod Toxicol. 2013;42:132-155.
21. Gao H, Yang BJ, Li N, Feng LM, Shi XY, Zhao WH, Liu SJ. Bisphenol A and hormone-associated cancers: current progress and perspectives. Medicine. 2015;94:e211.
22. Singh S, Li SS. Epigenetic effects of environmental chemicals bisphenol A and phthalates. Int J Mol Sci. 2012;13:10143-10153.
23. Casati L, Sendra R, Sibilia V, Celotti F. Endocrine disrupters: the new players able to affect the epigenome. Front Cell Dev Biol. 2015;3:37.
24. Maqbool F, Mostafalou S, Bahadar H, Abdollahi M. Review of endocrine disorders associated with environmental toxicants and possible involved mechanisms. Life Sci. 2016;145:265-273.
25. Zhang X, Ho SM. Epigenetics meets endocrinology. J Mol Endocrinol. 2011;46:R11-R32.
26. Ma Y, Xia W, Wang DQ, Wan YJ, Xu B, Chen X, Li YY, Xu SQ. Hepatic DNA methylation modifications in early development of rats resulting from perinatal BPA exposure contribute to insulin resistance in adulthood. Diabetologia. 2013;56:2059-2067.
27. Faulk C, Kim JH, Jones TR, McEachin RC, Nahar MS, Dolinoy DC, Sartor MA. Bisphenol A-associated alterations in genome-wide DNA methylation and gene expression patterns reveal sequence-dependent

and non-monotonic effects in human fetal liver. Environ Epigenet. 2015;1:dvv006.

28. Wang T, Han J, Duan X, Xiong B, Cui XS, Kim NH, Liu HL, Sun SC. The toxic effects and possible mechanisms of bisphenol A on oocyte maturation of porcine in vitro. Oncotarget. 2016;7:32554-32565.

29. Du YP, Peng JS, Sun A, Tang ZH, Ling WH, Zhu HL. Assessment of the effect of betaine on *p16* and *c-myc* DNA methylation and mRNA expression in a chemical induced rat liver cancer model. BMC Cancer. 2009;9:261.

30. Tao L, Yang S, Xie M, Kramer PM, Pereira MA. Hypomethylation and overexpression of *c-jun* and *c-myc* protooncogenes and increased DNA methyltransferase activity in dichloroacetic and trichloroacetic acid-promoted mouse liver tumors. Cancer Lett. 2000;158:185-193.

31. Tao L, Wang W, Li L, Kramer PK, Pereira MA. DNA hypomethylation induced by drinking water disinfection by-products in mouse and rat kidney. Toxicol Sci. 2005;87:344-352.

Turk J Pharm Sci 2020;17(3):343-348
DOI: 10.4274/tjps.galenos.2020.38801

ORIGINAL ARTICLE

Phytochemical Constituents, Antioxidant Activity, and Toxicity Assessment of the Seed of *Spondias mombin* L. (Anacardiaceae)

Spondias mombin L. (Anacardiaceae) Tohumunun Fitokimyasal Bileşenleri, Antioksidan Aktivitesi ve Toksisite Değerlendirmesi

Oyindamola Olajumoke ABIODUN*, Mesoma Esther NNORUKA, Rasidat Olufunke TIJANI

University of Ibadan College of Medicine, Department of Pharmacology and Therapeutics, Ibadan, Nigeria

ABSTRACT

Objectives: Increased generation of free radicals exceeding the antioxidant capacity of the host is deleterious. Thus new, potent, and safe antioxidants will be a valuable addition to the limited antioxidant arsenals available. Therefore, the antioxidant activity, cytotoxicity potential, and phytochemical constituents of the methanol extract of *Spondias mombin* seed (MESSM) were investigated.

Materials and Methods: 2,2-diphenyl-1-picrylhydrazyl (DPPH), nitric oxide (NO), and hydrogen peroxide (H_2O_2) were the antioxidant assays used. The cytotoxicity of MESSM was evaluated against a rhabdomyosarcoma (RD) cell line in a 3-(4,5-dimethylthiazol-2-yl)-2,5-diphenyl tetrazolium bromide based assay. The phytochemical constituents of MESSM were identified using gas chromatography-mass spectrometry.

Results: MESSM produced better antioxidant activity in the DPPH (IC_{50}=58.64±1.49 µg/mL) and H_2O_2 (IC_{50}=44.03±5.57 µg/mL) assays than in the NO (IC_{50}=494.55±12.68 µg/mL, p<0.0001) assay. Moreover, MESSM was nontoxic (CC_{50}=139.6±0.54 µg/mL) in comparison to cyclophosphamide (CC_{50}=0.97±0.03 µg/mL) against the RD cell line. The major compounds in MESSM were dodecanoic acid (22.48%), tetradecanoic acid (17.95%), n-hexadecanoic acid (15.35%), capsaicin (12.11%), and dihydrocapsaicin (5.23%).

Conclusion: The seed extract of *Spondias mombin* contains nontoxic antioxidant compounds that could be explored in the pharmaceutical and cosmetics industries for the development of antioxidant agents.

Key words: Seed of *Spondias mombin*, antioxidants, cytotoxicity, GC-MS

ÖZ

Amaç: Konağın antioksidan kapasitesini aşan serbest radikallerin artması zararlıdır. Bu nedenle, yeni, güçlü ve güvenli antioksidanlar, mevcut sınırlı antioksidanlara değerli katkı sağlayacaktır. Bu nedenle, *Spondias mombin* tohumunun (MESSM) metanol ekstraktının antioksidan aktivitesi, sitotoksisite potansiyeli ve fitokimyasal bileşenleri araştırıldı.

Gereç ve Yöntemler: 2,2-difenil-1-pikrilhidrazil (DPPH), nitrik oksit (NO) ve hidrojen peroksit (H_2O_2) kullanılan antioksidan deneylerdi. MESSM'nin sitotoksisitesi, 3-(4,5- dimetil tiyazol-2-yl)-2,5- difenil tetrazolium bromür ile bir rabdomiyosarkom (RD) hücre hattında değerlendirildi. MESSM'nin fitokimyasal bileşenleri gaz kromatografisi-kütle spektrometresi kullanılarak tanımlandı.

Bulgular: MESSM, DPPH (IC_{50}=58,64±1,49 µg/mL) ve H_2O_2 (IC_{50}=44,03±5,57 µg/mL) deneylerinde NO (IC_{50}=494,55±12,68 µg/mL, p<0,0001) deneyinden daha iyi antioksidan aktivite gösterdi. Ayrıca, MESSM'in RD hücre hattına karşı siklofosfamide (CC_{50}=0,97±0,03 µg/mL) kıyasla toksik olmadığı (CC_{50}=139,6±0,54 µg/mL) bulundu. MESSM'deki ana bileşiklerin, dodekanoik asit (%22,48), tetradekanoik asit (%17,95), n-heksadekanoik asit (%15,35), kapsaisin (% 12,11) ve dihidrokapsaisin (% 5,23) olduğu bulundu.

Sonuç: *Spondias mombin*'in tohum ekstresinin, ilaç ve kozmetik endüstrilerinde antioksidan ajanların geliştirilmesi için araştırılabilecek toksik olmayan antioksidan bileşikler içerdiği sonucuna varıldı.

Anahtar kelimeler: *Spondias mombin* tohumu, antioksidanlar, sitotoksisite, GC-MS

*Correspondence: **E-mail:** oyindamolaabiodun1@gmail.com, **Phone:** +234 703 096 4774 **ORCID-ID:** orcid.org/0000-0002-6629-3016
Received: 25.04.2019, **Accepted:** 11.05.2020

INTRODUCTION

Free radicals such as reactive oxygen species (ROS) in the form of superoxide anion (O_2), hydroxyl radical, and hydrogen peroxide (H_2O_2), and reactive nitrogen species (NOS) in the form of nitric oxide (NO) radical are by-products of the human body's metabolism and can also be generated from exogenous stimuli.[1] A physiological amount of ROS is considered to function in signal delivering while an excessive amount damages DNA, proteins, and lipids, which can induce cell death, implicated in the pathogenesis of cancer, ageing,[2] ophthalmological diseases,[3] cardiovascular diseases,[4] and many general neurodegenerative pathologies like Alzheimer's disease,[5] Parkinson's disease,[6] and prion disease.[7]

Excessive ROS are neutralized by a controlled and balanced complex web of antioxidant defenses in the body.[8] Antioxidants help to minimize the effect of free radicals on biomolecules by scavenging them. However, if production of free radicals overwhelms the biological antioxidants, there will be a need for introduction of an external source of antioxidants. An external source of antioxidants offers a promising way to prevent the deleterious effect of excessive exposure to ROS.[8] It has been reported by previous studies that phytochemicals such as flavonoids and polyphenols can help in preventing the development of chronic diseases.[9] Moreover, the use of extracts from pomegranate, green tea, grape seed, and mushrooms as antioxidants in skin care products to prevent the clinical signs of photoaging is on the increase.[2,10] Thus, the interest in naturally occurring antioxidants in foods, cosmetics, and pharmaceutical products has significantly increased. Prolonged use of antioxidants necessitates the need for safe and effective antioxidants that the natural agents symbolize, unlike the synthetic antioxidants that have been associated with toxicity[11] and carcinogenic effects[12] after prolonged use.

There is a need to search for more antioxidants of natural origin that can be added to the limited arsenals of antioxidants available. *Spondias mombin* (*S. mombin*) is a fructiferous tree that is commonly found in Nigeria, Brazil, Peru, southern Mexico, Sierra Leone, Equatorial Guinea and Côte d'Ivoire.[13] In Nigeria, it is commonly known as *iyeye* in the Yoruba ethnomedicine. Antidiarrheal, antimicrobial, diuretic, febrifuge, and emetic activities of the fruit, leaf, or bark of *S. mombin* leaf have been reported.[14-18] The flower, leaf, or bark are used for wound healing and to treat stomachache and various inflammatory conditions.[19] Antioxidant activity of the leaf and fruit has been reported.[20,21] Despite the information on the leaf, fruit, flower, and stem bark of *S. mombin,* little is known about the usefulness of its seed, which is considered a waste product. Therefore, we report the antioxidant, cytotoxicity, and phytochemical composition of the seed of *S. mombin*.

MATERIALS AND METHODS

Reagents

Sodium bicarbonate, sodium hydroxide, 2,2-diphenyl-1-picryl-hydrazyl (DPPH), rutin, Folin-Ciocalteu reagent, rutin, gallic acid, ascorbic acid, sodium nitroprusside, sulfanilamide, N-naphthyl-ethylenediamine dihydrochloride, and 3-(4,5-dimethylthiazol-2-yl)-2,5-diphenyl tetrazolium bromide (MTT) were obtained from Sigma Aldrich Co., St. Louis, MO, USA.

Plant collection

The fresh fruit of *S. mombin* was collected behind the Pharmacology and Therapeutics building, University of Ibadan on 20 September 2017. Identification of the plant was done by Mr. D. P. Esimekhuai of the Botany Department, University of Ibadan (UIH-22764).

Plant extraction

The fleshy part of the *S. mombin* fruit was removed completely; thereafter the seed was oven dried at 40 °C and pulverized. The maceration method of extraction was employed by soaking 203 g of *S. mombin* seed in a mixture of methanol:water (70:30) for 72 h. The solvent was removed at reduced pressure and temperature in order to obtain the extract, which was kept at 4 °C.

Total phenolic content (TPC)

The determination of the TPC of methanol extract of *Spondias mombin* (MESSM) was carried out by following the procedures of a previously reported method.[22] Briefly, 0.1 mL of MESSM (1 mg/mL) and 0.1 mL of Folin-Ciocalteu phenol were mixed and left for 5 min. Thereafter, 1 mL of 7% Na_2CO_3 and 1.3 mL of distilled water were added. The mixture was allowed to stand for 90 min at 29 °C. Optical density (OD) was obtained at 750 nm. The TPC was estimated in triplicate and expressed as milligrams of gallic acid equivalents (GAE) per gram of the dried seed of *S. mombin*.

Total flavonoid content (TFC)

The determination of MESSM TFC was done according to a previously reported method.[23] First, 0.3 mL of MESSM (1 mg/mL), 0.15 mL of $AlCl_3.6H_2O$ (0.3 M), 0.15 mL of $NaNO_2$ (0.5 M), and 3.4 mL of methanol (30%) were mixed. After 5 min, the reaction was stopped with 1 mL of NaOH (1 M). The absorbance was obtained at 506 nm. The TFC was estimated in triplicate and expressed as milligrams of rutin equivalents (RE) per gram of the dried seed of *S. mombin*.

Antioxidant assays of MESSM

DPPH assay

A modified version of the method described by Silva et al.[24] was followed. Briefly, gradient concentrations of MESSM (6.25-400 µg/mL) or the standard drug ascorbic acid (0.25-16 µg/mL) were prepared in ethanol and incubated with 0.04 mg/mL DPPH (1:1.5 vol/vol) for 30 min at 29 °C in the dark. OD was obtained at 517 nm and expressed as percentage of the control.

Hydrogen peroxide assay

A previously reported method was used.[25] H_2O_2 free radical was generated from H_2O_2 solution. Briefly, 2 mM of freshly prepared H_2O_2 (6:1 v/v) was mixed with gradient concentrations of MESSM (6.25 to 400 µg/mL) or ascorbic acid (2.5-160 µg/mL). The mixture was left in the dark for 10 min at 29 °C. Thereafter, absorbance was recorded at 230 nm.

Nitric oxide assay

Briefly, sodium nitroprusside in aqueous solution (40 mM) was added to graded concentrations (50-800 µg/mL) of MESSM (1:4 v/v) and kept in the dark at 29 °C for 2 h. Subsequently, the resulting solution was mixed with Griess reagent (1:1 v/v) and kept for 15 min in the dark at 29 °C.[26] Absorbance was obtained at 550 nm and the amount of NO in each of the wells was estimated from the sodium nitrite curve. Ascorbic acid at 2.5-160 µg/mL served as the standard drug.

Data analysis for antioxidant assays

OD values of MESSM or ascorbic acid in all the antioxidant assays were calculated and represented as the percentage of the negative control. Percentage scavenging activity in respect to the negative control was calculated. The 50% inhibitory concentration of MESSM (IC_{50}) was determined using linear regression in a commercial statistical package, Origin®.

Toxicity assessment of MESSM against the rhabdomyosarcoma (RD) cell line

A published method was used.[27] Briefly, a ten-fold serial dilution of 1 mg/mL MESSM was prepared in culture media resulting in 0.01-1000 µg/mL. A confluent monolayer of RD cells cultured in a microtiter plate for 24 h was incubated with the graded concentrations of MESSM or cyclophosphamide (positive control) at 37 °C in 5% CO_2. After 72 h, 25 µL of 2 mg/mL MTT solution was added and further incubation was done for 1.5 h at 37 °C in 5% CO_2. Finally, 125 µL of DMSO was added to the cells and they were agitated for 15 min. Absorbance was recorded at 492 nm and expressed as percentage of the negative control. The 50% cytotoxic concentration (CC_{50}) was determined using nonlinear regression in GraphPad Prism 5®.

Chemical composition of MESSM using gas chromatography-mass spectrometry (GC-MS)

In the identification of the phytochemical constituents of MESSM, GC-MS was used according to a previously described method.[28] The model of the instrument used was an Agilent Technologies 7890 GC system with a 5975 MC detector. The mobile phase was a carrier gas, helium (99.99% purity), and the column was an HP5 MS 30 m in length, 0.320 mm in internal diameter, and 0.25 µm in thickness. To identify the compounds, the retention time and fragmentation pattern were compared to the NIST library database.

Statistical analysis

The antioxidant and cytotoxicity assays were performed in duplicate and repeated in three independent experiments. The IC_{50} or CC_{50} values were expressed as mean ± standard error of mean. The mean IC_{50} or CC_{50} of the MESSM was compared to that of the standard drug using the Mann-Whitney U test and difference was significant at $p<0.05$.

RESULTS

The percentage yield, following the extraction of MESSM in 70% methanol, was 2.72%. The TPC and TFC of MESSM were 239.50±7.9 mg GAE/g sample and 105.3±3.6 mg RE/g sample, respectively. In addition, the IC_{50} of MESSM in the DPPH, hydrogen peroxide, and NO scavenging assays was 58.64±1.49, 44.03±5.57, and 494.55±12.68 µg/mL, respectively (Table 1). Ascorbic acid, the standard drug used in the 3 antioxidants assays, gave an IC_{50} of 4.31±0.26, 10.63±0.31, and 48.74±1.46 µg/mL, respectively. Moreover, MESSM and cyclophosphamide showed CC_{50} of 139.6±0.54 and 0.97±0.03 µg/mL, respectively, on the RD cell line in the cytotoxicity assay. The GC-MS chromatogram of MESSM showed 21 distinct peaks (Figure 1) corresponding to 21 compounds (Table 2). The identified compounds can be grouped into alkanes (42.86%), fatty acids (28.57%), phenol amide (9.52%), phenolic lipids (9.52%), saponin (4.76%), and terpenoids (4.76%). Peaks 3, 7, 12, 18, and 19 represent dodecanoic acid, the most abundant (22.48%), followed by tetradecanoic acid (17.95%), n-hexadecanoic acid (15.35%), capsaicin (12.11%), and dihydrocapsaicin (5.23%). The m/z, fragmentation pattern, and structures of dodecanoic acid, tetradecanoic acid, n-hexadecanoic acid, capsaicin, and dihydrocapsaicin are presented in Figures 2-6.

DISCUSSION

The seed extract of *S. mombin* contains nontoxic antioxidant components. Ascorbic acid, a standard drug, had better activity than the MESSM, a crude extract. Purification of this extract might yield more potent compounds. In the present study, MESSM was 8-11 times less active in scavenging NO free radicals than scavenging the DPPH and H_2O_2 free radicals. In water, plants, the human body, food, microorganisms, and air, H_2O_2 occurs in low quantities.[12] The decomposition of H_2O_2 yields hydroxyl radicals, which can damage DNA and cause lipid peroxidation.[29] Similar reports on the antioxidant activity of other components of *S. mombin* have been published.[20,21,30] However, it appears this is the first report of the antioxidant activity of the seed of *S. mombin*. The seed, a waste product, has not been investigated. In the spirit of turning waste into wealth, this study was performed. In order to rule out the toxicity of MESSM, its cytotoxicity was evaluated. The MESSM was 143 times less toxic than cyclophosphamide, the standard drug against RD cells. This implies MESSM is nontoxic to RD cells.

Table 1. *In vitro* antioxidant activity and toxicity assessment of methanol extract of the seed of *Spondia mombin* (MESSM)

***In vitro* assays**	**IC_{50} (µg/mL)**	
	MESSM	**Standard drugs**
Antioxidant		
DPPH radical scavenging	58.64±1.49*	4.31±0.26[a]
Hydrogen peroxide radical scavenging	44.03±5.57*	10.63±0.31[a]
Nitric oxide radical scavenging	494.55±12.68*	48.74±1.41[a]
Cytotoxicity		
Using rhabdomyosarcoma cell line	139.6±0.54**	0.97±0.03[b]

a: Ascorbic acid, b: Cyclophosphamide, *Ascorbic acid compared with MESSM, **Cyclophosphamide compared with MESSM, $p<0.05$, MESSM: Methanol extract of *Spondias mombin*, DPPH: 2,2-diphenyl-1-picryl-hydrazyl

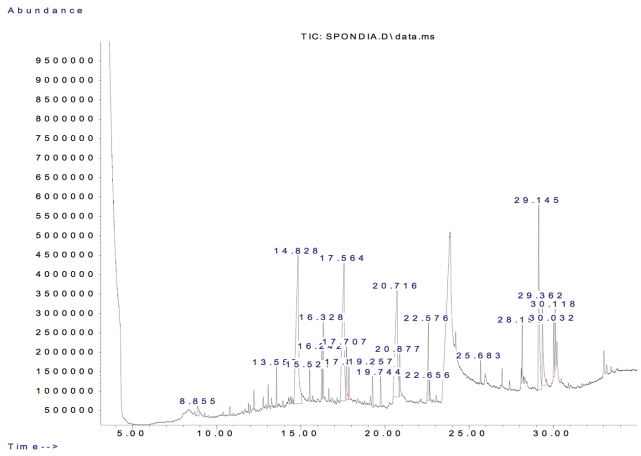

Figure 1. A gas chromatogram showing a plot of intensity against retention time (minutes)

In addition, MESSM showed high total flavonoid and phenolic contents. Phenolic compounds are secondary metabolites that contain hydroxyl groups that confer them with scavenging ability. The MESSM had a higher phenolic content (>100) than some fruits such as *S. mombin*, guava, strawberry, pineapple, soursop, and passion fruit.[21,31]

The following major compounds were identified in the seed of *S. mombin*: dodecanoic acid (22.48%), tetradecanoic acid (17.95%), n-hexadecanoic acid (15.35%), and phenol amides capsaicin (12.11%) and dihydrocapsaicin (5.23%). Dodecanoic acid, also known as lauric acid, showed *in vitro* antimicrobial activity against *Propionibacterium acnes* and beneficial effects in a mouse ear model of *Propionibacterium acnes*-induced inflammation.[32] Lauric acid is one of the reagents for making soaps and cosmetics.[33] Tetradecanoic acid (myristic acid), another constituent of MESSM, is used as a dietary supplement and a flavoring agent in the food industry. It is also used in the cosmetic industry, for making toiletries, emulsifiers, facial creams, and lotions, and in the pharmaceutical industry.[34,35] Furthermore, hexadecanoic acid (palmitic acid) possesses antioxidant, anticancer, and anti-inflammatory activities.[36-39] Capsaicin and dihydrocapsaicin, other constituents of MESSM, are phenol amides, majorly found in pepper. Capsaicin and dihydrocapsaicin possess antioxidant activity.[40] Capsaicin is also used for the treatment of pain. It can be administered in topical ointments, nasal sprays, and dermal patches.[41] A transdermal patch of capsaicin (Qutenza®) was approved by the Food and Drug Administration for the management of pain due to postherpetic neuralgia.[42] Other minor compounds in the seed of *S. mombin* with antioxidant activity that have been previously reported include (9*Z*, 12*Z*)-9,12-octadecadienoic acid (linoleic acid), 4-H-pyran-4-one, 2.3-dihydro-3.5-dihydroxy-6-methyl, and hexadecanoic acid-methyl ester.[43]

CONCLUSION

The seed extract of *S. mombin* lacked cytotoxicity potential. It contains nontoxic antioxidant compounds that could be explored in the pharmaceutical and cosmetics industries for the development of antioxidant agents.

Table 2. Chemical components of methanol extract of *Spondias mombin* using GC-MS

S/N	Compound	Peak no.	GC-MS-RT (min)	Percentage abundance (%)	M/Z value
	Saponin				
1	4H-Pyran-4-one,2,3-dihydro-3,5-dihydroxy-6-methyl-	1	8.86	0.90	144
	Alkanes				
2	Pentadecane	2	13.55	1.05	212
3	Pentadecane, 2,6,11-trimethyl-	4	15.52	1.15	254
4	Heptadecane	5	16.24	1.36	240
5	Pentadecane, 2,6,10,14-tetramethyl	6	16.33	2.63	268
6	Octadecane	8	17.71	2.21	254
7	Hexadecane, 2,6,10,14-tetramethyl-	9	17.86	1.33	282
8	Nonadecane	10	19.26	1.41	268
9	Eicosane	13	20.88	1.92	282
10	Octadecane, 1-bromo-	16	25.68	0.76	332
	Fatty acid				
11	Dodecanoic acid	3	14.83	22.48	200
12	Tetradecanoic acid	7	17.56	17.95	228
13	Hexadecanoic acid, methyl ester	11	19.74	1.13	270
14	n-Hexadecanoic acid	12	20.72	15.35	256
15	9,12-Octadecadienoic acid (Z,Z)-methyl ester	14	22.58	3.92	294
16	11-Octadecenoic acid, methyl ester	15	22.66	0.76	335
	Phenolic lipids				
17	(Z)-3-(pentadec-8-en-1-yl) phenol	17	28.16	1.95	302
18	3-(4Z,7Z)-Heptadeca-4,7-dien-1-yl) phenol	20	30.03	2.32	328
	Phenol amide				
19	Capsaicin	18	29.15	12.11	305
20	Dihydrocapsaicin	19	29.36	5.23	307
	Monoterpenoids				
21	Pyridine, 2-ethoxy-	21	30.12	2.09	123

GC-MS: Gas chromatography-mass spectrometry, RT: Retention time

ACKNOWLEDGEMENTS

The technical assistance of Ms. Faridah Abdulhameed and Owoola Azizat during the course of the study is acknowledged.

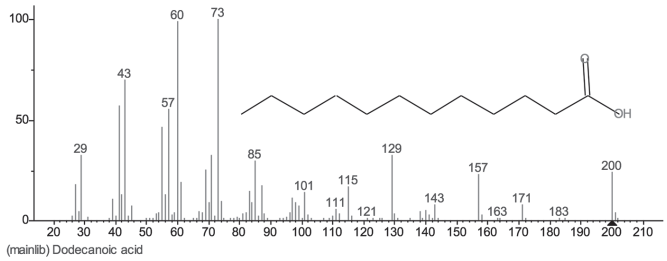

Figure 2. Profile of mass spectra and chemical structure of dodecanoic acid present in seed of *Spondias mombin*

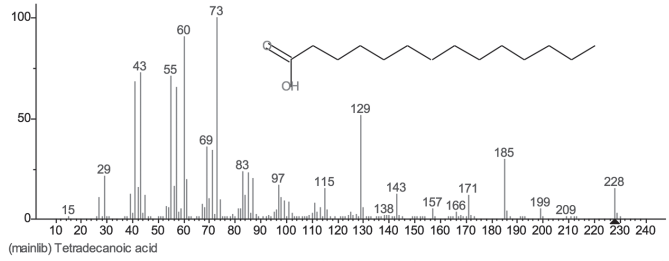

Figure 3. Mass spectra of tetradecanoic acid, a plot of relative abundance against mass to charge ratio

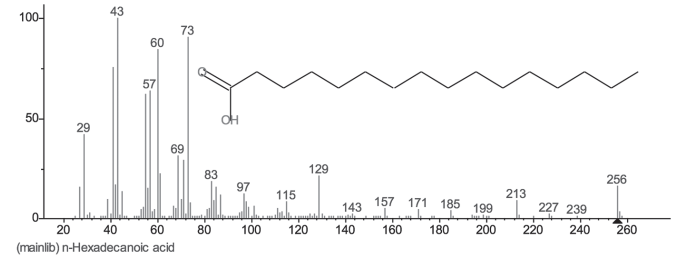

Figure 4. Mass spectra of n-hexadecanoic acid, a plot of relative abundance against mass to charge ratio

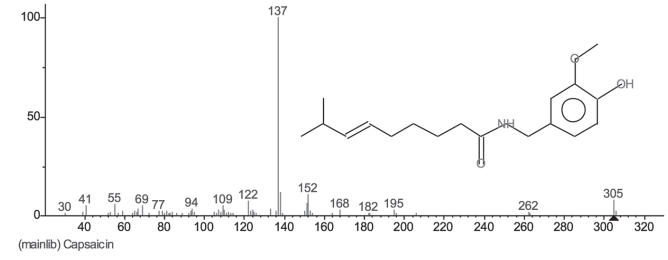

Figure 5. Mass spectra of capsaicin, a plot of relative abundance against mass to charge ratio

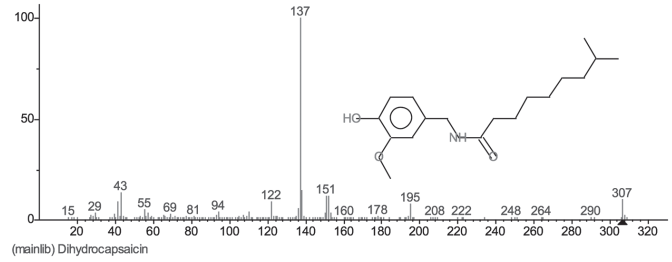

Figure 6. Mass spectra of dihydrocapsaicin, a plot of relative abundance against mass to charge ratio

Conflicts of interest: No conflict of interest was declared by the authors. The authors alone are responsible for the content and writing of this article.

REFERENCES

1. Birben E, Sahiner UM, Sackesen C, Erzurum S, Kalayci O. Oxidative stress and antioxidant defense. World Allergy Organ J. 2012;5:9-19.
2. Bogdan AI, Baumann L. Antioxidants used in skin care formulations. Skin Therapy Lett. 2018;13:5-9.
3. Tezel G. Oxidative stress in glaucomatous neurodegeneration: mechanisms and consequences. Prog Retin Eye Res. 2006;25:490-513.
4. Lobo V, Patil A, Phatak A, Chandra N. Free radicals, antioxidants and functional foods: Impact on human health. Pharmacogn Rev. 2010;4:118-126.
5. Butterfield DA, Drake J, Pocernich C, Castegna A. Evidence of oxidative damage in Alzheimer's disease brain: central role for amyloid β-peptide. Trends Mol Med. 2001;7:548-554.
6. Agil A, Durán R, Barrero F, Morales B, Araúzo M, Alba F, Miranda MT, Prieto I, Ramírez M, Vives F. Plasma lipid peroxidation in sporadic Parkinson's. Role of the L-dopa. J Neurol Sci. 2006;240:31-36.
7. Kim JI, Cho SI, Kim NH, Jin JK, Choi EK, Carp RI, Kim YS. Oxidative stress and neurodegeneration in prion diseases. Ann N Y Acad Sci. 2001;928:182-186.
8. He L, He T, Farrar S, Linbao J, Liu T, Ma Xi. Antioxidants and Cellular Homeostasis by Elimination of Reactive Oxygen Species. Cell Physiol Biochem. 2017;44:532-553.
9. Pandey KB, Rizvi SI. Plant polyphenols as dietary antioxidants in human health and disease. Oxid Med Cell Longev. 2009;2:270-278.
10. Simo A, Kawal N, Paliyath G, Bakovic M. Botanical antioxidants for skin health in the world of cosmeceuticals. International Journal of Advanced Nutritional and Health Science. 2014;2:67-88.
11. López VGC, Cortés RC. Medicinal plants, antioxidants and health. J Tox Health. 2013;103:257-265.
12. Gülçin I, Berashvili D, Gepdiremen A. Antiradical and antioxidant activity of total anthocyanins from Perilla pankinensis decne. J Ethnopharmacol. 2005;101:287-293.
13. Irvine JR. Woody plants of Ghana. 2nd ed. London: Oxford University press; 1961:51.
14. Abo KA, Ogunleye VO, Ashidi JS. Antimicrobial potential of Spondias mombin, Croton zambesicus and Zygotritonia crocea. Phytother Res. 1999;13:494-497.
15. Ajao AO, Shonukan O, Onadeko BF. Antibacterial effect of aqueous and alcohol extracts of Spondias mombin and Alchomea cordifolia - Two local antimicrobial remedies. Int J Crude Drug Res. 1985;23:67-72.
16. Akubue PI, Mittal GC, Aguwa CN. Preliminary pharmacological study of some Nigerian medicinal plants. J Ethnopharmacol. 1983;8:53-63.
17. Corthout J, Pieters LA, Claeys M, Vanden BDA, Viletinck AJ. Antiviral; Ellagitannins from Spodias mombin. Phytochemistry 1991;30:1129-1130.
18. Rodrigues KF, Hesse M, Werner C. Antimacrobial activities of secondary metabolites produced by endophytic fungi from Spondias mombin. J Basic Microbiol. 2000;40:261-267.
19. Villegas LF, Fernadz TD, Maldonado H, Torres R, Zavaleta A, Vaisberg AJ, Hammond GB. Evaluation of the wounds - healing activity of selected

traditional medical plants from Peru. J Ethnopharmacol. 1997;55:193-200.

20. Cabral B, Siqueira EMS, Bitencourt MAO, Lima MCJS, Lima AK, Ortmann CF, Chaves VC, Fernandes-Pedrosa MF, Rocha HAO, Scortecci KC, Reginatto FH, Giordani RB, Zucolotto SM. Phytochemical study and anti-inflammatory and antioxidant potential of Spondias mombin leaves. Rev Bras Farmacogn. 2016;26:304-311.
21. Tiburski JH, Rosenthal A, Deliza R, De Oliveira Godoy RL, Pacheco S. Nutritional properties of yellow mombin (*Spondias mombin* L.) pulp. Food Res Int. 2011;44:2326-2331.
22. Kim DO, Jeong SW, Lee CY. Antioxidant capacity of phenolic phytochemicals from various cultivars of plums. Food Chem. 2003;81:321-326.
23. Park YS, Jung ST, Kang SG, Heo BG, Arancibia AP, Toledo F, Drzewiecki J, Namiesnik J, Gorinstein S. Antioxidants and proteins in ethylene-treated kiwifruits. Food Chem. 2008;107:640-648.
24. Silva EM, Souza JNS, Rogez H, Rees JF, Larondelle Y. Antioxidant activity and polyphenolic contents of fifteen selected plant species from the Amazonian region. Food Chem. 2006;101:1012-1018.
25. Ruch RJ, Cheng SJ, Klaunig JE. Prevention of cytotoxicity and inhibition of intracellular communication by antioxidant catechins isolated from Chinese green tea. Carcinogenesis. 1989;10:1003-1008.
26. Balakrishnan N, Panda AB, Raj NR, Shrivastava A, Prathani R. The evaluation of nitric oxide scavenging activity of Acalyphaindica Linn Root. Chem Asian J. 2009;2:148-150.
27. Mosmann T. Rapid colorimetric assay for cellular growth and survival: application to proliferation and cytotoxicity assays. J Immunol Methods.1983;65:55-63.
28. Wangchuk P, Navarro S, Shepherd C, Keller PA, Pyne SG, Loukas A. Diterpenoid alkaloids of Aconitum laciniatum and mitigation of inflammation by 14-O-acetylneoline in a murine model of ulcerative colitis. Sci Rep. 2015;5:12845.
29. Sahreen S, Khan MR, Khan RA. Phenolic compounds and antioxidant activities of Rumex hastatus D. Don. Leaves. J Med Plant Res. 2011;5:2755-2765.
30. Akinmoladun AC, Khan MF, Sarkar J, Farombi EO, Maurya R. Distinct radical scavenging and antiproliferative properties of Spondias mombin and antioxidant activity-guided isolation of quercetin-3-O-β-Dglucopyranoside and undec-1-ene. Afr J Pharm Pharmacol. 2015;9:506-513.
31. Kuskoski EM, Asuero AG, Morales MT, Fett R. Frutos tropicais silvestrese polpas de frutas congeladas: atividade antioxidante, polifenóise antocianinas. Ciênc Rural. 2006;36:1283-1287.
32. Nakatsuji T, Kao MC, Fang JY, Zouboulis CC, Zhang L, Gallo RL, Huang CM. Antimicrobial Property of Lauric acid against Propionibacterium acnes: Its Therapeutic Potential for Inflammatory Acne Vulgaris. J Invest Dermatol. 2009;129:2480-2488.
33. Anneken DJ, Both S, Christoph R, Fieg G, Steinberner U, Westfechtel, A. "Fatty Acids" in Ullmann's Encyclopedia of Industrial Chemistry. Weinheim: Wiley-VCH; 2006.
34. Meng Q, Yu M, Gu B, Li J, Liu Y, Zhan C, Xie C, Zhou J, Lu W. Myristic acid-conjugated polyethylenimine for brain-targeting delivery: *In vivo* and *ex vivo* imaging evaluation. J Drug Target. 2010;18:438-446.
35. Or-Rashid MM, Odongo NE, Subedi B, Karki P, McBride BW. Fatty acid composition of yak (Bos grunniens) cheese including conjugated linoleic acid and trans-18:1 fatty acids. J Agric Food Chem. 2008;56:1654-1660.
36. Aparna V, Dileep KV, Mandal PK, Karthe P, Sadasivan C, Haridas M. Anti-inflammatory property of n-hexadecanoic acid: Structural evidence and kinetic assessment. Chem Biol Drug Des. 2012;80:434-439.
37. Graikou K, Kapeta S, Aligiannis N, Sotiroudis G, Chondrogianni N, Gonos E, Chinou L. Chemical analysis of Greek pollen-antioxidant, antimicrobial and proteasome activation properties. Chem Cent J. 2011;5:33.
38. Harada H, Yamashita U, Kurihara H, Fukushi E, Kawabata J, Kamei Y. Antitumor activity of palmitic acid found as a selective cytotoxic substance in a marine red alga. Anticancer Res. 2002;22:2587-2590.
39. Kumar P, Kumaravel S, Lalitha C. Screening of antioxidant activity, total phenolics and GC-MS study of Vitex negundo. Afr J Biochem Res. 2010;4:191-195.
40. Murakami K, Ito M, Htay HH, Tsubouchi R, Yoshino M. Antioxidant effect of capsaicinoids on the metal-catalyzed lipid perox idation. Biomed Res. 2001;22:15-17.
41. Fattori V, Hohmann MS, Rossaneis AC, Pinho-Ribeiro FA, Verri WA. Capsaicin: Current Understanding of Its Mechanisms and Therapy of Pain and Other Pre-Clinical and Clinical Uses. Molecules. 2016;21:844.
42. FDA. "FDA Approves New Drug Treatment for Long-Term Pain Relief after Shingles Attacks". U.S. Food and Drug Administration. 17 November 2009. Retrieved 5 January 2016.
43. Cechovska L, Cejpek K, Konecny M, Velısek J. On the role of 2,3-dihydro-3,5-dihydroxy-6-methyl-(4H)-pyran-4-one in antioxidant capacity of prunes. Eur Food Res Technol. 2011;233: 367-376.

Turk J Pharm Sci 2020;17(3):349-356
DOI: 10.4274/tjps.galenos.2019.47123

REVIEW

The Cardiopulmonary Effects of the *Calcitonin* Gene-related Peptide Family

Kalsitonin-Geni İle İlişkili Peptit Ailesinin Kardiyopulmoner Etkileri

Gökçen TELLİ[1], Banu Cahide TEL[1], Bülent GÜMÜŞEL[2]*

[1]Hacettepe University Faculty of Pharmacy, Department of Pharmacology, Ankara, Turkey
[2]Lokman Hekim University Faculty of Pharmacy, Department of Pharmacology, Ankara, Turkey

ABSTRACT

Cardiopulmonary diseases are very common among the population. They are high-cost diseases and there are still no definitive treatments. The roles of members of the calcitonin-gene related-peptide (CGRP) family in treating cardiopulmonary diseases have been studied for many years and promising results obtained. Especially in recent years, two important members of the family, adrenomedullin and adrenomedullin2/intermedin, have been considered new treatment targets in cardiopulmonary diseases. In this review, the roles of CGRP family members in cardiopulmonary diseases are investigated based on the studies performed to date.

Key words: CGRP family, cardiopulmonary diseases, adrenomedullin, adrenomedullin2/intermedin, pulmonary hypertension

ÖZ

Kardiyopulmoner hastalıklar toplumda sık görülen, tedavi maliyeti oldukça yüksek ve halen kesin bir tedavisi bulunmayan hastalıklardır. Kalsitonin-geni ile ilişkili peptit (CGRP) ailesinin üyelerinin bir çok kardiyopulmoner hastalıktaki rolleri uzun yıllardır çalışılmakta ve umut vadeden sonuçlar elde edilmektedir. Özellikle son yıllarda CGRP ailesine ait peptitlerden adrenomedullin ve intermedin kardiyopulmoner hastalıklarda yeni tedavi hedefleri olarak değerlendirilmektedir. Bu derleme ile CGRP ailesi peptitlerinin kardiyopulmoner hastalıklardaki rolleri günümüze kadar yapılan çalışmalar doğrultusunda incelenmiştir.

Anahtar kelimeler: CGRP ailesi, kardiyopulmoner hastalıklar, adrenomedullin, adrenomedullin2/intermedin, pulmoner hipertansiyon

INTRODUCTION

The calcitonin gene-related peptide (CGRP) family consists of calcitonin, amylin (AMY), CGRP, adrenomedullin (ADM), calcitonin receptor (CTR) stimulating peptides 1-3, and the latest member of the family, ADM2/intermedin (IMD).[1,2] These peptides are included in the same family because of their similar chemical structures and they have important roles in the homeostasis of the body.[3-6] The effects of these peptides on the cardiovascular and pulmonary systems, especially ADM and ADM2/IMD, sparked interest as many studies were presented for the new targets of cardiovascular diseases.[7-9] In this review, we aim to summarize the cardiopulmonary effects of the CGRP family.

DISTRIBUTION OF MEMBERS OF THE CGRP FAMILY

Peptides of the CGRP family are widely expressed in the body. The first peptide of this family, calcitonin, was synthesized by a calcium-dependent mechanism and released from thyroid C-cells.[10,11] Another peptide, AMY, was isolated from amyloid plaques in β-cells found in pancreatic islets of Langerhans.[12] The rest of the family, CGRP, ADM, and ADM2/IMD, have more effect on the cardiovascular and pulmonary system. CGRP is expressed in both central and peripheral nerves associated with blood vessels. Perivascular nerves were suggested as important sources of plasma CGRP. Although CGRP is mainly expressed in nerves, it is also located in endothelial cells, adipocytes, keratinocytes, and immune cells.[13]

ADM was isolated for the first time from human pheochromocytoma cells; however, in following years it has been shown to be expressed in many tissues in the body.[14] It is found in the adrenal medulla, kidneys, lungs, ventricles, and especially endothelial cells in high amounts.[15,16]

The distribution of ADM2/IMD is largely similar to that of ADM. The expression of ADM2/IMD was demonstrated in the brain, liver, intestines, heart, kidneys, plasma, hypothalamus, and

*Correspondence: E-mail: bulent.gumusel@lokmanhekim.edu.tr, Phone: +90 532 435 21 90 ORCID-ID: orcid.org 0000-0002-7533-7949
Received: 12.06.2019 , Accepted: 27.06.2019

like ADM widely in endothelial cells.[17-22] In addition to being expressed widely in physiological conditions, their levels change under pathological conditions.[13,23-26]

RECEPTORS OF THE CGRP FAMILY

The peptides of the CGRP family interact with CTRs or calcitonin receptor-like receptors (CLRs). CTRs were first identified in pigs in 1991 and two different variants were found in humans, named hCT_aR and hCT_bR. These receptors are located on the cell surface. hCT_aR is widely distributed in the body, while hCT_bR was found in the placenta, ovaries, lungs, and bone marrow.[27] CLRs were first demonstrated in rats in 1993 and 2 years later were shown in different tissues of humans.[28,29] CLRs were found in the central nervous system, kidneys and spleen, endothelial cells, vascular smooth muscle cells, and the heart. CTRs and CLRs are G protein-dependent receptors and contain 7 transmembrane regions.[30,31] The receptors must also interact with the related receptor-activating modified protein (RAMP), depending on the type of peptide. These proteins facilitate the transfer of receptors from the plasma membrane and translocations of them into the cells.[32,33] RAMPs are composed of 148 to 189 amino acids and although they exhibit a homology less than 30%, they are structurally similar to each other. These proteins are named RAMP1, RAMP2, and RAMP3.[13] AMY shows high affinity when CTRs are activated by RAMPs.[33,34] RAMPs that bind to CTRs allow the receptor to show affinity to AMY instead of calcitonin. When the CTRs are connected with RAMP1, RAMP2, and RAMP3 they are called AMY1, AMY2, and AMY3, respectively. CGRP and ADM are activated by binding to CLRs. CLRs must interact with RAMP1 in order to function as CGRP receptors. CLRs must be bound to RAMP2 and -3 to act as ADM receptors (AM1 and AM2, respectively) (Table 1).

RAMP1 is commonly found in the uterus, bladder, brain, pancreas, and gastrointestinal tract.[35-37] It has been also shown in the veins, perivascular nerves, arteries, and endothelial cells of arterioles and smooth muscle cells and cardiomyocytes.[38] RAMP2 is found in the lungs, spleen, immune system, and kidneys, and widely distributed in the cardiovascular system, especially in vascular endothelium and smooth muscle cells.[39] RAMP3 is found in high levels in the kidneys, lungs, and spleen, similar to RAMP2.[35,36]

Table 1. The receptors and receptor components that interact with the CGRP family

Receptor	Receptor component	Agonist
CGRP	CLR/RAMP1	CGRP, ADM2/IMD
AM1	CLR/RAMP2	ADM, ADM2/IMD
AM2	CLR/RAMP3	ADM, CGRP, ADM2/IMD
Calcitonin	CTR	CT, CRSP
AMY1	CTR/RAMP1	AMY, CGRP
AMY3	CTR/RAMP3	AMY

CGRP: Calcitonin-gene related-peptide, AMY: Amylin, CLR: Calcitonin receptor-like receptor, RAMP: Related receptor-activating modified protein, CTR: Calcitonin receptor, ADM: Adrenomedullin, IMD: intermedin

Other than RAMPs, CLRs need another adapter protein to show optimum activity. This protein is called receptor component protein (RCP) and provides more effective binding with stimulator G protein and thus increases the activity of peptides[32,40] (Figure 1).

CARDIOPULMONARY EFFECTS OF THE CGRP FAMILY

Peptides of the CGRP family show widespread biological activity in the body, and in the cardiopulmonary system especially CGRP, ADM, and ADM2/IMD have remarkable effects.

Amylin

AMY acts on the cardiovascular system via CGRP receptors.[41] However, AMY has to reach a high plasma concentration to show activity. Intravenous (i.v.) AMY application provided potent vasodilatation and decreased arterial blood pressure in rats.[42] However, human studies showed no significant effect after AMY application.[43] In studies on rat cardiomyocytes and isolated heart, AMY showed a direct inotropic effect that was mediated by CGRP receptors. However, because of the side effects on the heart of high doses of AMY, it was stated that it could not be applied clinically.[44,45]

Calcitonin gene-related peptide

CGRP is one of the most potent and effective vasodilators and it has a longer duration of action.[46,47] Its relaxing effects on coronary, cerebral, pulmonary, and renal arteries were shown in both *in vitro* and *in vivo* experiments. CGRP has also regulatory effects on the vascular system; it was shown to reduce the vascular resistance and to increase the blood supply to organs in both normotensive and hypertensive animals.[48,49] In hypertensive rats, systemically administrated CGRP decreased blood pressure and had positive inotropic and chronotropic effects. After ischemic injury CGRP released in rats and also CGRP infusion reduced ischemia-reperfusion-induced arrhythmias. In addition, many studies have shown that CGRP is also protective against ischemic damage. These

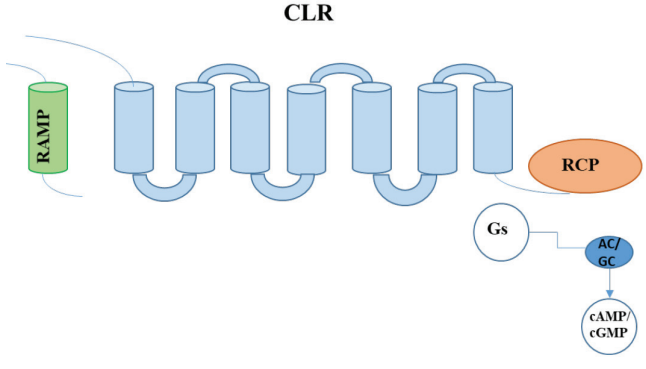

Figure 1. CLRs are G protein-dependent receptors and contain 7 transmembrane domains. CLRs require RAMPs and RCP for activation. The activated CLRs stimulate the G protein complex and provide activity
RCP: Receptor component protein, CLRs: Calcitonin receptor-like receptors, RAMPs: Related receptor-activating modified proteins, cAMP: Cyclic adenosine monophosphate, cGMP: Cyclic guanosine monophosphate

effects of CGRP are generally thought to be the result of its vasodilatory effect.[50-52] Furthermore, CGRP also suppressed the release of potent vasoconstrictor agents such as endothelin and angiotensin.[53]

CGRP provided important relaxation in the pulmonary vascular system and was found in high amounts in lung tissue.[54] In pulmonary hypertension (PH), plasma CGRP levels were decreased and CGRP infusion has been shown to be effective in treatment.[13,23-25] Adenovirus-mediated CGRP transfection before chronic hypoxia exposure in mice lungs provided cyclic adenosine monophosphate (cAMP)-mediated protection against pulmonary vascular resistance and decreased vascular remodeling.[53] CGRP has been shown to provide protection against hypoxia-induced remodeling in human tissue studies[55] and it was shown that in rat hypoxic lung the expression levels of the CGRP receptor adapter protein RAMP1 were increased.[26]

CGRP shows all these effects through CGRP receptor and the effects of CGRP on the cardiovascular system are inhibited in the presence of selective CGRP antagonist $CGRP_{8-37}$.[46,56-58] It is suggested that both endothelium-dependent and endothelium-independent mechanisms have roles in CGRP-mediated vasodilatation.[5,59,60] In many tissues, such as cat cerebral artery, rat mesenteric artery, and pig coronary artery, the increase in cAMP was measured after CGRP administration and in the endothelium-damaged vessels vasodilation was also observed. However, even high doses of CGRP did not stimulate the cyclic guanosine monophosphate (cGMP) levels directly.[59,60] Therefore, it may indicate that CGRP directly activates cAMP-dependent vasodilation.[61-63] In the studies that were performed in the pig coronary artery and guinea pig ureter, CGRP-mediated vasodilation was inhibited by the K_{ATP} channel inhibitor glibenclamide. Therefore, it was stated that the increase in cAMP activates protein kinase A and subsequently K_{ATP} channels.[61,63-67] Basal and nitric oxide (NO)-stimulated CGRP release were increased in the human right atrium in patients that underwent cardiopulmonary bypass.[68,69] However, there are also contradictory studies that indicated the role of endothelium in CGRP-mediated vasodilation. CGRP provided NO- and cGMP-dependent vasodilation in the rat aorta.[70]

On the other hand, in the perivascular nerves of the rat mesentery artery, CGRP was found more sensitive to endothelin-1 mediated constructions and this effect was not associated with NO or cyclic nucleotides.[71]

Adrenomedullin

For many years, the effects of ADM on the cardiovascular system have attracted attention. Potent, NO-mediated hypotension was observed after the infusion of ADM both in animals and in humans.[72-74] After acute and chronic administration of ADM in rats, total peripheral vascular resistance and blood pressure were decreased significantly. The heart rate and cardiac output were increased simultaneously. Similar effects were also observed in hypertensive rats.[75,76] ADM is an important vasorelaxant agent, especially in the mesentery, renal, pulmonary, and cerebral arteries and aorta, but the mechanism of this effect varies according to species and the vascular bed.[77-80] The vasorelaxing effects act through CGRP and ADM receptors. In the rat mesenteric artery and dog renal arteries, the relaxing effect of ADM was inhibited in the presence of CGRP receptor antagonist, whereas in some studies that were performed in the cerebral arteries of cat and rat hind limb, inhibition of CGRP receptors did not alter the relaxation response.[78,81,82] Similarly, the role of endothelium and NO in the relaxation effect of ADM also varies between different studies. Numerous studies have shown that endothelium-mediated vasorelaxation occurred in different vessels such as the rat renal, pulmonary, and mesenteric arteries and vasorelaxation was inhibited in the presence of NO synthase (NOS) inhibitors.[72,83,84] However, in contrast to these studies, no changes were observed in the presence of NOS inhibitor in studies that were performed in isolated rat lung, cat hind limb arteries, and the cat penile artery.[85-87] Studies in human and dog coronary arteries and rat cerebral arteries showed inhibited ADM response with high potassium.[78,88,89] Although there are contradictory results in the literature, it has been shown in many studies that ADM provides relaxation through the cAMP, NO, or K^+ channels in vascular systems.[90]

According to its potent and long-lasting vasodilatory activity in the peripheral microcirculation, ADM also could be effective in PH.[91] In hypoxia-induced PH, ADM reduced pulmonary arterial pressure.[92] Systemic i.v. administration of ADM reduced pulmonary vascular resistance and increased arterial oxygen levels with no effect on systemic blood pressure.[93] In the studies performed in PH patients, the plasma level of ADM increased along with the severity of the disease. In contrast to the increase in the endogenous production of ADM, i.v. ADM administration reduced pulmonary artery pressure and pulmonary vascular resistance in PH patients.[94,95] In another study performed with a small number of PH patients, acute inhaled ADM was shown to improve selectively the hemodynamic parameters in the pulmonary system and increase exercise capacity.[96] Multicenter, randomized, controlled clinical trials should be conducted to evaluate the long-term safety and efficacy of ADM, to be able to consider it as a future treatment target in PH.[9]

Adrenomedullin2/intermedin

ADM2/IMD has quite a similar structure and function to CGRP and ADM. Therefore, it is also expected that ADM2/IMD can be effective in the vascular system. In many studies, blood pressure and vascular resistance were decreased and the heart rate was increased with the application of ADM2/IMD.[17,30,97,98] After cardiac ischemia/reperfusion injury, the administration of ADM2/IMD increased the coronary perfusion and contractile strength of the left ventricle and reduced myocardial infarct size, hypertrophy, and cardiac fibrosis.[99-101] In normotensive and hypertensive rats, i.v. infusion of ADM2/IMD increased cardiac output by reducing total peripheral vascular resistance.[102] ADM2/IMD has been shown to be a potent vasodilator in many vessel beds such as pulmonary, renal, and abdominal arteries.[103-106]

$CGRP_{8-37}$ and ADM receptor antagonist AM_{22-52} inhibited the effects of ADM2/IMD on the cardiovascular system under both

physiological and pathophysiological conditions. The CLR/RAMP receptors are responsible for the actions of ADM2/IMD in the cardiovascular system.[17,20,103] Although the effects of ADM2/IMD on the cardiovascular system frequently act through the CGRP receptors, in different vascular beds ADM2/IMD can interact with the both CGRP and ADM receptors.[5,57] The ADM2/IMD-mediated response acts through CGRP receptor in the hypotension of rat systemic pressure and the vasodilation of rat coronary, carotid, supramesenteric, and pulmonary arteries. However, the ADM2/IMD responses were AM1 and AM2 receptor-mediated in pig coronary and rat renal arteries.[17,20,103,105,107,108] Several studies have shown that the cardiovascular effects of ADM2/IMD are endothelium-mediated and NO-dependent. In the pulmonary vascular system and aorta, the relaxation responses were inhibited by the presence of NOS inhibitor Nω-Nitro-L-arginine methyl ester hydrochloride and in the damaged endothelium.[99,103,109] The NO production increased dose-dependently with ADM2/IMD administration in cerebral endothelial cells and pulmonary smooth muscle cells.[110,111]

The positive inotropic effects of ADM2/IMD and the role in cell proliferation, apoptosis, and cell migration were related to the increase in cAMP production.[112-114] The mRNA and protein levels of ADM2/IMD increased in the right ventricles, lung tissues, and plasma of hypoxia-induced pulmonary hypertensive rats.[115-117] The symptoms of PH were alleviated by ADM2/IMD treatment in rats, right ventricular hypertrophy was prevented, and hypoxic pulmonary vascular remodeling was inhibited.[111] According to studies that were performed in pulmonary hypertensive rats, ADM2/IMD is thought to be effective in PH.[118] In chronic hypoxia-induced PH ADM2/IMD provided potent vasodilation in the pulmonary arteries of rats and intraarterial administration reduced the perfusion pressure of hypoxic lungs. This reduction indicates the possible application of ADM2/IMD administration in humans with PH.[119,120]

CONCLUSION

Peptides of the CGRP family exhibit cardiopulmonary effects and have been investigated for many years. Especially CGRP and ADM were proposed as new vasodilator agents in the treatment of many cardiovascular disease, such as hypertension and PH. ADM2/IMD is also a potent vasodilator in the cardiopulmonary system and in recent years it has been shown as a new drug candidate for cardiometabolic disease. However, further investigations should be performed for understanding these possible effects of ADM2/IMD before clinical investigations.

Conflicts of interest: No conflict of interest was declared by the authors. The authors alone are responsible for the content and writing of this article.

REFERENCES

1. Born W, Fischer JA. The Calcitonin Peptide Family: What Can We Learn from Receptor Knock Out and Transgenic Mice. In: Hay DL, Dickerson IM, eds. The Calcitonin Gene-related Peptide Family Form, Function and Future Perspectives. Springer Dordrecht Heidelberg London New York; Springer; 2010:75-86.
2. Ghatta S, Ramarao P. Increased contractile responses to 5-Hydroxytryptamine and Angiotensin II in high fat diet fed rat thoracic aorta. Lipids Health Dis. 2004;3:19.
3. Wimalawansa SJ. Amylin, calcitonin gene-related peptide, calcitonin, and adrenomedullin: a peptide superfamily. Crit Rev Neurobiol. 1997;11:167-239.
4. Muff R, Born W, Fischer JA. Adrenomedullin and related peptides: receptors and accessory proteins. Peptides. 2001;22:1765-1772.
5. Brain SD, Grant AD. Vascular actions of calcitonin gene-related peptide and adrenomedullin. Physiol Rev. 2004;84:903-934.
6. Ren YS, Yang JH, Zhang J, Pan CS, Yang J, Zhao J, Pang YZ, Tang CS, Qi YF. Intermedin 1-53 in central nervous system elevates arterial blood pressure in rats. Peptides. 2006;27:74-79.
7. Zhang SY, Xu MJ, Wang X. Adrenomedullin 2/intermedin: a putative drug candidate for treatment of cardiometabolic diseases. Br J Pharmacol. 2018;175:1230-1240.
8. Nagaya N, Kangawa K. Adrenomedullin in the treatment of pulmonary hypertension. Peptides. 2004;25:2013-2018.
9. Raja SG, Raja SM. Treating pulmonary arterial hypertension: current treatments and future prospects. Ther Adv Chronic Dis. 2011;2:359-370.
10. Copp DH. Calcitonin: discovery, development, and clinical application. Clin Invest Med. 1994;17:268-277.
11. Copp DH, Cameron EC. Demonstration of a hypocalcemic factor (calcitonin) in commercial parathyroid extract. Science. 1961;134:2038.
12. Westermark P, Wernstedt C, Wilander E, Sletten K. A novel peptide in the calcitonin gene related peptide family as an amyloid fibril protein in the endocrine pancreas. Biochem Biophys Res Commun. 1986;140:827-831.
13. Russell FA, King R, Smillie SJ, Kodji X, Brain SD. Calcitonin gene-related peptide: physiology and pathophysiology. Physiol Rev. 2014;94:1099-1142.
14. Kitamura K, Sakata J, Kangawa K, Kojima M, Matsuo H, Eto T. Cloning and characterization of cDNA encoding a precursor for human adrenomedullin. Biochem Biophys Res Commun. 1993;194:720-725.
15. Sugo S, Minamino N, Shoji H, Kangawa K, Kitamura K, Eto T, Matsuo H. Production and secretion of adrenomedullin from vascular smooth muscle cells: augmented production by tumor necrosis factor-alpha. Biochem Biophys Res Commun. 1994;203:719-726.
16. Sugo S, Minamino N, Kangawa K, Miyamoto K, Kitamura K, Sakata J, Eto T, Matsuo H. Endothelial cells actively synthesize and secrete adrenomedullin. Biochem Biophys Res Commun. 1994;201:1160-1166.
17. Roh J, Chang CL, Bhalla A, Klein C, Hsu SY. Intermedin is a calcitonin/calcitonin gene-related peptide family peptide acting through the calcitonin receptor-like receptor/receptor activity-modifying protein receptor complexes. J Biol Chem. 2004;279:7264-7274.
18. Takei Y, Inoue K, Ogoshi M, Kawahara T, Bannai H, Miyano S. Identification of novel adrenomedullin in mammals: a potent cardiovascular and renal regulator. FEBS Lett. 2004;556:53-58.
19. Taylor MM, Bagley SL, Samson WK. Intermedin/adrenomedullin-2 acts within central nervous system to elevate blood pressure and inhibit food and water intake. Am J Physiol Regul Integr Comp Physiol. 2005;288:919-927.

20. Kobayashi Y, Liu YJ, Gonda T, Takei Y. Coronary vasodilatory response to a novel peptide, adrenomedullin 2. Clin Exp Pharmacol Physiol. 2004;31(Suppl 2):49-50.

21. Takei Y, Hyodo S, Katafuchi T, Minamino N. Novel fish-derived adrenomedullin in mammals: structure and possible function. Peptides. 2004;25:1643-1656.

22. Takahashi K, Kikuchi K, Maruyama Y, Urabe T, Nakajima K, Sasano H, Imai Y, Murakami O, Totsune K. Immunocytochemical localization of adrenomedullin 2/intermedin-like immunoreactivity in human hypothalamus, heart and kidney. Peptides. 2006;27:1383-1389.

23. Keith IM, Ekman R. Dynamic aspects of regulatory lung peptides in chronic hypoxic pulmonary hypertension. Exp Lung Res. 1992;18:205-224.

24. Keith IM, Looi STA, Kraiczi H, Ekman R. Three-week neonatal hypoxia reduces blood CGRP and causes persistent pulmonary hypertension in rats. Am J Physiol Heart Circ Physiol. 2000;279:1571-1578.

25. Looi STA, Ekman R, Lippton H, Cary J, Keith I. CGRP and somatostatin modulate chronic hypoxic pulmonary hypertension. Am J Phsiol. 1992;263:681-690.

26. Qing X, Svaren J, Keith IM. mRNA expression of novel CGRP1 receptors and their activity-modifying proteins in hypoxic rat lung. Am J Physiol Lung Cell Mol Physiol, 2001;280:547-554.

27. Kuestner RE, Elrod RD, Grant FJ, Hagen FS, Kuijper JL, Matthewes SL, O'Hara PJ, Sheppard PO, Stroop SD, Thompson DL. Cloning and characterization of an abundant subtype of the human calcitonin receptor. Mol Pharmacol. 1994;46:246-255.

28. Flühmann B, Muff R, Hunziker W, Fischer JA, Born W. A human orphan calcitonin receptor-like structure. Biochem Biophys Res Commun. 1995;206:341-347.

29. Njuki F, Nicholl CG, Howard A, Mak JC, Barnes PJ, Girgis SI, Legon S. A new calcitonin-receptor-like sequence in rat pulmonary blood vessels. Clin Sci (Lond). 1993;85:385-388.

30. Pan CS, Yang JH, Cai DY, Zhao J, Gerns H, Yang J, Chang JK, Tang CS, Qi YF. Cardiovascular effects of newly discovered peptide intermedin/adrenomedullin 2. Peptides 2005;26:1640-1646.

31. Park K-Y, Russo AF. Genetic Regulation of CGRP and Its Actions. In: Hay DL, Dickerson IM, eds. The Calcitonin Gene-related Peptide Family Form, Function and Future Perspectives. Springer Dordrecht Heidelberg London New York; Springer; 2010:97-114.

32. Juaneda C, Dumont Y, Quirion R. The molecular pharmacology of CGRP and related peptide receptor subtypes. Trends Pharmacol Sci. 2000;21:432-438.

33. McLatchie LM, Fraser NJ, Main MJ, Wise A, Brown J, Thomson N, Solari R, Lee MG, Foord SM. RAMPs regulate the transport and ligand specificity of the calcitonin-receptor-like receptor. Nature. 1998;393:333-339.

34. Muff R, Bühlmann N, Fischer JA, Born W. An amylin receptor is revealed following co-transfection of a calcitonin receptor with receptor activity modifying proteins-1 or -3. Endocrinology. 1999;140:2924-2927.

35. Just RSJ, Furness SGB, ChristopoulosA, Sexton PM. Understanding Amylin Receptors. In: Hay DL, Dickerson IM, eds. The Calcitonin Gene-related Peptide Family Form, Function and Future Perspectives. Springer Dordrecht Heidelberg London New York; Springer; 2010:41-57.

36. Nagae T, Mukoyama M, Sugawara A, Mori K, Yahata K, Kasahara M, Suganami T, Makino H, Fujinaga Y, Yoshioka T, Tanaka I, Nakao K. Rat receptor-activity-modifying proteins (RAMPs) for adrenomedullin/CGRP receptor: cloning and upregulation in obstructive nephropathy. Biochem Biophys Res Commun. 2000;270:89-93.

37. Cottrell GS, Roosterman D, Marvizon JC, Song B, Wick E, Pikios S, Wong H, Berthelier C, Tang Y, Sternini C, Bunnett NW, Grady EF. Localization of calcitonin receptor-like receptor and receptor activity modifying protein 1 in enteric neurons, dorsal root ganglia, and the spinal cord of the rat. J Comp Neurol. 2005;490:239-255.

38. Autelitano DJ, Ridings R. Adrenomedullin signalling in cardiomyocytes is dependent upon CRLR and RAMP2 expression. Peptides. 2001;22:1851-1857.

39. Kamitani S, Asakawa M, Shimekake Y, Kuwasako K, Nakahara K, Sakata T. The RAMP2/CRLR complex is a functional adrenomedullin receptor in human endothelial and vascular smooth muscle cells. FEBS Lett. 1999;448:111-114.

40. Evans BN, Rosenblatt MI, Mnayer LO, Oliver KR, Dickerson IM. CGRP-RCP, a novel protein required for signal transduction at calcitonin gene-related peptide and adrenomedullin receptors. J Biol Chem. 2000;275:31438-31443.

41. Young A. Cardiovascular effects. Adv Pharmacol. 2005;52:239-250.

42. Young AA, Crocker LB, Wolfe-Lopez D, Cooper GJ. Daily amylin replacement reverses hepatic glycogen depletion in insulin-treated streptozotocin diabetic rats. FEBS Lett. 1991;287:203-205.

43. Young A, Kolterman O, Hall J. Amylin innocent in essential hypertension? Diabetologia. 1999;42:1029.

44. Bell D, McDermott BJ. Activity of amylin at CGRP1-preferring receptors coupled to positive contractile response in rat ventricular cardiomyocytes. Regul Pept. 1995;60:125-133.

45. Kaygisiz Z, Ozden H, Erkasap N, Koken T, Gunduz M, İkizler M, Kural T. Positive inotropic, positive chronotropic and coronary vasodilatory effects of rat amylin: mechanisms of amylin-induced positive inotropy. Acta Physiol Hung. 2010;97:362-374.

46. Brain SD, Cambridge H. Calcitonin gene-related peptide: vasoactive effects and potential therapeutic role. Gen Pharmacol. 1996;27:607-611.

47. Brain SD, Tippins JR, Morris HR, MacIntyre I, Williams TJ. Potent vasodilator activity of calcitonin gene-related peptide in human skin. J Invest Dermatol. 1986;87:533-536.

48. Deng PY, Li YJ. Calcitonin gene-related peptide and hypertension. Peptides. 2005;26:1676-1685.

49. Li Y, Zhang Y, Furuyama K, Yokoyama S, Takeda K, Shibahara S, Takahashi K. Identification of adipocyte differentiation-related regulatory element for adrenomedullin gene repression (ADRE-AR) in 3T3-L1 cells. Peptides. 2006;27:1405-1414.

50. Ando K, Pegram BL, Frohlich ED. Hemodynamic effects of calcitonin gene-related peptide in spontaneously hypertensive rats. Am J Physiol. 1990;258:425-429.

51. Gardiner SM, Compton AM, Kemp PA, Bennett T, Foulkes R, Hughes B. Regional haemodynamic effects of prolonged infusions of human alpha-calcitonin gene-related peptide in conscious, Long Evans rats. Br J Pharmacol. 1991;103:1509-1514.

52. Wu D, Bassuk J, Adams JA. Calcitonin gene-related peptide protects against whole body ischemia in a porcine model of cardiopulmonary resuscitation. Resuscitation 2003;59:139-145.

53. Champion HC, Bivalacqua TJ, Lambert DG, McNamara DB, Kadowitz PJ. The influence of candesartan and PD123319 on responses to

angiotensin II in the hindquarters vascular bed of the rat. J Am Soc Nephrol. 1999;10(Suppl 11):95-97.

54. Mulderry PK, Ghatei MA, Spokes RA, Jones PM, Pierson AM, Hamid QA, Kanse S, Amara SG, Burrin JM, Legon S. Differential expression of alpha-CGRP and beta-CGRP by primary sensory neurons and enteric autonomic neurons of the rat. Neuroscience. 1988;25:195-205.

55. Tjen ALS, Ekman R, Lippton H, Cary J, Keith I. CGRP and somatostatin modulate chronic hypoxic pulmonary hypertension. Am J Physiol. 1992;263:681-690.

56. Tam CW, Husmann K, Clark NC, Clark JE, Lazar Z, Ittner LM, Götz J, Douglas G, Grant AD, Sugden D, Poston L, Poston R, McFadzean I, Marber MS, Fischer JA, Born W, Brain SD. Enhanced vascular responses to adrenomedullin in mice overexpressing receptor-activity-modifying protein 2. Circ Res. 2006;98:262-270.

57. Bell D, McDermott BJ. Calcitonin gene-related peptide in the cardiovascular system: characterization of receptor populations and their (patho)physiological significance. Pharmacol Rev. 1996;48:253-288.

58. Marshall I. Mechanism of vascular relaxation by the calcitonin gene-related peptide. Ann N Y Acad Sci. 1992;657:204-215.

59. Hirata Y, Takagi Y, Takata S, Fukuda Y, Yoshimi H, Fujita T. Calcitonin gene-related peptide receptor in cultured vascular smooth muscle and endothelial cells. Biochem Biophys Res Commun. 1988;151:1113-1121.

60. Crossman DC, Dashwood MR, Brain SD, McEwan J, Pearson JD. Action of calcitonin gene-related peptide upon bovine vascular endothelial and smooth muscle cells grown in isolation and co-culture. Br J Pharmacol. 1990;99:71-76.

61. Han SP, Naes L, Westfall TC. Calcitonin gene-related peptide is the endogenous mediator of nonadrenergic-noncholinergic vasodilation in rat mesentery. J Pharmacol Exp Ther. 1990;255:423-428.

62. Edvinsson L. Calcitonin gene-related peptide (CGRP) and the pathophysiology of headache: therapeutic implications. CNS Drugs. 2001;15:745-753.

63. Yoshimoto R, Mitsui-Saito M, Ozaki H, Karaki H. Effects of adrenomedullin and calcitonin gene-related peptide on contractions of the rat aorta and porcine coronary artery. Br J Pharmacol. 1998;123:1645-1654.

64. Nelson MT, Huang Y, Brayden JE, Hescheler J, Standen NB. Arterial dilations in response to calcitonin gene-related peptide involve activation of K+ channels. Nature. 1990;344:770-773.

65. Maggi CA. Tachykinins and calcitonin gene-related peptide (CGRP) as co-transmitters released from peripheral endings of sensory nerves. Prog Neurobiol. 1995;45:1-98.

66. Wellman GC, Quayle JM, Standen NB. ATP-sensitive K+ channel activation by calcitonin gene-related peptide and protein kinase A in pig coronary arterial smooth muscle. J Physiol. 1998;507:117-129.

67. Edvinsson L, Fredholm BB, Hamel E, Jansen I, Verrecchia C. Perivascular peptides relax cerebral arteries concomitant with stimulation of cyclic adenosine monophosphate accumulation or release of an endothelium-derived relaxing factor in the cat. Neurosci Lett. 1985;58:213-217.

68. Strecker T, Dieterle A, Reeh PW, Weyand M, Messlinger K. Stimulated release of calcitonin gene-related peptide from the human right atrium in patients with and without diabetes mellitus. Peptides. 2006;27:3255-3260.

69. Isaka M, Imamura M, Sakuma I, Makino Y, Shiiya N, Yasuda K. Cardiopulmonary bypass influences the plasma levels of calcitonin gene-related peptides in dogs: effects of hemofiltration and hemodilution. Res Vet Sci. 2007;82:110-114.

70. Gray DW, Marshall I. Nitric oxide synthesis inhibitors attenuate calcitonin gene-related peptide endothelium-dependent vasorelaxation in rat aorta. Eur J Pharmacol. 1992;212:37-42.

71. Meens MJ, Fazzi GE, van Zandvoort MA, De Mey JG. Calcitonin gene-related peptide selectively relaxes contractile responses to endothelin-1 in rat mesenteric resistance arteries. J Pharmacol Exp Ther. 2009;331:87-95.

72. Feng CJ, Kang B, Kaye AD, Kadowitz PJ, Nossaman BD. L-NAME modulates responses to adrenomedullin in the hindquarters vascular bed of the rat. Life Sci. 1994;55:433-438.

73. Miura K, Ebara T, Okumura M, Matsuura T, Kim S, Yukimura T, Iwao H. Attenuation of adrenomedullin-induced renal vasodilatation by NG-nitro L-arginine but not glibenclamide. Br J Pharmacol. 1995;115:917-924.

74. Hirata Y, Hayakawa H, Suzuki Y, Suzuki E, Ikenouchi H, Kohmoto O, Kimura K, Kitamura K, Eto T, Kangawa K. Mechanisms of adrenomedullin-induced vasodilation in the rat kidney. Hypertension. 1995;25:790-795.

75. He H, Bessho H, Fujisawa Y, Horiuchi K, Tomohiro A, Kita T, Aki Y, Kimura S, Tamaki T, Abe Y. Effects of a synthetic rat adrenomedullin on regional hemodynamics in rats. Eur J Pharmacol. 1995;273:209-214.

76. Khan AI, Kato J, Kitamura K, Kangawa K, Eto T. Hypotensive effect of chronically infused adrenomedullin in conscious Wistar-Kyoto and spontaneously hypertensive rats. Clin Exp Pharmacol Physiol. 1997;24:139-142.

77. Shimekake Y, Nagata K, Ohta S, Kambayashi Y, Teraoka H, Kitamura K, Eto T, Kangawa K, Matsuo H. Adrenomedullin stimulates two signal transduction pathways, cAMP accumulation and Ca2+ mobilization, in bovine aortic endothelial cells. J Biol Chem. 1995;270:4412-4417.

78. Terata K, Miura H, Liu Y, Loberiza F, Gutterman DD. Human coronary arteriolar dilation to adrenomedullin: role of nitric oxide and K (+) channels. Am J Physiol Heart Circ Physiol. 2000;279:2620-2626.

79. Hinson JP, Kapas S, Smith DM. Adrenomedullin, a multifunctional regulatory peptide. Endocr Rev. 2000;21:138-167.

80. Gumusel B, Hao Q, Hyman AL, Kadowitz PJ, Champion HC, Chang JK, Mehta JL, Lippton H. Analysis of responses to adrenomedullin-(13-52) in the pulmonary vascular bed of rats. Am J Physiol. 1998;274:1255-1263.

81. Parkes DG, May CN. Direct cardiac and vascular actions of adrenomedullin in conscious sheep. Br J Pharmacol. 1997;120:1179-1185.

82. Stangl D, Muff R, Schmolck C, Fischer JA. Photoaffinity labeling of rat calcitonin gene-related peptide receptors and adenylate cyclase activation: identification of receptor subtypes. Endocrinology. 1993;132:744-750.

83. Majid DS, Kadowitz PJ, Coy DH, Navar LG. Renal responses to intra-arterial administration of adrenomedullin in dogs. Am J Physiol. 1996;270:200-205.

84. Nossaman BD, Feng CJ, Kaye AD, Dewitt B, Coy DH, Murphy WA, Kadowitz PJ. Pulmonary vasodilator responses to adrenomedullin are reduced by NOS inhibitors in rats but not in cats. Am J Physiol. 1996;270:782-789.

85. Champion HC, Lambert DG, McWilliams SM, Shah MK, Murphy WA, Coy DH, Kadowitz PJ. Comparison of responses to rat and human adrenomedullin in the hindlimb vascular bed of the cat. Regul Pept. 1997;70:161-165.

86. Champion HC, Wang R, Shenassa BB, Murphy WA , Coy DH, Hellstrom WJ, Kadowitz PJ. Adrenomedullin induces penile erection in the cat. Eur J Pharmacol. 1997;319:71-75.

87. Champion HC, Wang R, Santiago JA, Murphy WA , Coy DH, Kadowitz PJ, Hellstrom WJ. Comparison of responses to adrenomedullin and calcitonin gene-related peptide in the feline erection model. J Androl. 1997;18:513-521.

88. Lang MG, Paterno R, Faraci FM, Heistad DD. Mechanisms of adrenomedullin-induced dilatation of cerebral arterioles. Stroke. 1997;28:181-185.

89. Sabates BL, Pigott JD, Choe EU, Cruz MP, Lippton HL, Hyman AL, Flint LM, Ferrara JJ. Adrenomedullin mediates coronary vasodilation through adenosine receptors and KATP channels. J Surg Res. 1997;67:163-168.

90. Brain SD, Poyner DR, Hill RG. CGRP receptors: a headache to study, but will antagonists prove therapeutic in migraine? Trends Pharmacol Sci. 2002;23:51-53.

91. Dewachter L, Dewachter C, Naeije R. New therapies for pulmonary arterial hypertension: an update on current bench to bedside translation. Expert Opin Investig Drugs 2010;19:469-488.

92. Zhao L, Brown LA, Owji AA, Nunez DJ, Smith DM, Ghatei MA, Bloom SR, Wilkins MR. Adrenomedullin activity in chronically hypoxic rat lungs. Am J Physiol. 1996;271:622-629.

93. Nagaya N, Nishikimi T, Uematsu M, Satoh T, Oya H, Kyotani S, Sakamaki F, Ueno K, Nakanishi N, Miyatake K, Kangawa K. Haemodynamic and hormonal effects of adrenomedullin in patients with pulmonary hypertension. Heart. 2000;84:653-658.

94. Vizza CD, Letizia C, Sciomer S, Naeije R, Rocca GD, Roma AD, Musaro S, Quattrucci S, Gaudio C, Battagliese A, Badagliacca R, Erasmo ED, Fedele F. Increased plasma levels of adrenomedullin, a vasoactive peptide, in patients with end-stage pulmonary disease. Regul Pept. 2005;124:187-193.

95. Kakishita M, Nishikimi T, Okano Y, Satoh T, Kyotani S, Nagaya N, Fukushima K, Nakanishi N, Takishita S, Miyata A, Kangawa K, Matsuo H, Kuniea T. Increased plasma levels of adrenomedullin in patients with pulmonary hypertension. Clin Sci (Lond). 1999;96:33-39.

96. Nagaya N, Kyotani S, Uematsu M, et Ueno K, Oya H, Nakanishi N, Shirai M, Mori H, Miyateke K, Kangawa K. Effects of adrenomedullin inhalation on hemodynamics and exercise capacity in patients with idiopathic pulmonary arterial hypertension. Circulation. 2004;109:351-356.

97. Takei Y, Joss JMP, Kloas W, Rankin JC. Identification of angiotensin I in several vertebrate species: its structural and functional evolution. Gen Comp Endocrinol. 2004;135:286-292.

98. Dong F, Taylor MM, Samson WK, Ren J. Intermedin (adrenomedullin-2) enhances cardiac contractile function via a protein kinase C- and protein kinase A-dependent pathway in murine ventricular myocytes. J Appl Physiol. 1985;2006;101:778-784.

99. Yang JH, Jia YX, Pan CS, Zhao J, Ouyang M, Yang J, Chang JK, Tang CS, Qİ YF. Effects of intermedin (1-53) on cardiac function and ischemia/reperfusion injury in isolated rat hearts. Biochem Biophys Res Commun. 2005;327:713-719.

100. Yang JH, Cai Y, Duan XH, Ma CG, Wang X, Tang CS, Qİ YF. Intermedin 1-53 inhibits rat cardiac fibroblast activation induced by angiotensin II. Regul Pept. 2009;158:19-25.

101. Song JQ, Teng X, Cai Y, Tang CS, Qi YF. Activation of Akt/GSK-3beta signaling pathway is involved in intermedin (1-53) protection against myocardial apoptosis induced by ischemia/reperfusion. Apoptosis. 2009;14:1061-1069.

102. Fujisawa Y, Nagai Y, Miyatake A, Miura K, Nishiyama A, Kimura S, Abe Y. Effects of adrenomedullin 2 on regional hemodynamics in conscious rats. Eur J Pharmacol. 2007;558:128-132.

103. Burak Kandilci H, Gumusel B, Wasserman A, Witriol N, Lippton H. Intermedin/adrenomedullin-2 dilates the rat pulmonary vascular bed: dependence on CGRP receptors and nitric oxide release. Peptides. 2006;27:1390-1396.

104. Fujisawa Y, Nagai Y, Miyatake A, Takei Y, Miura K, Shoukouji T, Nishiyama A, Kimura S, Abe Y. Renal effects of a new member of adrenomedullin family, adrenomedullin2, in rats. Eur J Pharmacol. 2004;497:75-80.

105. Jolly L, March JE, Kemp PA, Bennett T, Gardiner SM. Mechanisms involved in the regional haemodynamic effects of intermedin (adrenomedullin 2) compared with adrenomedullin in conscious rats. Br J Pharmacol. 2009;157:1502-1513.

106. Telli G, Erac Y, Tel BC, Gumusel B. Mechanism of adrenomedullin 2/intermedin mediated vasorelaxation in rat main pulmonary artery. Peptides. 2018;103:65-71.

107. Grossini E, Molinari C, Mary DA, Uberti F, Caimmi PP, Vacca G. Intracoronary intermedin 1-47 augments cardiac perfusion and function in anesthetized pigs: role of calcitonin receptors and beta-adrenoreceptor-mediated nitric oxide release. J Appl Physiol (1985) 2009;107:1037-1050.

108. Pfeil U, Aslam M, Paddenberg R, Quanz K, Chang CL, Park JII, Gries B, Rafiq A, Faulhammer P, Goldenberg A, Papadakis T, Noll T, Hsu SYT, Weissmann N, Kummer W . Intermedin/adrenomedullin-2 is a hypoxia-induced endothelial peptide that stabilizes pulmonary microvascular permeability. Am J Physiol Lung Cell Mol Physiol. 2009;297:837-845.

109. Kandilci HB, Gumusel B, Lippton H. Intermedin/adrenomedullin-2 (IMD/AM2) relaxes rat main pulmonary arterial rings via cGMP-dependent pathway: role of nitric oxide and large conductance calcium-activated potassium channels (BK(Ca)). Peptides. 2008;29:1321-1328.

110. Chen L, Kis B, Hashimoto H, Busija DW, Takei Y, Yamashita H, Ueta Y. Adrenomedullin 2 protects rat cerebral endothelial cells from oxidative damage in vitro. Brain Res. 2006;1086:42-49.

111. Mao SZ, Fan XF, Xue F, Chen R, Ying Chen XY, Yuan GS, Gang Hu L, Liu SF, Gong YS. Intermedin modulates hypoxic pulmonary vascular remodeling by inhibiting pulmonary artery smooth muscle cell proliferation. Pulm Pharmacol Ther. 2014;27:1-9.

112. Chen H, Wang X, Tong M, Wu D, Wu S, Chen J, Wang X, Wang X, Kang Y, Tang H, Tang C, Jiang W. Intermedin suppresses pressure overload cardiac hypertrophy through activation of autophagy. PLoS One. 2013;8:64757.

113. Li P, Sun HJ, Han Y, Wang JJ, Zhang F, Tang CS, Zhou YB. Intermedin enhances sympathetic outflow via receptor-mediated cAMP/PKA signaling pathway in nucleus tractus solitarii of rats. Peptides. 2013;47:1-6.

114. Chang CL, Roh J, Hsu SYT. Intermedin, a novel calcitonin family peptide that exists in teleosts as well as in mammals: a comparison with other calcitonin/intermedin family peptides in vertebrates. Peptides. 2004;25:1633-1642.

115. Gong YS, Fan XF, Wu XM, Hu LG, Tang CS, Pang YZ, Qİ YF. [Changes of intermedin/adrenomedullin 2 and its receptors in the right ventricle of rats with chronic hypoxic pulmonary hypertension]. Sheng Li Xue Bao. 2007;59:210-214.

116. Gong YS, Zhang L, Guo YM, Gang Hu L, Mao SZ, Fang XF, Huang P, Hong L. [Effect of hypoxia on the expressions of intermedin/ adrenomedullin2 in plasma and the tissues of heart and lung in rats]. Zhongguo Ying Yong Sheng Li Xue Za Zhi. 2009;25:8-11.

117. Fan XF, Huang P, Gong YS, Wu XM, Hu LG, Tian LX, Tang CS, Pang YZ. [Changes of adrenomedullin 2/intermedin in the lung of rats with chronic hypoxic pulmonary hypertension]. Zhongguo Ying Yong Sheng Li Xue Za Zhi. 2007;23:467-471.

118. Ni XQ, Zhang JS, Tang CS, Qi YF. Intermedin/adrenomedullin2: an autocrine/paracrine factor in vascular homeostasis and disease. Sci China Life Sci. 2014;57:781-789.

119. Telli G, Tel BC, Yersal N, Korkusuz P, Gumusel B. Effect of intermedin/ adrenomedullin2 on the pulmonary vascular bed in hypoxia-induced pulmonary hypertensive rats. Life Sci. 2018;192:62-67.

120. Telli G, Kandilci HB, Tel BC, Gümüşel B. Intermedin/Adrenomedullin 2 (IMD/AM2) is a potent vasodilator in chronic hypoxia induced pulmonary hypertensive isolated rat lungs. Faseb Journal 2016;30(Suppl 1).